U.PORTO
FACULDADE DE FARMÁCIA
UNIVERSIDADE DO PORTO

Brígida Ribeiro de Pinho

Naphthoquinones and Ubiquinone Analogues' Biological Properties: Modulation of Immune and Neurological Systems

Thesis for Doctor Degree in Pharmaceutical Sciences
Phytochemistry and Pharmacognosy Speciality

Work performed under the supervision of
Prof. Paula Cristina Branquinho de Andrade, PhD
and co-supervision of
Prof. Patrícia Carla Ribeiro Valentão, PhD
Prof. Jorge Miguel de Ascenção Oliveira, PhD

December 2013

To my parents

The financial support was provided by “Fundação para a Ciência e a Tecnologia” (FCT) (SFRH/BD/63852/2009), under the POPH – QREN – Type 4.1 – Advanced Training, funded by the European Social Fund and by National funds from “Ministério da Educação e Ciência”, and by PTDC/NEU-NMC/0237/2012 (FCT), FCOMP-01-0124-FEDER-029649 (COMPETE).

PUBLICATIONS

The data contained in the following works make part of this thesis:

Publications in international peer-reviewed journals indexed at *Journal Citation Reports* from *ISI Web of Knowledge*:

1. **Pinho BR**, Sousa C, Valentão P, Andrade PB. Is nitric oxide decrease observed with naphthoquinones in LPS stimulated RAW 264.7 macrophages a beneficial property? **PLoS ONE** 2011 Aug; 6 (8): e24098.

2. **Pinho BR**, Santos MM, Fonseca-Silva A, Valentão P, Andrade PB, Oliveira JMA. How mitochondrial dysfunction affects zebrafish development and cardiovascular function: An *in vivo* model for testing mitochondria-targeted drugs. **Br J Pharmacol** 2013 Mar; 169 (5): 1072-90.

3. **Pinho BR**, Sousa C, Valentão P, Oliveira JMA, Andrade PB. Modulation of basophils' degranulation and allergy-related enzymes by monomeric and dimeric naphthoquinones. Submitted for publication.

4. **Pinho BR**, Leitão-Rocha A, Quintas C, Valentão P, Andrade PB, Santos MM, Oliveira JMA. Mitochondrial and behavioural deficits in the zebrafish MPP^+ Parkinson model: Effect of ubiquinone analogues and lysine deacetylase inhibitors. Manuscript in preparation.

Book chapter:

1. **Pinho BR**, Sousa C, Oliveira JMA, Valentão P, Andrade PB. Naphthoquinones' biological activities and toxicological effects. In: Bitterlich, A., Fischl, S. (Eds.) Bioactive compounds: Type, biological activities and health effects. New York: Nova Science Publishers; 2012. p. 181-218.

Communications at conferences or workshops:

Oral communications

1. **Pinho BR**, Magalhães JSO, Valentão P, Andrade PB, Santos MM, Oliveira JMA. Pharmacological and toxicity screening of naphthoquinones in a zebrafish model validated with HDAC inhibitors. **XLI Reunião Anual da Sociedade Portuguesa de Farmacologia**. February 2-4, 2011. Coimbra, Portugal.

2. **Pinho BR**, Fonseca-Silva A, Santos MM, Valentão P, Andrade PB, Oliveira JMA. *In vivo* modelling of mitochondrial dysfunction and testing of ubiquinone analogues in zebrafish. **XLII Reunião Anual da Sociedade Portuguesa de Farmacologia**. February 1-3, 2012. Lisboa, Portugal.

3. Fonseca-Silva A, **Pinho BR**, Maia-Amaral R, Santos MM, Oliveira JMA. A zebrafish model of cardiac insufficiency by mitochondrial dysfunction: Insights for ubiquinone analogues and lysine deacetylase inhibitors in Friedreich's ataxia. **XLIII Reunião Anual da Sociedade Portuguesa de Farmacologia**. February 6-8, 2013. Porto, Portugal.

4. **Pinho BR**, Leitão-Rocha A, Faustová Z, Valentão P, Andrade PB, Oliveira JMA. Lysine deacetylase inhibitors and ubiquinone analogues in a zebrafish (*Danio rerio*) Parkinson model. **XLIII Reunião Anual da Sociedade Portuguesa de Farmacologia**. February 6-8, 2013. Porto, Portugal.

5. Fonseca-Silva A, **Pinho BR**, Mendes JM, Maia-Amaral R, Santos MM, Oliveira JMA. Experimental therapeutics in a zebrafish model of cardiac insufficiency by mitochondrial dysfunction: Insights for Friedreich's ataxia. **IJUP13 – 6th Meeting of Young Researchers of University of Porto**. February 13-15, 2013. Porto, Portugal.

Poster communications

1. **Pinho BR**, Sousa C, Oliveira JMA, Valentão P, Andrade PB. *Diospyros chamaethamnus*: Naphthoquinones' bioactivity in inflammation. **1st Annual Workshop MAP-BioPlant**. March 29-30, 2010. Porto, Portugal.

2. **Pinho BR**, Sousa C, Valentão P, Oliveira JMA, Andrade PB. Anti-inflammatory activity of naphthoquinones isolated from *Diospyros chamaethamnus*. **International Workshop: Drugs from Nature Targeting Inflammation**. April 8-10, 2010. Innsbruck, Austria.

3. **Pinho BR**, Magalhães JSO, Valentão P, Andrade PB, Santos MM, Oliveira JMA. *In vivo* toxicity profile of naphthoquinones in zebrafish embryos. **2nd Annual Workshop MAP-BioPlant**. April 18-19, 2011. Braga, Portugal.

4. **Pinho BR**, Fonseca-Silva A, Santos MM, Valentão P, Andrade PB, Oliveira JMA. Ubiquinone analogues and histone deacetylase inhibitors in an induced zebrafish model of mitochondrial dysfunction. **5th Meeting of Young Researchers of University of Porto**. February 22-24, 2012. Porto, Portugal.

5. **Pinho BR**, Sousa C, Valentão P, Andrade PB. Anti-allergic properties of natural naphthoquinones: Menadione inhibits leukotrienes production and naphthazarin inhibits degranulation. **3rd Annual Workshop MAP-BioPlant**. December 4-5, 2012. Aveiro, Portugal.

AUTHOR'S DECLARATION

The author states to have afforded a major contribution to the conceptual design, technical execution of the work, interpretation of the results and manuscript preparation of the works included in this thesis.

ACKNOWLEDGMENTS

The completion of this PhD thesis was only possible due to the contribution of several people and institutions, to whom I am profoundly grateful. Therefore, I would like to thank the following people and organisations:

"Fundação para a Ciência e a Tecnologia" (FCT) for the financial support given by awarding me a doctoral grant (SFRH/BD/63852/2009) under the POPH – QREN – Type 4.1 – Advanced Training, funded by the European Social Fund and by National funds from the "Ministério da Educação e Ciência".

Prof. Paula Cristina Branquinho de Andrade, supervisor of this thesis. Without her, this thesis would not be possible. Prof. Paula aroused my interest in scientific research, having welcomed me in her laboratory, the Laboratory of Pharmacognosy of the Faculty of Pharmacy of the University of Porto. Prof. Paula offered all the necessary conditions for the realization of this PhD work, being an example of persistence and dedication. I greatly admire her due to her wide professional experience and the way she maintains a strong and growing laboratory in a harmonious, cohesive and competitive group. I am very grateful for all of her availability and scientific supervision.

Prof. Patrícia Carla Ribeiro Valentão, co-supervisor of this thesis, for her encouraging words, availability, perfectionism and scientific knowledge. I deeply appreciate the intensive work developed by Prof. Patrícia, who always had the time to accompany the students' works even when she was too busy. Thank you very much.

Prof. Jorge Miguel de Ascenção Oliveira, co-supervisor of this thesis, who welcomed me in the Laboratory of Pharmacology of the Faculty of Pharmacy of the University of Porto. I immensely appreciate his scientific rigour and knowledge and his constant pursuit to know more and more. I am greatly grateful to Prof. Jorge for all his teaching, as well as for encouraging me to work with zebrafish. Thank's to Prof. Jorge, it was possible to establish a significant scientific relationship with the Interdisciplinary Centre of Marine and Environmental Research (CIIMAR), where I learned about zebrafish husbandry, management and care and about molecular biology.

Doctor Carla Sara Ferreira Sousa for her friendship, support and knowledge about cell culture.

Prof. Maria Clara Ferreira de Oliveira Quintas for her friendship, availability and training concerning the western blot technique.

Doctor Miguel Alberto Fernandes Machado e Santos, researcher of the Interdisciplinary Centre of Marine and Environmental Research (CIIMAR), for all his know-how about zebrafish management and molecular biology. I am deeply grateful for his availability and for having received me in his lab (Environmental toxicology – LETOX lab).

The staff of the Laboratory of Pharmacognosy from the Faculty of Pharmacy of the University of Porto for all the support hence contributing to the normal functioning of the lab and the development of this thesis.

The staff of the Laboratory of Pharmacology from the Faculty of Pharmacy of the University of Porto for all the support every time that it was required.

My PhD colleagues of the Laboratory of Pharmacognosy of the Faculty of Pharmacy of the University of Porto, Graciliana Lopes, Marcos Monteiro, Andreia Oliveira, Fátima Fernandes and Eduarda Moita, and my colleagues of the Laboratory of Pharmacology of the Faculty of Pharmacy of the University of Porto, Pedro Dias and Ana Rocha, for their companionship.

The research members of the Environmental toxicology (LETOX) lab of CIIMAR for having welcomed me in their laboratory and sharing their knowledge about molecular biology. A special acknowledgement to Ana André, Ana Capitão and Raquel Ruivo.

My parents, Olga Pinho e António Pinho, to whom this thesis is dedicated. Thank you very much for your unconditional love.

Joana Pinho e Daniel Pinho, my siblings, of whom I am very proud of. I am grateful for their friendship, companionship and affection. Joana, thank you very much for your useful information about image processing and Daniel, thank you very much for being my “English teacher”.

Válter Costa, my husband, for all his dedication, patience, understanding and affection.

ABSTRACT

ABSTRACT

Quinones are compounds present in nature with essential functions to the survival of living beings, such as defence or energy production. The great majority of quinones may be divided into three groups according to the number of aromatic rings: benzoquinones, naphthoquinones and anthraquinones. In the work developed for this thesis, naphthoquinones (diospyrin, diosquinone, juglone, menadione, naphthazarin and plumbagin) and ubiquinone analogues (idebenone and decylubiquinone), which are prenylated benzoquinones, were the studied compounds. Although several biological activities of naphthoquinones have been explored, little is known about their ability to modulate the immune system. On the other hand, ubiquinone analogues are promising drugs for the treatment of neurodegenerative disorders. Nevertheless, until now, idebenone and decylubiquinone were not studied in a model of mitochondrial dysfunction or in a model of Parkinsonism induced by MPP^+ in zebrafish. Therefore, the main goals of this thesis were: naphthoquinones screening as potential anti-inflammatory and anti-allergic drugs; the study of naphthoquinones' toxicity in an *in vivo* model; and the study of the ubiquinone analogues' potential in rescuing a Parkinsonian phenotype or a mitochondrial dysfunction in an *in vivo* model.

In order to evaluate naphthoquinones' anti-inflammatory properties, we studied their ability to reduce nitric oxide production in lipopolysaccharide-stimulated cells (RAW 264.7 macrophages). Diosquinone was the only naphthoquinone that reduced nitric oxide production. However, as naphthoquinones may undergo redox cycles, they may generate superoxide anion that can react with nitric oxide, consuming it and forming peroxynitrite. Therefore, we quantified the superoxide radical and 3-nitrotyrosine, which is an important hallmark of peroxynitrite-induced toxicity. Both superoxide radical and 3-nitrotyrosine were not increased in the presence of diosquinone, with the diosquinone anti-inflammatory activity being confirmed by the associated reduction in pro-inflammatory cytokines' production. Diosquinone anti-inflammatory properties might be valuable in the process of developing novel treatments for other pathologies with an associated inflammatory process, such as allergy. However, diosquinone was unable to inhibit RBL-2H3 basophils' degranulation induced by either antibody-antigen complex or calcium ionophore. In contrast, diospyrin reduced calcium ionophore-induced degranulation and naphthazarin reduced antibody-antigen complex-induced degranulation. These results suggest that diospyrin and naphthazarin have different mechanisms of action. Also related to the study of naphthoquinones' anti-allergic properties, results from this thesis suggest that the tested naphthoquinones are weak hyaluronidase inhibitors, but able to inhibit soybean lipoxidase, an enzyme structurally similar to 5-lipoxygenase. Menadione, diospyrin and

diosquinone were the naphthoquinones with strongest lipoxidase inhibitory activity. As these naphthoquinones were the most lipophilic among tested compounds, it is possible that they compete with natural lipoxidase substrates, which are also lipophilic. From these three naphthoquinones, only menadione inhibited leukotriene C_4 production in intact cells.

When tested in zebrafish embryos, most naphthoquinones were more toxic than in cell lines, such as RAW 264.7 or RBL-2H3 cells. Naphthoquinones showed different patterns of toxicity, which may be related with their lipophilic properties. Among monomeric naphthoquinones, naphthazarin and juglone directly killed zebrafish embryos without intermediate abnormalities, whereas menadione and plumbagin primarily evoked morphological/developmental abnormalities. Menadione in particular caused hyprochromic anaemia in zebrafish embryos, possibly via reduced hematopoiesis related with mitochondrial membrane potential disruption.

In order to assess the putative protective effects of ubiquinone analogues in mitochondrial dysfunction and Parkinson's disease models, we exposed zebrafish embryos/larvae to mitochondrial inhibitors and MPP^+, a dopaminergic toxin inhibiting mitochondrial complex I. Inhibitors of complexes I and II induced abnormalities in zebrafish embryos, while complex III inhibitors were highly lethal without inducing prior abnormalities, likely due to lack of alternative downstream pathways to feed the mitochondrial respiratory chain. In fact, ubiquinone analogues delayed cardio-circulatory arrest in zebrafish larvae acutely exposed to rotenone (a mitochondrial complex I inhibitor), while failing to delay the arrest induced by complex III inhibition. Attending to these results and to the fact that oligomycin (an ATP synthase inhibitor) also delayed the heartbeat arrest of rotenone-treated larvae, the protection induced by ubiquinone analogues might be due to sustaining/delaying energy dissipation. Ubiquinone analogues may directly feed the complex III, provided they are firstly reduced by dehydrogenases, such as cytosolic NAD(P)H quinone-oxidoreductase. Ubiquinone analogues, however, failed to rescue/delay chronic rotenone toxicity, suggesting only transient effects at the respiratory chain, or additional toxicity pathways of chronic rotenone exposure.

MPP^+ (500 μM) induced an abnormal locomotor profile and sensorimotor reflexes, apparently without peripheral toxicity, as assessed by normal neuromast labelling; and no generalized mitochondrial toxicity, as assessed in mitochondrial extracts from whole-larvae or even head/body splits. Despite the protective effect verified against an acute complex I dysfunction, the ubiquinone analogues did not rescue the MPP^+-induced locomotor phenotype. One possible explanation is that MPP^+ toxicity may rely on its mitochondrial membrane potential-dependent uptake, and with this being sustained by ubiquinone analogues, it would also sustain MPP^+ incorporation and toxicity.

Summing up: diosquinone reduced nitric oxide and pro-inflammatory cytokine production; naphthazarin reduced basophils' degranulation upstream from intracellular calcium increase, while diospyrin reduced calcium ionophore-induced basophils' degranulation; menadione reduced leukotrienes levels in a cellular system; ubiquinone analogues were protective against an acute mitochondrial complex I dysfunction in zebrafish embryos, but they did not rescue the MPP^+-induced Parkinsonian phenotype in zebrafish larvae.

Keywords: Naphthoquinones, Ubiquinone analogues; Inflammation; Allergy; Neurodegenerative disorders; Mitochondria; Zebrafish.

RESUMO

RESUMO

As quinonas são compostos presentes na Natureza com funções essenciais à sobrevivência dos seres vivos, tais como a defesa ou a produção energia. A maioria das quinonas pode ser dividida em três grupos de acordo com o número de anéis aromáticos: benzoquinonas, naftoquinonas e antraquinonas. As naftoquinonas (diospirina, diosquinona, juglona, menadiona, naftazarina e plumbagina) e os análogos de ubiquinona (idebenona e decilubiquinona), que são benzoquinonas preniladas, foram os compostos estudados no trabalho desenvolvido para esta tese. Várias atividades biológicas das naftoquinonas têm sido exploradas; contudo, o conhecimento sobre a sua capacidade para modularem o sistema imunitário é reduzido. Por outro lado, os análogos de ubiquinona são compostos promissores no tratamento de doenças neurodegenerativas, apesar de, até à data, a idebenona e a decilubiquinona não terem sido estudadas num modelo de disfunção mitocondrial ou num modelo de Parkinsonismo induzido pelo MPP^+, em peixe-zebra. Deste modo, os principais objetivos desta tese foram: o *screening* de naftoquinonas como potenciais fármacos anti-inflamatórios e antialérgicos; o estudo da toxicidade das naftoquinonas num modelo *in vivo*; e o estudo do potencial de análogos de ubiquinona em resgatar um fenótipo Parkinsónico ou uma disfunção mitocondrial num modelo *in vivo*.

Para avaliar as propriedades anti-inflamatórias das naftoquinonas, estudou-se a capacidade destas reduzirem a produção de óxido nítrico por um sistema celular (macrófagos RAW 264.7) sujeito à ação pró-inflamatória do lipopolissacarídeo. A diosquinona foi a única naftoquinona testada capaz de induzir um decréscimo na produção de óxido nítrico. Porém, as naftoquinonas podem sofrer ciclos de oxidação-redução com geração do radical superóxido que, por sua vez, pode reagir com óxido nítrico, levando ao seu consumo e à formação de peroxinitrito. Assim, o radical superóxido e a 3-nitrotirosina, que constitui um dos principais marcadores de toxicidade do peroxinitrito, foram quantificados. Nenhum destes parâmetros estava aumentado na presença da diosquinona e a atividade anti-inflamatória desta foi confirmada pela redução da produção de citoquinas pró-inflamatórias. As propriedades anti-inflamatórias da diosquinona podem ser uma mais-valia para o tratamento de outras patologias com um processo inflamatório associado, como é o caso da alergia. Porém, a diosquinona não teve capacidade de inibir a desgranulação de basófilos RBL-2H3 quando estimulados por um complexo anticorpo-antigénio ou por um ionóforo de cálcio. Contrariamente à diosquinona, a diospirina reduziu a desgranulação induzida pelo ionóforo de cálcio, enquanto que a naftazarina reduziu a desgranulação induzida pelo complexo anticorpo-antigénio. Estes resultados sugerem que a diospirina e a naftazarina apresentam

diferentes mecanismos de ação. Ainda relacionado com o estudo da atividade antialérgica, resultados desta tese sugerem que as naftoquinonas testadas são fracos inibidores da hialuronidase, mas que apresentam capacidade para inibir a lipoxidase de soja, que é uma enzima estruturalmente semelhante à 5-lipoxigenase. As naftoquinonas que apresentaram uma maior atividade na inibição da lipoxidase foram a menadiona, a diospirina e a diosquinona. Como essas naftoquinonas são as que apresentam maior lipofilia entre as testadas, é provável que possam competir com os substratos naturais da lipoxidase, que são igualmente lipofílicos. Dessas três naftoquinonas, a menadiona foi a única que conseguiu inibir a produção de leucotrieno C_4 num sistema celular.

Quando testadas em embriões de peixe-zebra, as naftoquinonas foram, no geral, mais tóxicas do que quando testadas em linhas celulares, como nas células RAW 264.7 e RBL-2H3. As naftoquinonas mostraram diferentes perfis de toxicidade, que podem estar relacionados com as suas propriedades lipofílicas. Entre as naftoquinonas monoméricas, naftazarina e a juglona induziram diretamente a morte de embriões sem indução de anomalias, enquanto que a menadiona e a plumbagina promoveram inicialmente o desenvolvimento de anomalias. Em particular, a menadiona induziu uma anemia hipocrómica nos embriões de peixe-zebra, provavelmente devido a uma redução da hematopoiese relacionada com uma perturbação do potencial membranar mitocondrial.

Para avaliar, os possíveis efeitos protetores dos análogos de ubiquinona num modelo de disfunção mitocondrial e num de Doença de Parkinson, embriões/larvas de peixe-zebra foram expostos a inibidores mitocondriais e ao MPP^+, uma toxina dopaminérgica que inibe o complexo I mitocondrial. Os inibidores dos complexos I e II induziram anomalias nos embriões de peixe-zebra, enquanto que os inibidores do complexo III foram altamente letais, sem induzirem um estado de anormalidade, o que pode estar relacionado com a falta de alternativas ao complexo III na cadeia respiratória mitocondrial. De facto, os análogos de ubiquinona testados atrasaram a paragem cardiocirculatória de larvas de peixe-zebra tratadas de forma aguda com rotenona (inibidor do complexo I mitocondrial), enquanto que não foi verificada nenhuma proteção face à toxicidade induzida pelos inibidores do complexo III. Atendendo a estes resultados e ao facto da oligomicina (inibidor da ATP sintase) ter, igualmente, atrasado a perda de batimento cardíaco de larvas tratadas com rotenona, a proteção induzida pelos análogos de ubiquinona deve-se, provavelmente, a um atraso na depleção de energia. Os análogos de ubiquinona podem alimentar diretamente o complexo III mitocondrial, quando reduzidos previamente por desidrogenases, como a citosólica NAD(P)H quinona-oxidoreductase. Contudo, os análogos de ubiquinona não induziram proteção contra a toxicidade crónica induzida pela rotenona, sugerindo que os análogos de ubiquinona possam ter apenas efeitos transientes na cadeia respiratória, ou que os efeitos tóxicos

decorrentes do tratamento crónico com rotenona não sejam apenas devido à inibição do complexo I.

O MPP^+ (500 μM) induziu um perfil de locomoção e de reflexos sensório-motores anormais, sem aparente toxicidade periférica (como foi avaliado pela normal marcação de neuromastos) e sem uma toxicidade mitocondrial generalizada (como foi verificado em extratos mitocondriais de larva-inteira ou mesmo em extratos mitocondriais da cabeça/corpo). Apesar do efeito protetor verificado face a uma disfunção aguda do complexo I, os análogos de ubiquinona não foram capazes de reverterem ou reduzirem a gravidade do fenótipo locomotor induzido pelo MPP^+. Uma possível explicação para este resultado é que a acumulação do MPP^+ na mitocôndria pode ser dependente do potencial de membrana mitocondrial, pelo que, como os análogos de ubiquinona são capazes de manterem esse potencial, podem contribuir para uma maior incorporação MPP^+ na mitocôndria e consequentemente para o aumento da sua toxicidade.

Retendo as principais observações/conclusões: a diosquinona diminuiu a produção de óxido nítrico, bem como de citoquinas pró-inflamatórias; a naftazarina inibiu a desgranulação de basófilos num passo da via metabólica anterior ao aumento de cálcio intracelular, enquanto que a diospirina reduziu a desgranulação de basófilos induzida por um ionóforo de cálcio; a menadiona reduziu os níveis de leucotrienos num sistema celular; os análogos de ubiquinona mostraram efeitos protetores contra uma disfunção aguda do complexo I mitocondrial em embriões de peixe-zebra, mas não resgataram o fenótipo Parkinsoniano induzido pelo MPP^+ em larvas de peixe-zebra.

Palavras-chave: Naftoquinonas; Análogos de ubiquinona; Inflamação; Alergia; Doenças neurodegenerativas; Mitocôndria; Peixe-zebra.

GENERAL INDEX

GENERAL INDEX

INDEX OF FIGURES

INDEX OF FIGURES

1. General Introduction

Experimental Section

3.1. Is nitric oxide decrease observed with naphthoquinones in LPS stimulated RAW 264.7 macrophages a beneficial property?

3.2. Modulation of basophils' degranulation and allergy-related enzymes by monomeric and dimeric naphthoquinones

3.3. How mitochondrial dysfunction affects zebrafish development and cardiovascular function: An *in vivo* model for testing mitochondria-targeted drugs

3.4. Mitochondrial and behavioural deficits in the zebrafish MPP^+ Parkinson model: Effect of ubiquinone analogues and lysine deacetylase inhibitors

4. General Discussion

INDEX OF TABLES

INDEX OF TABLES

ABBREVIATIONS AND SYMBOLS

ABBREVIATIONS AND SYMBOLS

3NP	3-Nitropropionic acid
4HB	4-Hydroxybenzoic acid
4NB	4-Nitrobenzoic acid
5-HETE	5-Hydroxyeicosatetraenoic acid
5-HPETE	5(*S*)-Hydroperoxy-6-*trans*-8,11,14-*cis*-eicosatetraenoic acid
5-LO	5-Lipoxygenase
AA	Arachidonic acid
Acetyl-CoA	Acetyl coenzyme A
AD	Alzheimer's disease
ADP	Adenosine-5'-diphosphate
ALS	Amyotrophic lateral sclerosis
AMP	Adenosine-5'-monophosphate
ANT	Antimycin
ATP	Adenosine-5'-triphosphate
ATV	Atovaquone
BP	Base pairs
Bpm	Beats per minute
BSA	Bovine serum albumin
CNS	Central nervous system
COX	Cyclooxygenase
CRM-1	Chromosome region maintenance 1
DAD	Diode array detector
DAT	Dopamine transporter
DCB	Decylubiquinone
DCM	Dicoumarol
DCPIP	2,6-Dichlorophenolindophenol
DD	Deacetylase domain
DHODH	Dihydroorotate dehydrogenase
DMAB	*p*-Dimethylaminobenzaldehyde
DMB	Dynein motor binding
DMEM	Dulbecco's modified Eagle medium
DMSO	Dimethyl sulfoxide
DNA	Deoxyribonucleic acid
DNP	Dinitrophenyl
DPBS	Dulbecco's phosphate buffered saline

Dpf	Days post fertilization
DPR	Diospyrin
DQN	Diosquinone
DTT	DL-dithiothreitol
EBSS	Earle's balanced salt solution
EDTA	Ethylenediaminetetraacetic acid
EGTA	Ethylene glycol-bis(2-aminoethylether)-*N*,*N*,*N*',*N*'-tetraacetic acid
ELISA	Enzyme linked immunosorbent assay
ERK	Extracellular signal-regulated kinases
ETC	Electron transport chain
ETF	Electron transfer flavoprotein
ETFDH	Electron transfer flavoprotein dehydrogenase
FAD	Flavin adenine dinucleotide, oxidized form
$FADH_2$	Flavin adenine dinucleotide, reduced form
FCCP	Carbonyl cyanide 4-(trifluoromethoxy)phenylhydrazone
FcεRI	High-affinity IgE receptor
FITC	Fluorescein isothiocyanate
Fps	Frames per second
FRDA	Friedreich's ataxia
GAS6	Growth arrest-specific 6
GFP	Green fluorescent protein
GM-CSF	Granulocyte-macrophage colony-stimulating factor
GPDH	Glycerol-3-phosphate dehydrogenase
GSH	Reduced glutathione
GSSG	Oxidized glutathione
H_2O_2	Hydrogen peroxide
HD	Huntington's disease
HMG-CoA	3-Hydroxy-3-methylglutaryl-coenzyme A
$HO^{\bullet}$	Hydroxyl radical
HOCl	Hypochlorous acid
Hpf	Hours post fertilization
HPLC	High-performance liquid chromatography
HRP	Horseradish peroxidase
HSP90	Heat shock protein 90
IC	Inhibitory concentration
IDB	Idebenone
IKK	IκB kinase

IL	Interleukin
IMM	Inner mitochondrial membrane
IMS	Intermembrane space
INF	Interferon
iNOS	Inducible nitric oxide synthase
IRF	Interferon regulatory factor
IκB	Inhibitory factor-κB
JAK/STAT	Janus kinase/ Signal transducer and activator of transcription
JGL	Juglone
JNK	*c*-Jun N-terminal kinase
KDAC	Lysine deacetylase
KDACi	KDAC inhibitors
LC	Lethal concentration
LDH	Lactate dehydrogenase
LHON	Leber's hereditary optic neuropathy
LPC	Lapachol
LPS	Lipopolysaccharide
LRRK2	Leucine-rich repeat kinase 2
LT	Leukotriene
MADD	Multiple acyl-CoA dehydrogenase deficiency
MAO	Monoamine oxidase
MAP	Mitogen-activated protein
MAPK	Mitogen-activated protein kinase
mDNA	Mitochondrial DNA
MELAS	Mitochondrial encephalomyopathy, lactic acidosis and stroke-like episodes
MHCII	Major histocompatibility complex class II
MKK/MEK	MAPK kinase
MND	Menadione
$MPDP^+$	1-Methyl-4-phenyl-2,3-dihydropyridinium
MPP^+	1-Methyl-4-phenylpyridinium
MPPP	1-Methyl-4-phenyl-4-propionoxypiperidine
MPTP	1-Methyl-4-phenyl-1,2,3,6-tetrahydropyridine
mPTP	Mitochondrial permeability transition pore
MTN	Methanol
MTT	3-(4,5-Dimethylthiazol-2-yl)-2,5-diphenyltetrazolium bromide
MYX	Myxothiazol
NAD^+	β-Nicotinamide adenine dinucleotide, oxidized form

NADH	β-Nicotinamide adenine dinucleotide, reduced form
NADPH	β-Nicotinamide adenine dinucleotide phosphate, reduced form
NBT	Nitrotetrazolium blue chloride
ND1	NADH dehydrogenase subunit 1
nDNA	Nuclear DNA
NES	Nuclear export signal
NF-κB	Nuclear factor κB
NLS	Nuclear localization signal
NO	Nitric oxide
NOS	Nitric oxide synthase
NQO1	NAD(P)H quinone-oxidoreductase
NSAID	Non-steroidal anti-inflammatory drug
NTZ	Naphthazarin
Nu	Nucleophile
O_2	Molecular oxygen
$O_2^{\bullet-}$	Superoxide anion
OCT	Organic cation transporter
OLG	Oligomycin
$ONOO^-$	Peroxynitrite
OPA	*o*-Phthalaldehyde
PAF	Platelet activating factor
PAGE	Polyacrylamide gel electrophoresis
PAMP	Pathogen-associated molecular pattern
PAP	3'-Phosphoadenosine 5'-phosphate
PAPS	3'-Phosphoadenosine 5'-phosphosulfate
PARL	Presenilin-associated rhomboid-like
PBMC	Peripheral blood mononuclear cells
PBS	Phosphate buffered solution
PBST	PBS with 0.05% Tween-20
PD	Parkinson's disease
PG	Prostaglandin
PGC-1α	PPAR-γ coactivator 1α
PHA	Phytohemagglutinin
Pi	Phosphate
PIN1	Peptidyl-prolyl *cis-trans* isomerase NIMA-interacting 1
PINK1	PTEN-induced putative kinase 1
PKC	Protein kinase C

PLA_2	Phospholipase A_2
PLB	Plumbagin
PMSF	Phenylmethanesulfonyl fluoride
PP	Pyrophosphate
PPAR	Peroxisome proliferator-activated receptor
PRR	Pattern-recognition receptor
QCT	Quercetin
Q_i	Ubiquinone reduction site
Q_o	Ubiquinone oxidation site
qPCR	Quantitative polymerase chain reaction
RNA	Ribonucleic acid
ROS	Reactive oxygen species
rRNA	Ribosomal RNA
RTN	Rotenone
SD	Standard deviation
SDS	Sodium dodecyl sulfate
SE14	Serine-glutamate tetradecapeptide
SEM	Standard error of the mean
SyK	Spleen tyrosine kinase
TBS	Tris-buffered saline
TBS-T	TBS with 0.05% Tween-20
TCR	T cell receptor
Th	T helper
TLR	Toll-like receptor
TNF	Tumour necrosis factor
TPA	12-*O*-Tetradecanoylphorbol-13-acetate
tRNA	Transfer RNA
TSA	Trichostatin A
TUB	Tubastatin A
UDP	Uridine diphosphate
UDPGA	Uridine diphosphate glucuronic acid
UQ	Ubiquinone
UQH_2	Ubiquinol
UV	Ultraviolet
VMAT	Vesicular monoamine transporter
VPA	Valproic acid
Znf-UBP	Zinc-finger ubiquitin-binding protein

α-Syn	α-Synuclein
βLPC	β-Lapachone
$\Delta\psi_m$	Mitochondrial membrane potential

THESIS OUTLINE

THESIS OUTLINE

The present thesis contains four main sections:

- CHAPTER I – INTRODUCTION AND OBJECTIVES

This is a General Introduction section, addressing the main topics from the work-plan of this thesis, including the study of naphthoquinones in the modulation of inflammation and allergy, as well as the study of ubiquinone analogues in the modulation of neurodegenerative disorders. This section includes only the essential information required to understand the experimental findings (results). Therefore, the first part of the General Introduction includes a brief approach to quinones and their chemical reactions, naphthoquinones and ubiquinone analogues. Moreover, it includes a focused description of the anti-inflammatory and anti-allergic properties of naphthoquinones (the two properties addressed in this thesis), and a more general review of the literature concerning naphthoquinones and their antitumoral and antimicrobial properties (the two properties more extensively studied in the literature). As the interest in ubiquinone analogues study in this thesis was due to the application of these drugs in mitochondrial dysfunction, only this topic was approached regarding ubiquinone analogues. The second part of the General Introduction comprises a brief description of inflammatory and allergic processes, as well as of neurodegenerative disorders, namely Parkinson's disease, with special attention to mitochondrial function. This section ends with the objectives of this thesis.

- CHAPTER II – EXPERIMENTAL SECTION

The Experimental Section is divided in four items that correspond to the research papers originated from this thesis. Each paper includes a small introduction, material and methods section, results and discussion.

- CHAPTER III – GENERAL DISCUSSION AND CONCLUSIONS

This chapter discusses the key aspects of the different works and how they integrate with each other. Furthermore, the approached subjects are discussed according to recent bibliographic references. The thesis' conclusions are enumerated at the end of this section.

- CHAPTER IV – BIBLIOGRAPHIC REFERENCES

This section comprises all the bibliographic references used in the writing of this thesis.

CHAPTER I

INTRODUCTION

OBJECTIVES

1. General Introduction

Plants are living beings devoid of or with very limited motility, being susceptible to biotic and abiotic aggressions. Over the course of evolution, plants developed biosynthetic pathways to synthesize a wide variety of organic molecules, commonly named secondary metabolites (1, 2). These compounds can have several functions, such as structure stabilization, protection against ultraviolet (UV) radiation, insects and predators, as well as attractants, being responsible for colour and scents (1, 3).

The study of secondary metabolites suffered a significant development in the last 50 years (4), in which more than 200,000 compounds were described. However, it is expected that the number of compounds synthesized by all living organisms could be much higher (2, 5). The secondary metabolites are mainly classified according to their biosynthetic origin and/or structural features (1): alkaloids, flavonoids, terpenes and quinones are examples of some classes. This thesis will focus on the latter group.

1.1. Quinones

Quinones are ubiquitously present in nature, more than 1200 compounds being already described (6). Chemically, quinones are oxygen-containing compounds, in which a dione is conjugated with an aromatic nucleus. Three main groups are known: benzoquinones, naphthoquinones and anthraquinones (**Figure 1.1**).

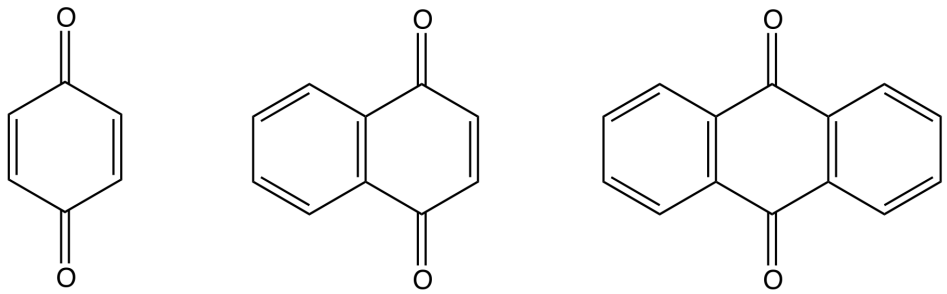

Figure 1.1. Basic chemical structure of the main groups of quinones.

Despite several metabolic pathways being described for quinone biosynthesis, a limited number of precursors are known: precurors are derived from acetate or shikimate pathways (**Figure 1.2**). By the acetate pathway, a β-ketoester cyclization may originate anthraquinones and naphthoquinones (**Figure 1.2*A***). The reaction of α-ketoglutaric acid

from acetate pathway with isochorismic acid from shikimate pathway forms 1,4-dihydroxy-2-naphthoic acid, which is a direct precursor of naphthoquinones. Additionally, the addition of an isoprene unit to 1,4-dihydroxy-2-naphthoic acid may originate some anthraquinones (**Figure 1.2*B***). 4-Hydroxybenzoic acid, which is formed from the shikimate pathway, is also a precursor of naphthoquinones and benzoquinones, such as ubiquinones (**Figure 1.2*C***) (6).

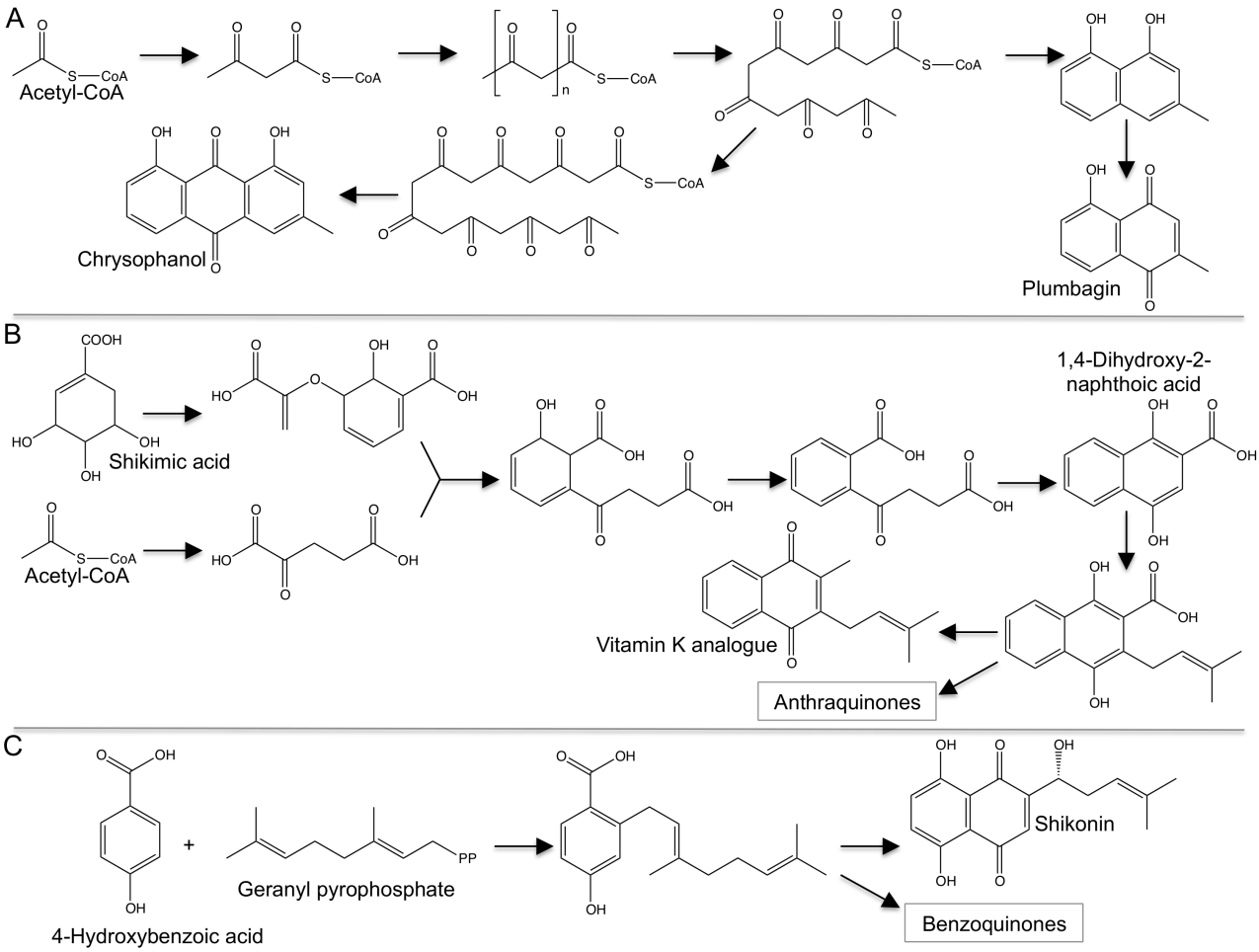

Figure 1.2. Main pathways for quinone biosynthesis. *A*, Acetate pathway. ***B***, Acetate and shikimate pathway. ***C***, 4-Hydroxybenzoic acid pathway. Adapted from Bruneton (6) and Babula and collaborators (7).

In this thesis, naphthoquinones and ubiquinones were the studied quinones. Regarding naphthoquinones, these compounds are generally more lipophilic than benzoquinones, whose majority has only one aromatic ring, and they are normally more reactive than anthraquinones, since naphthoquinones have in general higher redox potential than anthraquinones (8). Attending to naphthoquinones' chemical characteristics and to the existence of little information about some dimeric naphthoquinones derived

from *Diospyros* species, naphthoquinones were chosen as object of study of this thesis. Additionally, ubiquinone analogues were also considered, because, in general, they have better lipophilic properties than non-prenylated benzoquinones and they are interesting compounds to modulate mitochondrial function (9).

1.1.1. Chemical reactions

Several quinones have important functions in cellular biochemistry, being essential for energy production or for defence, avoiding the proliferation of bacteria, parasites or fungi (8). The diversity of biological activities attributed to quinones is partially explained by their pro-oxidant character. Quinones, mainly benzoquinones and naphthoquinones, may undergo redox cycles, as well as addition and substitution reactions with nucleophiles, attending to the high electron density of the quinone moiety (8, 10, 11). The presence of substituents in the quinone skeleton, which can be electron-donating or electron-attracting groups, determines the quinones' redox properties and, consequently, the tendency to react with nucleophiles or the semiquinone radical stability (12).

Quinones may undergo one- or two-electron reduction, forming semiquinone radical or hydroquinone, respectively (**Figure 1.3*A***) (10). These reactions can be catalyzed by flavoenzymes, which are oxidoreductases responsible by a large variety of different reactions (13). Flavoenzymes present in endoplasmic reticulum (β-nicotinamide adenine dinucleotide reduced form (NADH) cytochrome b_5 reductase or β-nicotinamide adenine dinucleotide phosphate reduced form (NADPH) cytochrome *c* reductase) or in mitochondria (NADH dehydrogenase or lipoyl dehydrogenase) catalyze a single–electron reduction, transforming the quinone into a semiquinone radical. In the cytosol, the NAD(P)H quinone-oxidoreductase (NQO1), also known as DT-diaphorase, catalyzes two-electron reduction, directly converting the quinone into hydroquinone (**Figure 1.3*A***). Also in the cytosol, xanthine oxidase and xanthine dehydrogenase catalyse one- or two-electron reductions (8). Despite the possibility of undergoing through autoxidation with a semiquinone radical formation, hydroquinones are, in general, less reactive than semiquinone radicals, being easily eliminated by conjugation with glucuronic acid or sulfate (**Figure 1.3*B*, *C***) (10). Furthermore, hydroquinones autoxidation may be largely inhibited by glutathione, an endogenous antioxidant (8). In contrast, the majority of semiquinones are reoxidized under aerobic conditions, inducing the formation of superoxide anion radical ($O_2^{\bullet -}$) (**Figure 1.3*A***) that may lead to the production of other reactive species, such as peroxynitrite ($ONOO^-$), hydrogen peroxide (H_2O_2), hypochlorous acid (HOCl) or hydroxyl radical ($HO^\bullet$) (**Figure 1.3*D***) (8, 14). In addition to inducing a

depletion of cells' antioxidant defences like the pool of reduced glutathione (GSH), reactive species induce damage in several macromolecules (proteins, nucleic acids and lipids), compromising their several functions (8). Thus, regarding the oxidative stress generated by semiquinones, NQO1 has been regarded as a cellular protector (8, 15).

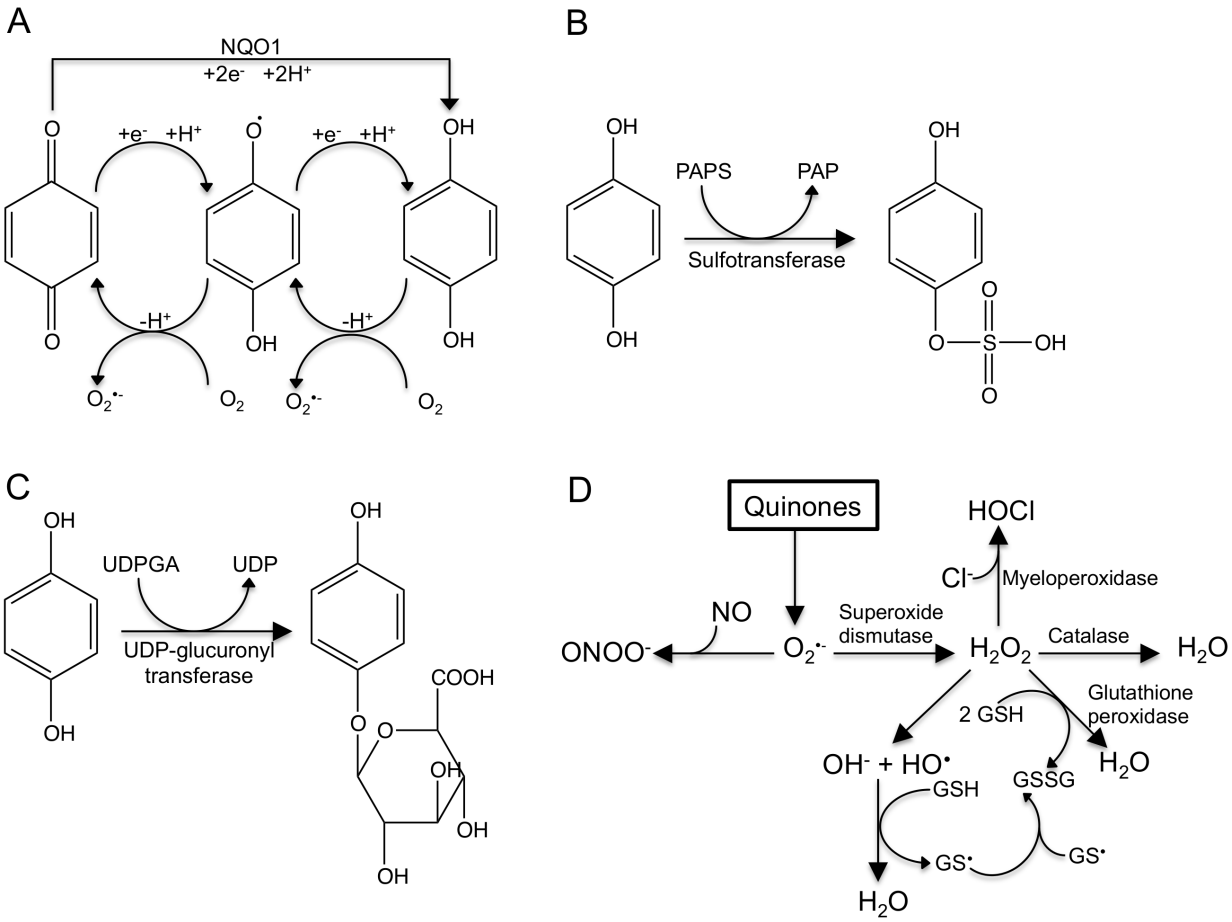

Figure 1.3. Quinones-induced oxidative stress and quinones' metabolism phase 2 reactions. ***A***, Reduction of quinone into semiquinone and hydroquinone. Hydroquinone and semiquinone may undergo oxidation with superoxide anion ($O_2^{\bullet -}$) formation. NQO1 [NAD(P)H quinone-oxidoreductase] catalyses the reduction of quinone directly into hydroquinone. ***B***, Conjugation of hydroquinone with sulfate. PAPS, 3'-phosphoadenosine 5'-phosphosulfate; PAP, 3'-phosphoadenosine 5'-phosphate. ***C***, Conjugation of hydroquinone with glucuronic acid. UDPGA, uridine diphosphate glucuronic acid; UDP, uridine diphosphate. ***D***, Oxidative stress generated from $O_2^{\bullet -}$. GSH, reduced glutathione; GSSG, oxidized glutathione. Adapted from Powis (10).

Quinones are electrophilic Michael acceptors', whereby they establish adducts with several macromolecules, compromising or modifying their functions as well. The reaction of quinones with nucleophiles, such as proteins or nucleic acids, may form a

hydroquinone adduct, which can be oxidized to a quinone adduct with reactive oxygen species (ROS) formation, or can react with a parent quinone forming the quinone adduct and hydroquinone (**Figure 1.4**) (10). Glutathione-quinone adduct formation may also occur, contributing to reduced glutathione depletion.

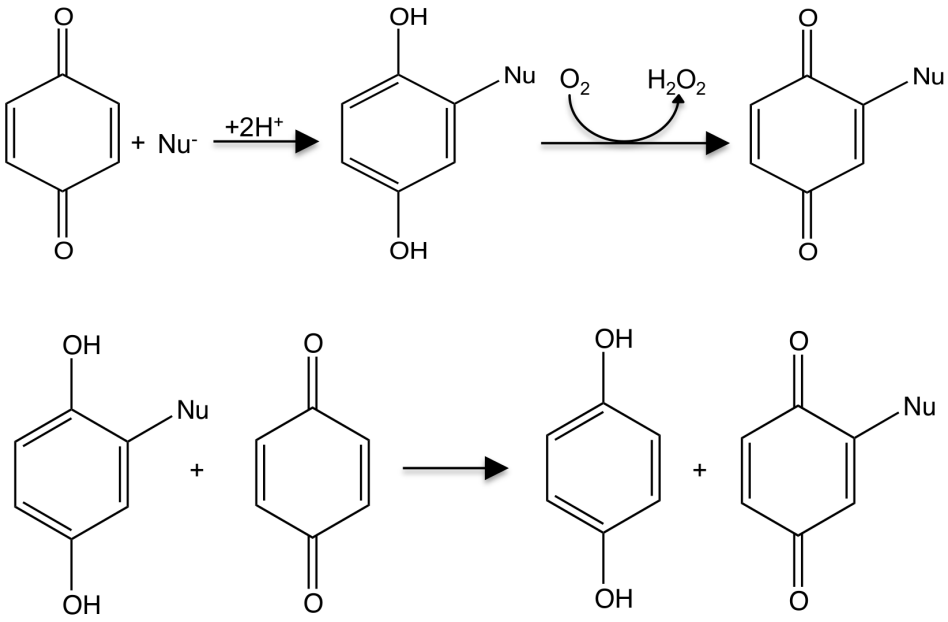

Figure 1.4. Quinone-nucleophile (Nu) adduct formation.

1.1.2. Naphthoquinones

Naphthoquinones are widespread in nature, being produced by plants (7), actinomycetes (16, 17), fungi (18, 19), lichens (20, 21) and algae (22). Regarding plants, the main producing families are Avicenniaceae, Bignoniaceae, Boraginaceae, Droseraceae, Ebenaceae, Juglandaceae, Nepenthaceae and Plumbagnaceae (7). Chemically, naphthoquinones may be present as monomers, dimers or tetramers. The monomeric naphthoquinone is characterized by the presence of a naphthalene skeleton substituted in C1 and C4 (1,4-naphthoquinones) or in C1 and C2 (1,2-naphthoquinones) by two carbonyls (**Figure 1.5**) (7).

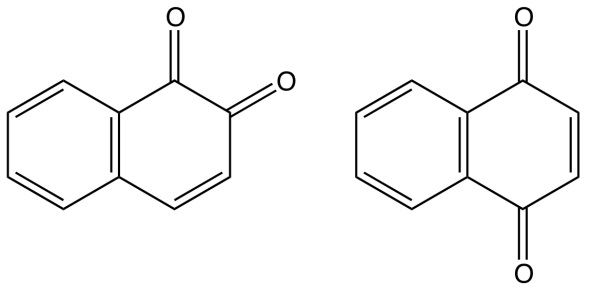

1,2-Naphthoquinone 1,4-Naphthoquinone

Figure 1.5. Basic chemical structure of naphthoquinones.

1.1.2.1. Biological importance

Naphthoquinones are produced by several organisms, possibly for their survival advantage. For example, naphthoquinones constitute a group of vitamins, influence the development of neighbouring living beings, and contribute to attracting pollinators since they are generally coloured (yellow, orange and brown), thus influencing the pigmentation of living beings (7).

Naphthoquinones are also known as allelochemicals (23). Allelopathy is a biological phenomenon by which an organism influences the survival, growth and reproduction of neighbouring organisms through chemical substances. Juglone (5-hydroxy-1,4-naphthoquinone) (**Figure 1.6**), which is a well-known example of allelochemical, may be released to the environment by black walnut (*Juglans nigra* L.), avoiding the development of other species (7, 24). The mechanisms linked to this activity include inhibition of plastoquinone biosynthesis, by inhibition of phenylpyruvate dioxygenase activity (25) and reduction of water reuptake by the roots (26).

Naphthoquinones constitute an important group of vitamins: vitamin K. The vitamin K group is constituted by isoprenoid naphthoquinones, whose core skeleton is menadione (2-methyl-1,4-naphthoquinone) (**Figure 1.6**). Several organisms are able to synthesize vitamin K, such as plants, algae and bacteria, in contrast to mammals that need to obtain it from the diet or symbiotic bacteria living in their gut (7, 27). In mammals, vitamin K is important for coagulation, because it is an essential cofactor for γ-glutamyl carboxylase, an enzyme responsible for the activation of four procoagulant factors (II, VII, IX and X). Additionally, vitamin K is essential to bone tissue homeostasis, through regulation of mineralization and calcium homeostasis (28). Vitamin K's function in the brain is related to sphingolipid metabolism modulation and the discovery of two vitamin K-dependent proteins closely associated with the nervous system [growth arrest-specific 6 (Gas6) and the protein S] (29).

1.1.2.2. *Diospyros* spp. naphthoquinones

Diospyros is an important genus of the Ebenaceae family, with more than 350 species (trees and shrubs) distributed mainly by tropical zones. *Diospyros* is characterized by the synthesis of 1,4-naphthoquinones metabolites, from which non-monomeric naphthoquinones are mainly juglone derivatives (30). Naphthazarin derivatives, such as 2-methylnaphthazarin, and plumbagin derivatives are also found in *Diospyros* species (7, 30-32). Naphthoquinones may be present in several organs, especially in the bark, and they commonly occur in reduced and glycosidic form (7).

Diospyros chamaethamnus Dinter ex Mildbr. is an African species from which little is known. Eight naphthoquinones were identified in its root barks, two of them being isolated in higher amounts: diospyrin and diosquinone (**Figure 1.6**) (31).

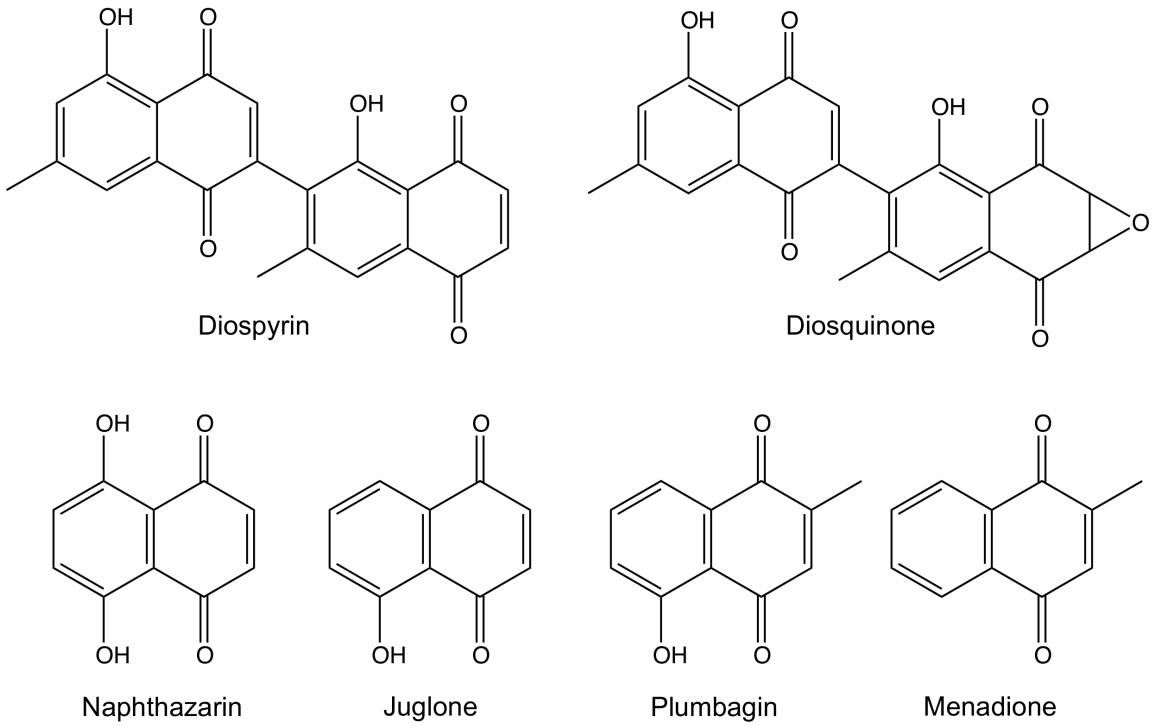

Figure 1.6. Menadione and naphthoquinones that are commonly found in *Diospyros* spp.

1.1.2.3. Pharmacological activities attributed to naphthoquinones

Plants rich in naphthoquinones have been employed in folk medicine for the tentative treatment of several health problems: root extracts of the Chinese medicinal herb

Lithospermum erythrorhizon Siebold & Zucc., which is rich in shikonin/alkannin derivatives (**Figure 1.7**), is used in burns, haemorrhoids, external wounds and dermatitis (33); root extracts of *Plumbago zeylanica* L., rich in plumbagin, is used in Indian medicine as a putative antiatherogenic, cardiotonic, hepatoprotective and neuroprotective agent (34); *Tabebuia impetiginosa* (Mart. ex DC.) Standl extracts were used by native populations of South America in the context of several diseases like cancer, fever and infections (35).

Different naphthoquinones' pharmacological activities were already explored, these being mostly antitumoral and antimicrobial activities. Nevertheless, little is known about naphthoquinones' anti-inflammatory and anti-allergic properties. In the following sections a brief description of the antitumoral and antimicrobial activity of naphthoquinones is presented, because these activities are the most explored concerning naphthoquinones. Additionally, a review of the literature concerning anti-inflammatory and anti-allergic activities of naphthoquinones is also presented, because these were the naphthoquinones' activities studied in this thesis.

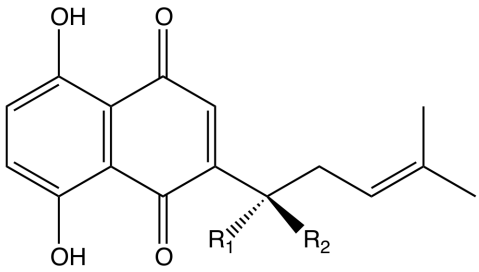

	R_1	R_2
Shikonin	OH	H
Alkannin	H	OH

Figure 1.7. Chemical structure of shikonin and alkannin.

1.1.2.3.1. Antitumoral activity

Antitumoral activity of naphthoquinones has been studied in tumour cell lines from prostate (36), breast (37), ovary (38), colon (39), lungs (40), skin (39), pancreas (41), among others organs. Lapachol and β-lapachone (**Figure 1.8**), extracted from *T. impetiginosa* (also known as red lapacho), were extensively studied concerning antitumoral properties, showing activity against several tumour cell lines (42). Lapachol was even tested in phase I clinical trials, but showed a low oral bioavailability (43).

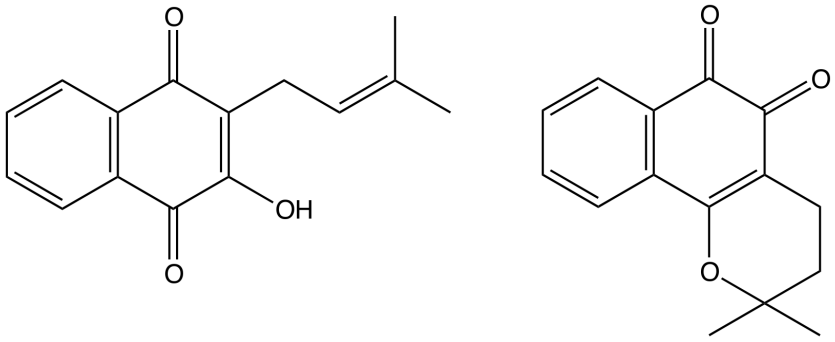

Lapachol β-Lapachone

Figure 1.8. Chemical structures of lapachol and β-lapachone.

The antitumoral activities of naphthoquinones may be explained by several mechanisms: a) intercalation into DNA base pairs through establishment of electrostatic bonds (44); b) inhibition of topoisomerases, which are regulatory enzymes of the DNA overwinding, and thus important to DNA replication (45); c) inhibition of nuclear factor (NF)-κB, which is a transcription factor involved in inflammation and proliferation (46); d) activation by cytochrome P450 reductase, which induces a one-electron reduction of naphthoquinones with the formation of highly reactive semiquinone radical (8); normally, the activity of cytochrome P450 reductase is increased in tumour cells in comparison to normal ones, conferring a selective toxicity of naphthoquinones to cancer cells (47). Naphthoquinones may also potentiate the anti-tumoral activity of other treatments: menadione derivatives and plumbagin induce sensitization to radiotherapy (48, 49); additionally, menadione showed synergic antitumoral effect with methotrexate and with 5-fluorouracil (50, 51).

1.1.2.3.2. Antimicrobial activity

Antimicrobial activity is probably one of the best-studied naphthoquinones' biological properties. Naphthoquinones are active against a wide variety of bacteria [*Clostridium* spp. (52), *Mycobacterium* spp. (53-55), *Neisseria gonorrhoeae* Zopf (55), *Escherichia coli* (Migula) Castellani and Charmers, *Staphylococcus aureus* Rosenbach (56) among others] and fungi [*Candida* spp. (57-59), *Cryptococcus neoformans* (San Felice) Vuill. (60), *Aspergillus* spp., *Fusarium* sp. and *Trychophyton* spp. (61)].

Naphthoquinones are also effective against a wide spectrum of parasites with atovaquone (**Figure 1.9**) being a licensed antiparasitic drug. Atovaquone is a hydroxynaphthoquinone with activity against *Plasmodium* spp., *Pneumocystis jirovecii*

Frenkel (pneumonia) and *Toxoplasma gondii* (Nicolle & Manceaux) (toxoplasmosis). Atovaquone selectively inhibits ubiquinone (UQ) biosynthesis (62) and the mitochondrial complex III of the parasites, through the binding to the ubiquinol oxidation (Q_o) site. Thus, atovaquone interrupts the parasites' electron transport chain (ETC) and pyrimidine synthesis (63, 64), because complex III inhibition by atovaquone avoids regeneration of oxidized ubiquinone (required as electron acceptor of dihydroorotate dehydrogenase), an essential step of *de novo* pyrimidine biosynthesis (65). The inhibition of *de novo* pyrimidine biosynthesis is particularly toxic to malaria parasites, because salvage of pyrimidines in these organisms is minimal (65). Commercially, atovaquone is available alone or in combination with proguanil, an inhibitor of dihydrofolate reductase, which is an essential protein for pyrimidine biosynthesis (63).

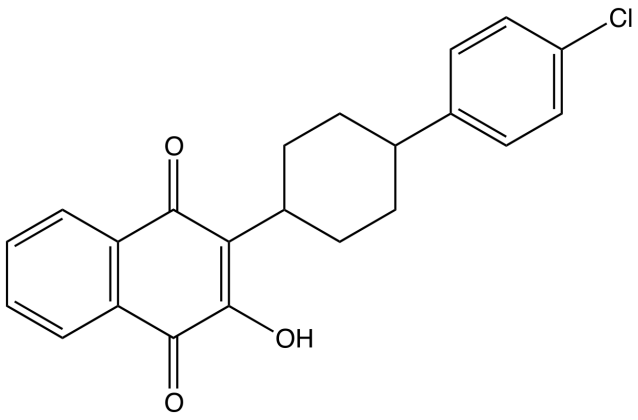

Figure 1.9. Chemical structure of atovaquone.

Beyond *Plasmodium* spp., naphthoquinones have been studied against *Schistosoma mansoni* Sambon (64), *Leishmania donovani* Laveran et Mesnil (65, 66), *Theileria parva* Muguga (67) and *Trypanosoma cruzi* Chagas (68). Naphthoquinones' action mechanisms against trypanosomatids (e.g. *Trypanosoma* spp. and *Leishmania* spp.) have been explored, being related with redox properties of naphthoquinones. Trypanosomatids have a NADPH-dependent flavoprotein disulphide, named trypanothione reductase, which is responsible for maintaining the trypanothione, a molecule similar to glutathione, in the thiol form. The absence of trypanothione reductase in mammalian hosts and the high susceptibility of these parasites to oxidative stress make this enzyme a potential target for new antiparasitic drugs (69, 70). According to 1,4-naphthoquinones redox properties, these compounds constitute "subversive" substrates for trypanothione reductase, avoiding the enzymatic reduction of the enzyme's physiological substrate and subverting the physiological function of the enzyme, which becomes a prooxidant (69, 70).

1.1.2.3.3. Anti-inflammatory activity

β-Lapachone, shikonin and plumbagin are the most studied naphthoquinones as anti-inflammatory compounds and little is known about the other naphthoquinones, explaining the interest in exploring their anti-inflammatory potential.

β-Lapachone induced a reduction in the expression of the inducible cyclooxygenase (COX)-2, decreasing prostaglandin (PG) E_2 synthesis, but without significant changes in COX-1 levels (constitutive enzyme) in a cell system (71). The selective inhibition of inducible enzymes isoforms by β-lapachone was also confirmed for nitric oxide synthase (NOS): β-lapachone reduced inducible nitric oxide synthase (iNOS) expression after lipopolysaccharide (LPS) stimulation of rat alveolar macrophages and aortic rings, without affecting the constitutive isoforms of NOS (endothelial and neuronal) (72). *In vivo*, β-lapachone was efficient in LPS-induced mice lung oedema reduction. This effect was attributed to the inhibition of NF-κB expression, which consequently led to the inhibition iNOS expression (73). NF-κB is a ubiquitous transcription factor involved in cellular proliferation and expression of immunoregulatory genes (74) that will be approached in more detail in section 1.2.1. β-Lapachone suppressed also the development of experimental autoimmune encephalomyelitis in a mouse model, decreasing the expression of interleukin (IL)-12 family cytokines (IL-12, IL-23 and IL-17) (75).

Contrarily to β-lapachone, shikonin is reported to directly inhibit all NOS isoforms (inducible and constitutive) at the same range of concentrations (4-7 μM). Thus, in addition to reducing nitric oxide (NO) production in LPS-stimulated cells, shikonin alone induced a strong inhibition of the aorta relaxation response (76). However, these authors verified that shikonin decreased the NO production in stimulated cells to concentrations lower (< 1 μM) than the ones required to inhibit the enzymes *in vitro,* suggesting that shikonin reduced NO production through other mechanisms without direct enzyme inhibition (76). In fact, several research groups showed that shikonin suppresses extracellular signal-regulated kinase (ERK)1/2 phosphorylation and NF-κB expression (77-79). NF-κB expression inhibition explains the COX-2 and NOS expression decrease (78) and the reduction of tumour necrosis factor (TNF)-α, IL-1β, IL-6 and myeloperoxidase activity in a mouse model of acute pancreatitis (80). Other mechanisms of action, beyond NF-κB inhibition, have been suggested. Shikonin supressed TNF-α transcription independently from inhibition of ERK1/2 phosphorylation or NF-κB activation and, therefore, the effects were attributed to the inhibition of transcription factor IID binding to TATA box, present in TNF-α promotor region (81). Inhibition of proteasome by shikonin was also suggested, given the observed accumulation of inhibitory factor κB (IκB) and

ubiquitinated proteins in a rat primary macrophage culture (82). Shikonin was also previously studied in animal models: shikonin reduced the 12-*O*-tetradecanoylphorbol-13-acetate (TPA)-induced acute ear oedema in mice (78); it ameliorated the macroscopic lesions and cartilage destruction in a murine model of collagen-induced arthritis, with a decrease of pro-inflammatory mediators (TNF-α, IL-12 and IL-6) and an increase of anti-inflammatory cytokines (IL-10 and IL-4) (83); additionally, it suppressed the allergic airway inflammation in a mouse model of asthma (84).

Similarly to β-lapachone and shikonin, plumbagin also inhibits NF-κB activation, through the suppression of IκB kinase (IKK) activation and consequently IκB phosphorylation and degradation and through direct inhibition of p65 binding to DNA (34, 85). The exact mechanism by which plumbagin inhibits IKK activation and the binding of p65 to DNA is not clear; however, some authors suggest that plumbagin interacts directly with critical serine residues of IKK and p65, given its redox properties (34). The interference with the NF-κB pathway is used to explain anti-inflammatory effects observed with plumbagin: plumbagin suppressed the paw oedema induced by carrageenan in rats with a decrease in pro-inflammatory mediators, such as IL-1β, IL-6, TNF-α, iNOS and COX-2 (86); it also inhibited cytokines production by phytohemagglutinin (PHA)-stimulated peripheral blood mononuclear cells (PBMC) (87). Immunossupressive properties of plumbagin have also been reported. Plumbagin inhibited activation, proliferation and the functions of T-cells, inhibiting the entry of concanavalin A-stimulated T cell in S phase of the cell cycle, reducing the expression of early (CD69) and late (CD25) activation markers, as well as reducing the cytokines release in activated T-cells (85). Plumbagin improved the clinical symptoms of experimental autoimmune encephalomyelitis in a mouse model, decreasing interferon (INF)-γ and IL-17 production, through the regulation of Janus kinase (JAK) / Signal transducer and activator of transcription (STAT) signalling pathway (88). Another work explained plumbagin's anti-inflammatory effects with ROS generation, because the inhibition of cytokine production, the ERK mitogen-induced phosphorylation, as well as the inhibition of IκB proteins degradation, were abrogated by thiol antioxidants (89).

Juglone and its 5-*O*-acyl derivatives (conjugation with acetic acid to C22:6 fatty acids) reduced the TPA-induced acute inflammation in mouse ears and decreased the TNF-α production using LPS-stimulated RAW 264.7 macrophages (90).

1.1.2.3.4. Anti-allergic activity

Little information exists about the anti-allergic properties of naphthoquinones. Menadione avoided the antigen-stimulated RBL-2H3 cells (basophilic cell line) degranulation through inhibition of the cellular calcium influx. Furthermore, menadione inhibited 5-lipoxygenase (5-LO) translocation from the cytoplasm to the nuclear membrane [an important mechanism to leukotrienes (LT) production] and no effect was observed in phosphorylation of some important 5-LO regulators (mitogen-activated protein (MAP), ERK or p38). As the inhibition of LT production induced by menadione was reverted by antioxidants, ROS generated by menadione were considered to be important to its activity (91). Naphthoquinones extracted from *Rhinacanthus nasutus* Kuertz leaves (rhinacanthin-C, -D and –N) also reduced the degranulation and the release of TNF-α by IgE/antigen-stimulated RBL-2H3 cells (92). Chloro-1,4-naphthoquinones derivatives also decreased the degranulation of mast cells (93).

Anti-allergic properties of juglone were related to its capacity to inhibit the peptidyl-prolyl *cis-trans* isomerase NIMA-interacting 1 (PIN1), which regulates eosinophil differentiation (94). Juglone treatment of allergen-sensitized rats induced an improvement of allergic pathology, with reduction of eosinophilia and reduction of granulocyte-macrophage colony-stimulating factor (GM-CSF) and IL-5 expression, without alterations in the other leukocytes and in the cytokines PIN1-independent (95).

The known anti-inflammatory and anti-allergic properties of naphthoquinones studied in this thesis are resumed in **Table 1.1**.

Table 1.1. Naphthoquinones studied in this thesis and known activities and targets concerning anti-inflammatory and anti-allergic properties.

Naphthoquinones	Target	Activity	References
Juglone	PIN1	Inflammatory mediators reduction; Eosinophilia reduction	(95)
Menadione	5-LO	Leukotrienes synthesis reduction	(91)
Plumbagin	NF-κB JAK/STAT ERK1/2	Inflammatory mediators reduction; COX-2 and iNOS expression reduction	(34, 85, 86, 88, 89)

1.1.3. Benzoquinones

Benzoquinones are ubiquitous compounds that present a unique aromatic ring with two carbonyl groups. The most important are the prenylated benzoquinones, which vary in the length and in the saturation degree of the side chain, as well as in the

presence of additional groups (96). Examples of prenylated benzoquinones groups are plastoquinones, rhodoquinones and ubiquinones (**Figure 1.10**) (96). Due to their importance for energy production, ubiquinones (UQ) are approached in detail.

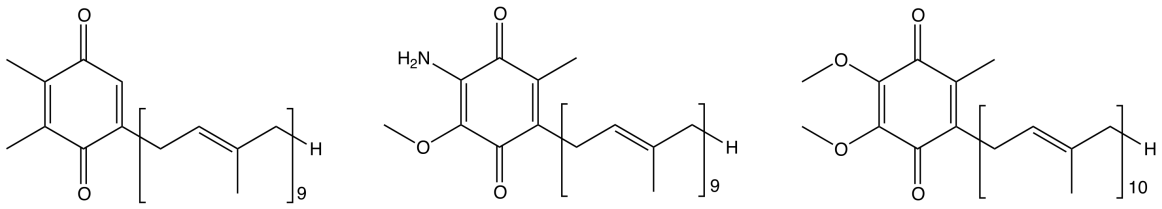

Figure 1.10. Chemical structures of prenylated benzoquinones.

1.1.3.1. Ubiquinones

UQ are prenylated benzoquinones (2,3-dimethoxy-5-methyl-6-polyprenyl-1,4-benzoquinone) in which the number of isoprenoid units of the side chain may vary between 6 and 10 units long (96, 97). Some organisms have more than one type of UQ, despite one of them being the most abundant (96). UQ_{10} (**Figure 1.10**) is the most abundant UQ in humans, but UQ_9 is also present. In contrast, in rodents there is a prevalence of UQ_9 (96). Ubiquinones are found in prokaryotic and eukaryotic cells, being components of all membranes (98). The biosynthetic pathway of ubiquinones is highly conserved, being mainly constituted by three metabolic sequences (**Figure 1.11**). One is the synthesis of *p*-hydroxybenzoate, which can be formed by shikimate pathway or directly from tyrosine (and sometimes from phenylalanine) mainly in higher eukaryotes. Another is the synthesis of the polyprenyl side chain by the mevalonate pathway: from acetyl-coenzyme A (acetyl-CoA), a hydrophobic polyisoprenoid side chain with 6 to 10 isoprene units is obtained; regarding UQ_{10}, acetylCoA is transformed in farnesyl-pyrophosphate (PP), which is also a precursor of cholesterol and of dolichol, and then in decaprenyl-PP. Afterwards, the condensation of *p*-hydroxybenzoate with the polyprenyl side chain, catalyzed by *p*-hydroxybenzoate prenyltransferases, occurs (98-100). Following condensation, the benzoquinone ring may undergo several modifications, such as *C*-hydroxylation, decarboxylation, *O*-methylation and *C*-methylation (98). The exact subcellular location of the several steps involved in UQ biosynthesis remains uncertain (101). Some authors suggest that it begins in the endoplasmic reticulum and ends in the Golgi apparatus, from where UQ is transported to other cellular compartments (99, 102, 103). However, other authors consider that UQ biosynthesis localization may be more

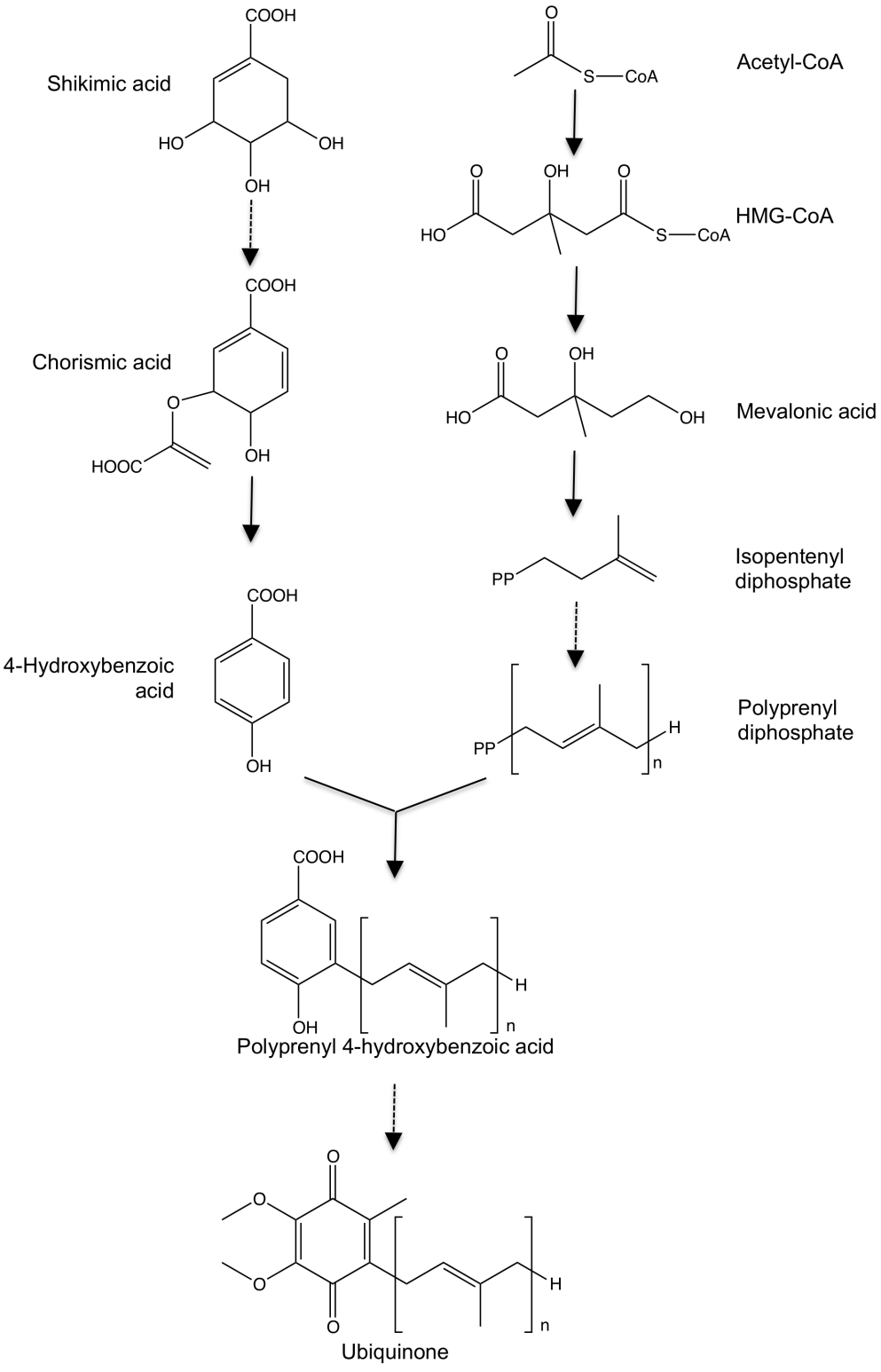

Figure 1.11. Ubiquinone's biosynthesis pathway. HMG-CoA, 3-hydroxy-3-methylglutaryl-coenzyme A.

complex and probably the same reaction may be performed in different cell compartments (104). For example, some enzymes are present in several cell compartments: farnesyl-PP synthase is present in cytoplasm, mitochondria and peroxisomes (105, 106), while *trans*-

prenyltransferase was found in mitochondria, endoplasmic reticulum and peroxisomes (106-108).

Among the most important UQ cellular functions are those related with energy production. The UQ functions are: a) electron carrier in several electron transport chains - mitochondrial respiratory chain, extramitochondrial electron transport (plasma membranes and lysosomes), photosynthetic and in chemosynthetic electron chain, where reduced inorganic compounds supply electrons (96, 104); b) stabilization of mitochondrial permeability transition pore (mPTP) in the closed conformation (109); c) activation of mitochondrial uncoupling proteins (110); d) regulation of physicochemical properties of the membranes (104); e) lipid-soluble antioxidant (111); f) regulation of NAD^+/NADH ratio - the majority of plasma membranes contains a UQ-dependent NADH oxidase (112); g) anti-inflammatory - regulation of NF-κB expression (113); h) prevention of endothelial dysfunction - stimulation of NO release (114).

1.1.3.2. Ubiquinone analogues

Modifications of the alkyl chain of physiological UQ have been made in order to improve their biological effects and physicochemical properties (115). UQ analogues are thus mainly characterized by lower lipophilicity than endogenous UQ. In this section, the main groups of UQ analogues are described: the mitoQ group *vs*. the idebenone and decylubiquinone group.

Quinones containing a UQ moiety and a lipophilic alkyl chain with variable length, terminating in a lipophilic cation (methyltriphenylphosphonium), constitute the mitoQ group (**Figure 1.12**). The lipophilic cation allows the accumulation of these UQ analogues in the mitochondria, due to the negatively charged environment characteristic of an established mitochondrial membrane potential ($\Delta\psi_m$) (116). The mitoQ analogues series has been less explored than idebenone and decylubiquinone, probably because they cannot act as electron carriers in ETC, since they are not oxidized by complex III. However, mitoQ analogues are efficient antioxidants against lipid peroxidation, $ONOO^-$ and $O_2^{\bullet-}$ (117).

Both idebenone and decylubiquinone have an UQ head group linked to a ten-carbon alkyl tail, differing only in the end of the tail: idebenone has a hydroxyl group, while decylubiquinone presents a methyl group (**Figure 1.12**) (117). Thus far, idebenone has been more extensively studied than decylubiquinone.

Idebenone rescued the toxicity induced by digitonin, which consists on the solubilisation of mitochondrial membranes, impairing the mitochondrial ETC (118). Furthermore, despite the oxidized form of idebenone inhibiting complex I (119), idedebone

protected a rodent RGC cell line against complex I dysfunction (120). These effects of idebenone in mitochondrial activity increased the interest in idebenone as potential drug for mitochondrial disorders. In fact, idebenone was initially available on the Japanese market as a drug to ameliorate age-dependent brain functions impairment (101).

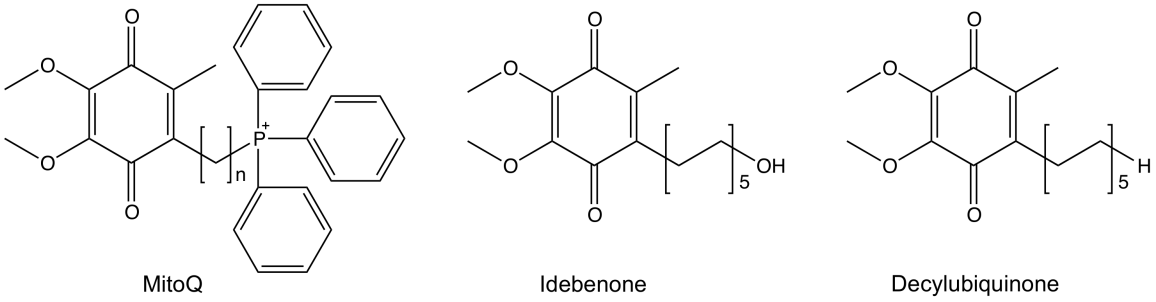

Figure 1.12. Chemical structures of ubiquinone analogues.

In contrast to UQ_{10}, idebenone is rapidly absorbed by humans when taken orally (121). While there are studies suggesting that idebenone does not rescue UQ_{10} deficiencies (122), there are also reports of its successfull use in the treatment of other pathologies. Several studies in animal models of Friedrich's ataxia (FRDA) were made to test the therapeutic potential of idebenone in this pathology: idebenone revealed to be a promising drug, ameliorating the pathological condition (123, 124). FRDA is a hereditary disease caused by a deficiency in frataxin, a protein involved in mitochondrial iron content regulation, whereby in FRDA there is an increase of oxidative stress that compromises several mitochondrial proteins with iron-sulphur clusters, such as complexes I, II and III (125). Administration of idebenone during 4-9 months to FRDA patients ameliorated cardiomyopathy, with substantial decrease of myocardial hypertrophy (125). However, higher doses than needed to improve cardiac function were required to improve neurological function of FRDA patients (126). Several other clinical trials showed the beneficial effects of idebenone in FRDA (127, 128). Idebenone avoided stroke-like episodes and improved neurological symptoms in a patient with mitochondrial encephalomyopathy, lactic acidosis and stroke-like episodes (MELAS) (129), and also improved colour vision in patients with Leber's hereditary optic neuropathy (LHON) (130). Idebenone was reported beneficial in several other diseases, such as Leigh syndrome, Duchenne muscular dystrophy, OPA-1 dominant optic atrophy, as well as in Alzheimer's disease (AD) and Huntington's disease (131-134).

Regarding decylubiquinone, it was reported to improve mitochondrial function in synaptosomes, increasing complex I/II and complex II/III activities (135). Additionally,

decylubiquinone rescued respiration of isolated muscle mitochondria from a patient with UQ_{10} deficiency (136) and restored respiration in yeast mitochondria lacking UQ (117).

Some authors attribute the effects of UQ analogues to their antioxidant properties (125), but the possibility of working as electron carriers has been studied (9, 119). A balance between hydrophilicity and lipophilicity is important so that UQ analogues rescue the adenosine-5'-triphosphate (ATP) levels, as well as for their antioxidant activity: hydrophilicity is essential to cytoplasmic reduction by NQO1, while lipophilicity determines membrane access (137). Thus, an advantage of idebenone and decylubiquinone is the ability to cross membranes that allows the UQ analogues to be either in the cytosol or in the mitochondria. Short-chain quinones can be reduced in the cytosol by NQO1 and their respective hydroquinones may be shuttled into mitochondria, transferring the electrons to complex III, passing any dysfunction of mitochondrial dehydrogenases (9). In contrast, UQ_{10} does not have polarity properties to go to cytosol and be reduced by NQO1, explaining the results obtained by Haefeli and collaborators that observed a rescue of ATP levels by idebenone (and not by UQ_{10}), in a cell system, dependent on both NQO1 and mitochondrial complex III after acute inhibition of complex I (9). Furthermore, both idebenone and decylubiquinone are good substrates of complex III (117, 119). Thus, the side chain of UQ analogues has an important role in determining the activity of the compound: decylubiquinone has better antioxidant, cytoprotective properties, and better ability to maintain $\Delta\psi_m$ than idebenone in CEM leukaemia cells (115); however, idebenone was more effective in increasing ATP levels in rotenone-treated cells than decylubiquinone (137).

UQ analogues have other biological effects beyond antioxidant and respiratory chain improvement: idebenone inhibited COX enzymes, showing anti-inflammatory activity (138), and inhibited the respiration of *Helicobacter pylori* (Marshall et al.) Goodwin et al., having antibacterial activity (139).

1.2. An overview of the immune system

The main function of the immune system is to protect the organism against potential aggressors, normally a pathogenic infectious agent. Mammalian immune system is divided in innate and acquired immunity (140, 141). The innate immune response is the first line of host defence against an infectious agent, discriminating between self and foreign molecules (140). Pathogens are recognized by conserved molecular structures essential to microorganism survival, named pathogen-associated molecular patterns (PAMP), which include microbial structural components, proteins or nucleic acids that may

be shared by different classes of microorganisms (140, 142). PAMP are recognized by pattern-recognition receptors (PRR) that are constitutively expressed by the host (140). Depending on the PRR group, PRR binding may induce endocytosis, enhancing antigen-presentation, induce opsonisation or even activate multiple signalling pathways, such as NF-κB, mitogen-activated protein kinases (MAPK) and interferon regulatory factors (IRF), controlling the expression of pro-inflammatory cytokines (142, 143). Thus, PRR initiate the innate immunity process: opsonisation, phagocytosis, complement and pro-inflammatory signalling pathways activation and apoptosis (141). Several classes of PRR are known, such as retinoic acid-inducible gene I-like receptors, nucleotide oligomerization domain-like receptors and Toll-like receptors (TLR), the latter being the most explored (142). The innate immune response contributes to the initiation of adaptive immunity, characterized by immunological memory due to generation of pathogen antigen-specific B and T lymphocytes (141, 144). Adaptive immunity has two stages: a) antigen presentation and recognition specific T or B cells, leading to cell priming, activation and differentiation; this process normally occurs within lymphoid tissues; b) T cells leave the lymphoid tissue and move towards the disease site, while activated B cells release antibodies into blood and tissue fluids (143). Several pathological conditions are related with the immune system, more commonly exaggerated immunological responses, such as inflammation and allergy.

1.2.1. Inflammation

The inflammatory process is an essential response to tissue injury induced by invading pathogens (145). However, chronic inflammation is a persistent phenomenon that induces extensive tissue damage (146). Furthermore, inflammation is a pathophysiological condition associated with many other diseases, such as atherosclerosis (147) and cancer (145).

During an inflammatory process, adhesion molecule activation and chemotactic cytokine release activate leukocyte migration from blood to damaged tissues (145). This process initiates with recognition of a PAMP such as LPS. LPS, the main outer membrane component of Gram-negative bacteria, is a glycolipid composed by a hydrophilic polysaccharide and a ‘lipid A’ hydrophobic domain (148). LPS binds TLR4 and activates NF-κB transcription and the MAPK cascade (**Figure 1.13**) (74, 149). MAPK are serine/threonine protein kinases regulating cell proliferation, differentiation and survival genes (150). ERK1/2, *c*-Jun N-terminal kinase (JNK) and p38 MAP kinase (151) are the major members of the MAPK family, representing three different signalling cascades that transduce a broad range of extracellular stimuli. All MAPK are activated through

phosphorylation by specific MAPK kinases (MKK or MEK) (150), inducing phosphorylation and activation of several other cytoplasmically- or nuclear-located transcription factors (149).

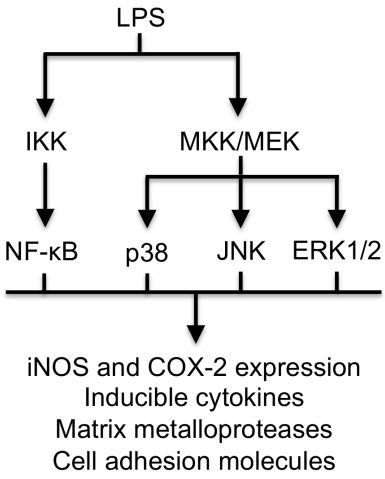

Figure 1.13. Main signalling pathways involved in LPS inflammatory response.

NF-κB is a family of seven structurally related transcription factor subunits, including proteins with a conserved amino-terminal region with dimerization, nuclease-localization and DNA binding domains. The most frequent form of NF-κB comprises a p65 subunit heterodimer associated with either a p50 or a p52 subunit (74, 152). NF-κB proteins interact with cytoplasmic anchoring-domain containing proteins, the IκB proteins (74, 153). IκB proteins retain NF-κB in the cytoplasm by masking the nuclear-localization signal (NLS), and with some IκB proteins containing a nuclear-export signal (NES) (74). NF-κB activation is most frequently triggered by IκB degradation (74). IKK-mediated phosphorylation of IκB proteins on specific serine residues induces their polyubiquitination and 26S proteasome-mediated degradation (74, 153). After IκB protein degradation, NF-κB may translocate to the nucleus and activate κB-dependent gene transcription (74). NF-κB activity may also be regulated by phosphorylation and acetylation of NF-κB proteins (74). NF-κB regulates the expression of more than 150 genes related with cell proliferation and inflammation (inducible cytokines, cell adhesion molecules, matrix metalloproteases, COX-2, iNOS and other vasoactive mediators), being important to innate and adaptive immune responses (74, 152, 153). COX-2 and iNOS are known inducible enzymes essential to inflammation and thus relevant therapeutic targets. While iNOS generates NO, COX are key enzymes for prostanoid (prostaglandins and tromboxans) synthesis from arachidonic acid (154). Prostanoids are essential for inflammation, platelet aggregation and vasoconstriction/relaxation (155). In addition to prostanoids synthesis during

inflammation, COX-2 is also constitutively expressed in the brain, kidney, pancreas, intestine and blood vessels (156).

NF-κB is highly active in inflammatory disorders such as rheumatoid arthritis or asthma, and in tumour tissues (74, 157). Thus, several anti-inflammatory drugs act by NF-κB inhibition, such as the glucocorticoid dexamethasone (158). Non-steroidal anti-inflammatory drugs (NSAID) are the most widely-used anti-inflammatory drugs. Currently available NSAID, however, are associated with long-term gastrointestinal and renal side-effects, stressing the need for new anti-inflammatory drugs with improved safety profile (154).

RAW 264.7 cells are murine macrophages frequently used to test anti-inflammatory compounds. LPS is frequently used to induce an inflammatory response in these cells (159, 160), but other agents such as INF-γ are also useful for this purpose (161). In response to these stimuli, RAW 264.7 cells produce NO, TNF-α, interleukins, prostaglandins, and increase COX-2 and iNOS expression (77, 159, 162, 163). RAW 264.7 cells have also been used to study TLR role in autophagy (164) and transmembrane transport of organic molecules (165).

1.2.2. Alllergy

Inflammation and allergy are increasingly recognized and interconnected pathologies, thus prompting the designation of “allergic inflammation” (166). Allergic responses are associated with exposure to otherwise innocuous substances present in the environment, named allergens. Thus, the therapeutic challenges are to induce immunological tolerance to allergens and to manipulate immune responses avoiding allergy development (166). However, these are mostly unmet challenges, with current anti-allergic therapies being focused on symptomatic management.

Allergic disorders (allergic rhinitis, hay fever, eczema or asthma) affect about 25% of people in developed countries and its prevalence is increasing (167). The “hygiene hypothesis” associates the increasing number of allergic disorders with reduced microorganism exposure due to improved hygiene, vaccination and antibiotics. Contact with microorganisms promotes normal development of immune responses by T-helper (Th) 1 cells, associated to autoimmune diseases, bacterial and viral infections. In contrast, in the absence of microorganism contact the immune system responds inappropriately to innocuous substances, with Th2 cells prevalence associated to helminthic infections and allergic disorders (166-168). Thus, the “hygiene hypothesis” helps explain the lower prevalence of allergic diseases in developing countries and rural *vs*. urban areas of the

same country (167). Furthermore, there is a genetic predisposition to allergic disorders: in contact with an allergen non-atopic adults produce allergen-specific IgG antibodies and tipically modest Th1 cell proliferation; atopic individuals, however, present exaggerated Th2 cell allergen-specific IgE response (169).

Allergic responses may be IgE- or non-IgE-mediated, i.e., mediated by allergen-specific lymphocytes or IgG antibodies. However, IgE-mediated reactions are the most prevalent (170). The first step in allergic reaction is the sensitization process, where the allergen may elicit a Th2 cell response, in which IL-4, IL-13 and the binding of CD40 on B cells induce IgE production, by promoting immunoglobulin class-switch recombination in B cells (166, 171) (**Figure 1.14**). Allergen binding to high-affinity IgE receptor (FcεRI) complex induces calcium influx, mast-cell degranulation, and synthesis of lipid mediators. Cytokines and chemokines released in this early phase initiate the late phase with recruitment and activation of inflammatory cells (172).

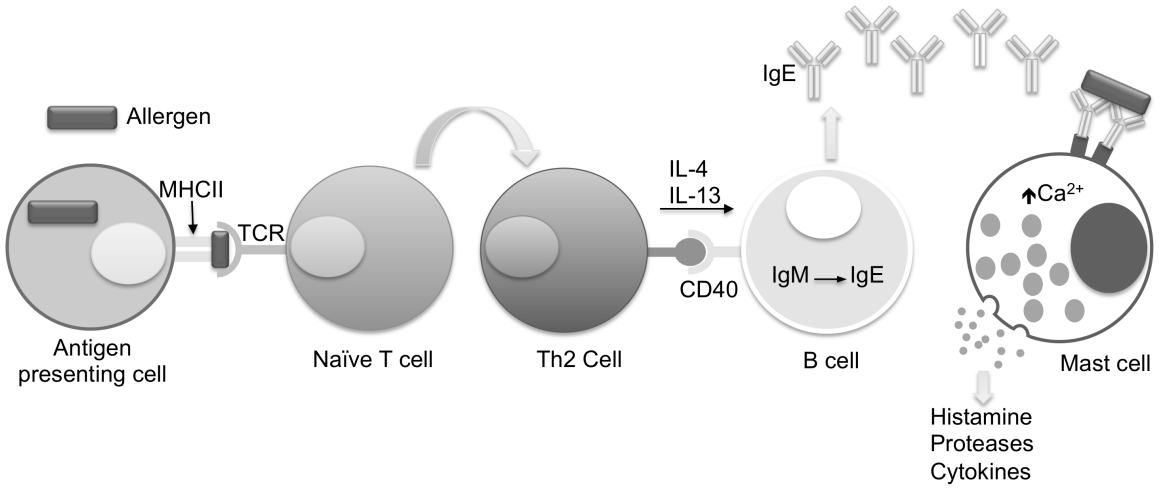

Figure 1.14. IgE-mediated allergic response. MHCII, major histocompatibility complex class II; TCR, T-cell receptor.

Mast cells are present in skin and mucosae, participating in inflammation and allergy, and being considered the major effectors of IgE-associated reactions (173, 174). Mast cells can partially or totally degranulate upon several factors: immune mechanisms (IgE-dependent or IgE-independent); endogenous mediators (tissues proteases or proteins derived from eosinophils and neutrophils); chemical substances (toxins and proteases) (173, 174). Mast cell granules contain several inflammatory mediators, such as chemotactic factors, histamine, proteoglycans (heparin), serotonin and proteases (tryptase, chymase, peroxidase, carboxidase or β-glucosidase) (171, 173, 174). Proteases are major mast cell products that degrade extracellular matrix proteins in defence against pathogens. For example, β-triptase is the major constituent of human

mast cell secretory granules (175). Histamine is a hallmark of allergic reaction that increases vascular permeability (176). Furthermore, mast cell activation increases calcium influx and induces synthesis of secondary mediators whose release pathophysiologically changes several organs: arachidonic acid metabolism derivatives (PG and LT) and other pro-inflammatory mediators [platelet activating factor (PAF), GM-CSF and TNF-α] (171, 173, 174).

Leukotrienes are synthesised from arachidonic acid released from the nuclear membrane by phospholipase A_2 (PLA_2) and converted in 5(*S*)-hydroperoxy-6-*trans*-8,11,14-*cis*-eicosatetraenoic acid (5-HPETE) by 5-LO (177). 5-HPETE is not stable and may be reduced by peroxidases to 5-hydroxyeicosatetraenoic acid (5-HETE) or converted into leukotrienes. The first leukotriene, LTA_4, has a labile epoxide intermediate, being metabolised into LTB_4 or LTC_4 (178, 179). LTB_4 contrasts with other leukotrienes by lacking cysteine. LTC_4 and LTD_4 induce smooth muscle spasms, molecular adhesion, venopermeability and airway mucus secretion (178).

Treatment of allergic disorders includes three main topics: environmental control and allergen avoidance, pharmacotherapy and immunotherapy. The pharmacotherapy approach includes corticosteroids, antihistamines, leukotrienes antagonists, β_2-adrenoreceptor agonists and α-adrenoreceptor agonists. Current pharmacotherapy, however, ameliorates symptoms only. The allergen-specific immunotherapy might be efficient to reduce the prevalence of allergic disorders by inducing immunological tolerance and decreasing allergen-specific IgE (180).

RBL-2H3 cells are immortalized basophils used to model allergic inflammation. Basophils are granulocytes with some similarities to mast cells: FcεRI and Th2 cytokine expression, and mediator release (171). The calcium ionophore A23187 or IgE/antigen are known degranulation inducers in RBL-2H3 cells (181).

1.3. Neurodegenerative disorders

1.3.1. Mitochondrial function – electron transport chain

Mitochondria are fundamental organelles for calcium homeostasis (182), amino acid and steroids biosynthesis (183, 184), fatty acid β-oxidation (185), iron-sulphur cluster biogenesis (186), apoptotic signalling (187), but primarily known for its role in energy production in the form of ATP (184, 188). Distinguishing mitochondrial features are the double membrane and the mitochondrial DNA (mDNA). Human mDNA is maternally

inherited and has been completely sequenced (189): it has only 37 genes, encoding 13 polypeptides of the ETC, 22 transfer RNAs (tRNA) and 2 ribossomal RNAs (rRNA) (12S and 16S) (189, 190). Mitochondria depend on nuclear DNA (nDNA) for its mDNA replication, repair, transcription and translation (191), and also for the synthesis of the overwhelming majority of mitochondrial components.

The ETC is located in the inner mitochondrial membrane (IMM), being responsible for the majority of ATP production of most cells. The ETC includes both nDNA- and mDNA-encoded proteins (190). The main ETC components are four large protein complexes (complexes I, II, III and IV) with ubiquinone between complexes I/II and III and cytochrome *c* between complexes III and IV (**Figure 1.15**) (192). The supercomplex model considers that mitochondrial complexes organize into supramolecular complexes (193). In the ETC, electrons from donor compounds are transferred through several protein complexes towards a more positive oxidative potential, allowing proton pumping from the matrix to the inter membrane space (IMS), establishing a proton gradient and a negatively charged membrane potential towards the matrix side. The final electron acceptor is molecular oxygen (O_2) (**Figure 1.15**) (192, 194). The proton gradient associated to electric potential across the IMM constitutes the proton-motive force, which is important to generate energy and to import proteins and calcium to the mitochondria (195, 196). The UQ moiety may accept two electrons and two protons, being reduced to ubiquinol (UQH_2), transferring electrons from several dehydrogenases to the mitochondrial complex III (also known as ubiquinol-cytochrome *c* oxidoreductase or bc_1 complex). The most common electron donors are NADH and succinate formed during glycolysis, fatty acid oxidation and the Krebs cycle (192, 194). Complex I (also known as NADH:ubiquinone oxidoreductase or NADH dehydrogenase) constitutes the main route of electron entry in the ETC. It allows the transference of electrons from NADH to UQ and then to complex III. Complex I may be selectively inhibited by rotenone, which is highly lipophilic and crosses the blood brain barrier. Rotenone binds the ubiquinone-binding site, preventing electron flow from complex I to ubiquinone and thus to complex III (191). Complex II (also known as succinate:ubiquinone oxidoreductase or succinate dehydrogenase) participates in both Krebs cycle and the ETC, catalyzing succinate oxidation to fumarate and, consequently, ubiquinone reduction. NADH yields more ATP than succinate partly because complex II does not induce proton pumping (**Figure 1.15**) (192). Once reduced, UQ binds the outer UQ oxidation site (Q_o; inhibited by myxothiazol) (197) and transfers one electron to the Rieske iron-sulphur (FeS) protein, and then to cytochrome c_1 (C_1) within complex III and posteriorly to cytochrome *c* (Cyt *C*). Consequently, UQ is transiently converted into semiubiquinone and then into oxidized UQ, due to loss of the second electron to the UQ reduction (Q_i) site *via* two cytochrome *b*

hemes (b_L and b_H). Antimycin A, which is also a complex III inhibitor, binds to the inner Q_i site, increasing $O_2^{\bullet-}$ generation (192, 198). At the Q_i site, an UQ is again reduced into ubiquinol, whereby one UQ reduction at the Q_i site is linked with two ubiquinol oxidations at the Q_o site (**Figure 1.15**). However, the two electrons from the ubiquinol at the Q_o site can also be directly transferred to the cytochrome *c* instead of going to the Q_i site, because in each Q-cycle two electrons are transferred from ubiquinol to two molecules of cytochrome *c* (192). Some authors have proposed that three UQ molecules bind to complex III: one binds at the Q_i site, and two molecules bind at the Q_o site (199). Lastly, complex IV, also known as cytochrome *c* oxidase, receives four electrons from four cytochrome *c* molecules and four protons, transfering them to one O_2 molecule, generating two water molecules (**Figure 1.15**) (192).

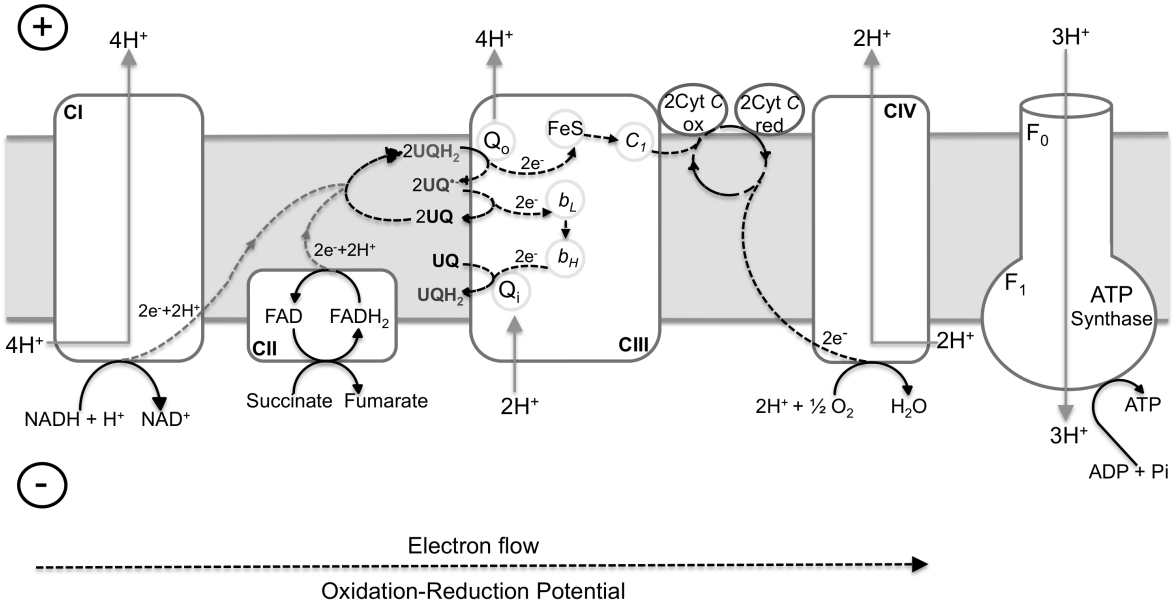

Figure 1.15. Mitochondrial respiratory chain. FAD, flavin adenine dinucleotide oxidized form; $FADH_2$, flavin adenine dinucleotide reduced form;

ATP synthase contains two domains: F_1 with the catalytic site for ATP synthesis from adenosine-5'-diphosphate (ADP) and phosphate (Pi), being localized in the matrix side; and F_o with the proton channel across the IMM (**Figure 1.15**) (200). ATP is exchanged with cytosolic ADP by inner-membrane adenine nucleotide translocators (195). ATP synthase is inhibited by oligomycin that putatively binds to F_o 9 and 6 subunits (200). Mitochondria may reverse ATP synthase, consuming ATP to maintain the $\Delta\psi_m$. Proton leak or mitochondrial uncoupling may be induced by protonophores [such as, carbonyl cyanide 4-(trifluoromethoxy)phenylhydrazone (FCCP)] or uncoupling proteins (194).

In addition to complex I and II, several other dehydrogenases may supply the ETC with electrons through UQ reduction: glycerol-3-phospate dehydrogenase (enzyme of the IMM's outer surface involved in lipid metabolism and glycolysis), electron transfer flavoprotein dehydrogenase (enzyme present in the IMM's matrix surface, mainly involved in fatty acids oxidation) and dihydroorotate dehydrogenase (enzyme of the IMM's outer surface, responsible for the dihydroorotate oxidation into orotate, a step of *de novo* pyrimidine biosynthesis). Other alternative dehydrogenases are located in both sides of IMM of plants, bacteria and fungi, catalyzing the NAD(P)H oxidation and the UQ reduction. The major differences of these complex I alternative dehydrogenases in relation to complex I are their rotenone insensitivity and lack of proton pumping capability (97). Similarly, other ubiquinol oxidases alternative to complex III are present in plants and fungi, however complex III appears to be the only ubiquinol-oxidase in mammals (201).

Mitochondria are an important source of ROS and possess antioxidant defences such as superoxide dismutase, catalase and glutathione peroxidase (198, 202). Some authors suggest mitochondria as the major ROS source of the cell; however, Brown and Borutaite consider that this may not be true due to the existence of other ROS sources, such as lysosomes (203). In fact, under normal physiological conditions, ROS are formed at relatively low levels, being neutralized by mitochondrial antioxidants (204). Complexes I and III are the main sources of ROS in a mitochondrion (198).

1.3.2. Mitochondrial disorders

Mitochondrial dysfunction disorders may have as primary cause mutations in mDNA (MELAS or LHON) or nDNA (Charcot-Marie Tooth neuropathy type 2A or Leigh syndrome), but may also be acquired as a secondary event in disease pathogenesis (AD or PD) (205). mDNA is particularly susceptible to mutations, possibly due to less efficient DNA repair mechanisms and the absence of protective histones. Additionally, proximity to the ETC may favour mDNA damage by ROS (196). Regarding acquired mitochondrial dysfunction, the most important risk factor is ageing (206). With ageing, mitochondria tend to decrease in number, exhibiting cristae abnormalities, and decreased ETC activity (207). These alterations may result of accumulated mDNA mutations and oxidative damage. Ageing also down-regulates genes associated with synaptic plasticity, vesicular transport and mitochondrial function (206, 208).

Mitochondrial dysfunction primarily impair organs with high-energy demand (195), such as brain, muscle and heart. These organs have a high density of mitochondria and

most energy is provided by oxidative phosphorylation (209, 210). Symptomatically, mitochondrial disorders may affect either single or, most frequently, several organs (205).

No effective treatment exists for mitochondrial dysfunctions (205, 211, 212), but some metabolic approaches may provide modest improvement in patients' life quality: UQ_{10} and its analogues, thiamine, uridine, dichloroacetate, L-arginine, antioxidants, mPTP modulators (cyclosporin A) and regulation of mitochondrial biogenesis and turnover [caloric restriction, Sirt1 agonists, activators of peroxisome proliferator-activated receptor (PPAR)/ PPAR-γ coactivator 1α (PGC-1α), phosphoinositide 3-kinase antagonists and agonists] (195).

1.3.2.1. Parkinson's disease

Parkinson's disease (PD) is the most frequent movement disorder and the second most common neurodegenerative disorder (213). PD presents motor (bradykinesia, hypokinesia, resting tremor, gait difficult, postural instability and rigidity) and non-motor symptoms (cognitive impairment, depression and sleep disturbances) (196, 213). Biochemically, PD exhibits progressive loss of *substantia nigra* dopaminergic neurons, dopamine deficiency in the striatum, and cytoplasmic protein aggregates mainly composed by α-synuclein (α-syn), ubiquitin and molecular chaperones (Lewy bodies) (188, 196, 213).

Sporadic PD likely combines genetic and environmental factors. Industrialization, rural environment, plant derived-toxins, pesticide exposure, bacterial and viral infection and ageing, have all been associated with sporadic PD (214). Ageing is the most important risk factor (196). 10% of PD cases have a genetic cause (196). Such familial variants are characterized by earlier onset of the symptoms, otherwise similar to sporadic PD (215).

Mitochondrial dysfunction is associated with PD's pathophysiology, being proposed to occur before the onset of the symptoms (204, 213, 216). Moreover, mitochondrial complex I is tipically impaired in PD patients. Deficient complex I activity was reported in dopaminergic neurons, in the frontal cortex, and in peripheral tissues (e.g. platelets and muscle), thus suggesting global complex I impairment in PD (217-221). Deficient complex III in lymphocytes and platelets was also reported in PD patients (217, 222). Furthermore, mutations in several genes encoding mitochondrial proteins or proteins implicated in mitochondrial function have been linked with familial PD: e.g. α-syn (223), parkin (224), PTEN-induced putative kinase 1 (PINK1) (225) and leucine-rich repeat kinase 2 (LRRK2) (226). Parkin contains an ubiquitin E3 ligase domain and can have both cytosolic and mitochondrial localization. Parkin is proposed to have a crucial role in

mitochondrial turnover by mitophagy and biogenesis (224, 227, 228). The PINK1/Parkin pathway promotes mitochondrial fission (229) and controls motility (230). Dysfunctional PINK1/Parkin pathway associates with reduced proteasomal activity in PD *substantia nigra* (231), favoring accumulation and aggregation of potential cytotoxic proteins such as α-syn (232). α-Syn may directly bind the proteasome inhibiting its ubiquitin-dependent function (233). Significantly, proteosomal inhibitors (e.g. lactacystin) are known to induce neurodegeneration (234).

α-Syn is expressed at high levels in the brain, localizing mainly at neuronal synaptic terminals (235). α-Syn inhibits mitochondrial fusion independently from the PINK1/Pakin pathway (236). Mutant α-syn accumulates on the IMM, being unclear whether as cause or consequence of complex I dysfunction and ROS (237). One hypothesis is that complex I inhibition and associated ROS induce α-syn aggregation, which subsequently impairs proteostasis thus causing dopaminergic neurodegeneration (238, 239). This hypothesis is supported by the report that mice lacking α-syn are resistant to the complex I inhibitor 1-methyl-4-phenyl-1,2,3,6-tetrahydropyridine (MPTP) (240). Alternative hypothesis suggest that Lewy bodies may be neuroprotective, sequestering potentially toxic proteins (241), this being supported by the observation of familiar forms of PD without Lewy bodies (242).

Complex I impairment is associated with oxidative stress. PD patients present oxidative stress markers such as L-dopa and dopamine oxidation products (243, 244). Elevated iron in the *substantia nigra* of PD patients and decreased antioxidant enzymes is reported to favour oxidative stress (245). NQO1, an inducible flavoprotein involved in quinone detoxification (e.g. quinones derived from dopamine), is increased in PD brains, possibly in response to oxidative stress (244). Thus, ETC generated oxidative stress may have an important role in PD pathophysiology (204).

Mitochondrial complex I inhibitors, like rotenone (246), paraquat (247) or MPTP (248) (**Figure 1.16**), have been used to induce PD. Rotenone is unselective for dopaminergic neurons, but can nevertheless induce preferential degeneration of dopaminergic neurons, suggesting that these are particularly sensitive to complex I inhibition (238). The pesticide paraquat, structurally related to MPTP's active metabolite [1-methyl-4-phenylpyridinium (MPP^+)] (**Figure 1.16**), also induces preferential dopaminergic neurodegeneration (249). Increased paraquat exposure is a PD risk factor (250). However, a Parkinsonism without complex I deficiency has also been reported, highlighting the limitations of the complex I impairment hypothesis in PD (242).

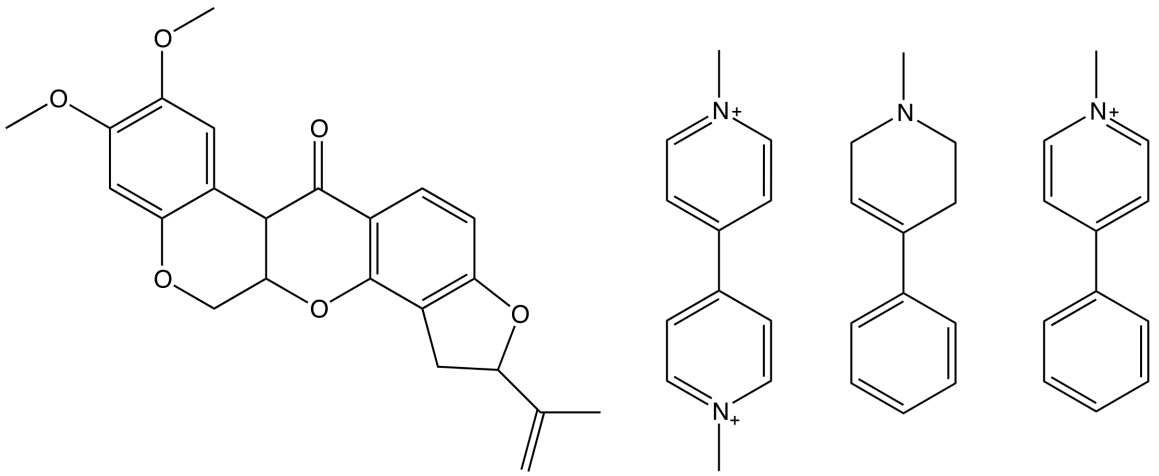

Figure 1.16. Mitochondrial complex I inhibitors used to induce Parkinsonism: Rotenone, paraquat, MPTP and MPTP's active metabolite, MPP^+.

The main PD pharmacological approaches aim to rescue dopaminergic neurotransmission deficits, most frequently by combining the precursor L-dopa with a peripheral dopa decarboxylase inhibitor (e.g. carbidopa or benserazide) (251). Dopaminergic agonists (e.g. ropinirole) monoamine oxidase (MAO)-B inhibitors (e.g. selegiline), and amantadine have also been used in PD therapeutics (251, 252). These, however, are symptomatic therapies and no available treatment can rescue neurodegeneration or delay disease progression (252, 253).

1.3.2.1.1. MPTP and MPP^+

MPTP, a neurotoxin inducing severe Parkinsonism was identified as a byproduct of 1-methyl-4-phenyl-4-propionoxypiperidine (MPPP), a meperidine analogue with heroin-like properties (254, 255). MPTP crosses the blood brain barrier, being metabolised into 1-methyl-4-phenyl-2,3-dihydropyridinium ($MPDP^+$) by glial MAO-B. $MPDP^+$ is then oxidized to the active metabolite MPP^+, exits glia *via* the organic cation transporter (OCT)-3, and accumulates in dopaminergic neurons via their dopamine transporters (DAT) (**Figure 1.17**) (256). Pre-treatment with MAO-B inhibitors (e.g. deprenyl) or with DAT inhibitors (e.g. nomifensine) can prevent MPTP toxicity (257-259). Intracellularly, MPP^+ accumulates in mitochondria in a $\Delta\psi_m$ dependent manner, where it inhibits complex I (260, 261). $\Delta\psi_m$ dependent accumulation of MPP^+ is in accordance with higher MPP^+ toxicity in intact mitochondria *vs*. submitochondrial particles (262, 263). While complex I is the main

MPP^+ target, some studies suggest that MPP^+ may also inhibits complexes III and IV (264). Additionally, MPP^+ may accumulate in synaptosomal vesicles through the vesicular monoamine transporter (VMAT)-2 (265) or interact with cytosolic proteins carrying negative charges (**Figure 1.17**) (266).

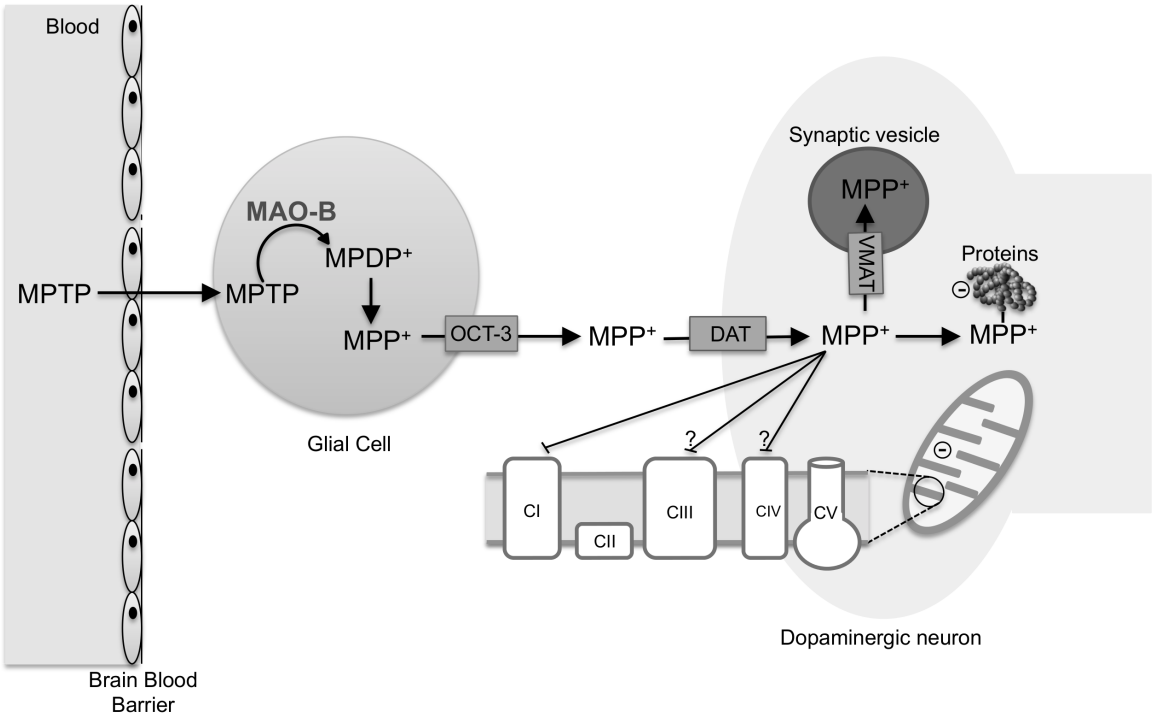

Figure 1.17. Mechanism of action of MPTP and its active metabolite, MPP^+.

MPTP induced Parkinsonism has several similarities to sporadic PD. MPTP can induce Lewy bodies formation (267), impair mitochondrial ATP production, generate ROS, and activate pro-apoptotic pathways (268, 269); MPTP toxicity is selective to dopaminergic neurons (270); and L-dopa attenuates symptoms induced by MPTP (271). Thus, MPTP and MPP^+ have been used to induce Parkinsonian phenotype in several animal models, such as monkeys (272, 273), tree shrews (274), mice (275, 276), and zebrafish (259), among others, despite variation of MPTP susceptibility among species (277). Specially in rodents, only specific strains of mice are sensitive to MPTP-induced toxic effects, which is perhaps related with metabolic differences, namely in MPP^+ clearance (278).

1.4. Zebrafish as an experimental model

Mammalian models, such as mice or rats, have been widely used to study human diseases, due to high homology between mammalian genomes and similarities in anatomy, physiology and cell biology. Mammalian models, however, are expensive, laborious, time- and drug-consuming, and there are increasing ethical and legislative pressures to limit their use in research (279, 280). Given the high conservation of basic cell biology between mammals and invertebrates, *Drosophila melanogaster* Meigen and *Caenorhabditis elegans* (Maupas) have been extensively used in biomedical research (281, 282). The major advantages of these models are their lower price and size, the possibility of high-throughput drug screening and the sequenced genome that allows easy genetic modifications. However, several structures and organs that are involved in human pathology are missing in invertebrates, limiting the use of these models (279).

Zebrafish (*Danio rerio* Hamilton) (**Figure 1.18**) is a popular robust tropical pet that became a frequent biomedical model. Zebrafish allows the study of organogenesis, physiology and behaviour, associating genes to functions (280). Zebrafish has multiple advantages: less expensive than mammals, small size, high spawning rate (about 300 eggs per female), external and optically transparent embryonic development, no feeding requirement for at least the first 7 days post fertilization (dpf), short generation time (3 months), high-throughput drug screening potential, sequenced genome, easy genetic manipulation and high physiological and genetic homology to mammals (280, 283). Despite obvious differences between fish and humans, it is clear that zebrafish offers several advantages that make it a good complement to mammalian models. The majority of zebrafish experiments have been made in embryos or larvae; however, the use of adult zebrafish is critical for developmental/age dependent biological processes. Several regeneration and behaviour studies have been carried out in adults (284, 285). Additionally, several methodologies have been optimized/developed for zebrafish, such as *in situ* hybridization, antisense morpholino oligonucleotides and transgenic lines generation (286-288).

Zebrafish allows high-throughput drug screening, where small molecules normally added to water are absorbed into the fish. Embryos/larvae can be assayed in multi-well plates without invasive or time-consuming injections (289). Zebrafish is also used as disease model for obesity and metabolic dysfunction (283), leukaemia (290), muscular dystrophies (291), cardiovascular, neurodegenerative, and multiple other human disorders.

Zebrafish cardiac development begins very early with heartbeat starting at about 24 h post fertilization (hpf) (292). Zebrafish needs no cardiac function to survive until 5 dpf, subsisting with simple oxygen diffusion, thus allowing the study of severe heart

abnormalities otherwise lethal to other key animal models (289, 293). Moreover, heart and blood vessels are easily visualised in transgenic zebrafish expressing fluorescent proteins driven by organ specific promotors (294). Zebrafish has thus been used to model dilated cardiomyopathy (295), long QT syndrome (296), aortic coarctation (297), and vascular lipid deposition (298) among other cardiovascular diseases.

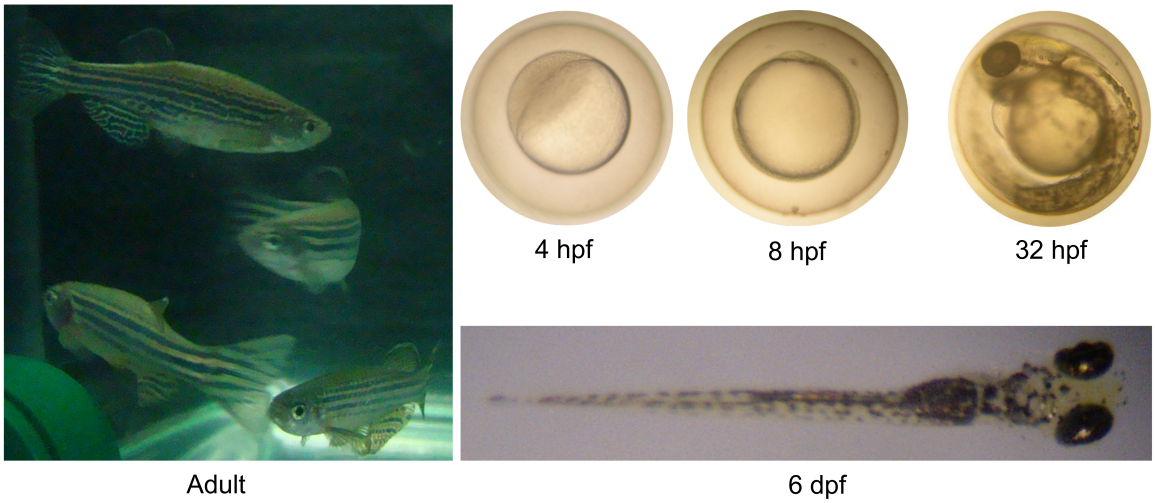

Figure 1.18. Zebrafish. Zebrafish at embryonic, larval and adult stage. (photos by Brígida R. Pinho).

Zebrafish has been used to study the nervous system, under physiological and pathological conditions, and to search novel neuroactive molecules. The zebrafish brain has several common features with the mammalian brain: glial cells; a similar blood brain barrier (299, 300); similar central nervous system (CNS) organization, conventionally divided into spinal cord, hindbrain, midbrain and forebrain (292); and similar neuronal pathways, cellular homeostasis and pathology (300). Screening of neuroactive molecules can be easily made in zebrafish through photomotor- and embryonic touch-response (301). Mechanosensory stimuli evoke locomotor responses in larvae. Also, changes in ambient temperature, presence of chemical irritants, or olfactory stimuli may all promote locomotion as escape behaviour (302, 303). Zebrafish has been used to study neuronal circuits involved in learning and behaviour (303), and to model nervous system disorders such as such as Huntington's disease (304), retinal degeneration (305), anxiety (306), Charcot-Marie Tooth disease (307), amyotrophic lateral sclerosis (ALS) (308), AD (309), PD (310). Zebrafish has also been used to model mitochondrial disorders such as multiple acyl-CoA dehydrogenase deficiency (MADD) (311). Some homologues genes associated with human neurodegenerative disorders were already identified in zebrafish. Zebrafish has a partial genome duplication, resulting in a subfunctionalization of some genes that

assists their study (300). One example is the presenilin-associated rhomboid-like (*PARL*) gene, recently associated to familial PD, that has two paralogs (*parl-a* and *parl-b*) in zebrafish (312). Examples of other neurodegeneration-linked genes in zebrafish are Parkin, PINK-1 (310, 313), LRRK2 (314), β-secretase, γ-secretase and presenilin-1 (315).

The zebrafish dopaminergic system has been mostly explored in the context of PD. Dopaminergic neurons are first detected at 18 hpf (316) and at 3 dpf they form a cluster in the posterior tuberculum of the ventral diencephalon. At 3 dpf, the zebrafish has a well-developed CNS with a spatial distribution of dopaminergic neurons equivalent to the nigrostriatal system observed in adults. In fact, as zebrafish mature into adults, their dopaminergic neurons in the posterior tuberculum ascend to the subpallium basal telencephalon, considered equivalent to the mammalian dopaminergic system (312, 316, 317). Zebrafish dopaminergic neurons are also detected in the olfactory bulb, pretectum and retina (316). Similarly to mammals, zebrafish dopaminergic neurons also regulate locomotion and behaviour (318).

Zebrafish allows the study of PD associated genes as well as PD phenotypes. Dopaminergic neurotoxins such as paraquat, rotenone, 6-hydroxydopamine, and MPTP/MPP^+, have been used to induce PD phenotypes in zebrafish (319, 320). Zebrafish is equally susceptible to MPTP during all life stages, showing a locomotor activity deficit when exposed to this neurotoxin (257, 259). Selective MPTP concentrations induce a locomotor phenotype in zebrafish without morphological changes in treated larvae (319). Zebrafish, however, has a higher neurogenesis potential than mammals, which may influence its neurotoxin susceptibility 16 different neurogenesis regions were identified in zebrafish *vs*. 2 specially involved in mammalian neurogenesis (subventricular and subgranular zone of the telencephalon) (321), which may explain the higher zebrafish capacity for axonal and neuronal regeneration after local lesions (300).

2. Objectives

This thesis had the following objectives:

1. Evaluate naphthoquinones' anti-inflammatory potential:
    a. Reduction of NO and pro-inflammatory cytokines release in LPS-treated cells;
    b. Contribution of naphthoquinone-generated oxidative stress to NO reduction.
2. Evaluate naphthoquinones' anti-allergic properties:
    a. Inhibition of basophils' degranulation induced by IgE-antigen complex or calcium ionophore;
    b. Inhibition of allergy-related enzymes;
    c. Inhibition of leukotriene production induced by IgE-antigen complex.
3. Characterize the consequences of mitochondrial dysfunction for zebrafish development and cardiovascular function, and test mitochondria-targeted quinones:
    a. Compare mitochondrial complex subunits between zebrafish and other species;
    b. Characterise mitochondrial inhibitors' effects on zebrafish embryonic development and cardiovascular function;
    c. Characterise naphthoquinones and ubiquinone analogues' effects on zebrafish embryonic development and cardiovascular function;
    d. Evaluate ubiquinone analogues' potential for rescuing chronic and acute mitochondrial dysfunction in zebrafish.
4. Evaluate ubiquinone analogues' potential for rescuing the MPP^+-induced PD model in zebrafish:
    a. Characterise locomotor profiles and sensorimotor reflexes under control conditions during the post-hatching period;
    b. Characterise MPP^+-induced phenotypes in zebrafish larvae, including viability, effects on locomotion, reflexes, neuromast labelling and mitochondrial function;
    c. Characterise ubiquinone analogues' effects on locomotion, reflexes and mitochondrial function in zebrafish larvae;
    d. Evaluate ubiquinone analogues' potential for rescuing the MPP^+-induced locomotor phenotype in zebrafish larvae.

CHAPTER II

EXPERIMENTAL SECTION

3.1. Is nitric oxide decrease observed with naphthoquinones in LPS stimulated RAW 264.7 macrophages a beneficial property?

PLoS ONE 2011 Aug; 6 (8): e24098

OPEN ACCESS Freely available online

PLoS one

Is Nitric Oxide Decrease Observed with Naphthoquinones in LPS Stimulated RAW 264.7 Macrophages a Beneficial Property?

Brígida R. Pinho, Carla Sousa, Patrícia Valentão, Paula B. Andrade*

REQUIMTE/Laboratório de Farmacognosia, Departamento de Química, Faculdade de Farmácia, Universidade do Porto, Porto, Portugal

Is nitric oxide decrease observed with naphthoquinones in LPS Stimulated RAW 264.7 macrophages a beneficial property?

Brígida R. Pinho, Carla Sousa, Patrícia Valentão and Paula B. Andrade*

REQUIMTE/Laboratório de Farmacognosia, Departamento de Química, Faculdade de Farmácia, Universidade do Porto, Porto, Portugal

Abstract

The search of new anti-inflammatory drugs has been a current preoccupation, due to the need of effective drugs, with less adverse reactions than those used nowadays. Several naphthoquinones (plumbagin, naphthazarin, juglone, menadione, diosquinone and 1,4-naphthoquinone), plus *p*-hydroquinone and *p*-benzoquinone were evaluated for their ability to cause a reduction of nitric oxide (NO) production, when RAW 264.7 macrophages were stimulated with lipopolysaccharide (LPS). Dexamethasone was used as positive control. Among the tested compounds, diosquinone was the only one that caused a NO reduction with statistical importance and without cytotoxicity: an IC_{25} of 1.09 ± 0.24 μM was found, with 38.25 ± 6.50% ($p < 0.001$) NO reduction at 1.5 μM. In order to elucidate if this NO decrease resulted from the interference of diosquinone with cellular defence mechanisms against LPS or to its conversion into peroxynitrite, by reaction with superoxide radical formed by naphthoquinones redox cycling, 3-nitrotyrosine and superoxide determination was also performed. None of these parameters showed significant changes relative to control. Furthermore, diosquinone caused a decrease in the pro-inflammatory cytokines: tumour necrosis factor-alpha (TNF-α) and interleukin 6 (IL-6). Therefore, according to the results obtained, diosquinone, studied for its anti-inflammatory potential for the first time herein, has beneficial effects in inflammation control. This study enlightens the mechanisms of action of naphthoquinones in inflammatory models, by checking for the first time the contribution of oxidative stress generated by naphthoquinones to NO reduction.

Keywords: Naphthoquinones; diosquinone; anti-inflammatory; nitric oxide; pro-inflammatory cytokines; 3-nitrotyrosine; superoxide.

Introduction

Naphthoquinones are secondary metabolites widely distributed in nature. They are present mainly in several families of higher plants, as *Diospyros* spp., including the species producing the edible fruit persimmon, but also in fungi, lichens and in bacteria (7). Naphthoquinones present a diversity of structures, exhibiting several substituents and can group together forming dimers, trimers and more seldom tetramers (30). This chemical diversity probably explains the several activities described for them. Naphthoquinones exhibit very interesting pharmacological properties, being *Diospyros* extracts widely used in African, Chinese and Indian traditional medicine (7). In particular, *Diospyros chamaethamnus* is characterized by the presence of several 7-methyljuglone derivatives, including five dimers (diospyrin, isodiospyrin, diosquinone, mamegakinone and biramentaceone), a trimer (xylospyrin) and a tretramer (6-[2-(7-methyl-juglonyl)]-isoxylospyrin) (31).

Antibacterial (53), antimalarial (322), antipyretic (323) and antitumor (324) activities are some of the properties attributed to naphthoquinones. Although naphthoquinones have also a toxicological potential, mainly due to their ability to induce oxidative stress (8), they can be good lead compounds for new anti-inflammatory drugs, as several previous studies evidence. Bisnaphthoquinones inhibit platelet aggregation (325), plumbagin inhibits cytokines release (85), shikonin derivatives inhibit cyclooxygenase-2 expression (326), mast cell degranulation (327) and iNOS (an inducible calcium-independent isoform of nitric oxide (NO) synthases) (77), interfering with NO production (328). However more studies are needed to confirm a really beneficial property.

During inflammation highly reactive species, such as superoxide radical, peroxynitrite, hydrogen peroxide, hypochlorous acid and NO are produced. NO is a small diffusible molecule with important biological functions, including vasodilatation, neurotransmission and inflammation. NO generated by iNOS in activated macrophages is important for host defences. NO modulates the synthesis of prostaglandins, tromboxans and other inflammatory molecules (329).

Macrophages are important producers of pro-inflammatory cytokines, such as tumour necrosis factor-alpha (TNF-α), interleukin 1β (IL-1β) and interleukin 6 (IL-6), when they are stimulated by an aggression, like lipopolysaccharide (LPS) exposure (330). These pro-inflammatory cytokines allow an increase in blood flow and permeability into capillaries, leading to infiltration of immune cells. TNF-α has a central role in the inflammatory and destructive processes found in several human autoimmune and chronic inflammatory diseases (331). IL-1β is important for the initiation and enhancement of inflammatory response to proliferation of some microorganisms (332) and IL-6 is regarded as an endogenous mediator of LPS-induced fever (333). Furthermore, there is some evidence of the involvement of these cytokines in carcinogenicity (334).

Although inflammatory mediators like cytokines are necessary for successful defence against foreign invaders, their production also results in collateral damage to host tissue components, including proteins, lipids/membranes and DNA. A delicate balance between formation and detoxification of reactive species produced in inflammation process allows directing signalling pathways to physiological or pathological conditions. Therefore, inflammation plays a pivotal role in the pathogenesis and development of some diseases, like certain cancers, neurodegenerative lesions and chemical toxicity (335).

For the management of inflammation a broad range of immunosuppressive drugs, as calcineurin inhibitors, steroids and anti-inflammatory non-steroids have been used. Nevertheless, these drugs have undesirable side effects like metabolic derangements, development of infections, cancers and gastric toxicity (85).

In the present work, the ability to induce a decrease of NO in LPS-stimulated RAW 264.7 macrophages of several naphthoquinones (plumbagin, naphthazarin, juglone, menadione, diosquinone and 1,4-naphthoquinone), *p*-hydroquinone and *p*-benzoquinone (**Figure 3.1.1**) was evaluated. This chemical mediator was chosen due to its importance in inflammatory processes and for inflammatory damage, besides being easily quantified. Regarding the anti-inflammatory potential of the involved naphthoquinones, naphthazarin and 1,4-naphthoquinone were already studied for their ability to decrease NO in LPS-stimulated RAW 264.7 macrophages (77). Nevertheless, naphthoquinones are also known to undergo redox cycling, causing oxidative stress in cells (8). As far as we know, there are no reports assessing whether the decrease of NO in this model is due to a reduction of its production or to the reaction of NO with superoxide generated during redox cycling of naphthoquinones. If the second hypothesis is true, the generation of peroxynitrite can lead to protein nitration, impairing cellular functioning, and no beneficial effect can be attributed to naphthoquinones. Thus, this work intended to: extend the knowledge on the ability to cause a NO decrease in the LPS – RAW 264.7 macrophages model to other naphthoquinones (juglone, menadione, plumbagin and diosquinone) and related compounds (*p*-hydroquinone and *p*-benzoquinone); establish possible structure-activity relationships; determine if NO decrease induced by naphthoquinones is due to its consumption in peroxynitrite formation. Pro-inflammatory cytokines (TNF-α, IL-1β and IL-6), superoxide radical and protein nitration levels were determined for the most promising compound.

As far as we know, the contribution of oxidative stress induced by naphthoquinones to NO reduction has not been studied yet. Furthermore, diosquinone, an epoxide dimeric naphthoquinone found in several *Diospyros* species (31, 336), was evaluated for its anti-inflammatory potential for the first time herein.

Materials and Methods

Materials

DPBS (Dulbecco's Phosphate Buffered Saline), DMEM (Dulbecco's Modified Eagle Medium)+GlutaMAXTM-I, heat inactivated foetal bovine serum and penicillin + streptomycin (Pen Strep) were obtained from Gibco, Invitrogen™ (Grand Island, NY, USA). Plumbagin, naphthazarin, juglone, 1,4-naphthoquinone, *p*- hydroquinone, *p*-benzoquinone, menadione, sulphanilamide, potassium nitrite, β-nicotinamide adenine dinucleotide reduced disodium salt hydrate (NADH), sodium pyruvate, 3-(4,5-di- methylthiazol-2-yl)-2,5-diphenyltetrazolium bromide (MTT), methanol, triton, tris-HCl, ethylene glycol-bis(2-aminoethylether)-*N*,*N*,*N*',*N*'-tetraacetic acid (EGTA), brilliant blue G, dimethyl sulfoxide (DMSO), DL-dithiothreitol (DTT), phenylmethanesulfonyl fluoride (PMSF), nitrotetrazolium blue chloride (NBT), bovine serum albumin, lipopolysaccharide from *Salmonella enteric* serotype *Typhimurium*, monoclonal anti-3-nitrotyrosine antibody produced in mouse and GBX fixer and developer of Kodak processing chemicals for autoradiography films were purchased from Sigma-Aldrich (St. Louis, MO, USA). *N*-(1)-Naphthylethylenediamine, glycerol and ethylenediaminetetraacetic acid (EDTA) were obtained from Merck (Darmstadt, Germany). Sodium chloride and potassium hydroxide (KOH) were purchased from Vaz Pereira (Lisbon, Portugal) and *ortho*-phosphoric acid 85% was obtained from Panreac (Barcelona, Spain). Goat

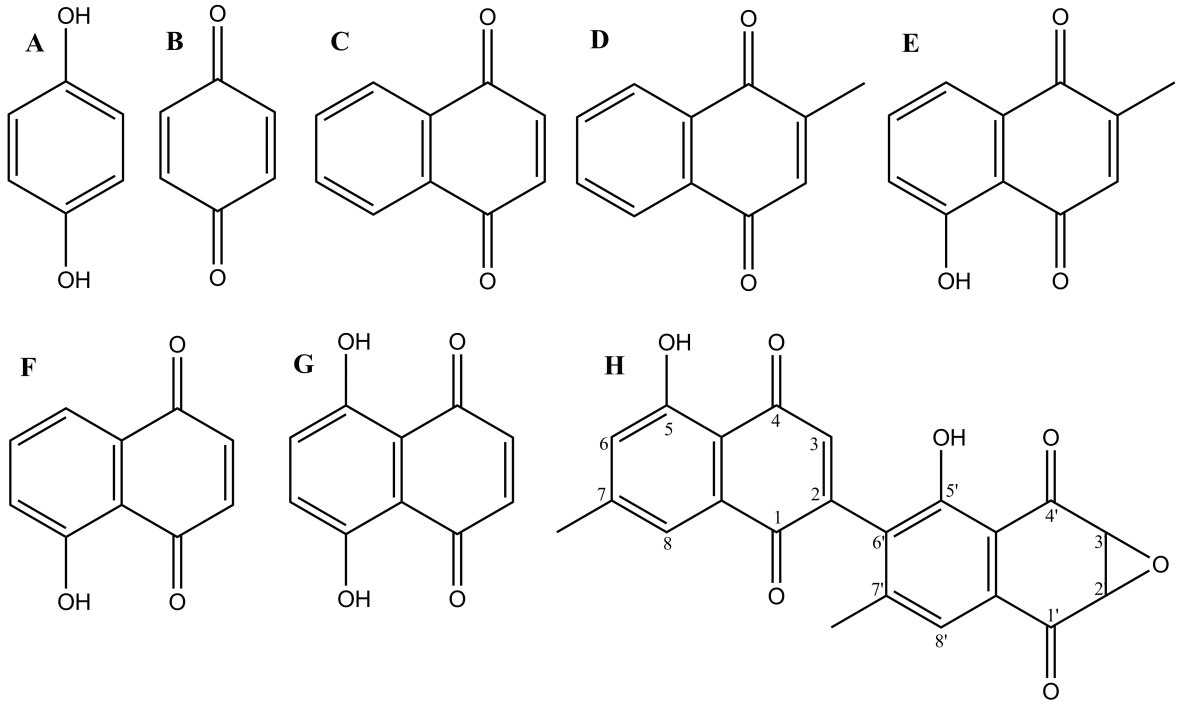

Figure 3.1.1. **Chemical structures of the tested compounds.** ***A***, *p*-hydroquinone; ***B***, *p*-benzoquinone; ***C***, 1,4-naphthoquinone; ***D***, menadione; ***E***, plumbagin; ***F***, juglone; ***G***, naphthazarin; ***H***, diosquinone.

antibody to mouse IgG (horseradish peroxidase) (0.8 mg/mL), TNF-α, IL-1β and IL-6 mouse ELISA kits were purchased from Abcam (Cambridge, United Kingdom). Hybond – ECL, Hyperfilm^{TM} ECL and the enhanced chemiluminescence (ECL)-Plus reagent Kit were obtained from Amersham^{TM} (GE Healthcare, Piscataway, NJ, USA). Diosquinone was isolated from root barks of *D. chamaethamnus* (31) and its purity was checked by HPLC-DAD.

Diosquinone HPLC-DAD analysis

Chloroform solution of diosquinone was analysed in a HPLC system (Gilson), using a Spherisorb OSD2 column (Waters, Milford, USA) (250 x 4.6 mm, i. d., 5 µm). The solvent used was a mixture of acetic acid 5% in water (A) and methanol (B) and the gradient was as follows: 0 min - 75% B, 10 min - 75% B, 25 min - 85% B, 35 min - 100% B and 60 min - 100% B. The HPLC system was equipped with a Gilson diode array detector (DAD). Spectroscopic data of the peak was accumulated in the range of 200–400 nm, and chromatogram was recorded at 255 nm. The data was processed on Unipoint system software (Gilson Medical Electronics, Villiers le Bel, France).

Cell culture and treatments

The mouse macrophage-like cell line RAW 264.7 was kindly provided by Prof. Maria S. J. Nascimento (Laboratório de Microbiologia, Departamento de Ciências Biológicas, Faculdade de Farmácia, Universidade do Porto). Cells were grown in DMEM+GlutaMAX^{TM} – I supplemented with 10% heat inactivated foetal bovine serum, 100 U/mL penicillin and 100 µg/mL streptomycin, under 5% CO_2 at 37ºC, in humidified air. Cells were plated at $1.5x10^5$ cells/mL in a plate with 48 wells (1 mL/well). The tested compounds were dissolved in DMSO, at 10 mM, and stored, as small aliquots, at -20ºC. The compounds were diluted with supplemented DMEM as needed, before cell exposure. When cells reach confluence, the compounds were added, 1 h before exposure to LPS (1 µg/mL). After addition of LPS, the cells were maintained in culture for 18 h. Dexamethasone at a concentration of 50 µM was used as positive control. The effect of all tested compounds in the absence of LPS was also evaluated, in order to observe if they induced changes in NO basal levels. In negative controls, no LPS was added. The final concentration of DMSO was 0.5% (v/v) and all control groups received the same amount of DMSO.

Lactate dehydrogenase (LDH) leakage assay

The release of the cytosolic enzyme LDH into culture medium was evaluated as follows: an aliquot of culture medium was taken and mixed with a NADH buffered solution and pyruvate solution (337). LDH activity was measured spectrophotometrically by following the conversion of NADH to NAD^+, at 340 nm. Results are expressed as a percentage of the respective control (with or without LPS).

MTT reduction assay

Cellular viability was also assessed by the mitochondria dependent reduction of MTT to formazan, according to Sousa and collaborators (338) with some modifications. After described incubation with tested compounds, culture medium removal and cells washing with DPBS, cells in 48-wells plates were incubated with 1 mL/well of MTT (0.5 mg/mL), during 30 min at 37ºC. In the end, supernatant was rejected and formazan was solubilized in DMSO (1 mL). The extent of reduction of MTT to formazan within cells was quantified by measurement of optical density at 550 nm, using a microplate reader (Multiskan ASCENT Thermo®). Results are expressed as a percentage of the respective control (with or without LPS).

NO determination

In culture, the NO released by the macrophages into the medium is converted to several nitrogen derivatives, from which only nitrite is stable, being easily measured by Griess reagent (1.0% sulphanilamide and 0.1% *N*-(1)-naphthylethylenediamine in 2% phosphoric acid) (77). After incubation, 100 µL of culture medium supernatant was mixed with the same volume of Griess reagent, during 10 min, at room temperature. The nitrite produced was determined by measuring the optical density at 550 nm, in a microplate reader (Multiskan ASCENT Thermo®). Nitrite was quantified by external standard, using potassium nitrite to generate a standard curve. Results are expressed as a percentage of the control with LPS.

Measurement of superoxide radical

Superoxide radical was measured by the NBT reduction assay (338). Each well of a 12-wells plate was seeded with 2 mL of RAW 264.7 macrophages suspension containing $1.5x10^5$ cells/mL. The treatment of cells proceeded as described previously: pre-exposure to tested compounds for 1 h, followed by addition of 1 mg/mL or vehicle and further incubation for 18 h. After incubation, 40 µL of a NBT solution at 1 µg/mL was added to the medium and incubated at 37ºC, for 1 h. Then, the incubation medium was removed and cells were lysed with DMSO: 4 mM KOH (1:1). The absorbance of reduced NBT, formazan, was measured at 630 nm, in a microplate reader (Multiskan ASCENT Thermo®). Results are expressed as a percentage of the control without LPS.

Protein quantification

Protein quantification was performed by addition of 200 µL of Bradford dye reagent (brilliant blue G, 0.1 mg/mL; ethanol, 5% (v/v); phosphoric acid, 10% (v/v) and water) to 40 µL of samples, pre-diluted 100 times. The photometrical measure was performed at 595 nm. Bovine serum albumin was used to generate a standard curve.

Slot-immunoblotting analysis of 3-nitrotyrosine

RAW 264.7 macrophages were plated with 4 mL/well at a density of $1.5x10^5$ cells/mL, in a plate with 6 wells. After treatment with dexamethasone (50 µM), diosquinone (1.5 µM) and LPS (1 µg/mL), as described above, the cells were washed and subjected to 200 µL triton lysis buffer (1% triton, 20 mM tris HCl, 150 mM NaCl, 5 mM EGTA, 10 mM EDTA and 10% glycerol) with 1 mM DTT and 0.5 mM PMSF, as proteases inhibitors, during 60 min. Samples were centrifuged at 12 000 rpm, for 10 min, at 4ºC, and respective supernatants were collected. Samples solutions were diluted to contain the same protein concentration (0.5 mg/mL) and 100 µL of these solutions were applied in a nitrocellulose membrane, pre-washed with 10% of methanol and pre-hydrated during 5 min. Negative pressure was applied after application of all samples (in duplicate). The membrane was then disassembled from the apparatus and incubated in a TBS-T blocking solution with 5% milk for 5 h, at room temperature. A mouse polyclonal anti-3-nitrotyrosine antibody was used at a dilution of 1:1000 in TBS-T blocking solution with 5% milk. The membrane and the antibody were incubated overnight, at 4ºC, and further incubated at room temperature for 2 h. After washing the membrane with TBS-T, during 5 min, three times, a goat anti-mouse secondary antibody conjugated with horseradish peroxidase (1:2000) was applied to the membrane for 2 h, at room temperature. All incubations were made with mixing. Finally, the membrane was washed three times with TBS-T buffer and one time with TBS. Blots were revealed using the ECL system kit and 3-nitrotyrosine were visualized on high performance chemiluminescence film, after 15 min of exposure of film to membrane. Three assays were performed. This method is in accordance to Moreira-Gonçalves and collaborators with some modifications (339). Three-dimensional surface plot analyses were generated with the ‘‘Surface Plot’’ function of Image J 1.44 (http://rsbweb.nih.gov/ij/download. html).

Enzyme linked immunosorbent assay (ELISA)

RAW 264.7 macrophages were plated with 4 mL/well at a density of $1.5x10^5$ cells/mL, in a 6 wells plate. Supernatants from dexamethasone (50 µM), diosquinone (1.5 µM) exposed macrophages, either without or with LPS (1 µg/mL) stimulation, were collected at 18 h and centrifuged at 4000 rpm for 3 min, to remove any cells. Cell free culture media were stored at -70ºC until use. TNF-α, IL-1β

and IL-6 secreted cytokines were measured in duplicate, using purified biotinylated antibodies in ELISA sets according to the protocol provided by the supplier (Abcam, Cambridge, United Kingdom). The ELISA plates were read using a microplate reader (Multiskan ASCENT Thermo®).

Statistical analysis

OneWay ANOVA and Dunnett test, as post-hoc test, were used to determine the statistical significance in comparison to control. Data are expressed as the mean ± standard error of the mean (SEM) of at least four independent experiments, performed in duplicate or triplicate, as described above. *P* values of 0.05 or less were considered statistically significant. Statistical analysis was made using: PAWS Statistic 18 Software (Chicago, IL, USA) and Graphpad Prism 5 Software (San Diego, CA, USA).

Results

Cellular viability

The exposure to LPS (1 µg/mL) for 18 h induced a decrease in cellular viability (14.22 ± 2.50 % relative to control, in MTT assay), with statistical importance ($P < 0.001$) (**Figure 3.1.2**). Dexamethasone (1–50 µM) was used as positive control. At 50 µM, dexamethasone alone caused 22.98 ± 4.11 % ($P < 0.001$) of cell death, as evaluated by MTT assay. However, for the same concentration of dexamethasone and in the presence of LPS, cell viability of RAW 264.7 macrophages was higher than 100% relative to control ($P < 0.01$). These differences in cell viability were not verified in the LDH assay (**Figure 3.1.2.**). Therefore, as MTT assay allowed detecting more alterations on cells' survival than the measure of LDH leakage (**Figures 3.1.2** and **3.1.3**), the results presented herein for cell viability after treatments with naphthoquinones were obtained by the first assay.

Naphthazarin was the most toxic compound (LC_{25} = 0.73 ± 0.07 µM), followed by plumbagin (LC_{25} = 1.26 ± 0.28 µM) (**Figure 3.1.4**). For plumbagin, at 5 µM, there was 70.50 ± 7.12 % ($P < 0.001$) of cell death, by MTT assay, while in the LDH assay cell viability was higher than 100% ($P < 0.01$) (**Figure 3.1.5**). In order to explore this result, a study of cell viability over time, with 5 µM of plumbagin was performed (data not shown). In the MTT assay, it was verified that cell death began to occur 2 h after treatment, rapidly increasing until 5 h and reaching 70% at the end of the treatment (19 h). Cell death measured by LDH assay showed the same profile during the first 8 h. After this period, the LDH quantified in the culture medium began to decrease. Cell death overtime was confirmed by microscopic evaluation.

1,4-Naphthoquinone ($P < 0.001$) and diosquinone ($P < 0.01$) showed some toxicity at concentrations of 5 µM and 2.5 µM, respectively (about 35% of cell death relative to control). Juglone caused nearly 20% of cell death at 10 µM ($P < 0.001$). Menadione (0.5 – 10 µM), *p*-hydroquinone and *p*-benzoquinone (0.5 – 5 µM) revealed no cytotoxicity under the concentration range used (**Figure 3.1.4**).

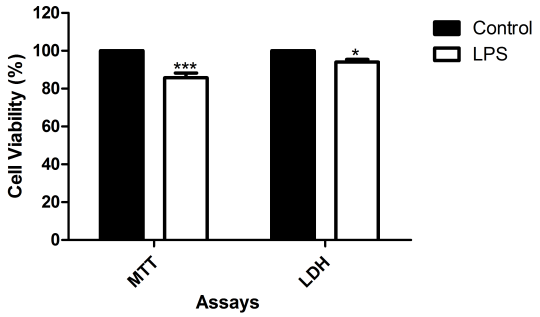

Figure 3.1.2. **Influence of LPS in cell viability.** RAW 264.7 macrophages were exposed to 1 µg/mL of LPS, during 18 h and cell viability were assessed by LDH and MTT assays. Results are expressed in percentage of control (mean ± SEM of five independent experiments, performed in duplicate). *$P < 0.05$, ***$P < 0.001$.

NO production

None of the tested compounds induced changes in NO basal levels, when incubated without LPS (data not shown).

Dexamethasone caused a decreased of NO for all tested concentrations, having an IC_{25} of 1.72 ± 0.54 µM. With 50 µM of dexamethasone, the amount of NO was similar to basal levels (**Figure 3.1.6**).

Diosquinone decreased NO to 38.25 ± 6.50 % ($P < 0.001$) relative to control at 1.5 µM, with an IC_{25} of 1.09 ± 0.24 µM (**Figure 3.1.7**). The IC_{25} found for 1,4-naphthoquinone was 0.72 ± 0.09 µM. However, at 1.5 µM, NO reduction by 1,4-naphthoquinone was 27.36 ± 0.28% ($P > 0.05$). Menadione did not induce NO reduction with statistical significance. Juglone, naphthazarin and plumbagin did not cause a decrease of NO at non-cytotoxic concentrations (**Figures 3.1.4**, **3.1.5** and **3.1.7**).

p-Benzoquinone and *p*-hydroquinone exhibited an IC_{25} of 1.82 ± 0.57 µM and 1.14 ± 0.28 µM, respectively, being the last more active than *p*-benzoquinone: *p*-hydroquinone caused a reduction of 50% of NO, at 3.74 ± 0.18 µM (**Figure 3.1.7**).

As diosquinone caused higher NO reduction than the other tested naphthoquinones to lower concentrations, it was chosen to study the effect on superoxide and pro-inflammatory cytokines production and protein nitration.

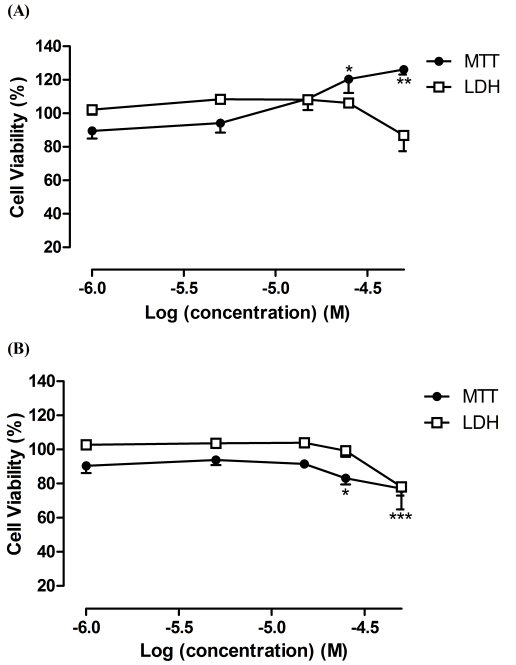

Figure 3.1.3. Influence of dexamethasone with and without LPS in cell viability. RAW 264.7 macrophages were pre-exposed for 1 h to dexamethasone followed by 18 h co-exposure with 1 μg/mL of LPS (***A***) or vehicle (***B***). The cell viability was assessed by MTT and LDH assays. All results are percentage of control (mean ± SEM of five independent experiments, performed in duplicate). **P* < 0.05, ***P* < 0.01, ****P* < 0.001.

Superoxide generation

The different treatments (without tested compounds, with 1.5 μM of diosquinone and 50 μM of dexamethasone, in the presence and in the absence of LPS) did not reveal significant differences (**Figure 3.1.8**). However, LPS seemed to increase superoxide generation, especially in control cells.

Protein nitration

Diosquinone (1.5 μM) alone did not increase protein nitration, relative to control. On the other hand, dexamethasone (50 μM) by itself led to protein nitration, which was potentiated by LPS (**Figure 3.1.9**).

Pro-inflammatory cytokines

Diosquinone (1.5 μM) was able to reduce TNF-α by 51.38 ± 9.72 % and IL-6 by 39.42 ± 19.79 % relative to LPS exposed cells only. With respect to IL-1β, macrophages stimulation with LPS did not cause a measurable increase of this cytokine under the assay conditions. So no reduction in this interleukin could be observed in cells exposed to diosquinone and LPS.

Discussion

Several compounds, the majority of them being naphthoquinones (**Figure 3.1.1**), were screened for their ability to alter NO production by LPS stimulated RAW 264.7 macrophages. In a second part of this work, assays were made to confirm the beneficial effect of diosquinone, the most promising one. Diosquinone, previously isolated from *D. chamaethamnus* (31), was pure, as ascertained by HPLC-DAD analysis (data not shown).

Macrophages, which express high levels of inducible NO synthase, play a central role in host's defence against bacterial infection, being the major cellular targets for LPS action (340).

Among inflammatory modulators produced in response to LPS, NO is an important cytotoxic mediator (341). The first precaution when studying the direct interference of a given compound on NO production is to guarantee that it does not cause cell death, decreasing the number of NO producing cells. Thus, the effect on cell viability should be assessed.

The results obtained after incubation with dexamethasone in MTT assay depended on the presence of LPS (**Figure 3.1.3**): when cells were treated with both LPS and dexamethasone the cellular viability was higher than 100% ($P < 0.01$), while the treatment only with dexamethasone gave the opposite result. This could be explained by the mechanism of action of dexamethasone, which inhibits NF-κB transcription factor (342). NF-κB is central to a series of cellular processes, like inflammation, cell proliferation and apoptosis (343). As constitutive expression of NF-κB is frequently found in tumour cells (34), the NF-κB inhibitory action of dexamethasone can be responsible for the decrease in RAW 264.7 macrophages viability. As LPS activates NF-κB (334) and dexamethasone has an opposite activity, the dexamethasone effect in cell survival is counterbalanced by the presence of LPS.

In this work, LDH and MTT assays revealed different effects on cellular viability. The decrease in cell survival, in the presence of 50 μM of dexamethasone, was not detected by LDH assay (**Figure 3.1.3**). Analogous observations had also been reported by other authors (337, 344). LDH assesses cell death due to cell membrane damage which leads to the release of LDH into culture medium (337). MTT assay provides information on mitochondrial function, as MTT reduction mainly occurs in this organelle through the action of succi-

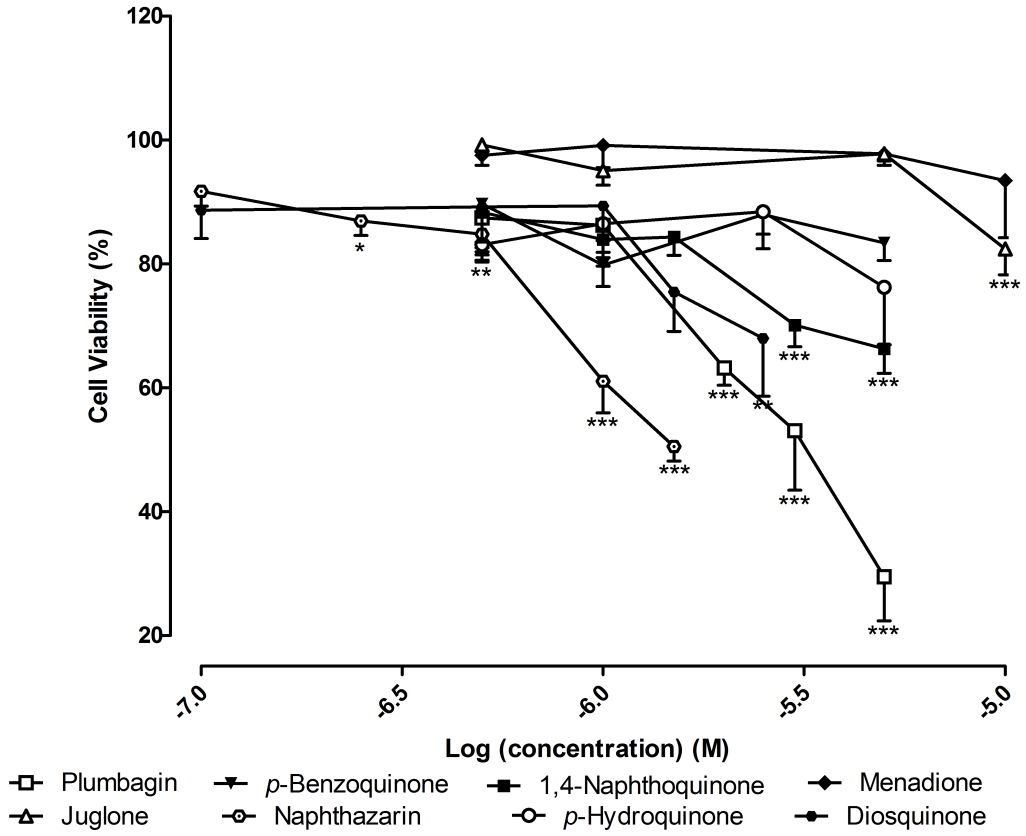

Figure 3.1.4. Influence of tested compounds in cell viability. Viability of LPS stimulated RAW 264.7 macrophages, after 19 h of exposure to the tested compounds, by MTT assay. All results are expressed in percentage of control with LPS (mean ± SEM of four independent experiments, performed in duplicate). **P* < 0.05, ***P* < 0.01, ****P* < 0.001.

nate dehydrogenase (337). The MTT assay is also a preferential method when cell death occurs long before cellular viability determination, as we observed for plumbagin treatment at 5 μM. With this naphthoquinone, cell viability after 19 h exposure assessed by the MTT assay was too low, while it reached a mean of 151.90 ± 41.39% (*P* < 0.01) in the LDH assay (**Figure 3.1.5**). Therefore, the influence of exposure time on cell viability was studied. It was observed that cell death occurred mainly in the beginning of the exposure period (data not shown). Thus the majority of the LDH leaked to the medium was degraded at 19 h. In this study, MTT assay appeared to be more sensitive in detecting toxicity compared to the LDH leakage assay. For these reasons, the MTT assay was chosen to assess the effect on cell viability.

Another important factor was the choice of the LPS concentration to be used in the assays. The LPS concentration must be such that not causes cell death, but allows a measurable NO amount. In this work, 1 μg/mL of LPS was used, which is a concentration currently applied by other authors (77, 345). However, the exposure of RAW 264.7 macrophages to 1 μg/mL of LPS for 18 h lead to 14.22 ± 2.50% (*P* < 0.001) of cell death relative to control (**Figure 3.1.2**). This result can be explained by excessive reactive oxygen species production (about 15% increase in superoxide relative to control), as it can be seen in **Figure 3.1.8**.

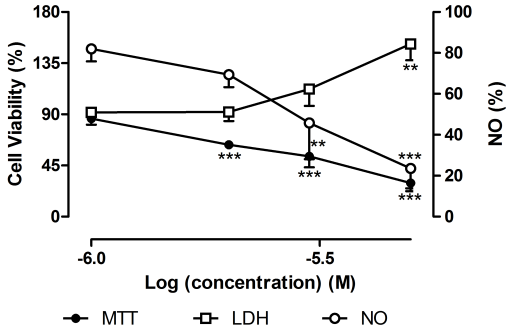

Figure 3.1.5. Influence of plumbagin in cell viability and in NO production. After pre-exposure with plumbagin and stimulation with LPS, RAW 264.7 macrophages viability was assessed by LDH and MTT assays and NO production was quantified. Results are expressed as percentage of control (mean ± SEM of four independent experiments, performed in duplicate).***P* < 0.01, ****P* < 0.001.

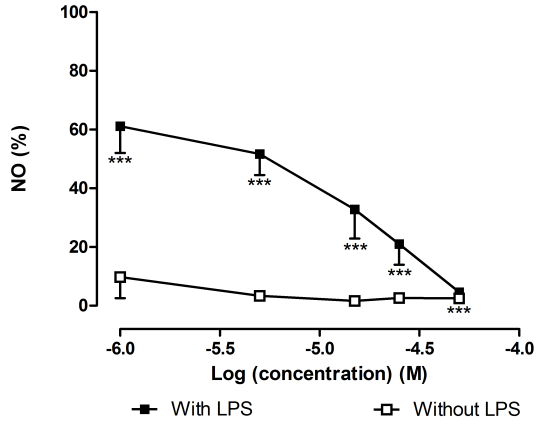

Figure 3.1.6. Dexamethasone effects on NO production. Quantification of NO produced by RAW 264.7 macrophages exposed to dexamethasone, in the presence and in the absence of 1 µg/mL of LPS (18 h). All results are expressed in percentage of control with LPS (mean ± SEM of four independent experiments, performed in duplicate). ***P < 0.001.

As so, the results of cell viability in the presence of LPS for the tested compounds are expressed in percentage of control with LPS. In addition, LPS (1 µg/mL) induced NO production in amounts easy to quantify (19.21 ± 0.274 µM) and we considered that NO produced by LPS exposed RAW 264.7 cells was 100%.

Concerning the cytotoxicity of tested compounds, naphthazarin and plumbagin were the most toxic ones (**Figure 3.1.4**). In general, tumour cells, as RAW 264.7 macrophages, are sensitive to the deleterious effects of naphthoquinones in low µM range. In studies involving other tumour and non-tumour cells (34, 85), the authors used plumbagin concentrations similar to those used in our work, but no significant cell death was noticed. This difference may be explained by distinct sensitivity of the cells to naphthoquinones.

The cytotoxicity of diosquinone was lower compared to most of the other tested hydroxy-naphthoquinones (**Figure 3.1.4**). Quinones

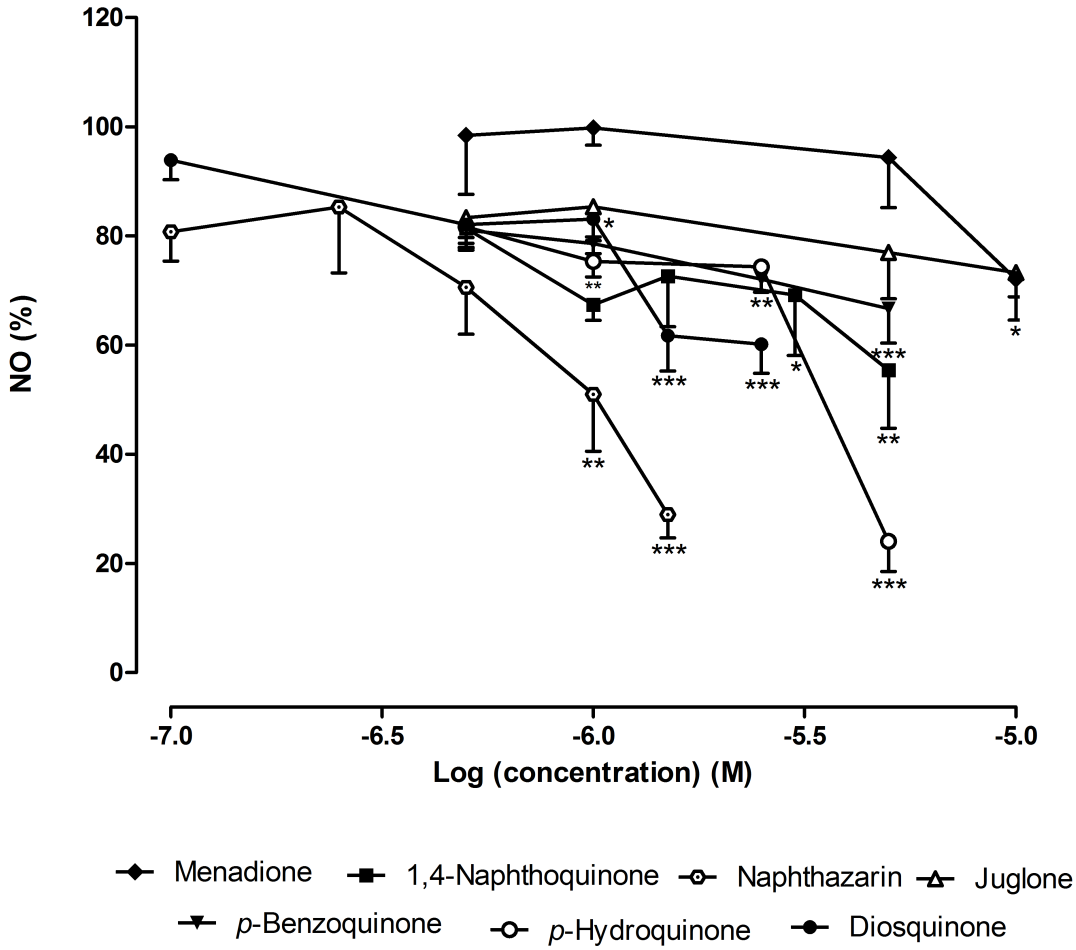

Figure 3.1.7. Influence of tested compounds in NO production. Quantification of NO produced by LPS stimulated RAW 264.7 macrophages after pre-exposure to tested compounds. Results are expressed in percentage of control (0.5% DMSO + 1 µg/mL LPS) (mean ± SEM of four independent experiments, performed in duplicate). *P < 0.05, **P < 0.01, ***P < 0.001.

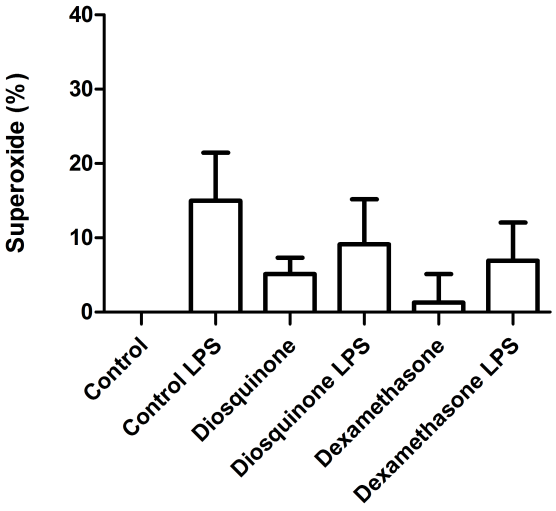

Figure 3.1.8. Superoxide radical quantification. Superoxide radical produced by RAW 264.7 macrophages, after pre-treatment (1 h) with diosquinone (1.5 μM) and dexamethasone (50 μM), in the presence and in the absence of 1 μg/mL of LPS (18 h). Results are expressed in percentage of control (mean ± SEM of four independent experiments, performed in duplicate).

cytotoxicity is related with their pro-oxidant properties and interaction with nucleophilic biomolecules (12, 346). It is known that nucleophilic attack to thiol groups involves positions 2 and 3 of naphthoquinones (347). As diosquinone has an epoxy group at positions 2 and 3 of one monomer and the C2 of the other monomer is involved in the linkage between the two monomers, probably diosquinone causes less oxidative stress and glutathione depletion than the other naphthoquinones. For the other compounds, the presence of a hydroxyl group in the benzene ring seems to be important for the exhibited toxicity, as the introduction of electron-donating hydroxyl groups increases the pro-oxidant potential of naphthoquinones (12, 346). This may explain the higher toxicity of naphthazarin and plumbagin and why juglone is more toxic than menadione. However, juglone is less toxic than the corresponding non-hydroxylated 1,4-naphtoquinone, which is in accordance with a previous work by Klaus and colleagues (346). In addition, hydroxyl groups at positions 5 and 8 of naphthazarin confer a high redox potential, explaining its higher toxicity relative to other naphthoquinones (8).

In what concerns to NO decrease (**Figure 3.1.7**), it seemed to follow the effect on cell viability (**Figure 3.1.4**). However, the decrease of NO was, in general, more pronounced. Furthermore, we only concluded about NO reduction if no cell death with statistical meaning occurred. Diosquinone, the only tested dimer, was the most interesting compound. Diosquinone caused 38.25 ± 6.50% (P < 0.001) of NO reduction relative to control at 1.5 μM (**Figure 3.1.7**). Although *p*-hydroquinone caused 75.92 ± 5.53% (P < 0.001) of NO reduction at 5 μM, NO reduction for 3.20 ± 0.16 μM corresponded to 40%. Thus, diosquinone was more active at lower concentrations than *p*-hydroquinone. Diosquinone had an IC_{25} of 1.09 ± 0.24 μM, lower than that of dexamethasone (1.72 ± 0.54 μM). However, dexamethasone caused a decrease in NO for all used concentrations, reaching basal levels at 50 μM (**Figure 3.1.6**). The greater activity of diosquinone in relation to the other naphthoquinones could be explained by its higher lipophilicity. Lipophilicity favours both the entrance of the compound in the cell and the establishment of hydrophobic bonds with a potential active site (348). The importance of lipophilicity may also be observed when comparing the activities of 1,4-naphthoquinone and *p*-benzoquinone: 1,4-naphthoquinone was more cytotoxic and leads to a higher NO decrease than *p*-benzoquinone (**Figures 3.1.4** and **3.1.7**).

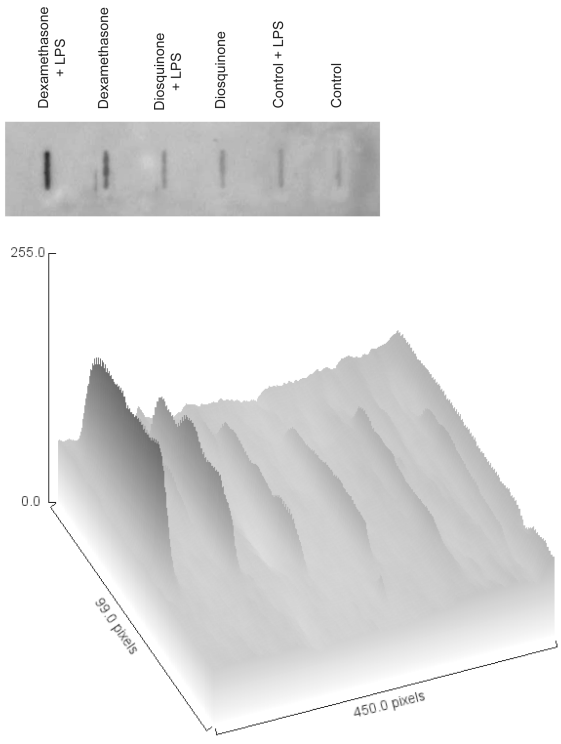

Figure 3.1.9. Semi-quantitative analysis of 3-nitrotyrosine. Image of slot-blot film, where 3-nitrotyrosine was detected by immunoblotting and respective surface plot analysis (Y axis represents intensity of bands). This assay was performed after RAW 264.7 macrophages pre-treatment (1 h) with diosquinone (1.5 μM) and dexamethasone (50 μM) in presence and in absence of 1 μg/mL of LPS (18 h). Control cells were exposed to vehicle (0.5% DMSO).

Although naphthoquinones may suppress NF-κB activation and, consequently, inhibit iNOS induction (34, 77), the observed NO reduction can also result from direct reaction of NO with superoxide radical, which is generated during quinone oxidation (349). The product of this reaction is peroxynitrite, which may react with thiol groups or nitrate hydroxylate phenolic amino acids, most importantly tyrosine residues, forming 3-nitrotyrosine. The increase of 3-nitrotyrosine has toxicological consequences, because it alters phosphorylation of tyrosine (350). Therefore, to clarify the effect of diosquinone we proceeded to the determination of superoxide radical and 3-nitrotyrosine.

It was observed that diosquinone (at 1.5 μM) did not induce more nitration than control (**Figure 3.1.9**), indicating that the decrease of NO is beneficial to cells, precluding LPS action and reducing inflammation. Some authors defend that nitration of tyrosine may not occur, having nitration of dityrosine (351, 352). However, that seemed to be not the case, as the used method allowed to detect high levels of 3-nitrotyrosine with dexamethasone and LPS treatment. With respect to superoxide radical, no significant differences were noticed, although cells treated with LPS tended to exhibit higher levels of this reactive species (**Figure 3.1.8**).

The potential of diosquinone to reduce LPS induced inflammation was confirmed by its ability to reduce the pro-inflammatory cytokines TNF-α and IL-6, which have a central role in inflammation. The decrease in TNF-α was the most expressive and since this cytokine has a fundamental role in the activation of macrophages themselves, being the first mediator in the inflammatory cascade (335), diosquinone may have interest to be explored as candidate to a new anti-inflammatory drug.

In conclusion, among the several compounds screened for anti-inflammatory activity, diosquinone, the only dimeric naphthoquinone, was the most promising naphthoquinone, causing a reduction of NO, without cytotoxicity. The NO decrease induced by this compound was probably due to its interference with the mechanism of action of LPS and not to NO consumption in the reaction with superoxide. This hypothesis was confirmed by the reduction of the inflammatory mediators TNF-α and IL-6 in macrophages stimulated with LPS. Thus, according to these results, diosquinone brings beneficial effects to cells by inhibiting the inflammatory response. This study contributes to the knowledge of naphthoquinones properties, mainly anti-inflammatory activity, and, as far as we are aware, constitutes the first work concerning diosquinone anti-inflammatory potential. Furthermore, it is the first study assessing whether the oxidative stress induced by naphthoquinones contributes to NO reduction, in this model.

Funding. B.R. Pinho is grateful to “Fundação para a Ciência e a Tecnologia” (FCT) for the grant (SFRH/BD/63852/2009).

3.2. Modulation of basophils' degranulation and allergy-related enzymes by monomeric and dimeric naphthoquinones

Submitted for publication

Modulation of basophils' degranulation and allergy-related enzymes by monomeric and dimeric naphthoquinones

Brígida R. Pinho[1], Carla Sousa[1], Patrícia Valentão[1], Jorge M. A. Oliveira[2] and Paula B. Andrade[1]*

[1]REQUIMTE/Laboratório de Farmacognosia, Departamento de Química, Faculdade de Farmácia, Universidade do Porto, Porto, Portugal and [2]REQUIMTE/Laboratório de Farmacologia, Departamento de Ciências do Medicamento, Faculdade de Farmácia, Universidade do Porto, Porto, Portugal

Abstract

Allergic disorders are characterized by an abnormal immune response towards non-infectious substances, being associated with life quality reduction and potential life-threatening reactions. The increasing prevalence of allergic disorders demands for new and effective anti-allergic treatments. Here we test the anti-allergic potential of monomeric (juglone, menadione, naphthazarin, plumbagin) and dimeric (diospyrin and diosquinone) naphthoquinones. Inhibition of RBL-2H3 rat basophils' degranulation by naphthoquinones was assessed using two complementary stimuli: IgE/antigen and calcium ionophore A23187. Additionally, we tested for the inhibition of leukotrienes production in IgE/antigen-stimulated cells, and studied hyaluronidase and lipoxidase inhibition by naphthoquinones in cell-free assays. Naphthazarin (0.1 μM) decreased degranulation induced by IgE/antigen but not A23187, suggesting a mechanism upstream of the calcium increase, unlike diospyrin (10 μM) that reduced degranulation in A23187-stimulated cells. Naphthoquinones were weak hyaluronidase inhibitors, but all inhibited soybean lipoxidase with the most lipophilic diospyrin, diosquinone and menadione being the most potent, thus suggesting a mechanism of competition with natural lipophilic substrates. Menadione was the only naphthoquinone reducing leukotriene C_4 production, with a maximal effect at 5 μM. This work expands the current knowledge on the biological properties of naphthoquinones, highlighting naphthazarin, diospyrin and menadione as potential lead compounds for structural modification in the process of improving and developing novel anti-allergic drugs.

Keywords: Allergy; Histamine and β-hexosaminidase; Hyaluronidase; Lipoxidase; Naphthoquinones.

Introduction

Allergy is an abnormal immune response against non-infectious environmental substances, named allergens (166). Allergy comprises chronic disorders associated with reduced quality of life, such as eczema or allergic rhinitis, and potential life-threatening reactions, including anaphylaxis and severe asthma episodes (353). The prevalence of allergic disorders has been increasing globally, affecting roughly 25% of people in developed countries. This increased prevalence has been associated to environmental changes, such as air pollution and ambient temperature increment, which may induce early springs with increased airborne pollen (166). On the other hand, the "hygiene hypothesis" suggests that reduced exposure to microorganisms in early life contributes to an immune system more susceptible to allergic and autoimmune diseases (168). In the allergic process, immune cells, such as mastocytes, eosinophils, basophils and macrophages, release several mediators (including histamine and leukotrienes) that are responsible for allergic symptoms (354). Additionally, these mediators may promote the development of different diseases, by inducing pathophysiological changes in the affected organs (173). A classic example is the role of leukotrienes in the pathogenesis of asthma and allergic rhinitis, by inducing bronchoconstriction and increased vascular permeability (179). Thus, the increased allergy prevalence, together with the deleterious consequences of repetitive exposure to allergens, stresses the need for new strategies to induce immunological tolerance to allergens as well as new anti-allergic drugs (166).

Nature continues to be a rich source of novel bioactive molecules, and several plant extracts have been probed for anti-allergic properties. Namely, the grape seed extract of *Vitis vinifera* L. (355), the rhizomes extract of *Dioscorea membranacea* Pierre ex Prain & Burkill, in which the main active compound was a quinone (dioscoreanone) (356), or the leaf extract of *Rhinacanthus nasutus* Kuntze, which is rich in naphthoquinones (92). In fact, *R. nasutus* contains three 1,4-naphthoquinones capable of inhibiting

RBL-2H3 basophils' degranulation in the micromolar range, and decreasing tumour necrosis factor (TNF)-α and interleukin production (92). Further studies, with synthetic naphthoquinones, support their anti-allergic properties: 2-alkyl/arylcarboxamido derivatives of 3-chloro-1,4-naphthoquinone inhibited the degranulation on mastocytes stimulated with compound 48/80 (93). On the other hand, allergic reactions are common after temporary tattoos with henna (derived from *Lawsonia inermis* L.), where lawsone (2-hydroxy-1,4-naphthoquinone) is the main compound responsible for dye properties. Still, allergic reactions to henna have been attributed only to the occasional additive *p*-phenylenediamine (357) (358).

In this work we studied the anti-allergic properties of naphthoquinones commonly produced by *Diospyros* species: diospyrin (DPR), diosquinone (DQN), juglone (JGL), menadione (MND), naphthazarin (NTZ) and plumbagin (PLB) (**Figure 3.2.1**). Several biological activities have been attributed to these compounds, namely, anti-inflammatory (359), antitumor (360) and antimicrobial (59), but anti-allergic properties were only identified for menadione (91) and plumbagin (87). To our knowledge, no anti-allergic data exists for the other *Diospyros'* naphthoquinones. For the initial screening, two different stimuli were used to induce RBL-2H3 basophils' degranulation (IgE/antigen or the calcium ionophore A23187) and the released β-hexosaminidase and histamine were quantified. Additionally, hyaluronidase and lipoxidase inhibition by naphthoquinones were evaluated, as well as the inhibition of leukotrienes production in IgE/antigen-exposed RBL-2H3 cells.

Materials and Methods

Test compounds

Plumbagin (PLB), naphthazarin (NTZ), menadione (MND) and juglone (JGL) were obtained from Sigma-Aldrich (St. Louis, MO, USA). Diospyrin (DPR) and diosquinone (DQN) (**Figure 3.2.1**) were isolated from the root barks of *Diospyros chamaethamnus* Dinter ex. Mildbr. (31) and their purity was evaluated by HPLC-DAD as b efore (359).

Chemicals and reagents

Medium, buffers and supplements for cell culture, including Earle's Balanced Salt Solution (EBSS) were from Gibco, Invitrogen™ (Grand Island, NY, USA) and bovine albumin fraction V solution 7.5% (BSA) was from Sigma-Aldrich (St. Louis, MO, USA).

Hyaluronic acid sodium salt from *Streptococcus equi*, hyaluronidase from bovine tests (type IV-S; EC 3.2.1.35), lipoxidase from *Glicine max* (L.) Merr. (type V-S; EC 1.13.11.12), as well as degranulation stimuli, monoclonal anti-dinitrophenyl (DNP) antibody produced in mouse, dinitrophenyl albumin (DNP-BSA) and calcium ionophore A23187 were from Sigma-Aldrich (St. Louis, MO, USA). Fluorescein-isothiocyanate (FITC)-conjugated recombinant annexin-V was from Immuno Tools (Friesoythe, Germany) and leukotriene C_4 EIA kit was from Abcam (Cambridge, United Kingdom). All other chemicals were from Sigma-Aldrich (St. Louis, MO, USA), with the exception of 3-(4,5-dimethylthiazol-2-yl)-2,5-diphenyltetrazolium bromide (MTT), which was from Duchefa Biochemie (Haarlem, The Netherlands).

Cell assays

Rat basophilic leukaemia cell line, RBL-2H3, was from the American Type Culture Collection (ATCC®) (LGC Standards S.L.U., Barcelona, Spain). Cells were cultured in DMEM (Dulbecco's Modified Eagle's Medium) + GlutaMAX™- I supplemented with 15% heat inactivated foetal bovine serum, 100 U/ml penicillin and 100 µg/ml streptomycin. Cells were maintained under 5% CO_2, at 37 ºC, in humidified air.

Cell treatment

Solvent, stimuli and drugs. RBL-2H3 cells were seeded at 3.0×10^5 cells/ml in 24-wells plate (1 ml/well), and assayed after 24 h at near-confluent stage (~90%). Two different degranulation stimuli were used: calcium ionophore A23187 500 ng/mL (1 µM) and an immunologic stimulus (100 ng/mL IgE anti-DNP followed by 100 ng/mL DNP-BSA) that we refer to as IgE/antigen (**Figure 3.2.2*A*** and **3.2.3*A***). Both stimuli induced degranulation, which was quantified by β-hexosaminidase and histamine release. With IgE/antigen, β-hexosaminidase release (*p*-nitrophenolate absorbance) increased by 65.4 ± 6.8 % above basal (n = 16; P < 0.001), whereas histamine increased from the basal value of 0.156 ± 0.151 µM towards 0.521 ± 0.186 µM (n = 10; P < 0.05). With A23187, β-hexosaminidase release increased by 187 ± 18.9 % above basal (n = 12; P < 0.001), whereas histamine increased towards 2.43 ± 0.330 µM (n = 12; P < 0.001). Thus, the ability of naphthoquinones to reduce β-hexosaminidase release was quantified for both stimuli, whereas effects upon histamine were only quantified with the A23187 stimulus, given the low histamine release and poor signal to noise achieved with IgE/antigen.

Quercetin was used as positive anti-degranulation control (361) and the anti-degranulation effects of diospyrin, diosquinone, juglone, menadione, naphathazarin and plumbagin

(**Figure 3.2.1**), were studied at non-toxic concentrations as inferred by the MTT assay. The concentrations of the tested compounds in the degranulation assays with different stimuli were kept constant [0.1 μM (NTZ), 1 μM (DQN and PLB), 5 μM (MND) and 10 μM (JGL)], except for diospyrin and quercetin, where a 10 fold higher concentration was also tested in the A23187 assay.

A23187, quercetin and naphthoquinones stocks were dissolved in dimethyl sulfoxide (DMSO), aliquoted and stored at -20 ºC. We determined the maximal non-interfering solvent concentrations (**Figure 3.2.2*B*** and **3.2.3*B***; 0.1% and 0.5% DMSO for IgE/antigen and A23187 assays, respectively), as this was a limiting factor for testing higher naphthoquinone concentrations.

IgE/antigen assay. When the IgE/antigen was used as stimulus, cells were incubated during 16 h with 100 ng/mL IgE anti-DNP and with individual naphthoquinones diluted in culture medium. After washing twice with Dulbecco's phosphate buffered saline (DPBS), cells were treated for 1 h, at 37 ºC, with 100 ng/mL DNP-BSA and with individual naphthoquinones diluted in EBSS supplemented with 0.1% BSA (**Figure 3.2.2*A***) (362). After treatments, supernatants were collected in order to quantify released β-hexosaminidase and released histamine, while cell viability assay was performed on adherent cells.

A23187 assay. Before treatment with A23187, cells were incubated with individual naphthoquinones during 15 min, at 37ºC. After that, A23187 1 μM was added and cells incubated for 30 min, at 37 ºC (**Figure 3.2.3*A***). Compounds were freshly diluted prior to cell exposure using EBSS supplemented with 0.1% BSA (362). β-hexosaminidase and histamine release was quantified in supernatants, whereas the MTT cell viability assay was performed on adherent cells.

Cell viability

Cell viability was assessed by the cellular dehydrogenases' dependent reduction of MTT to formazan, which was quantified by the measurement of optical density at 550 nm using a microplate reader (Multiskan ASCENT Thermo®), as described before (359).

Released β-hexosaminidase quantification

The release of β-hexosaminidase from stimulated-RBL-2H3 cells was measured as previously described (362). In a 96-wells plate, 50 μL of substrate solution [*p*-nitrophenyl N-acetyl-D-glucosamine 1.3 mg/mL in citrate buffer (pH 4.5)] were added to 30 μL of supernatant. The plate was incubated at 37ºC, during 1 h. The reaction was stopped by the addition of 80 μL of NaOH 0.5 M and the reaction product, *p*-nitrophenolate, was measured spectrophotometrically at 405 nm, in a microplate reader (Multiskan ASCENT Thermo®).

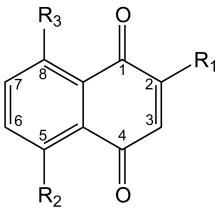

Monomeric naphthoquinone	R_1	R_2	R_3
Juglone (JGL)	H	OH	H
Menadione (MND)	CH_3	H	H
Naphthazarin (NTZ)	H	OH	OH
Plumbagin (PLB)	CH_3	OH	H
Shikonin	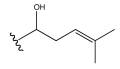	OH	OH

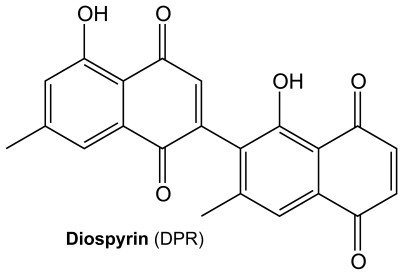

Diospyrin (DPR)

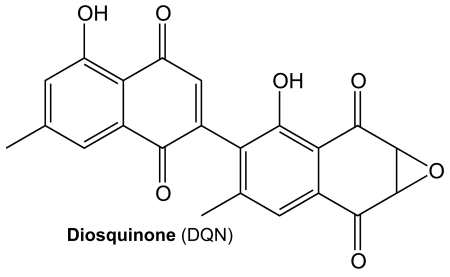

Diosquinone (DQN)

Figure 3.2.1. Chemical structures of monomeric and dimeric naphthoquinones.

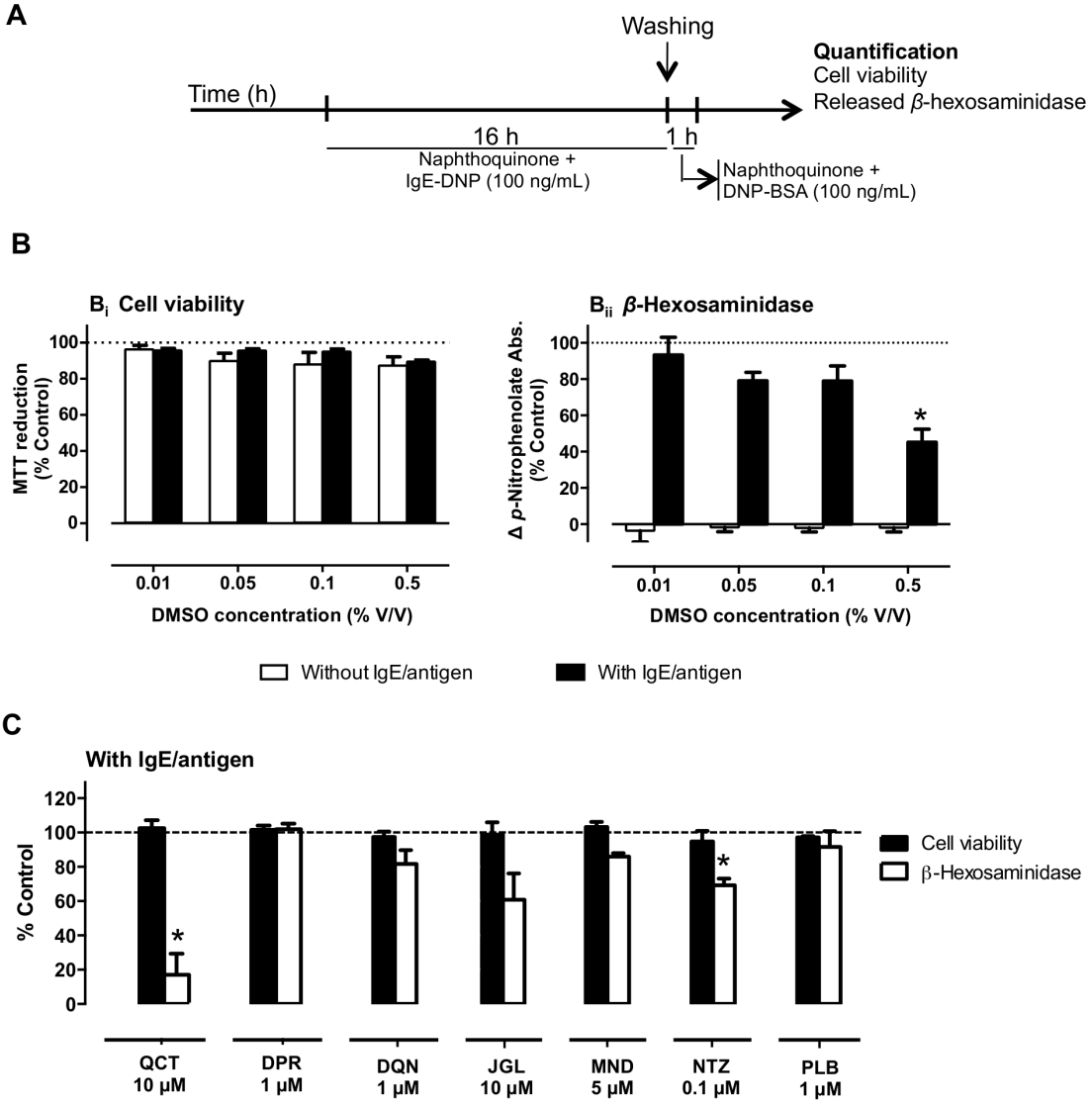

Figure 3.2.2. Effect of naphthoquinones pre-exposure in IgE/antigen-stimulated RBL-2H3 cells. ***A***, Protocol; ***B***, effect of the solvent (DMSO) on cell viability (***i***) and β-hexosaminidase release (***ii***) with/without IgE/antigen, *n*=3-4. **P*<0.05, One way ANOVA with Bonferroni post-hoc (*vs.* control); ***C***, effect on cell viability and β-hexosaminidase release in IgE/antigen-stimulated cells treated with quercetin (QCT) and naphthoquinones [diospyrin (DPR), diosquinone (DQN), juglone (JGL), menadione (MND), naphthazarin (NTZ) and plumbagin (PLB)], *n*=3-4. **P*<0.05, paired *t* test to respective control (100 ng/mL IgE/DNP + 0.1% DMSO).

β-hexosaminidase inhibitory activity

Beyond avoiding β-hexosaminidase release, individual naphthoquinones may directly inhibit β-hexosaminidase enzymatic activity. For this, the inhibition of β-hexosaminidase enzymatic activity by naphthoquinones and quercetin was evaluated in an assay similar to the one described above: individual naphthoquinones (5 μL) were incubated with supernatant of degranulated cells where β-hexosaminidase is present (25 μL of supernatant of cells treated with A23187), in presence of 50 μL of substrate solution, during 1 h, at 37ºC. The determination was made at 405 nm, in a microplate reader (Multiskan ASCENT Thermo®) (363).

Released histamine quantification

100 μL of NaOH 1 M and 25 μL of *o*-phthalaldehyde (OPA) 1% (w/v) were added to 500 μL of supernatant to convert histamine into fluorescent histamine-OPA-products. After 4 min incubation at room temperature, the reaction was stopped with of 50 μL of HCl 3 M. Precipitated proteins were removed by centrifugation at 14,000 rpm, during 3 min. The fluorescent histamine-OPA-products were quantified in the supernatant using 360 nm excitation and 450 nm emission in a microplate reader (Biotek Synergy HT®) (362). Changes in histamine release are expressed as the difference between maximal and basal release, in percentage of control.

FITC-Annexin-V labelling

After promoting degranulation with IgE/antigen treatment, cells were washed and exposed to FITC-conjugated annexin-V (5 µL/well with a final volume of 75 µL), according to the supplier's instructions (Immuno Tools, Friesoythe, Germany). After 15 min in the dark, cells were washed and visualized at 40x magnification in a system composed by an inverted microscope (Eclipse TE300, Nikon, Tokyo, Japan), a CCD camera (C6790; Hamamatsu Photonics, Japan) and a computer with an Aquacosmos software (version 2.5; Hamamatsu Photonics). FITC was excited at 488 nm with an exposure time of 727 ms and emission at 520 nm. 5 Random fields/well (2 wells per condition) were photographed

Leukotriene C_4 quantification

Leukotriene C_4 quantification was performed in the supernatant of IgE/antigen stimulated cells using a competitive enzyme immunoassay kit, according to the supplier's protocol (Abcam, Cambridge, United Kingdom) in a microplate reader (Multiskan ASCENT Thermo®) at 405 nm.

Assays of enzymatic inhibition in cell-free systems

Hyaluronidase. The enzymatic reaction mixture was composed by 50 µL hyaluronic acid (5 mg/mL in water), 100 µL buffer pH 3.68 (HCOONa 0.2 M, NaCl 0.1 M and BSA 0.2 mg/mL), 200 µL water, 50 µL individual naphthoquinones solution and 50 µL hyaluronidase 600 U. The enzymatic reaction occurred during 1 h, at 37ºC. The reaction product, *N*-acetyl-sugar, was quantified according Morgan-Elson colour reaction with minor modifications. The Morgan-Elson reaction was started by addition of 25 µL disodium tetraborate 0.8 M and subsequent heating in a boiling water bath during 3 min. After cooling, 750 µL *p*-dimethylaminobenzaldehyde (DMAB) was added and the reaction mixture was incubated at 37ºC for 20 min. DMAB stock solution was prepared by dissolving 2 g DMAB in glacial acetic acid with 12.5% of HCl 10 N. This solution was further diluted in glacial acetic acid (1:2) immediately before use. The measurement was made spectrophotometrically, at 560 nm, in a microplate reader (Multiskan ASCENT Thermo®) (364). Sodium cromoglycate was used as a positive control for inhibition (365). DMSO was kept constant at 1%, without inducing enzyme inhibition.

Lipoxidase. Lipoxidase catalyses the oxidation of linoleic acid to the conjugated diene, 13-hydroperoxy linoleic acid, which was measured spectrophotometrically at 234 nm on a UV/visible spectrophotometer (UNICAM Helios α) (366). The blank was measured in a reaction mixture with 20 µL of individual naphthoquinones solution, 1 mL of phosphate buffer (pH 9) and 20 µL of soybean lipoxidase 500 U. After 5 min pre-incubation at room temperature, the reaction was started by addition of 50 µL of substrate (linoleic acid) at 2 mM in ethanol. The reaction time was 3 min. DMSO was kept constant at 1.8%, without inducing enzyme inhibition. Quercetin was used as positive control (367).

Statistical analysis

Values are presented as mean ± standard error of mean (SEM) of at least three independent experiments (*n*), performed at least in duplicate. Results concerning cell viability, released histamine and released β-hexosaminidase are expressed in percentage of the respective control. The normality of the values was evaluated by Shapiro-Wilk test, which was performed using Statistical Package for the Social Sciences version 20.0 (SPSS Inc., Chicago, IL, USA). Paired *t*-test or One-Way ANOVA with Bonferroni as post-hoc test were used, respectively, to compare two or more groups (GraphPad Prism version 5.0, San Diego, CA, USA). *P* values under 0.05 were considered statistically significant.

Results

Naphthazarin and diospyrin decreased RBL-2H3 degranulation

To test the anti-allergic properties of naphthoquinones, we evaluated their ability to inhibit RBL-2H3 basophils' degranulation evoked by two different stimuli: IgE/antigen (100 ng/mL, 16h exposure) or the calcium ionophore A23187 (1 µM, 30 min exposure); Schematic protocols in **Figure 3.2.2*A*** and **3.2.3*A***. DMSO was used as a solvent, and we started by determining the maximal DMSO concentrations that could be used without interfering with the assays, and consequently the maximal concentrations that could be tested for the dissolved naphthoquinones (**Figure 3.2.2*B*** and **3.2.3*B***). DMSO at 0.5% decreased β-hexosaminidase release by 52.1 ± 11.9% when IgE/antigen was used ($P < 0.05$) (**Figure 3.2.2*B***), but it had no detectable effect on the release of β-hexosaminidase and histamine in A23187 stimulated cells (**Figure 3.2.3*B***), likely due to the shorter exposure time. Thus, the DMSO amount used in the IgE/antigen assay was 0.1%, while in the A23187 assay it was 0.5%, thus allowing for higher naphthoquinone concentration testing. None of the naphthoquinone concentrations used significantly affected cell

viability, as assessed by the MTT reduction assay (**Figure 3.2.2*C*** and **3.2.3*C***; black bars).

In the IgE/antigen assay, naphthazarin (NTZ; 0.1 μM) was the only naphthoquinone able to significantly reduce degranulation, decreasing β-hexosaminidase release by 30.8 ± 3.3% (n = 4; P < 0.05) (**Figure 3.2.2*C***). Naphthazarin (0.1 μM) and the positive control quercetin (1 μM) also decreased FITC-annexin-V labelling, consistent with a mechanism of degranulation inhibition (**Figure 3.2.4**). Juglone (JGL; 10 μM) also displayed a tendency to reduce the degranulation induced by IgE/antigen, since it induced a decrease of 39.2 ± 13.3% of released β-hexosaminidase (**Figure 3.2.2*C***).

In the A23187 assay, the positive control quercetin required a 10-fold higher concentration (100 μM) to reduce β-hexosaminidase release, when compared with the IgE/antigen assay. Diospirin (DPR) at the higher 10 μM concentration allowed by this assay, significantly decreased both β-hexosaminidase (56.8 ± 14.6%) and histamine (51.4 ± 12.8%) release, an amplitude of effect approaching that achieved with quercetin, and standing out amongst the other dimeric and monomeric naphthoquinones, none of which significantly affected degranulation at the maximal tested concentrations (**Figure 3.2.3*C***). None of the tested naphthoquinone concentrations induced degranulation in the absence of stimuli (IgE/Antigen or A23187) nor directly inhibited the β-hexosaminidase enzymatic activity (data not shown).

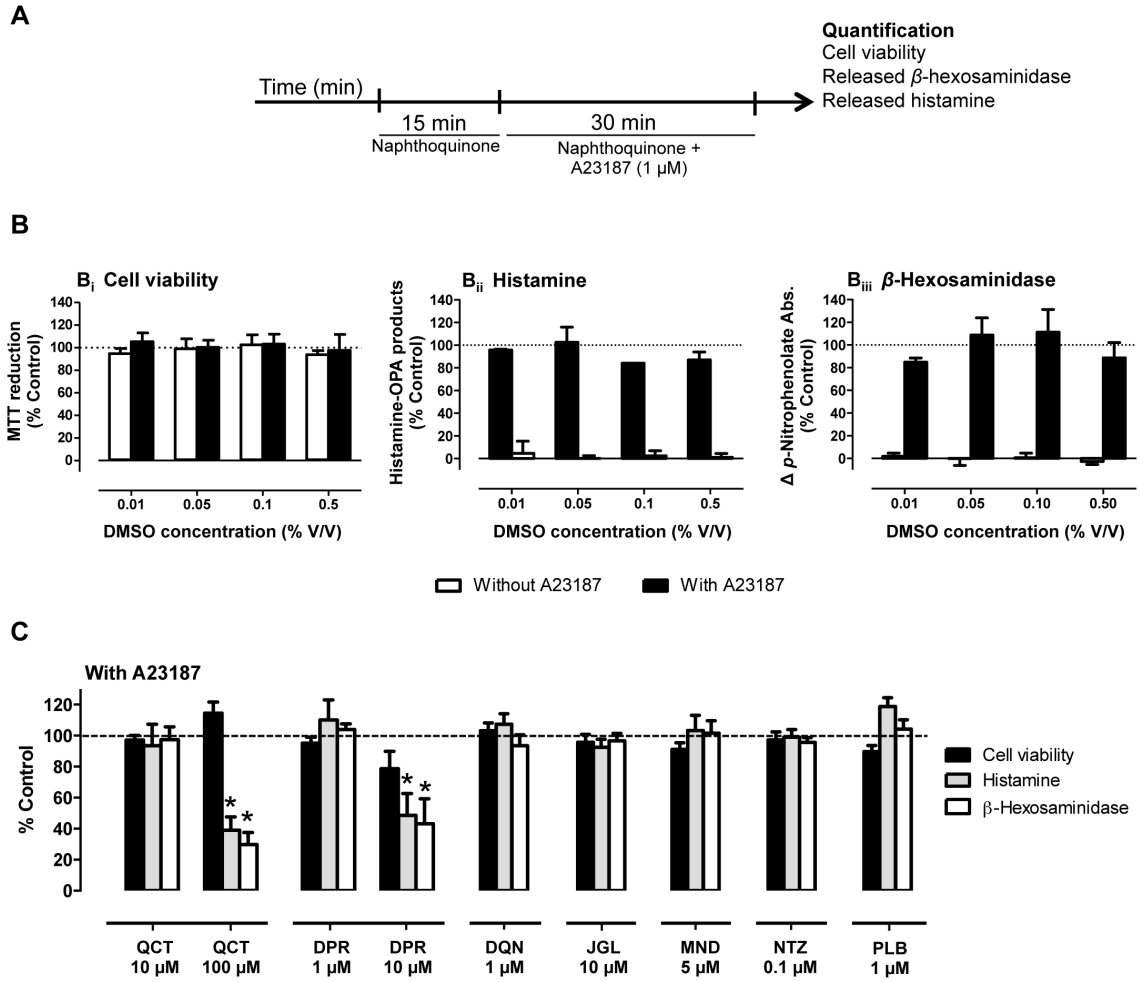

Figure 3.2.3. Effect of naphthoquinones pre-exposure in calcium ionophore (1 μM A23187) stimulated RBL-2H3 cells. ***A***, Protocol; ***B***, effect of solvent (DMSO 0.01-0.5%) on cell viability (***i***), released histamine (***ii***) and released β-hexosaminidase (***iii***) in cells with/without A23187 stimuli, n=3-4; ***C***, Cell viability (black), histamine release (grey) and β-hexosaminidase release (white) in A23187-stimulated cells treated with quercetin (QCT) or individual naphthoquinones [diospyrin (DPR), diosquinone (DQN), juglone (JGL), menadione (MND), naphthazarin (NTZ) and plumbagin (PLB)], n=5-10. *P<0.05, paired t test to respective control (1μM A23187 + 0.5% DMSO).

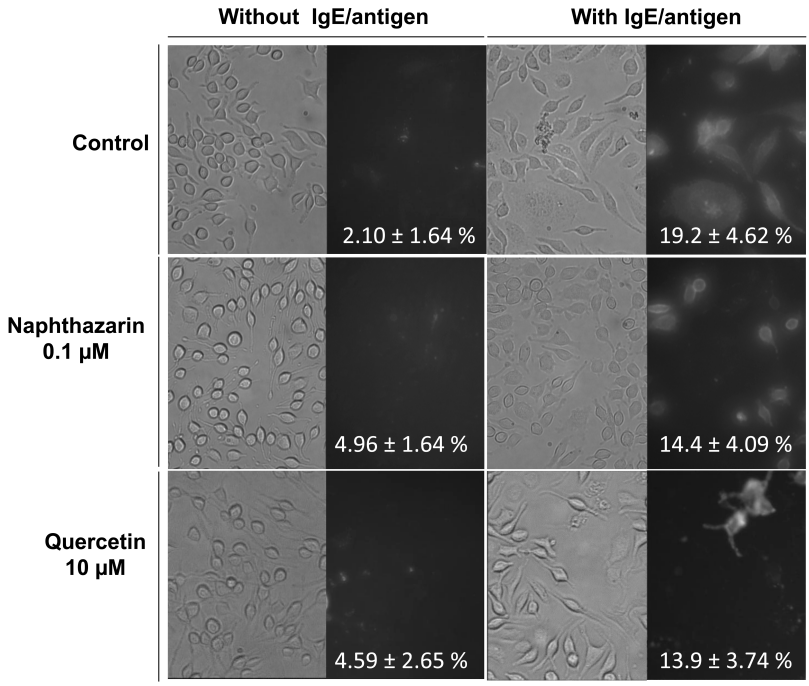

Figure 3.2.4. Degranulation quantification by FITC-annexin-V labelling. Images with (right) and without (left) IgE/antigen stimuli in RBL-2H3 cells treated with naphthazarin (NTZ, 0.1 µM) and quercetin (QCT, 10 µM) after exposure to FITC-annexin-V (40x magnification). Values are the percentage of annexin-V-labelled cells in relation to total number of the cells (mean ± SEM, *n*=3).

Naphthoquinones are weak hyaluronidase inhibitors

Sodium cromoglycate was used as a positive control for hyaluronidase inhibition (365). Complete hyaluronidase inhibition required 10 mM sodium cromoglycate (**Figure 3.2.5**). Solubility precluded the testing of naphthoquinone concentrations above 100 µM. Only menadione and naphthazarin significantly inhibited hyaluronidase. While their level of inhibition (about 20%) at 100 µM surpasses that achieved with the same sodium cromoglycate concentration (**Figure 3.2.5**), insolubility at higher concentrations, argues against these naphthoquinones as promising hyaluronidase inhibitors.

Naphthoquinones effects on soybean lipoxidase and in leukotriene levels

All tested naphthoquinones concentration-dependently inhibited soybean lipoxidase (**Figure 3.2.6*A***). Dimeric naphthoquinones, diospyrin and diosquinone, were the most potent with respective IC_{50} values of 28.9 and 83.8 µM, whereas all monomeric naphthoquinones displayed IC_{50} values above 100 µM, with the most potent being menadione with an IC_{50} of 128 µM (**Table 3.2.1**). These three most potent naphthoquinones were selected for an exploratory assay on leukotriene levels in IgE/antigen-stimulated RBL-2H3 cells. IgE/antigen treatment induced a robust increase in the levels of leukotriene (LT) C_4 in the supernatant of RBL-2H3 cells, which was unaffected by either diospyrin (1 µM) or diosquinone (1 µM), but completely abrogated by menadione (5 µM). We thus performed a concentration response curve for menadione on LTC_4 levels (**Figure 3.2.6*C***). Results showed that the lowest menadione concentration tested (5 nM) strongly decreased LTC_4 levels evoked by IgE/antigen, suggesting interference with LTC_4 synthesis mechanisms. Increasing menadione concentration-dependently decreased LTC_4 levels until full inhibition of the IgE/antigen evoked release, with an IC_{50} of 0.34 ± 0.018 µM (**Figure 3.2.6*C***).

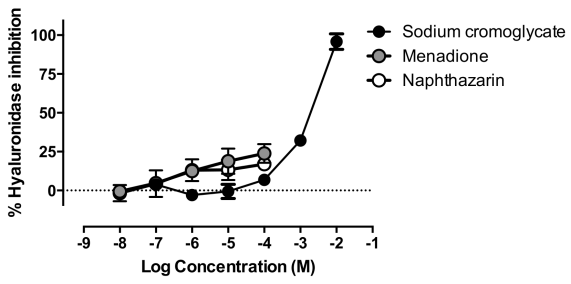

Figure 3.2.5. Concentration-dependent hyaluronidase inhibition by sodium cromoglycate (black circles) menadione (grey circles) and naphthazarin (white circles). *n*=3-4.

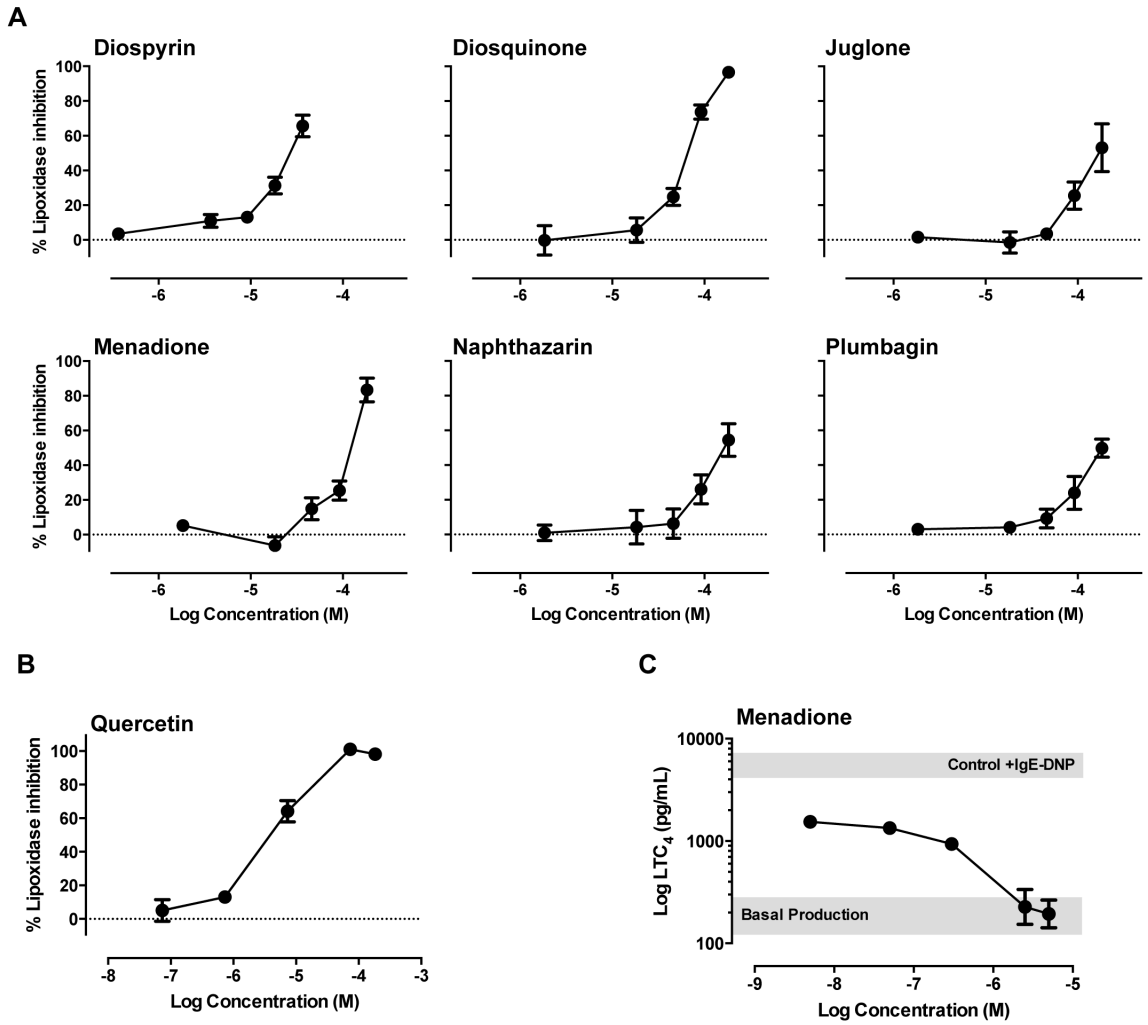

Figure 3.2.6. Lipoxidase inhibition and leukotriene C_4 production. Soybean lipoxidase inhibition by individual naphthoquinones (***A***) and by quercetin (***B***) in a cell-free assay and inhibition of leukotriene C_4 production in IgE/antigen-stimulated RBL-2H3 by menadione (***C***). Grey box represents LTC_4 production of stimulated (upper) and non-stimulated (lower) control cells. *n*=3-5.

Table 3.2.1. IC_{50} values (mean ± SEM) for soybean lipoxidase inhibition by naphthoquinones and quercetin, using a cell-free assay.

Compound	IC_{50} (μM)
Quercetin	10.6 ± 5.82
Dimeric naphthoquinones	
Diospyrin	28.9 ± 2.53
Diosquinone	83.8 ± 9.33
Monomeric Naphthoquinones	
Juglone	>184
Menadione	128 ± 9.38
Naphthazarin	142 ± 27.1
Plumbagin	>184

Discussion

In this work we investigated the anti-allergic potential of monomeric and dimeric naphthoquinones (**Figure 3.2.1**) by testing for inhibition of RBL-2H3 cells' degranulation. RBL-2H3 cells are a rat basophilic leukaemia cell line, expressing high affinity IgE receptors (FcεRI), being a model to study allergy and inflammation (181, 368). Potent inflammatory mediators (histamine, proteases, cytokines, arachidonic acid metabolites and chemotactic factors) are released from immune cells after an allergic stimulus that can be IgE-dependent or IgE-independent (174). To induce degranulation we used two previously described effective degranulation stimuli for RBL-2H3 (362): IgE/antigen (simulation of IgE-dependent allergic response) and calcium ionophore (A23187; simulation of events that

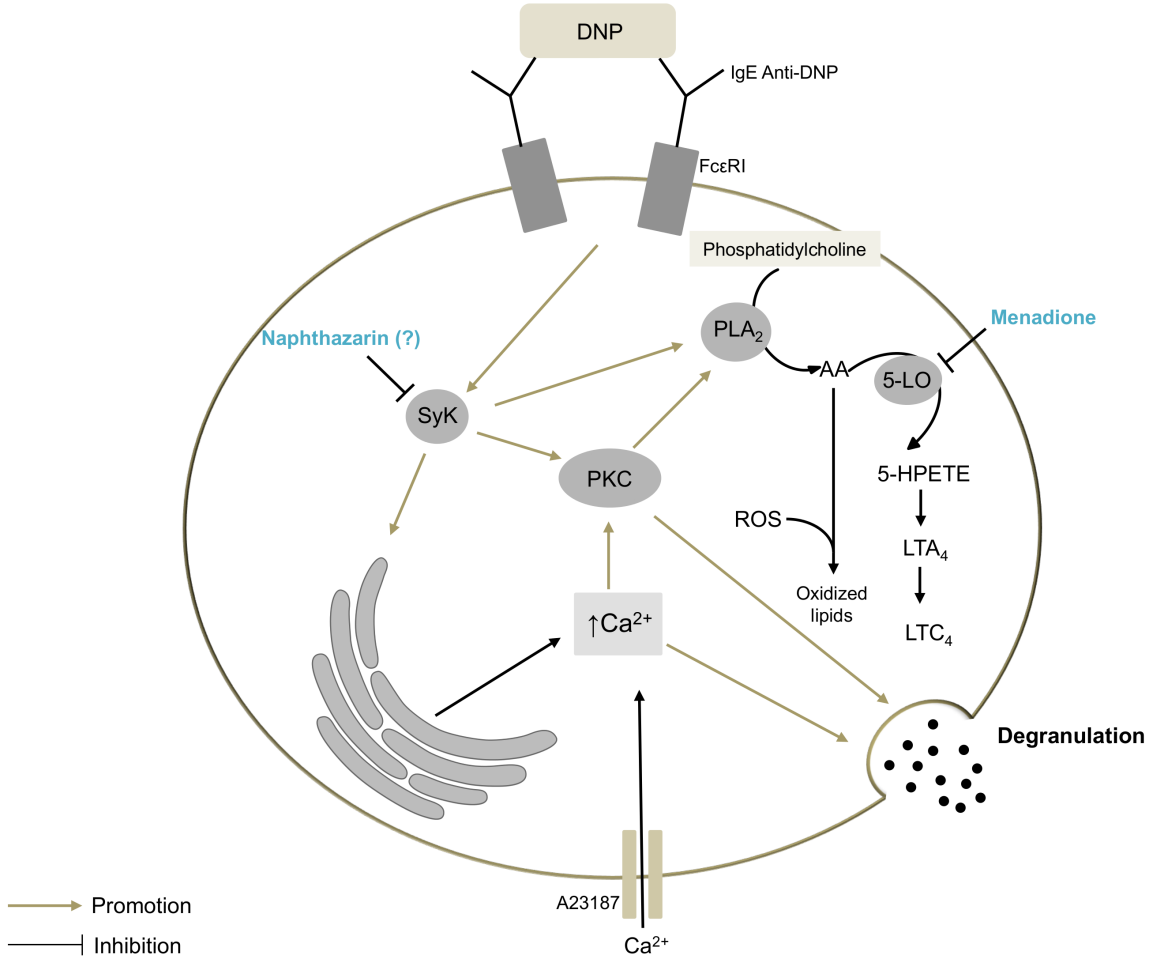

Figure 3.2.7. Simplified scheme of RBL-2H3 cells' degranulation pathways. The DNP antigen activates multiple signal transduction pathways via the IgE anti-DNP/FcεRI receptor complex. DNP receptor binding activates the immunoreceptor tyrosine activation motifs (ITAM)-Spleen tyrosine kinase (SyK) pathway that can be inhibited by shikonin (369) and probably by naphthazarin. Activated Syk catalyses protein phosphorylation of several proteins, leading indirectly to the activation of protein kinase C (PKC) that induces degranulation and the activation of phospholipase A_2 (PLA_2). PLA_2 increases arachidonic acid (AA) bioavailability that can be converted in leukotrienes (LT) by 5-lipoxygenase (5-LO; inhibited by menadione), or in oxidized lipids by means of ROS production. 5-LO converts AA into 5-hydroperoxyeicosatetraenoic acid (5-HPETE), which is metabolised to an unstable epoxide, LTA_4, and finally in LTC_4, in RBL-2H3 cells. The increase in intracellular calcium by SyK pathway, as well as by A23187 promotes degranulation.

immediately precede degranulation: increase of intracellular calcium) (**Figure 3.2.7**). These complementary stimuli assist characterization of the mechanisms by which the studied compounds reduce degranulation. In the present study, the release of immune cell degranulation markers – β-hexosaminidase and histamine (355) – was higher with ionophore than with IgE/antigen treatment, consistently with previous studies (370).

Naphthazarin (0.1 μM) decreased IgE/antigen-induced degranulation (**Figure 3.2.2*C***) and the labelling with FITC-annexin-V (**Figure 3.2.4**), reported to bind specifically to phosphatidylserine near sites of granule fusion (371). However, the same naphthazarin concentration failed to reduce ionophore-induced degranulation (**Figure 3.2.3*C***), suggesting that naphthazarin's mechanism of degranulation inhibition is upstream of intracellular calcium increase. While this is the first report for naphthazarin, a similar mechanism was previously described for another naphthoquinone, namely, shikonin (372). Shikonin reportedly inhibits the spleen tyrosine kinase (SyK), downstream from FcεRI activation, possibly explaining its anti-allergic properties (372). Meaningfully, naphthazarin displays the highest structural similarities to shikonin, among the naphthoquinones in the present study. In fact, both compounds share a 5,8-dihydroxy-1,4-naphthoquinone core (**Figure 3.2.1**). Thus, we propose that naphthazarin and shikonin act through a similar mechanism and that

both C5 and C8 hydroxyls modulate direct enzyme interaction via hydrogen bonds (373).

Diospyrin (10 μM) reduced degranulation in calcium ionophore-stimulated cells (**Figure 3.2.3*C***). Another naphthoquinone, acetylshikonin, was reported to attenuate ionophore-mediated intracellular calcium elevation in rat neutrophils (369). While, attenuation of calcium elevation might partly explain the effects of both diospyrin and acetylshikonin, their spectrum of activity does not necessarily overlap, since acetylshikonin is reported to decrease leukotriene B_4 and tromboxane A_2 (369), whereas in the present study diospyrin was unable to reduce leukotrien C_4, albeit in different cell models and stimuli.

Plumbagin was previously reported to exhibit anti-allergic properties, namely, at 5 μM plumbagin inhibited cytokines production by phytohemagglutinin-stimulated peripheral blood mononuclear cells (PBMC) (87). In the present study, the maximum non-toxic concentration of plumbagin that could be tested in RBL-2H3 cells was 1 μM, and at that concentration plumbagin did not prevent degranulation evoked by either IgE/antigen or A23187.

Following degranulation studies, we addressed the inhibition of enzymes involved in allergic responses: hyaluronidase and lipoxygenase. Hyaluronidase increases vascular permeability in inflammation, by cleavage of internal β-N-acetyl-D-glucosaminidic linkages of hyaluronic acid (374), thus being a possible target for anti-allergic drugs. Our data shows that the tested monomeric and dimeric naphthoquinones are poor hyaluronidase inhibitors, with only menadione and naphthazarin displaying modest inhibitory activity (**Figure 3.2.5**). 5-Lipoxygenase is a rate-limiting enzyme for leukotriene synthesis, converting arachidonic acid into 5-hydroperoxyeicosatetraenoic acid (5-HPETE). 5-HPETE is metabolised to an unstable epoxide LTA_4, which is transformed to LTB_4 or LTC_4 according with the cell type and the enzymes present (**Figure 3.2.7**) (375). In RBL-2H3 cells, LTC_4 is the major leukotriene released, while LTD_4 and LTE_4 are not produced (376). Soybean lipoxidase is often used to model human 5-, 12- and 15-lipoxygenases, given the high catalytic domain similarity between plant and mammalian lipoxygenases (377). All tested naphthoquinones exhibited lipoxidase inhibiting activity (**Figure 3.2.6*A***). Dimeric naphthoquinones (diospyrin and diosquinone), and the monomeric menadione were the most potent, showing the lowest IC_{50} values (**Table 3.2.1**). Considering that these three naphthoquinones are the most lipophilic of the studied compounds, our results raise the hypothesis that naphthoquinones inhibit lipoxidase by competing with natural lipophilic substrates.

Considering the results obtained with soybean lipoxidase, we tested the inhibition of leukotriene production by diospyrin, diosquinone and menadione. Menadione was the only naphthoquinone able to reduce leukotriene production, achieving full inhibition at 5 μM (**Figure 3.2.6*C***). Higher menadione concentrations (50-200 μM) were previously reported to reduce leukotriene production by inhibiting 5-lipoxygenase translocation to the nuclear membrane (91). Given that menadione is a known oxidative stress generator (378), and that reactive oxygen species (ROS) may react with arachidonic acid forming oxidized lipids (**Figure 3.2.7**) (379), decreased LTC_4 with our lower menadione concentrations may stem from decreased arachidonic acid availability. Consitently with our concentration range, menadione was reported to inhibit prostaglandin H_2 synthase via ROS production with an IC_{50} of 5 μM (380).

Concluding, we evaluated the anti-allergic properties of monomeric and dimeric naphthoquinones by studying the inhibition of RBL-2H3 basophils' degranulation and LTC_4 production induced by allergic stimuli, as well as by the evaluation of inhibition of enzymes involved in allergic responses. To our knowledge, this is the first study addressing the anti-allergic potential of diospyrin, diosquinone, naphthazarin and juglone. Naphthazarin and diospyrin reduced degranulation by different mechanisms of action. Naphthazarin and diospyrin acted, respectively, upstream and downstream of the intracellular calcium increase. In spite of being poor inhibitors of hyaluronidase, naphthoquinones inhibited lipoxidase and menadione reduced leukotriene production. Thus, this work expands the current knowledge on the biological properties of naphthoquinones, highlighting naphthazarin, diospyrin and menadione as potential lead compounds for structural modification in the process of improving and developing novel anti-allergic drugs.

Funding. The authors thank "Fundação para a Ciência e a Tecnologia" (FCT) for grant PEst-C/EQB/LA0006/2011. Brígida R. Pinho is grateful to FCT for her PhD fellowship (SFRH/BD/63852/2009).

3.3. How mitochondrial dysfunction affects zebrafish development and cardiovascular function: An *in vivo* model for testing mitochondria-targeted drugs

Br J Pharmacol 2013 Mar; 169 (5): 1072-90.

BJP British Journal of Pharmacology

DOI:10.1111/bph.12186
www.brjpharmacol.org

RESEARCH PAPER

How mitochondrial dysfunction affects zebrafish development and cardiovascular function: an *in vivo* model for testing mitochondria-targeted drugs

Brígida R Pinho[1,2], Miguel M Santos[3,4], Anabela Fonseca-Silva[1], Patrícia Valentão[2], Paula B Andrade[2] and Jorge M A Oliveira[1]

[1]*REQUIMTE, Department of Drug Sciences, Pharmacology Lab, Faculty of Pharmacy, University of Porto, Porto, Portugal,* [2]*REQUIMTE, Department of Chemistry, Pharmacognosy Lab, Faculty of Pharmacy, University of Porto, Porto, Portugal,* [3]*CIMAR/CIIMAR – Interdisciplinary Centre of Marine and Environmental Research, University of Porto, Porto, Portugal, and* [4]*FCUP – Department of Biology, Faculty of Sciences, University of Porto, Porto, Portugal*

Correspondence
Jorge M. Ascenção Oliveira, *REQUIMTE*, Departamento de Ciências do Medicamento, Laboratório de Farmacologia, Faculdade de Farmácia, Universidade do Porto, R. Jorge Viterbo Ferreira, 228, 4050-313 Porto, Portugal. E-mail: jorgemao@ff.up.pt

Keywords
mitochondria; zebrafish; *Danio rerio*; idebenone; decylubiquinone; atovaquone; menadione

Received
4 December 2012
Revised
8 March 2013
Accepted
15 March 2013

How mitochondrial dysfunction affects zebrafish development and cardiovascular function: An *in vivo* model for testing mitochondria-targeted drugs

Brígida R. Pinho[1,2], Miguel M. Santos[3,4], Anabela Fonseca-Silva[1], Patrícia Valentão[2], Paula B. Andrade[2] and Jorge M. A. Oliveira[1] *

[1]REQUIMTE, Department of Drug Sciences, Pharmacology Lab, Faculty of Pharmacy, University of Porto, Porto, Portugal, [2]REQUIMTE, Department of Chemistry, Pharmacognosy Lab, Faculty of Pharmacy, University of Porto, Porto, Portugal, [3]CIMAR/CIIMAR – Interdisciplinary Centre of Marine and Environmental Research, University of Porto, Porto, Portugal; and [4]FCUP – Department of Biology, Faculty of Sciences, University of Porto, Porto, Portugal

Abstract

BACKGROUND AND PURPOSE

Mitochondria are a drug target in mitochondrial dysfunction diseases and in antiparasitic chemotherapy. While zebrafish is increasingly used as a biomedical model, its potential for mitochondrial research remains relatively unexplored. Here, we perform the first systematic analysis of how mitochondrial respiratory chain inhibitors affect zebrafish development and cardiovascular function, and assess multiple quinones, including ubiquinone mimetics idebenone and decylubiquinone, and the antimalarial atovaquone.

EXPERIMENTAL APPROACH

Zebrafish (*Danio rerio*) embryos were chronically and acutely exposed to mitochondrial inhibitors and quinone analogues. Concentration-response curves, developmental and cardiovascular phenotyping were performed together with sequence analysis of inhibitor-binding mitochondrial subunits in zebrafish *versus* mouse, human and parasites. Phenotype rescuing was assessed in co-exposure assays.

KEY RESULTS

Complex I and II inhibitors induced developmental abnormalities, but their submaximal toxicity was not additive, suggesting active alternative pathways for complex III feeding. Complex III inhibitors evoked a direct normal-to-dead transition. ATP synthase inhibition arrested gastrulation. Menadione induced hypochromic anaemia when transiently present following primitive erythropoiesis. Atovaquone was over 1000-fold less lethal in zebrafish than reported for *Plasmodium falciparum*, and its toxicity partly rescued by the ubiquinone precursor 4-hydroxybenzoate. Idebenone and decylubiquinone delayed rotenone- but not myxothiazol- or antimycin-evoked cardiac dysfunction.

CONCLUSION AND IMPLICATIONS

This study characterizes pharmacologically induced mitochondrial dysfunction phenotypes in zebrafish, laying the foundation for comparison with future studies addressing mitochondrial dysfunction in this model organism. It has relevant implications for interpreting zebrafish disease models linked to complex I/II inhibition. Further, it evidences zebrafish's potential for *in vivo* efficacy or toxicity screening of ubiquinone analogues or antiparasitic mitochondria-targeted drugs.

Keywords: Mitochondria; zebrafish; *Danio rerio*; idebenone; decylubiquinone; atovaquone; menadione.

Introduction

Mitochondrial dysfunction is a common feature in multiple human diseases. Mitochondrial diseases present diverse clinical symptoms with the most common being neurological and cardiological manifestations, including cardiomyopathies and heart conduction defects (190, 210). Mutations in mitochondrial DNA (mDNA) may affect respiratory chain elements or ribosomal and transfer RNAs required for mitochondrial gene expression, causing diseases such as Leber's hereditary optic neuropathy or mitochondrial myopathy, encephalopathy, lactic acidosis and stroke syndrome (190). Also, mutations in nuclear encoded mitochondrial proteins are associated with human diseases (e.g. optic atrophy or Charcot-Marie-Tooth 2A). Furthermore, key neurodegenerative disorders such as Alzheimer, Parkinson and Huntington diseases, among others, have been associated with mitochondrial dysfunction (381). Current treatment options for mitochondrial dysfunction disorders are scarce and mostly

symptomatic (205). Further treatment development is partly hindered by limited *in vivo* models of mitochondrial disease. Notably, strong purifying selection in the mammalian female germ line imposes difficulties in establishing mouse models of mDNA mutations (382).

Zebrafish (*Danio rerio*) is increasingly used for modelling human diseases (383). Its mitochondrial genome is sequenced (384) and zebrafish is emerging as a model for studying mitochondria-linked disorders. Indeed, silencing mitofusin-2 in zebrafish generated an *in vivo* model of Charcot-Marie-Tooth 2A neuropathy (385). Similarly, depletion of cytochrome *c* oxidase, optic atrophy 3 protein and electron transfer flavoprotein dehydrogenase (ETFDH) were respectively used to model cytochrome *c* oxidase deficiency (386), Costeff syndrome (387) and multiple acyl-CoA dehydrogenase deficiency in zebrafish (388). Moreover, zebrafish was reported sensitive to mitochondrial toxins linked to Parkinson's disease (319), and parkin knockdown in embryos led to mitochondrial complex I deficiency (389). Currently, few studies addressed normal zebrafish mitochondrial physiology and bioenergetics. These include analysis of mDNA metabolism (390), oxygen consumption (391), calcium buffering and mitochondrial permeability transition (392) in zebrafish embryos. Still, further studies are required to validate zebrafish as a model to study mitochondrial dysfunction and its experimental treatment, including the identification of similarities and specific limitations when extrapolating towards mammalian physiology.

Here, we model mitochondrial dysfunction in zebrafish and use it to test mitochondria-targeted drugs. We characterize the effects of mitochondrial inhibitors and quinone analogues on zebrafish embryonic development and cardiovascular function, identifying morphological and functional phenotypes associated with impaired respiratory complexes and ubiquinone deficiency. Among several quinone analogues, we test the ubiquinone mimetics idebenone and decylubiquinone. Also, we test the antimalarial atovaquone, appraising zebrafish's potential for differential toxicity screening of the growing class of mitochondria-targeted antiparasitic drugs (393).

Methods

Drugs, solvents and solutions

Mitochondrial inhibitors [rotenone, 3-nitropropionic acid (3NP), myxothiazol, antimycin and oligomycin] and all other drugs/chemicals were from Sigma-Aldrich (St. Louis, MO, USA), unless otherwise stated. Quinones analogues were: natural monomeric naphthoquinones [menadione (MND), juglone (JGL), naphthazarin (NTZ), plumbagin (PLB), lapachol (LPC) and β-lapachone (βLPC)]; natural dimeric naphthoquinones [diospyrin (DPR) and diosquinone (DQN)]; synthetic naphthoquinone [atovaquone (ATV)]; and synthetic benzoquinones [idebenone (IDB) and decylubiquinone (DCB)]. Other drugs include the ubiquinone synthesis precursor [4-hydroxybenzoic acid (4HB)] and respective inhibitor [4-nitrobenzoic acid (4NB)]; the NAD(P)H:quinone oxidore- ductase (NQO1) inhibitor [dicoumarol (DCM)]; and the control abnormality inducer [valproic acid (VPA)]. DPR and DQN were isolated from root barks of *Diospyros chamaethamnus* Dinter ex Mildbr (31). 4HB was from Extrasynthese (Genay Cedex, France). For all drugs, chemical structures are in Supporting Information **Figure 3.3.S1**, summarized data in **Table 3.3.2** and **Figure 3.3.5*C***, and their mechanism/ sites of action depicted in **Figure 3.3.8**. Stock drug solutions were prepared in water, DMSO or methanol, according to their solubility. Prior to assays, stocks were diluted in dechlorinated autoclaved water (egg water). Non-water drug solvents, DMSO or methanol, were kept constant at all drug dilutions and always below 0.5 or 0.05% respectively. These solvent concentrations induced no significant effects (**Figure 3.3.1*B***).

Egg production

Adult wild-type zebrafish (*D. rerio*), were maintained at 28 ± 1°C on a 14 h:10 h light:dark cycle, and handled for egg production as we previously detailed (394). Briefly, adults (14:7 male:female) were placed in a 30 L breeding tank on the day before egg collection. Ninety minutes after starting the light period, eggs were collected and cleaned. This time point was recorded as 0 h post fertilization (hours post fertilization, hpf; **Figure 3.3.1*A***).

Chronic drug exposure assays

Embryo maintenance and drug treatment. Embryos were randomly distributed in 12-well plates (10 embryos/well; 2 mL egg water/well) and kept at 28 ± 1°C on a 14 h:10 h light:dark cycle throughout the assay. Embryos were continuously exposed to drugs from 4 to 80 hpf. VPA, a known teratogen in zebrafish, was used as positive control for developmental abnormalities and also cardiovascular abnormalities such as bradycardia (395). Dead embryos were removed during the readings (**Figure 3.3.1*A***) and two out of three of each well content was renewed with freshly prepared drug solution at 32 and 56 hpf. All drug concentrations were assayed in duplicate wells (10 + 10 eggs), in at least three independent experiments (≥60 eggs).

Monitoring of zebrafish development and cardiac function. At regular time points (8, 32, 56 and 80 hpf:

Figure 3.3.1*A*) embryos were scored as normal, abnormal or dead; hached/ unhatched; using a stereomicroscope (Stemi DV4, Zeiss, Göttinger, Germany) or an inverted microscope (Eclipse TS 100, Nikon, Tokyo, Japan) with colour camera (Nikon 8400; Tokyo, Japan) for digital recording. Normal development was as previously described (292). Abnormalities were organized as: pigmentation, cardiac and structural – for subdivisions description and photographs see **Table 3.3.1** and **Figure 3.3.2*A***. Heart rates (**Figure 3.3.5*A***) were measured in two embryos per phenotype per well, during 20 s, at 80 hpf. Weighted averages (**Figure 3.3.5*Ai***) consider the embryos with/ without cardiac oedema among the live population per well. For detailed heartbeat analyses (**Figure 3.3.5*B***), videos were recorded at 20x magnification in an inverted microscope (Eclipse TE300, Nikon), with CCD camera (C6790; Hamamatsu Photonics, Hamamatsu, Japan) and Aquacosmos software (version 2.5; Hamamatsu Photonics). Videos were captured at 28 Hz during 10 s and processed with ImageJ (NIH) for assessing atrioventricular coordination.

Parameters and abnormality indexes. NC_{50}, AC_{25} and LC_{50} signify concentrations required for, respectively, 50% decrease in normal embryos, 25% of embryos with abnormalities and 50% lethality. LS and NS are slopes from concentration-response curves depicting dead and normal embryos respectively. Abnormality indexes were expressed by LC_{50}/NC_{50} and LS/-NS ratios. Both are ~1 when increasing drug concentrations convert normal embryos directly into dead embryos. When abnormal embryos survive, the LC_{50}/ NC_{50} ratio is >1. The LS/-NS can still be ~1, but otherwise is inversely proportional to the resilience of abnormal embryos to increasing drug concentrations. Indeed, an LS steeper or shallower than -NS signifies a more or less abrupt abnormal-to-dead conversion respectively.

Acute drug exposure assays

Hatched embryos at 56 hpf were randomly distributed in 12-well plates (10 embryos in 2 mL egg water/well). Following acute exposure to isolated or combined drugs, embryos were scored for presence/absence of circulation and heartbeat at 10

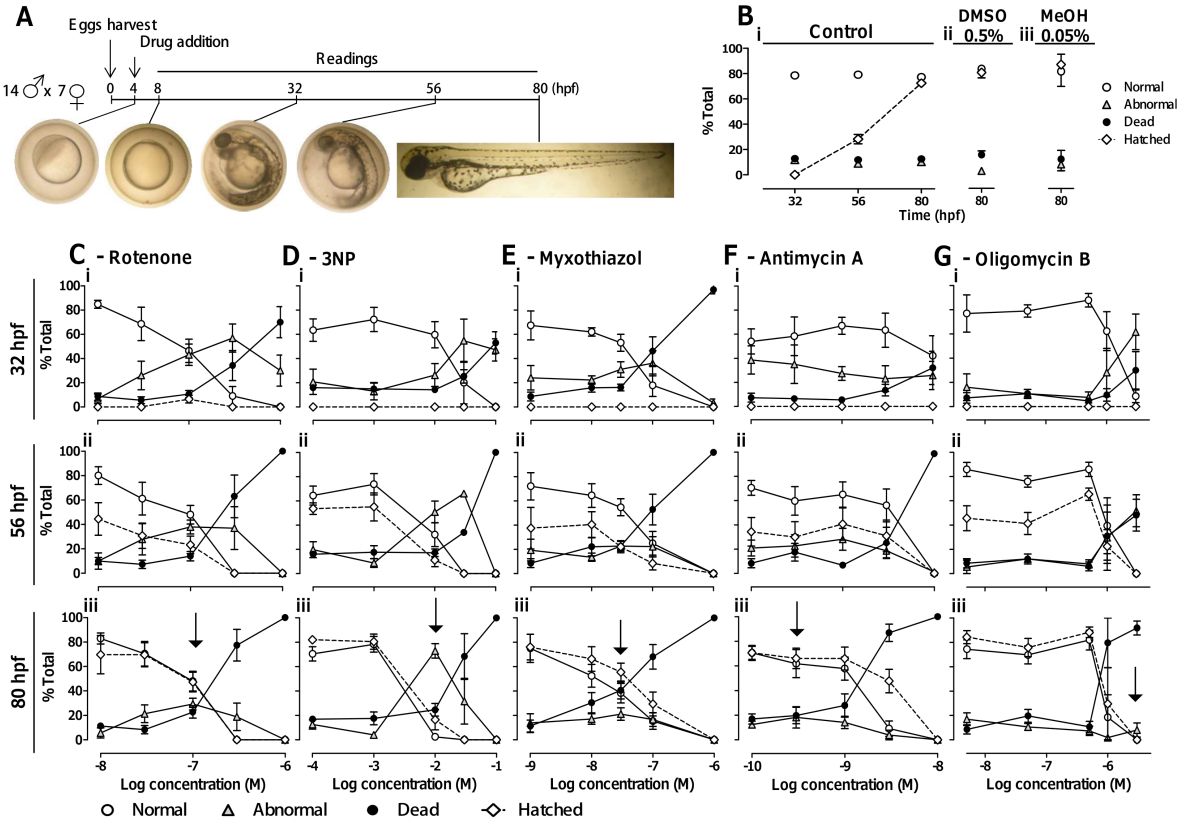

Figure 3.3.1. Mitochondrial inhibitors and zebrafish development. ***A***, Protocol and images of normal development. ***B***–***G***, Changes in normal (white *circles),* abnormal (grey *triangles),* dead (black *circles)* and hatched (white *diamonds)* embryos (% total) across time and drug concentrations. ***B***, Controls – egg water (***i***), with 0.5% DMSO (***ii***) and 0.05% methanol (***iii***, MeOH). ***C***–***G***, Mitochondrial inhibitors. Data are mean ± SEM of *n* independent experiments: control: *n* = 34, 4 and 4, for egg water, DMSO and MeOH, respectively; rotenone, *n* = 4–14; 3NP, *n* = 3–9; myxothiazol, *n* = 4–12; antimycin, *n* = 5–6; oligomycin, *n* = 3–5. C-Giii, Arrows – peak abnormalities at 80 hpf.

10 min intervals. For each treatment, 40–60 embryos, from two to three independent clutches, were assayed in two to three independent experiments, before data aggregation for Kaplan–Meier analysis.

Data sources and comparison of protein sequences

Protein sequence data of NADH dehydrogenase subunit 1 (ND1, complex I), succinate dehydrogenase complex subunit A (complex II), cytochrome *b* (complex III) and ATPase subunit 6 and 9 (complex V) were obtained from NCBI (http:// ncbi.nlm.nih.gov/ protein). Percentages of identity were calculated using BLAST (http://blast.ncbi.nlm.nih.gov/Blast. cgi). COBALT (http://www.ncbi.nlm.nih.gov/tools/cobalt) was used to align cytochrome *b* sequences (**Figure 3.3.3**).

Statistics

Values are mean ± SEM from *n* independent experiment, unless otherwise stated. Conventional 'E notation' is used when appropriate. For normally distributed data, *t*-test or ANOVA were used, respectively, to compare two or more groups. The Mann–Whitney test and Kruskal– Wallis ANOVA were used for non-normally distributed data. Changes in proportion of embryos with/without circulation or heartbeat were analysed via Kaplan–Meier. Cluster analysis was performed by *k*-means clustering, preceded by exploratory hierarchical clustering. Linear regressions (for computing NC_{50}, AC_{25}, LC_{50}, and slopes – NS, LS) and non-parametric tests were performed with GraphPad Prism version 5.0 (San Diego, CA, USA). All other statistical analyses were performed with SPSS 20.0 (SPSS Inc., Chicago, IL, USA). Differences from control were considered statistically significant when $P < 0.05$. Simultaneous biological relevance was assumed only for differences larger than 10% (Δ > 10%).

Results

Mitochondrial inhibitors induce different abnormalities in zebrafish

To assess how mitochondrial dysfunction affects zebrafish development, fertilized eggs were chronically exposed to different mitochondrial inhibitors. Protocol and concentration- response curves are in **Figure 3.3.1** and representative abnormalities (**Figure 3.3.2*A***) described in **Table 3.3.1**.

Complex I and II inhibitors (rotenone and 3NP, respectively) induced more abnormalities in surviving embryos than complex III inhibitors (myxothiazol and antimycin), which primarily induced a direct transition from normal to dead. The ATP synthase inhibitor (oligomycin) arrested surviving embryos at the gastrula stage, followed by a time-dependent death (**Figure 3.3.1*C*-*G*** and **Figure 3.3.2*B*-*G***). The order of potency for lethality was antimycin > myxothiazol > rotenone > oligomycin > 3NP (LC_{50} in **Table 3.3.2**). Comparing LC_{50}/ NC_{50} and LS/-NS ratios at 80 hpf (**Table 3.3.2**) highlights 3NP as the most frequent inducer of abnormalities among the mitochondrial inhibitors (highest LC_{50}/NC_{50} and lowest LS/-NS; AC_{25} = 3.4E3 ± 1.7E2 µM, *n* = 4), followed by rotenone, myxothiazol, antimycin and oligomycin. At 56 hpf, oligomycin stands out as an abnormality inducer, but the corresponding embryos do not survive until 80 hpf (**Table 3.3.2**, **Figure 3.3.2*G***).

Types and frequency of abnormalities varied across mitochondrial inhibitors (**Figure 3.3.2*B-G***). Rotenone and 3NP significantly decreased pigmentation (melanin) at 56 hpf suggesting developmental delay, and induced cardiovascular abnormalities (oedema and asystole); 3NP also caused necrotic lesions and head abnormalities (abnormal otoliths); **Figure 3.3.2*C*, *D***. Oligomycin-induced abnormalities were primarily arrests at the gastrula stage, lethal at 80 hpf (**Figure 3.3.2*G***). My-

Table 3.3.1. Description of zebrafish abnormalities. Criteria for scoring zebrafish as abnormal or dead, and respective reading times.

	Pigmentation		Cardiac abnormalities			Structural abnormalities			Dead
	Melanin	Anaemia	Oedema	Asystole	Lesions	Tail	Head	Gastrula	
Description	Decreased pigmentation	Hypochromic anaemia	Swelling in cardiac region and/or in yolk sac	Without heart beat and circulation	Necrosis - dark cell tissues Local clots or bleeding - accumulation of erythrocytes	Skeletal abnormalities - lordosis, kyphosis and other which cause tail curvature Abnormal caudal fins	Abnormal craniofacial structure Abnormal eyes Abnormal otoliths	Gastrulation arrest, without tissue decompostion	Generalized necrosis and desintegrated tissues
Reading time	≥32 hpf	≥56 hpf	≥32 hpf	≥56 hpf	≥32 hpf	≥32 hpf (except fins: ≥80hpf)	≥32 hpf (except otoliths: ≥80hpf)	≥32 hpf	≥8 hpf

xothiazol and antimycin evoked no statistically significant abnormalities (**Figure 3.3.2*E*, *F***), consistent with direct transition from normal to dead (**Figure 3.3.1*E*, *F***).

Heart rate analysis showed that bradycardia and cardiac oedema were strongly associated (**Figure 3.3.5*Aii*** *vs*. ***Aiii***; with few exceptions). Control heart rate was 179 ± 3 beats per minute (bpm) and 163 ± 5 bpm, for embryos without and with spontaneous oedema respectively (**Figure 3.3.5*Aiii***). Embryos with oedema caused by rotenone, 3NP, myxothiazol or oligomycin, all displayed concentration-dependent bradycardia, more pronounced than that caused by spontaneous oedema in controls (**Figure 3.35*Aiii***). In weighted average, however, only 3NP caused relevant bradycardia among the mitochondrial inhibitors (**Figure 3.3.5*Ai***), consistent with its higher proportion of oedema (**Figure 3.3.2*Diii***). Also, cluster analysis and scaling across three domains (cardiac, structural and pigmentation) clearly separated 3NP from all other mitochondrial inhibitors (Cluster 5; **Figure 3.3.5*C***).

Comparison of mitochondrial complex subunits between zebrafish, human, mouse and parasites targetable with quinone analogues

To appraise zebrafish for mitochondrial dysfunction modelling and drug testing, we compared inhibitor-binding subunits for rotenone (396), 3NP (397), myxothiazol, antimycin, atovaquone (393) and oligomycin (200) – (**Figure 3.3.3*A*, *B***). *Pneumocystis jiroveci* (398) and *Plasmodium falciparum* (399) are included because of relevant cytochrome *b* differences allowing selective targeting with atovaquone (393, 399). Zebrafish identity with human subunits is only 9–13% lower than mouse *versus* human, except for ATPase subunit 6 (**Figure 3.3.3*A***). Our LC_{50} for mitochondrial inhibitors in zebrafish were lower than LC_{50} or concentrations fully inhibiting mammalian mitochondrial complexes, except 3NP where only its AC_{25} approximated the LC_{50} reported for mammalian cells (**Table 3.3.2**). The

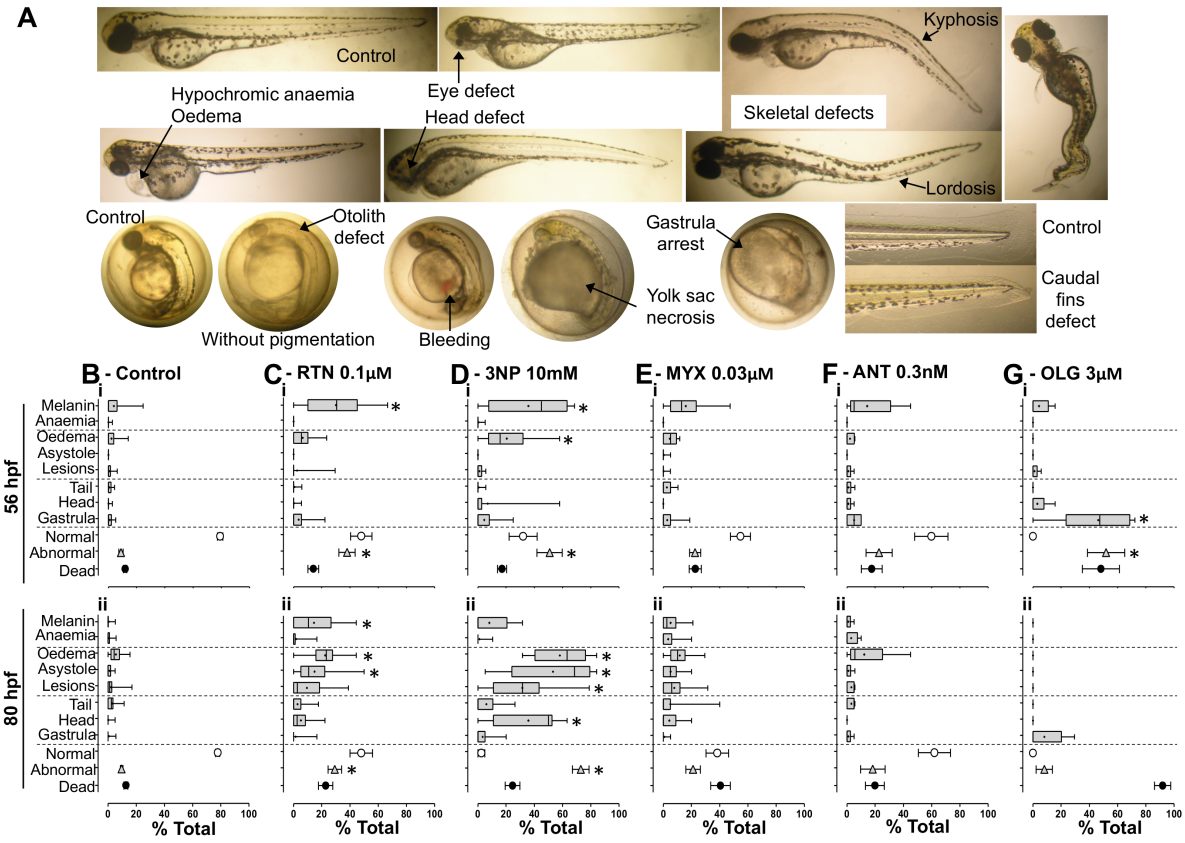

Figure 3.3.2. **Mitochondrial inhibitors and abnormalities in zebrafish.** ***A***, Representative abnormalities in comparison with post- and pre-hatched control embryos (top and bottom left, respectively) at 80 hpf. ***B***, Spontaneous abnormalities under control conditions; ***C***–***G***, Mitochondrial inhibitor induced abnormalities at the indicated concentrations (arrows in **Figure 1*C*-*Giii***); *Boxplots* (specific abnormalities, % total embryos) show median, mean (+), interquartile distances, maximum and minimum; *Symbols* (normal, *white circles;* abnormal, *grey triangles;* and dead; *black circles)* show mean ± SEM (% total, embryos). Data are from *n* independent experiments: control: *n* = 34; rotenone (RTN), *n* = 14; 3-nitropropionic acid (3NP), *n* = 9; myxothiazol (MYX), *n* = 12; antimycin (ANT), *n* = 5; oligomycin (OLG), *n* = 5. *P < 0.05 in *boxplots,* Kruskal–Wallis ANOVA with Dunn's *post hoc* (*vs*. control). *P < 0.05 in *grey triangles* (mean abnormalities), One-way ANOVA with Bonferroni *post hoc* (*vs*. control).

A - Percentage of identity

Mitocondrial complex	I			II			III				V			
Subunits/ sites	ND1			A			Cytrochome b				6 | 9			
Species	Human	Mouse	Zebrafish	Human	Mouse	Zebrafish	Human	Mouse	Zebrafish	*P. jiroveci*	Human	Mouse	Zebrafish	*P. jiroveci*
Mouse	78			95			79				76 | 90			
Zebrafish	67	69		83	83		70	74			52 | 77	52 | 76		
P. jiroveci	44	44	44	n.a.	n.a.	n.a.	51	51	56		31 | 70	32 | 70	30 | 70	
P. falciparum	n.a.	n.a.	n.a.	62	63	61	41	41	41	41	n.a.| 33	n.a.| 33	n.a.| 27	n.a.| 39

B - Cytochrome b sequence

Figure 3.3.3. Amino acid sequence comparison of mitochondrial inhibitor-binding subunits. ***A***, Percentage of identity among inhibitor-binding subunits of mitochondrial complexes I, II, III and V (NADH dehydrogenase subunit 1, ND1*;* succinate dehydrogenase subunit A, cytochrome *b,* and ATPase subunits 6 and 9), from human, mouse, zebrafish and parasites targetable with quinone analogues (*P. jiroveci* and *P. falciparum;* 'n.a.', not applicable – no homologue subunit in this species). ***B***, Comparison of Qo and Qi sites (grey *highlight). Xn* summarises non-Q_o/Q_i amino acids.

genetic and functional correlation is evidenced by ND1 and complex V subunit 6 absence in *Pl. falciparum versus* zebrafish/ mammals, and the associated 10-fold higher concentrations required for rotenone or oligomycin to kill *Pl. falciparum versus* zebrafish embryos in this study (**Table 3.3.2**). Differences in cytochrome *b* Q_o (binds myxothiazol/ atovaquone) and Q_i (binds antimycin) (**Figure 3.3.3B**) are functionally relevant since antimycin displays >1000-fold lower LC_{50} towards zebrafish/ mammals *versus* parasites. Therapeutically more relevant, atovaquone displays much higher toxicity towards *Pl. falciparum versus* zebrafish/ mammals (**Table 3.3.2**)

Quinone analogues and other ubiquinone-related compounds induce different abnormalities in zebrafish

Aiming to validate zebrafish as *in vivo* model for exploring the therapeutic potential of quinone analogues, we tested their effects in chronically (4–80 hpf) exposed embryos, along with other drugs for mechanistic studies (Supporting Information **Figure 3.3.S1**). All 11 quinone analogues were lethal within the tested range of concentrations (**Table 3.3.2**). The LC_{50} interval 0.5–1 µM includes PLB, DQN and JGL; 1–10 µM includes ATV, βLPC, DPR, MND, NTZ, IDB and LPC. The least lethal of all quinone analogues was decylubiquinone (DCB; LC_{50} at 80 hpf = 20.10 ± 0.74 µM, *n* = 3). Other drugs exhibited an LC_{50} comprised between 21 µM and 4 mM (DCM, VPA and 4NB); The LC_{50} for 4HB was > 5 mM, its AC_{25} at 80 hpf was 1.3 ± 0.66 mM, *n* = 5. Relatively few (4:11) quinone analogues induced a significant proportion of structural/functional abnormalities (ATV, LPC, MND and DCB; **Table 3.3.2**, LC_{50}/ NC_{50} > 1; **Figure 3.3.4**). Among the 'other drugs', 4NB, DCM and VPA exhibited an LC_{50}/NC_{50} > 1 at either 56 or 80 hpf (**Table 3.3.2** and **Figure 3.3.4**).

Atovaquone induced abnormalities were primarily cardiac oedema and focal lesions (e.g. bleedings/clots), most noticeable at 1 mM and 56 hpf (some lethal at 80 hpf; **Figure 3.3.4*A***). Meaningfully, although atovaquone shares complex III inhibition with myxothiazol and antimycin (**Figure 3.3.8*A***), it induces different abnormalities (**Figure 3.3.2*E***, ***F*** *vs.* **Figure 3.3.4*A***), which may be better explained by atovaquone's inhibition of ubiquinone synthesis (**Figure 8*D***). Consistently, the ubiquinone synthesis inhibitor 4NB replicated distinguishing atovaquone features, such as focal lesions and pronounced cardiac oedema without relevant bradycardia (**Figure 3.3.4*A*** *vs*. **Figure 3.3.4*D***; **Figure 3.3.5*Aiii***).

Decylubiquinone's lethality was strikingly time-dependent increasing about 90% from 56 to 80 hpf (**Figure 3.3.4*B***). Decylubiquinone caused a tail fin anomaly (**Figure 3.3.2*A***; ~50% embryos at 10 µM; **Figure 4*Eiv***, 80 hpf), also observed within 90 min of exposure in hatched embryos (experiments in **Figure 3.3.7A**), suggesting altered neuromuscular tonus and

not necessarily developmental defects. Interestingly, the structurally related idebenone (terminal –OH in decylubiquinone's aliphatic chain; Supporting Information **Figure 3.3.1**) displayed higher lethality (~3x lower LC_{50}; **Table 3.3.2**) and no significant abnormalities other than delayed pigmentation (melanin; **Figure 3.3.4C**).

Lapachol (10 mM) induced a diverse abnormality profile afflicting ~80% embryos at 56 hpf, precluding hatching and leading to >50% death at 80 hpf (**Figure 3.3.4*Fi*,*iii***). Lapachol caused decreased pigmentation (melanin), head defects (abnormal eyes, otoliths and craniofacial defects), gastrula arrest, oedema and asystole (**Figure 3.3.4 *Fii*,I *v***). Asystole was typically preceded by cardiac oedema and concentration-dependent bradycardia (**Figure 3.3.5*A***; with signs of atrioventricular block **Figure 3.3.5*Biii***). In contrast, dicoumarol (50 µM) abnormalities were merely decreased melanin (**Figure 3.3.4*G***).

Menadione (1 µM) was the single most powerful inducer of hypochromic anaemia among 20 compounds, affecting the majority of embryos at 80 hpf (**Figure 3.3.4*H***). We thus investigated hypochro-

Table 3.3.2. Comparative toxicity of mitochondrial inhibitors, quinone analogues and other drugs in zebrafish *vs*. other species.

[1]-[45] are literature references for drug effects, provided as supporting information Appendix S1.

Parameter index / Drug	Time (hpf)	Present Study: Zebrafish Embryos				Literature data: Mammals		Zebrafish	Parasites	
						Human (or Rat R)		*D. rerio*		
		LC_{50} (µM)	AC_{25} (µM)	LC_{50}/NC_{50}	LS/-NS	Normal cells	Cancer cells	ØEmbryo §Adult	*P. jiroveci*	*P. falciparum*
						LC_{50} (µM)				
Mitochondrial inhibitors						Neurons	Glioma			
Rotenone	56	0.36 ± 0.11	0.11 ± 0.02	2.8 ± 0.54	0.54 ± 0.15	2[1]#R	4.7-7.3[2]	Ø >1[3]		27.0±3.5[4]
(**RTN**, *n*=4)	80	0.30 ± 0.09	0.09 ± 0.03	2.2 ± 0.41	0.49 ± 0.18					
3-Nitropropionate	56	4.9E4 ± 2.1E3	9.5E3 ± 3.3E3	5.4 ± 2.49	0.13 ± 0.07	1.0E3[5]R				158.1±11.2[4]
(**3NP**, *n*=3)	80	3.7E4 ± 9.7E3	3.4E3 ± 1.7E2	6.8 ± 1.80	0.19 ± 0.09					
Myxothiazol	56	0.06 ± 0.01	n.a.	1.1 ± 0.21	1.19 ± 0.13	2[6]#R	1.4-22.6[2]	Ø >0.5[3]		0.21±0.01[7]
(**MYX**, *n*=4)	80	0.04 ± 0.01	n.a.	1.6 ± 0.27	1.20 ± 0.73					
Antimycin	56	5.4E-3 ± 1.1E-3	4.5E-4 ± 1.6E-4	1.1 ± 0.10	1.31 ± 0.13	3[1]#R	0.15-0.28[2]		>100[8]	6.2E3±3.3E3[9]
(**ANT**, *n*=4)	80	2.9E-3 ± 6.8E-4	n.a.	1.2 ± 0.24	0.98 ± 0.24					
Oligomycin	56	n.a.	1.20 ± 0.32	n.a.	0.45 ± 0.24	3[6]#R	0.27[10]¥	Ø >10[3]	>12.5[11]	>12.5[12]
(**OLG**, *n*=4)	80	1.23 ± 0.29	n.a.	1.0 ± 0.02	1.12 ± 0.11					
Quinone analogues						PBMC	Leukemic cells			
Atovaquone	56	1.76 ± 0.13	0.41 ± 0.05	2.0 ± 0.25	1.00 ± 0.54		15-30[13]¥	§ 0.86[14]	0.3-4.6[8,15]	3.4E-4±2.0E-3[4,9,16]
(**ATV**, *n*=4)	80	0.88 ± 0.24	n.a.	2.2 ± 0.74	0.98 ± 0.22					
β-Lapachone	56	1.92 ± 0.14	n.a.	1.1 ± 0.02	1.22 ± 0.06	8-16[17]	1.65[18]	Ø >2[19]		4.1±1.2[20]
(**βLPC**, *n*=3)	80	1.87 ± 0.12	n.a.	1.1 ± 0.05	1.30 ± 0.14					
Decylubiquinone	56	n.a.	11.28 ± 4.46	n.a.	0.18 ± 0.05		>50[21]			
(**DCB**, *n*=3)	80	20.10 ± 0.74	4.03 ± 0.70	1.7 ± 0.64	1.01 ± 0.35					
Diospyrin	56	2.04 ± 0.02	n.a.	1.2 ± 0.09	1.16 ± 0.08	78.3± 3.4[22]	>100[23]		2.6-7.8[15]	9.9[24]
(**DPR**, *n*=3)	80	2.00 ± 0.06	n.a.	1.1 ± 0.05	1.28 ± 0.13					
Diosquinone	56	0.57 ± 0.19	n.a.	1.1 ± 0.08	1.04 ± 0.15		0.46-7.95[25]¥			
(**DQN**, *n*=3)	80	0.54 ± 0.17	n.a.	1.1 ± 0.09	1.02 ± 0.07					
Idebenone	56	7.36 ± 0.07	n.a.	1.2 ± 0.16	1.06 ± 0.12	>1.0E3[26]R£	>15[27]¢			
(**IDB**, *n*=3)	80	5.65 ± 0.36	n.a.	1.2 ± 0.13	1.31 ± 0.13					
Juglone	56	0.62 ± 0.03	n.a.	1.0 ± 0.01	1.00 ± 0.04	>28.7[28]	4.1-8.4[29]			72.9[30]
(**JGL**, *n*=3)	80	0.62 ± 0.03	n.a.	1.0 ± 0.01	1.14 ± 0.04					
Lapachol	56	n.a.	2.47 ± 0.90	n.a.	0.29 ± 0.24	2.1-10[31]	16.0± 3.2[32]			18.7-42.1[20,30,33]
(**LPC**, *n*=4)	80	8.95 ± 3.65	3.25 ± 1.21	3.5 ± 0.91	0.19 ± 0.10					
Menadione	56	3.07 ± 0.49	0.89 ± 0.26	3.1 ± 0.88	0.68 ± 0.24	>10[34]	18±2.4[35]	§ 1.03[14]		
(**MND**, *n*=7)	80	1.56 ± 0.25	0.47 ± 0.06	2.6 ± 0.39	0.52 ± 0.10					
Naphthazarin	56	5.02 ± 0.28	n.a.	1.1 ± 0.04	1.07 ± 0.04					13.3[30]
(**NTZ**, *n*=3)	80	4.85 ± 0.37	n.a.	1.0 ± 0.04	1.04 ± 0.04					
Plumbagin	56	0.47 ± 0.04	n.a.	1.0 ± 0.02	1.01 ± 0.02	>100[36]	2.7[37]			0.27[38]
(**PLB**, *n*=5)	80	0.51 ± 0.08	0.27 ± 0.05	1.4 ± 0.10	1.37 ± 0.10					
Other drugs						PBMC	Leukemic cells			
4-Hydroxybenzoate	56	n.a.	2.0E3 ± 1.1E3	n.a.	0.71 ± 0.17	>1[39]			>1.0E4[40]	
(**4HB**, *n*=5)	80	n.a.	1.3E3 ± 6.6E2	n.a.	0.28 ± 0.44					
4-Nitrobenzoate	56	3.9E4 ± 4.6E3	2.0E4 ± 1.6E4	2.7 ± 1.44	0.82 ± 0.36		>2.0E3[41]	Ø 154[42]		
(**4NB**, *n*=3)	80	3.9E4 ± 4.8E3	3.7E3 ± 3.2E3	7.4 ± 1.02	0.37 ± 0.28					
Dicoumarol	56	23.42 ± 21.19	19.43 ± 1.24	7.8 ± 5.74	0.45 ± 0.20		>50[43]	Ø >5[19]		113.7±11.5[4]
(**DCM**, *n*=3)	80	21.24 ± 6.16	n.a.	1.7 ± 0.58	1.27 ± 0.03					
Valproate	56	4.6E3 ± 2.9E3	4.2E3 ± 2.6E3	2.4 ± 1.39	0.44 ± 0.32	3.0E3[44]	2.0E3[44]	Ø 940-3.6E3[45]		
(**VPA**, *n*=3)	80	3.1E3 ± 1.1E3	4.5E2 ± 90.92	3.2 ± 0.65	0.69 ± 0.19					

¥ - Leukemic cell data not found; data are mean values of several cell lines.

£ - PBMC data not found; data are from rat astrocytes .

¢ - Leukemic cell data not found; data are from neuroblastoma cell line (SHSY-5Y).

- LC_{50} not found; data are concentrations inducing maximal effects.

§ - Adult zebrafish.

R - Human data not found; data are from rat neurons.

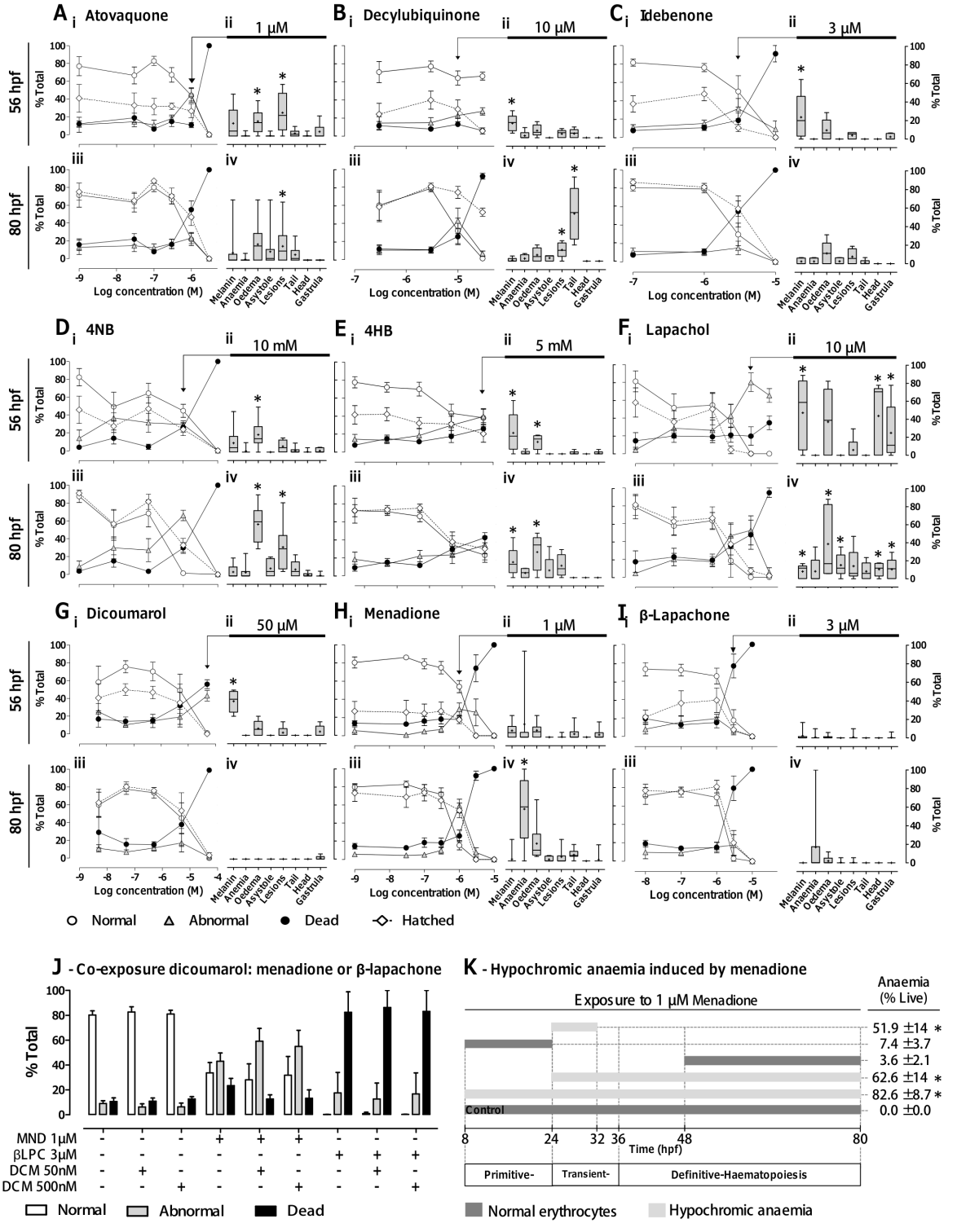

Figure 3.3.4. Influence of quinone analogues and ubiquinone related compounds on zebrafish development. ***A-I***, ***i***, ***iii***, Mean ± SEM of changes in normal, abnormal, dead and hatched embryos (% total) for the indicated times (56 and 80 hpf) and drug concentrations; ***ii***, ***iv***, *Boxplots* (specific abnormalities, % total embryos) show median, mean (+), interquartile distances, maximum and minimum, for the indicated concentrations (arrow; peak abnormalities at 80 hpf). Data are from *n* independent experiments with: ***A***, atovaquone, *n* = 3–12; ***B***, decylubiquinone, *n* = 4–8 ***C***, idebenone, *n* = 3–8; ***D***, 4NB, *n* = 3–11; ***E***, 4HB, *n* = 4–16; ***F***, lapachol, *n* = 3–5; ***G***, dicoumarol, *n* = 3–8; ***H***, menadione, *n* = 3–15; and ***I***, β-lapachone, *n* = 3–10. *P < 0.05, Mann–Whitney (*vs*. control) if difference in medians >10%. ***J***, Effect of dicoumarol [DCM; NQO1 inhibitor, (Preusch *et al.,* 1991)] upon abnormalities induced by menadione (MND) or β-lapachone (βLPC) at 80 hpf. *P* > 0.05 for differences between MND/βLPC alone versus combined with 50 or 500 nM DCM, one-way ANOVA with Bonferroni *post hoc, n* = 5–6. ***K***, Periods of menadione (1 µM) exposure and resulting mean ± SEM of embryos with hypochromic anaemia (% live, 80 hpf). **P* < 0.05 *versus* 48–80hpf exposure, ANOVA with Bonferroni *post hoc, n* = 3–4 independent experiments. The

periods of primitive, transient and definitive haematopoiesis were derived from Chen and Zon (400).

mic anaemia, modulating the duration and developmental stage of menadione exposure. Strikingly, a short exposure from 24 to 32 hpf sufficed to evoke over 50% hypochromic anaemia at 80 hpf, whereas longer exposures at earlier (8–24 hpf) or later (48-80 hpf) stages resulted in normally coloured erythrocytes at 80 hpf (**Figure 3.3.4*K***).

Rescue experiments with ubiquinone analogues or precursor during chronic mitochondrial inhibition

Idebenone and decylubiquinone fail to rescue chronic mitochondrial inhibition. Following individual drug titration, we tested whether ubiquinone analogues rescued the effects of chronic mitochondrial inhibition in zebrafish. Embryos were chronically exposed to concentrations inducing the highest percentage of abnormalities at 80 hpf for rotenone (0.1 µM), 3NP (10 mM), myxothiazol (0.03 µM) and atovaquone (1 µM), in the presence or absence of the highest concentration of ubiquinone analogues without detectable chronic toxicity (1 µM idebenone; 3 µM decylubiquinone). Neither idebenone nor decylubiquinone rescued changes in number of normal embryos, hatching, heart rate or oedema induced by chronic mitochondrial inhibition (**Figure 3.3.6*A***).

Zebrafish has active alternative ubiquinone reduction pathways. Lack of rescuing from chronic complex I or II inhibition with ubiquinone analogues prompted us to test whether combined rotenone and 3NP displayed additive toxicity. Results showed that the combination of rotenone (0.1 µM) with 3NP (10 mM) does not exceed the toxicity of 3NP alone (**Figure 3.3.6*C***). Together with development beyond the gastrula stage requiring mitochondrial ATP synthesis (oligomycin effect; **Figure 3.3.2*G***), these results suggest that alternative ubiquinone reduction pathways actively feed complex III (**Figure 3.3.8*C***), supporting mitochondrial ATP synthesis.

Given the possible contribution of NQO1 in the reduction of idebenone to idebenol and feeding of complex III [(9); **Figure 3.3.8*D***], we appraised the contribution of this enzyme by testing how its inhibitor dicoumarol modulated toxicity of its substrates – menadione and β-lapachone. Results showed that dicoumarol (50 or 500 nM; concentrations devoid of lethality, **Figure 3.3.4*G***) did not significantly increase the toxicity of 1 µM menadione [predicted to be detoxified by NQO1; (401)] and did not decrease the toxicity of 3 µM β-lapachone [predicted to be bioactivated by NQO1; (402) (**Figure 3.3.4*J***, **Figure 3.3.8*D***).

The ubiquinone precursor 4HB rescues atovaquone but not myxothiazol or antimycin toxicity. Given the central role of ubiquinone and complex III in energizing the mitochondrial respiratory chain, we tested whether the ubiquinone precursor 4HB (5 µM) could rescue the toxicity of complex III inhibitors (**Figure 3.3.6*B***). Although failing to rescue embryos from myxothiazol or antimycin toxicity, 4HB significantly rescued atovaquone toxicity, increasing the proportion of normal embryos (**Figure 3.3.36*Bi***; $P < 0.05$, $\Delta > 10\%$) and displaying a trend towards decreased oedema (**Figure 3.3.6*Biii***; ATV *vs*. ATV + 4HB). 4HB failed to rescue the effects of the ubiquinone synthesis inhibitor 4NB (**Figure 3.3.6*B***). The 2000-fold difference in concentrations required for 4NB toxicity (10mM; **Figure 3.3.4*D***) *vs*. 4HB efficacy (5 µM; **Figure 3.3.6*B***), and the toxicity displayed by ≥ 5 mM 4HB (**Figure 3.3.4*E***) precluded equimolar competition in rescue assays with 4HB and 4NB.

Rescue experiments with ubiquinone analogues upon acute mitochondrial inhibition

Acute complex I inhibition with rotenone induces cardiac insufficiency and asystole via ATP depletion. Following literature data supporting *in vitro* rescuing by ubiquinone analogues of decreased mitochondrial oxygen consumption or ATP levels in synaptosomes (135), cell lines (9) or isolated mitochondria (117), we aimed to establish an *in vivo* testing paradigm for ubiquinone analogues in zebrafish. Thus, we monitored circulation and heartbeat in 56 hpf embryos acutely challenged with mitochondrial inhibitors with or without ubiquinone analogues (idebenone or decylubiquinone; **Figure 3.3.7**). Circulatory arrest upon acute mitochondrial inhibition was associated with bradycardia and atrioventricular block (e.g. **Figure 3.3.5*Biii***) or supraventricular arrhythmia (e.g. **Figure 3.3.5*Biv***), and followed by asystole. Mitochondrial ATPase inhibition (oligomycin) evoked circulatory arrest. When combined, oligomycin did not modify rotenone's circulatory arrest (**Figure 3.3.7*Aii***), but delayed rotenone induced asystole by 18% (**Figure 3.3.7*Aiv***, $P < 0.05$). The latter can be explained by preventing ATP consumption upon rotenone induced ATPase reversal.

Idebenone and decylubiquinone delay the onset of cardiac dysfunction evoked by rotenone but not by myxothiazol or antimycin. Idebenone (3 µM) and decylubiquinone (30 µM) delayed rotenone induced cardiac insufficiency, respectively, by 61 and 79% (**Figure 3.3.7*Ai***, $P < 0.05$), and also delayed asystole

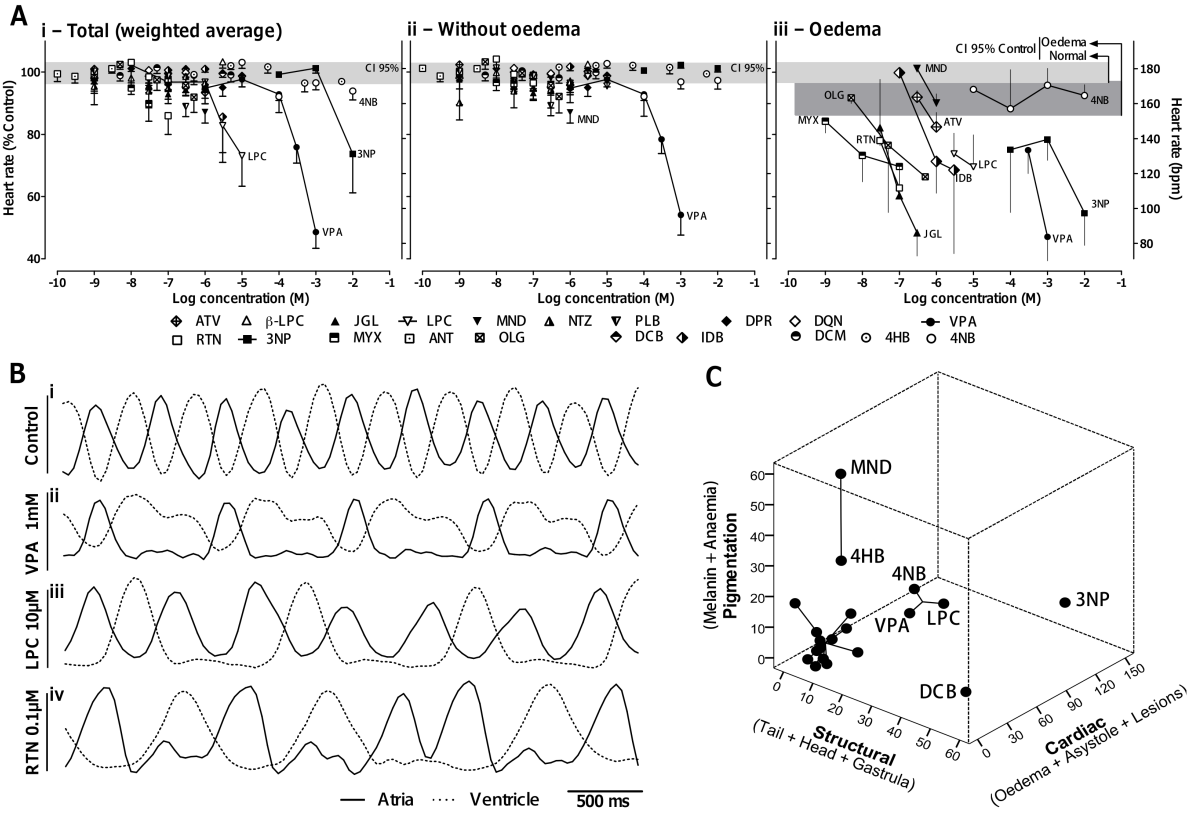

Figure 3.3.5. Detailed heartbeat analysis and multiple-abnormalities profiling. ***A***, Concentration-dependent changes in heart rate at 80 hpf, showing total weighted average (***i***, see Methods), and separating embryos without (***ii***) from those with (***iii***) cardiac oedema; embryos in asystole were excluded from calculations. Horizontal rectangles are the 95% confidence interval (CI) for control means without (light grey) and with (dark grey, ***iii***) spontaneous cardiac oedema, *n* = 33 experiments. Data for drugs are mean ± SEM from *n* = 3–14 experiments. ***B***, Detailed heartbeat analysis at 56 hpf showing examples of normal atrioventricular coordination and frequency (***i***), bradicardia (***ii***), atrioventricular block (***iii***) and supraventricular arrhythmia (***iv***). ***C***, Multi-dimensional scaling and clustering of abnormality profiles at 80 hpf. Axes are the sum of mean abnormalities for the respective subdomains (Table 3.3.1). Clusters: 1 (3NP); 2 (DCB); 3 (MND and 4HB); 4 (VPA, LPC and 4NB); 5 (all other drugs); *k-means* clustering.

respectively by 52 and 104% (**Figure 3.3.7*Aiii***, $P < 0.05$). In contrast, both ubiquinone analogues failed to protect from cardiac dysfunction induced by either myxothiazol (1 µM; **Figure 3.3.7*Bi***, ***iii***) or antimycin (100 nM, **Figure 3.3.7*Bii***, ***iv***).

Discussion and conclusions

Modelling mitochondrial dysfunction in zebrafish

Mitochondrial respiratory chain and inhibitors. Here, we show that zebrafish and mammalian mitochondria display high genetic and functional homology, and characterize the developmental and cardiovascular consequences of mitochondrial dysfunction evoked by respiratory chain inhibitors. Chronic complex I or II inhibition induced developmental abnormalities, whereas complex III inhibition directly converted normal into dead embryos, plausibly by lack of downstream alternatives to sustain mitochondrial ATP synthesis. Interestingly, when combining effective concentrations of rotenone and 3NP, lack of additive effects suggests a negligible residual complex I activity during complex II inhibition and vice versa. Yet, albeit abnormal, embryos undergo organogenesis and survive past 80 hpf. Because this cannot happen without mitochondrial ATP synthesis (oligomycin arrests gastrulation), data suggests alternative mitochondrial dehydrogenases [ETFDH, glycerol-3-phosphate dehydrogenase or dihydroorotate dehydrogenase (DHODH); **Figure 3.3.8**] actively reduce endogenous ubiquinone to support mitochondrial ATP production. This is important for interpreting zebrafish models of complex I or II deficiencies, for example in primary mitochondrial disease or in neurodegenerative disorders which have been associated with deficits in complexes I or II, such as Parkinson and Huntington's diseases respectively. Specifically, alternative feeding of complex III may explain why parkin knockout zebrafish presented 45% reduction of complex I activity without significant changes in swimming behaviour (403).

While the concentrations we have used for mitochondrial inhibitors are within the range commonly used in the literature, it is conceivable that in zebrafish, as with other models, there may be some contribution of off-target effects, such as microtubule depolymerization by rotenone (404), and fumarase inhibition by 3NP (405).

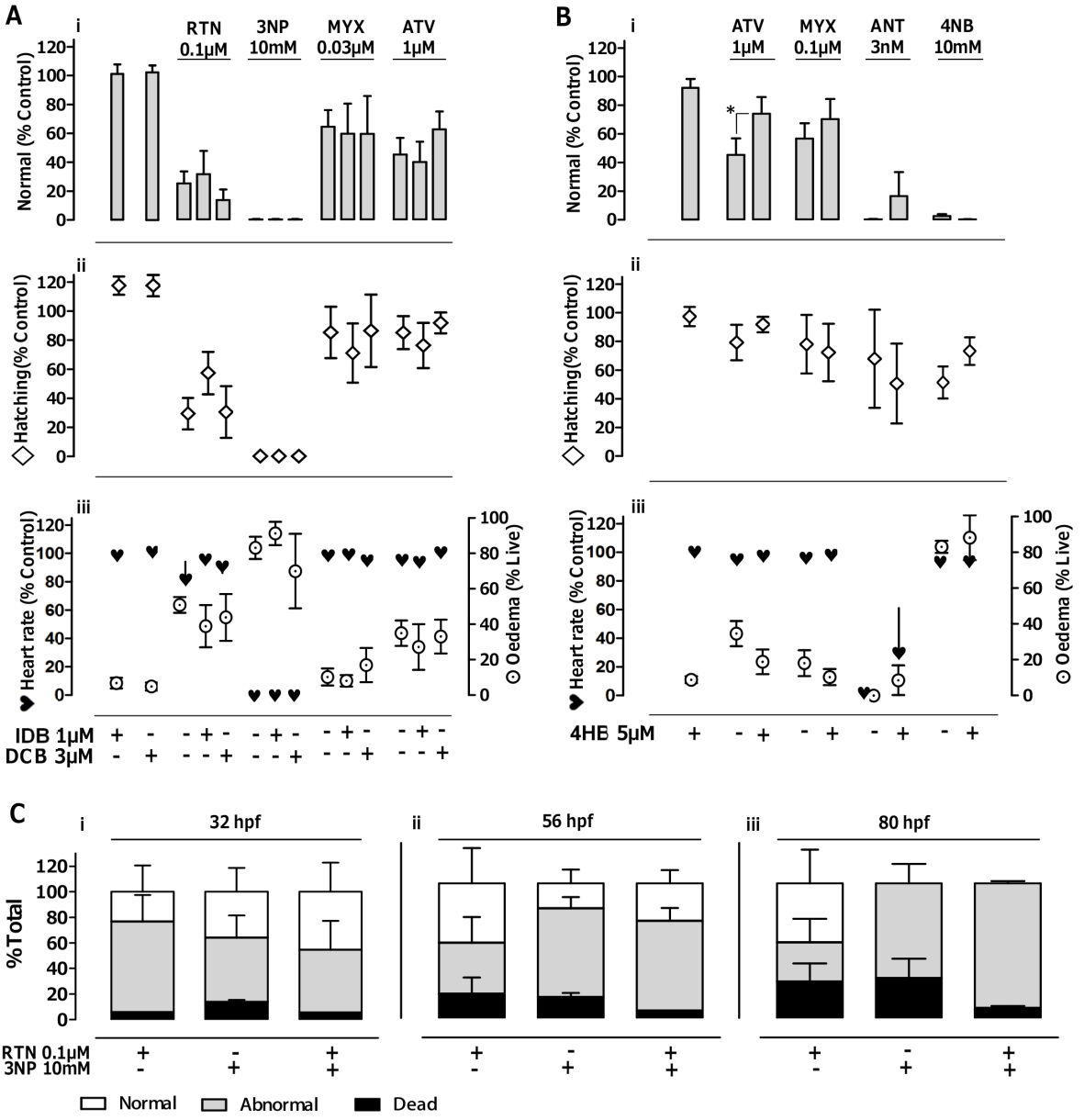

Figure 3.3.6. **Effect of ubiquinone analogues and precursor upon chronic mitochondrial inhibition.** ***A***,***B***, Normal embryos (***i***), hatching (***ii***), and average heart rate (***iii***; asystole included) in % of control, as well as oedema in surviving embryos (% live; ***iii***); Readings at 80 hpf, following chronic exposure to the indicated concentrations of drugs isolated *vs.* combined with idebenone (IDB, 1 µM, ***A)*** or decylubiquinone (DCB, 3 µM, ***A),*** or with 4-hydroxybenzoate (4HB, 5 µM, ***B***). Data are mean ± SEM on *n* independent experiments with rotenone (RTN, 0.1 µM, *n* = 4), 3-nitropropionic acid (3NP, 10 mM, *n* = 3), myxothiazol (MYX, 0.03 µM, *n* = 5; 0.1 µM, *n* = 6), atovaquone (ATV, 1 µM; *n* = 6), antimycin (ANT, 3 nM, *n* = 3), and 4-nitrobenzoate (4NB, 10 mM, *n* = 4). **P* < 0.05 for combined *vs*. isolated drug, unpaired *t-test.* ***C***, Normal, abnormal and dead embryos upon chronic exposure to 3NP (10 mM), alone or combined with RTN (0.1 µM). Data are mean ± SEM for *n* = 3 independent experiments, with readings at 32 (***i***), 56 (***ii***) and 80 hpf (***iii***). Note that 3NP toxicity (judged from abnormal and dead embryos *vs*. normal) does not increase upon combination with rotenone.

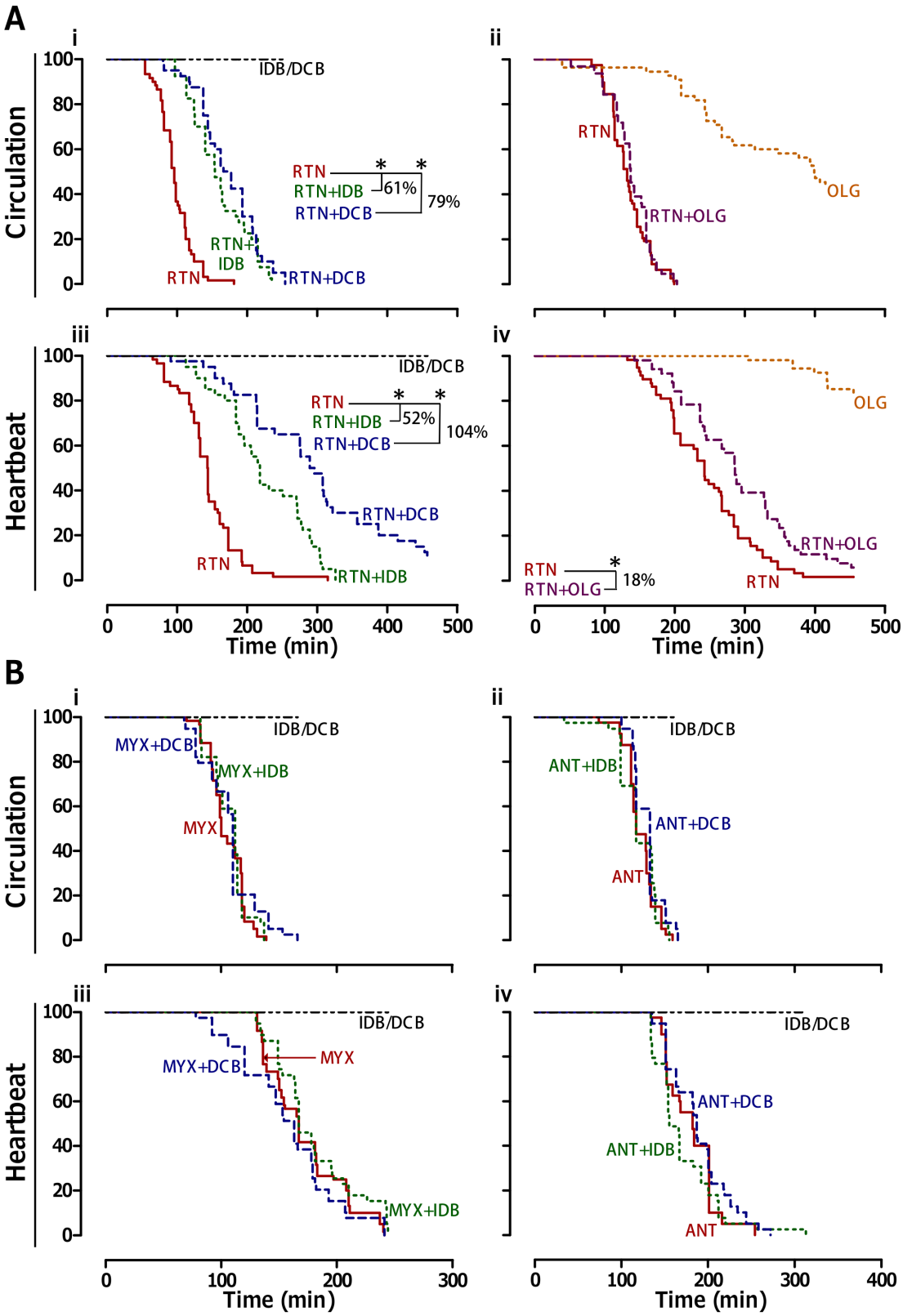

Figure 3.3.7. Effect of ubiquinone analogues upon acute mitochondrial inhibition. ***A***,***B***, Time-dependent changes in proportion of 56 hpf zebrafish with active circulation (***i***,***ii***) and heartbeat (***iii***,***iv***) following acute exposure to mitochondrial inhibitors (at time = 0 min). Ai,iii, Rotenone (RTN, 1 μM) with/without idebenone (IDB, 3 μM) or decylubiquinone (DCB, 30 μM); ***Aii***,***iv***, RTN (1 μM) and oligomycin (OLG, 3 μM), alone and combined. ***Bi-iv***, Myxothiazol (MYX, 1 μM) or antimycin (ANT, 0.1 μM), with/without IDB (3 μM) or DCB (30 μM). *P < 0.05 and % delay in circulatory arrest or assystole; Kaplan-Meier with Log Rank. Data are from 40–60 embryos per treatment, from 2–3 independent clutches. IDB or DCB (IDB/DCB) alone maintained 100% circulation or heartbeat throughout the experiment.

Cytosolic dehydrogenase: NQO1. In contrast with mitochondrial dehydrogenases, cytosolic NQO1, unlikely feeds complex III physiologically, since ubiquinone hydrophobicity precludes significant cytosolic-mitochondria shuttling. Pharmacologically, however, NQO1 may be quite relevant in reducing exogenous ubiquinone analogues (9, 134). Indeed, exogenous idebenone or decylubiquinone must travel the cytosol, where they may be reduced by NQO1, before feeding electrons to mitochondrial complex III. NQO1 inhibition was reported to decrease melanogenesis in zebrafish and melanoma cell lines (406). Here, we tested the NQO1 inhibitors dicoumarol and lapachol and both caused melanin defects in zebrafish embryos. Interestingly, lapachol was more potent than dicoumarol for melanin defects and presented a wider spectrum of abnormalities. Considering the higher NQO1 inhibiting potency of dicoumarol *versus* lapachol [IC_{50} = 10nM *vs*. 150nM, respectively; (407, 408)], we argue that effects may instead be mediated by DHODH inhibition, where lapachol was shown more potent than dicoumarol [IC_{50} = 61nM *vs*. 5 μM, respectively; (409, 410)]. Together, these findings suggest that the overall level of NQO1 activity during early zebrafish development is low, in contrast with that of DHODH. Consistently, dicoumarol failed to modulate chronic toxicity of menadione or β-lapachone suggesting they are not being significantly detoxified or bioactivated by NQO1. Still, specific organs like the heart may exhibit higher NQO1 activity, as addressed below.

Cardiovascular abnormalities and ubiquinone. Mitochondrial respiratory chain dysfunction and ubiquinone deficiency disorders are frequently associated with cardiovascular manifestations (210). Consistently, we show that mitochondrial inhibitors induce cardiac oedema associated with bradycardia and arrhythmia in zebrafish. Interestingly, we identified an unusual cardiovascular phenotype for 4NB and atovaquone, consisting in focal bleeding and necrosis, with pronounced cardiac oedema but normal heart rate. Meaningfully, 4NB inhibits ubiquinone biosynthesis (411), atovaquone was suggested to cause feedback inhibition of ubiquinone biosynthesis (62), and the ubiquinone precursor 4HB reduces atovaquone but not myxothiazol or antimycin toxicity. Therefore, data suggests that this unusual cardiovascular phenotype reflects ubiquinone deficiency, and may thus assist future study of related disorders in zebrafish.

In vivo testing of quinone analogues

Quinone analogues as research tools and chemotherapeutics. Quinone analogues are widespread in nature, playing key roles in electron transport chains and in interspecies chemical warfare. Their ability to interfere with biological processes stems from redox properties, and has promoted their use as research tools and as putative anticancer or antiparasitic drugs (8).

Menadione is a research tool for inducing oxidative stress, increasing mitochondria superoxide by redox cycling (412). While sometimes used as precursor for vitamin K, menadione may induce haemolysis in patients lacking glucose-6-phosphate dehydrogenase (413). Here, we report that menadione causes hypochromic anaemia in zebrafish when present between 24 and 32 hpf, following primitive erythropoiesis (400), but not when present for longer subsequent periods. Hence, instead of acute haemolysis, data suggests that menadione impairs zebrafish haematopoiesis, possibly by depolarizing mitochondria via redox-cycling or complex I inhibition (414) and disturbing membrane potential-dependent biosynthesis of the iron-sulfur cluster haem (**Figure 3.3.8*D***) (415). Thus, we suggest that menadione may be a useful research tool for studying erythropoiesis and its mitochondrial dependence in zebrafish.

Lapachol and β-lapachone are putative anticancer lead compounds, with their presence in plant extracts (e.g. *Tabebuia impetiginosa*) being associated with cytotoxicity against multiple cell lines (35). Similar reasoning applies to diospyrin, diosquinone, juglone and plumbagin. Here, we show that the LC_{50} of these quinone analogues in developing zebrafish is similar or even smaller than reported for cancer cells. Considering the similarities between cellular divisions in a developing embryo and in cancer cells, results suggest caution in interpreting data from zebrafish embryos whilst testing for selective anticancer toxicity.

Atovaquone is used therapeutically against *Pl. falciparum* malaria and *Pn. jiroveci* pneumonia. Selective toxicity for parasites *versus* humans is achieved by structural differences in atovaquone's target – the cytochrome *b* Q_o site in complex III (416). Here, we report a high amino acid homology of zebrafish, mice and humans at the Q_o and Q_i sites, confirming predicted functional differences by comparing LC_{50} of atovaquone, myxothiazol and antimycin with that reported for parasites. Together, data supports using *in vivo* zebrafish assays for comparative toxicity of mitochondria-targeted quinone analogues, namely in anti-malaric drug research.

Ubiquinone analogues and treatment of mitochondrial dysfunction. Ubiquinone analogues are among the few specific therapeutic options for mitochondrial diseases (129). Idebenone improved cardiac function in Friedrich ataxia (125), with higher doses required for improving neurological function

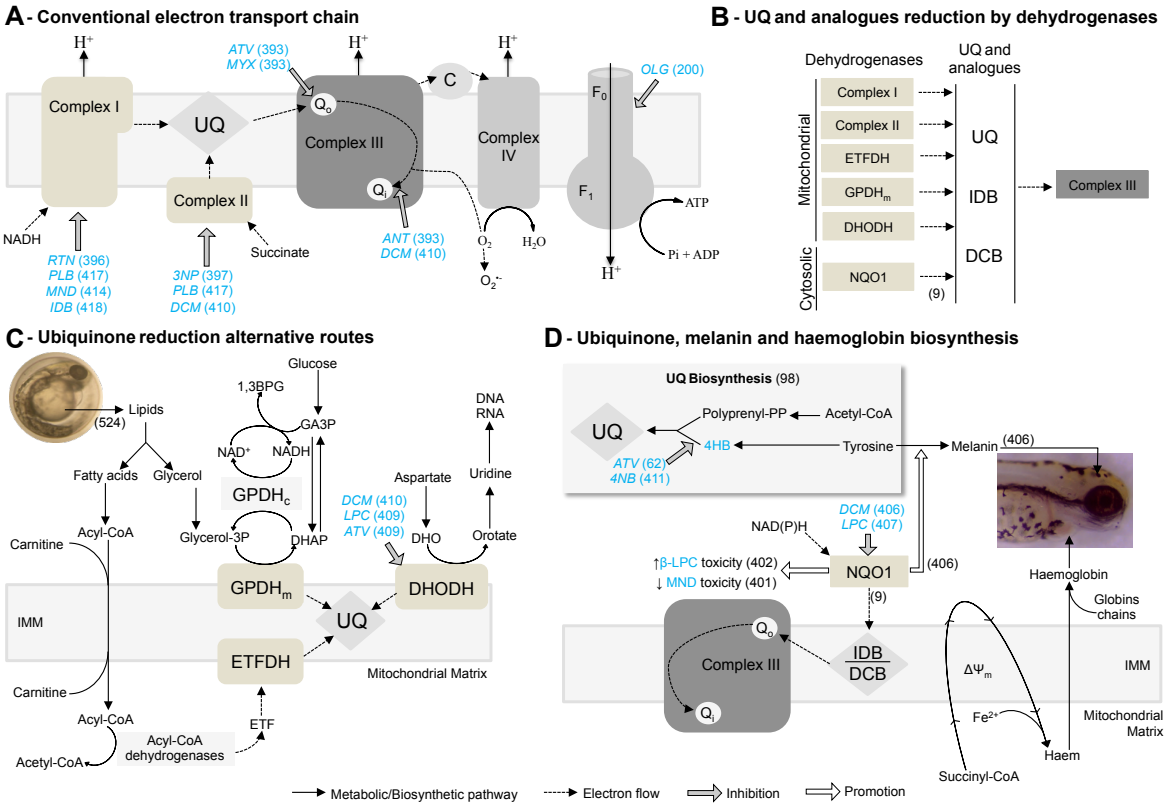

Figure 3.3.8. Mitochondrial and cytosolic biochemical pathways with sites of drug action. **A**, Mitochondrial respiratory chain, depicting electron flow (dashed-line *arrows*) from substrates to oxygen, and proton (H^+) pumping across the inner mitochondrial membrane (IMM). Drugs (blue *text*) and inhibitory sites (grey *arrows)*. Note that antimycin (ANT) binds Q_i, downstream of a potential electron exit site promoting superoxide ($O_2^{\bullet-}$) formation, whereas both myxothiazol (MYX) and atovaquone (ATV) bind the upstream Q_o in complex III. ***B***, Mitochondrial and cytosolic dehydrogenases, capable of reducing ubiquinone (UQ) or its analogues idebenone (IDB) and decylubiquinone (DCB). *Complex I,* NADH dehydrogenase; *Complex II,* succinate dehydrogenase; *ETFDH,* electron transfer flavoprotein (ETF) dehydrogenase; *GPDHm,* glycerol-3-phosphate dehydrogenase (mitochondrial); *DHODH,* dihydroorotate dehydrogenase; NQO1, NAD(P)H: quinone oxidoreductase. ***C***, Lipid metabolism and other metabolic pathways feeding dehydrogenases (ETFDH, GPDHm and DHDOH) that can reduce ubiquinone, thus being alternatives to Complex I and II. ***D***, Ubiquinone, melanin and haemoglobin biosynthesis. Note that: 4-hidroxibenzoate (4HB) is a precursor for UQ synthesis, inhibited by ATV and 4-nitrobenzoate (4NB); NQO1 promotes (white *arrows)* melanin synthesis, increases and decreases β-lapachone (βLPC) and menadione (MND) toxicity, respectively. Dicoumarol (DCM) and lapachol (LPC) inhibit NQO1; Haem synthesis is critically dependent on mitochondria and its membrane potential ($\Delta\psi_m$).

(126). Idebenone effects have been ascribed to antioxidant properties (101). Further, idebenone can mimic ubiquinone, transferring to complex III the electrons received from mitochondrial dehydrogenases, thus promoting mitochondrial ATP production (418). Although ubiquinone analogues have failed to rescue ubiquinone deficient cells (122), there are also evidences that idebenone's ability to rescue ATP levels correlates with NQO1 activity (9), promoting idebenone reduction and subsequent complex III feeding. Current support for this hypothesis stems from *in vitro* evidence, using cells or isolated mitochondria and predictive parameters such as ATP levels and oxygen consumption. Here, we explore this hypothesis *in vivo*, using zebrafish and cardiovascular parameters, testing the ability of ubiquinone analogues to prevent/delay cardiac insufficiency following induced mitochondrial dysfunction.

Idebenone and decylubiquinone significantly delayed cardiac insufficiency and asystole evoked by acute rotenone exposure. However, both drugs were ineffective against chronic rotenone exposure, as ubiquinone analogues clearly cannot sustainably protect from chronic multi-organ toxicity. The mechanisms of cardioprotection by idebenone and decylubiquinone in our zebrafish model are more likely related to increased ATP production efficiency than to antioxidant or reactive oxygen species (ROS) scavenging properties. Indeed, these ubiquinone analogues were without effect against both acute and chronic complex III inhibition, particularly with antimycin that is also an inducer of mitochondrial ROS production (419). Thus, transient cardiac

protection from acute rotenone exposure in zebrafish might be explained by higher NQO1 activity in the heart [as in mammals: (420, 421), allowing enhanced local ubiquinone analogue reduction (9, 134), and consequently more feeding of complex III and ATP production in the heart.

In future studies of mitochondrial dysfunction in zebrafish, it would be valuable to further explore ATP/ADP ratios as well as ROS production in this model organism. Significantly, Mendelsohn et al. (422) have monitored AMP/ ATP by HPLC and total ATP by luciferase assays in zebrafish. Also, Niethammer et al. (423) have successfully used a genetically encoded H_2O_2 sensor in zebrafish.

Concluding remarks

In summary, the present work supports zebrafish for studying mitochondrial dysfunction and testing mitochondria-targeted treatments. Our reported developmental and cardiovascular phenotypes should assist further research on mitochondrial diseases in this model organism. The present data, on mitochondrial sequence analysis and atovaquone effects, highlights zebrafish's potential for the *in vivo* differential toxicity screening of mitochondria-targeted antiparasitic drugs. Further, our *in vivo* assay identifying a delay of cardiac failure by idebenone and decylubiquinone may assist comparisons of other ubiquinone analogues, currently being developed as mitochondria-targeted drugs. Data on other quinone analogues (especially menadione) should assist their use as research tools. Lastly, our data showing a relatively low dependence of young zebrafish on mitochondrial complex I/II for ATP production should help interpret phenotypes of disease models linked to complex I/II inhibition.

Acknowledgements. This work was supported by "Fundação para a Ciência e a Tecnologia" (FCT), Strategic Project: PEst-C/EQB/LA006/ 2011, and by Research Grants (PI: J. M. A. O.) PTDC/NEU-NMC/0237/2012 (FCT), FCOMP-01-0124-FEDER-029649 (COMPETE), and PPII_CARDIAC and PPII_ZEBRA (Universidade do Porto and Santander-Totta). B. P. is grateful to FCT for her PhD grant (SFRH/BD/63852/2009).

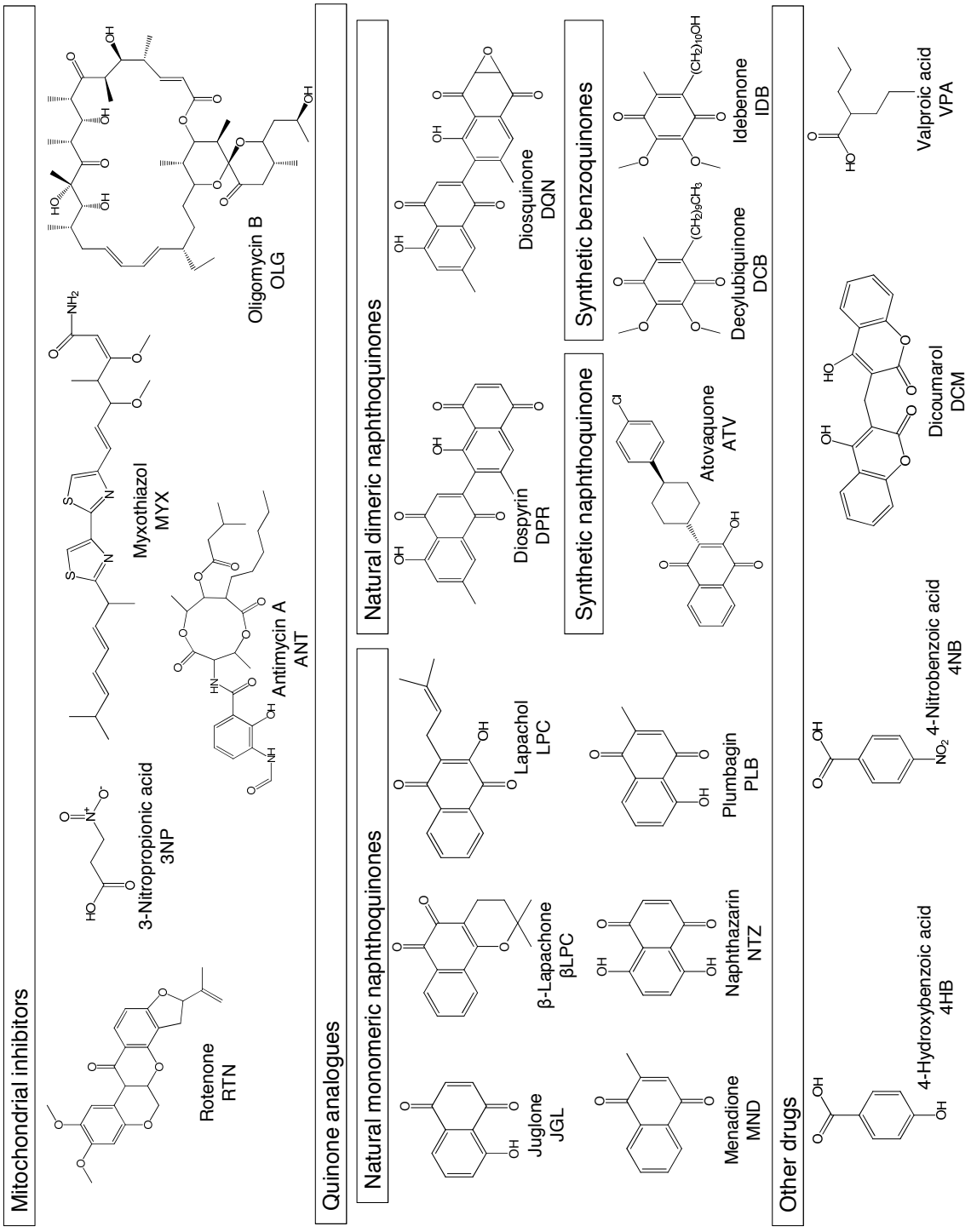

Figure 3.3.S1. Drug categories and structures.

Appendix S1. References of Table 2.

[1] Ward MW, Rego AC, Frenguelli BG, Nicholls DG. Mitochondrial membrane potential and glutamate excitotoxicity in cultured cerebellar granule cells. J Neurosci 2000 Oct; 20 (19): 7208-19.

[2] Turcotte ML, Parliament M, Franko A, Allalunis-Turner J. Variation in mitochondrial function in hypoxia-sensitive and hypoxia-tolerant human glioma cells. Br J Cancer 2002 Feb; 86 (4): 619-24.

[3] Mendelsohn BA, Kassebaum BL, Gitlin JD. The zebrafish embryo as a dynamic model of anoxia tolerance. Dev Dyn 2008 Jul; 237 (7): 1780-8.

[4] Biagini GA, Viriyavejakul P, O'Neill P M, Bray PG, Ward SA. Functional characterization and target validation of alternative complex I of *Plasmodium falciparum* mitochondria. Antimicrob Agents Chemother 2006 May; 50 (5): 1841-51.

[5] Pang Z, Geddes JW. Mechanisms of cell death induced by the mitochondrial toxin 3-nitropropionic acid: acute excitotoxic necrosis and delayed apoptosis. J Neurosci 1997 May; 17 (9): 3064-73.

[6] Oliveira JM, Gonçalves J. *In situ* mitochondrial Ca^{2+} buffering differences of intact neurons and astrocytes from cortex and striatum. J Biol Chem 2009 Feb; 284 (8): 5010-20.

[7] Korsinczky M, Chen N, Kotecka B, Saul A, Rieckmann K, Cheng Q. Mutations in *Plasmodium falciparum* cytochrome *b* that are associated with atovaquone resistance are located at a putative drug-binding site. Antimicrob Agents Chemother 2000 Aug; 44 (8): 2100-8.

[8] Ittarat I, Asawamahasakda W, Bartlett MS, Smith JW, Meshnick SR. Effects of atovaquone and other inhibitors on *Pneumocystis carinii* dihydroorotate dehydrogenase. Antimicrob Agents Chemother 1995 Feb; 39 (2): 325-8.

[9] Dong CK, Patel V, Yang JC, Dvorin JD, Duraisingh MT, Clardy J, et al. Type II NADH dehydrogenase of the respiratory chain of *Plasmodium falciparum* and its inhibitors. Bioorg Med Chem Lett 2009 Feb; 19 (3): 972-5.

[10] Salomon AR, Voehringer DW, Herzenberg LA, Khosla C. Understanding and exploiting the mechanistic basis for selectivity of polyketide inhibitors of F_0 F_1-ATPase. Proc Natl Acad Sci USA 2000 Dec; 97 (26): 14766-71.

[11] Chen F, Cushion MT. Use of an ATP bioluminescent assay to evaluate viability of *Pneumocystis carinii* from rats. J Clin Microbiol 1994 Nov; 32 (11): 2791-800.

[12] Elandaloussi LM, Lindt M, Collins M, Smith PJ. Analysis of P-glycoprotein expression in purified parasite plasma membrane and food vacuole from *Plasmodium falciparum*. Parasitol Res. 2006 Nov; 99 (6): 631-7.

[13] Zhou J, Duan L, Chen H, Ren X, Zhang Z, Zhou F, et al. Atovaquone derivatives as potent cytotoxic and apoptosis inducing agents. Bioorg Med Chem Lett 2009 Sep; 19 (17): 5091-4.

[14] Song WH, Ding F, Guo J, Li LY, Zhang JH, Lian J, et al. Study on acute toxicity and structure-activity relationship of zebrafish (*Danio rerio*) exposed to naphthoquinones. J Environ Sci Health B 2010 Oct; 45 (7): 601-5.

[15] Cushion MT, Collins M, Hazra B, Kaneshiro ES. Effects of atovaquone and diospyrin-based drugs on the cellular ATP of *Pneumocystis carinii* f. sp. *carinii*. Antimicrob Agents Chemother 2000 Mar; 44 (3): 713-9.

[16] Hughes LM, Lanteri CA, O'Neil MT, Johnson JD, Gribble GW, Trumpower BL. Design of anti-parasitic and anti-fungal hydroxy-naphthoquinones that are less susceptible to drug resistance. Mol Biochem Parasitol 2011 May; 177 (1): 12-9.

[17] Gupta D, Podar K, Tai YT, Lin B, Hideshima T, Akiyama M, et al. β-lapachone, a novel plant product, overcomes drug resistance in human multiple myeloma cells. Exp Hematol 2002 Jul; 30 (7): 711-20.

[18] da Silva EN, Jr., de Deus CF, Cavalcanti BC, Pessoa C, Costa-Lotufo LV, Montenegro RC, et al. 3-arylamino and 3-alkoxy-nor-β-lapachone derivatives: Synthesis and cytotoxicity against cancer cell lines. J Med Chem 2010 Jan; 53 (1): 504-8.

[19] Wu YT, Lin CY, Tsai MY, Chen YH, Lu YF, Huang CJ, et al. β-Lapachone induces heart morphogenetic and functional defects by promoting the death of erythrocytes and the endocardium in zebrafish embryos. J Biomed Sci 2011 Sep; 18: 70.

[20] Pérez-Sacau E, Estévez-Braun A, Ravelo AG, Gutiérrez Yapu D, Giménez Turba A. Antiplasmodial activity of naphthoquinones related to lapachol and β-lapachone. Chem Biodivers 2005 Feb; 2 (2): 264-74.

[21] Armstrong JS, Whiteman M, Rose P, Jones DP. The Coenzyme Q_{10} analog decylubiquinone inhibits the redox-activated mitochondrial permeability transition: Role of mitchondrial complex III. J Biol Chem 2003 Dec; 278 (49): 49079-84.

[22] Das Sarma M, Ghosh R, Patra A, Hazra B. Synthesis of novel aminoquinonoid analogues of diospyrin and evaluation of their inhibitory activity against murine and human cancer cells. Eur J Med Chem 2008 Sep; 43 (9): 1878-88.

[23] Chakrabarty S, Roy M, Hazra B, Bhattacharya RK. Induction of apoptosis in human cancer cell lines by diospyrin, a plant-derived bisnaphthoquinonoid, and its synthetic derivatives. Cancer Lett 2002 Dec; 188 (1-2): 85-93.

[24] Theerachayanan T, Sirithunyalug B, Piyamongkol S. Antimalarial and antimycobacterial activities of dimeric naphthoquinone from *Diospyros glandulosa* and *Diospyros rhodocalyx*. CMU J Nat Sci 2007; 6: 253-59.

[25] Adeniyi BA, Robert MF, Chai H, Fong HH. *In vitro* cytotoxicity activity of Diosquinone, a naphthoquinone epoxide. Phytother Res 2003 Mar; 17 (3): 282-4.
[26] Civenni G, Bezzi P, Trotti D, Volterra A, Racagni G. Inhibitory effect of the neuroprotective agent idebenone on arachidonic acid metabolism in astrocytes. Eur J Pharmacol 1999 Apr; 370 (2): 161-7.
[27] Tai KK, Pham L, Truong DD. Idebenone induces apoptotic cell death in the human dopaminergic neuroblastoma SHSY-5Y cells. Neurotox Res 2011 Nov; 20 (4): 321-8.
[28] Montenegro RC, Araújo AJ, Molina MT, Marinho Filho JD, Rocha DD, Lopez-Montero E, et al. Cytotoxic activity of naphthoquinones with special emphasis on juglone and its 5-O-methyl derivative. Chem Biol Interact 2010 Mar; 184 (3): 439-48.
[29] Xu HL, Yu XF, Qu SC, Zhang R, Qu XR, Chen YP, et al. Anti-proliferative effect of Juglone from *Juglans mandshurica* Maxim on human leukemia cell HL-60 by inducing apoptosis through the mitochondria-dependent pathway. Eur J Pharmacol 2010 Oct; 645 (1-3): 14-22.
[30] Kapadia GJ, Azuine MA, Balasubramanian V, Sridhar R. Aminonaphthoquinones-a novel class of compounds with potent antimalarial activity against *Plasmodium falciparum*. Pharmacol Res 2001 Apr; 43 (4): 363-7.
[31] da Silva EN, Jr., Guimaraes TT, Menna-Barreto RF, Pinto Mdo C, de Simone CA, Pessoa C, et al. The evaluation of quinonoid compounds against *Trypanosoma cruzi*: Synthesis of imidazolic anthraquinones, nor-beta-lapachone derivatives and β-lapachone-based 1,2,3-triazoles. Bioorg Med Chem 2010 May; 18 (9): 3224-30.
[32] Salustiano EJ, Netto CD, Fernandes RF, da Silva AJ, Bacelar TS, Castro CP, et al. Comparison of the cytotoxic effect of lapachol, α-lapachone and pentacyclic 1,4-naphthoquinones on human leukemic cells. Invest New Drugs. 2010 Apr; 28 (2): 139-44.
[33] Cockburn IL, Pesce ER, Pryzborski JM, Davies-Coleman MT, Clark PG, Keyzers RA, et al. Screening for small molecule modulators of Hsp70 chaperone activity using protein aggregation suppression assays: inhibition of the plasmodial chaperone PfHsp70-1. Biol Chem 2011 May; 392 (5): 431-8.
[34] Chowdhury R, Chowdhury S, Roychoudhury P, Mandal C, Chaudhuri K. Arsenic induced apoptosis in malignant melanoma cells is enhanced by menadione through ROS generation, p38 signaling and p53 activation. Apoptosis 2009 Jan; 14 (1): 108-23.
[35] Nutter LM, Cheng AL, Hung HL, Hsieh RK, Ngo EO, Liu TW. Menadione: Spectrum of anticancer activity and effects on nucleotide metabolism in human neoplastic cell lines. Biochem Pharmacol 1991 May; 41 (9): 1283-92.
[36] Subramaniya BR, Srinivasan G, Sadullah SS, Davis N, Subhadara LB, Halagowder D, et al. Apoptosis inducing effect of plumbagin on colonic cancer cells depends on expression of COX-2. PLoS One 2011; 6 (4): e18695.
[37] Kawiak A, Piosik J, Stasilojc G, Gwizdek-Wisniewska A, Marczak L, Stobiecki M, et al. Induction of apoptosis by plumbagin through reactive oxygen species-mediated inhibition of topoisomerase II. Toxicol Appl Pharmacol 2007 Sep 15; 223 (3): 267-76.
[38] Suraveratum N, Krungkrai SR, Leangaramgul P, Prapunwattana P, Krungkrai J. Purification and characterization of *Plasmodium falciparum* succinate dehydrogenase. Mol Biochem Parasitol 2000 Feb; 105 (2): 215-22.
[39] Monagas M, Khan N, Andres-Lacueva C, Urpi-Sarda M, Vazquez-Agell M, Lamuela-Raventos RM, et al. Dihydroxylated phenolic acids derived from microbial metabolism reduce lipopolysaccharide-stimulated cytokine secretion by human peripheral blood mononuclear cells. Br J Nutr 2009 Jul; 102 (2): 201-6.
[40] Sul D, Kaneshiro ES. *Pneumocystis carinii* f. sp. *carinii* synthesizes *de novo* four homologs of ubiquinone. J Eukaryot Microbiol 2001 Mar-Apr; 48 (2): 182-7.
[41] Forsman U, Sjoberg M, Turunen M, Sindelar PJ. 4-Nitrobenzoate inhibits coenzyme Q biosynthesis in mammalian cell cultures. Nat Chem Biol 2010 Jul; 6 (7): 515-7.
[42] Brust K. Toxicity of aliphatic amines on the embryos of zebrafish *Danio rerio* - experimental studies and QSAR. Doctor, Dresden: Technischen Universität Dresden; 2001.
[43] González-Aragón D, Ariza J, Villalba JM. Dicoumarol impairs mitochondrial electron transport and pyrimidine biosynthesis in human myeloid leukemia HL-60 cells. Biochem Pharmacol 2007 Feb; 73 (3): 427-39.
[44] Moog C, Kuntz-Simon G, Caussin-Schwemling C, Obert G. Sodium valproate, an anticonvulsant drug, stimulates human immunodeficiency virus type 1 replication independently of glutathione levels. J Gen Virol 1996 Sep; 77 (Pt 9): 1993-9.
[45] Selderslaghs IW, Blust R, Witters HE. Feasibility study of the zebrafish assay as an alternative method to screen for developmental toxicity and embryotoxicity using a training set of 27 compounds. Reprod Toxicol 2011 Aug; 33 (2): 142-54.

3.4. Mitochondrial and behavioural deficits in the zebrafish MPP^+ Parkinson model: Effect of ubiquinone analogues and lysine deacetylase inhibitors

Manuscript in preparation.

More experiments are required to conclude this work.

Mitochondrial and behavioural deficits in the zebrafish MPP$^+$ Parkinson model: Effect of ubiquinone analogues and lysine deacetylase inhibitors

Brígida R. Pinho[1,2], Ana Leitão-Rocha[1], Clara Quintas[1], Patrícia Valentão[2], Paula B. Andrade[2], Miguel M. Santos[3,4] and Jorge M. A. Oliveira[1] *

[1]REQUIMTE, Department of Drug Sciences, Pharmacology Lab, Faculty of Pharmacy, University of Porto, Porto, Portugal, [2]REQUIMTE, Department of Chemistry, Pharmacognosy Lab, Faculty of Pharmacy, University of Porto, Porto, Portugal, [3]CIMAR/CIIMAR – Interdisciplinary Centre of Marine and Environmental Research, University of Porto, Porto, Portugal; and [4]FCUP – Department of Biology, Faculty of Sciences, University of Porto, Porto, Portugal

Abstract

BACKGROUND AND PURPOSE

No current treatment avoids the progression of Parkinson's disease. Further understanding of Parkinson's disease pathophysiology and development of disease modifying drugs requires characterization of Parkinsonian animal models and validation of new drug targets. In this work, we further characterize the zebrafish Parkinson model induced by MPP$^+$ (a dopaminergic toxin) and tested lysine deacetylase inhibitors (KDACi) and ubiquinone (UQ) analogues in this model.

EXPERIMENTAL APPROACH

Zebrafish larvae were chronically exposed to MPP$^+$, UQ analogues (idebenone and decylubiquinone) and KDACi (tubastatin A and MS-275) from 3-6 days post fertilization (dpf) with sensorimotor reflexes, locomotor profile and mitochondrial complexes analysed at 6 dpf. KDAC's (HDAC1 and HDAC6) expression was evaluated by qPCR and KDAC inhibition confirmed by western blotting acetylated KDAC targets.

KEY RESULTS

HDAC1 and HDAC6 were expressed during zebrafish embryonic development and their deacetylase activity was inhibited by MS-275 and tubastatin A, respectively. Zebrafish HDAC1 displays high functional and structural homology with the human enzyme. Zebrafish HDAC6, however, displays substantially lower structural homology with the human enzyme but, nevertheless, exhibits tubulin deacetylase activity. MPP$^+$ inhibits zebrafish complex I, inducing intermittent and disorganized locomotion, and impairing head reflex. These phenotypes were not rescued by coexposure to UQ analogues or KDACi.

CONCLUSION AND IMPLICATIONS

This study further characterizes zebrafish MPP$^+$-induced Parkinsonian behavioural phenotypes, thus assisting further studies with this model. The characterization of KDAC transcription and active deacetylation profiles, validates KDACs as targetable enzymes in zebrafish, highlighting the value of this *in vivo* model for epigenetic drug testing.

Keywords: Parkinson's disease, *Danio rerio*, idebenone, decylubiquinone, HDAC1, HDAC6, mitochondria.

Introduction

Neurodegeneration is characterized by progressive and selective loss of specific groups of neurons. The causes of neurodegeneration remain uncertain, but mitochondrial function has been largely associated to neurodegenerative disorders, such as Alzheimer's (AD), Huntington's (HD) or Parkinson's diseases (PD) (424). The increasing prevalence of neurodegenerative diseases demands for currently unavailable disease modifying drugs. Lysine deacetylase (KDAC) inhibitors (KDACi) and ubiquinone analogues are emerging experimental therapeutics for neurodegeneration, whose cellular effects include the modulation of mitochondrial function (9, 135, 425).

Ubiquinone (UQ) analogues are drugs structurally similar to endogenous ubiquinone (coenzyme Q_{10}), but generally with lower lipophilicity and better pharmacokinetics than ubiquinone. UQ analogues have antioxidant properties, decreasing oxidative stress generated by mitochondrial dysfunction, and can act as

electron carriers, improving electron transport in the mitochondrial respiratory chain (9). UQ analogues, particularly idebenone, have been tested as treatment for several neurodegenerative disorders. Despite no rescue of primary ubiquinone deficiencies in *in vitro* experiments (426), idebenone reduced cardiomyopathy and improved neurological function of Friedreich's ataxia patients (125, 126). Additionally, idebenone improved vision in patients with Leber's hereditary optic neuropathy (130) and OPA-1 dominant optic atrophy (131). In AD, idebenone was reported to improve cognitive function and daily living activities of 50% treated patients (427). Idebenone also enhanced lifespan and motor function of mice with mitochondrial dysfunction induced by HtrA2 knockout, a mitochondrial protease associated with HD and PD (428).

KDACs catalyse the deacetylation of lysine residues in histone and non-histone proteins. Decrease histone acetylation promotes chromatin condensation, repressing gene transcription, the opposite occurring with increased histone acetylation (425). KDAC function is closely related to mitochondrial dynamics, regulating mitochondrial biogenesis, trafficking, fission-fusion and mitophagy (425). Valproic acid (VPA) and trichostatin A (TSA) are two pan-KDAC inhibitors largely used to study KDAC function: both drugs promoted neurogenesis and neurite outgrowth in rat primary cortical neurons subjected to ischemic conditions (429). VPA also decreased retinal neuronal death induced by optic nerve crush (430) and TSA improved the pathological conditions and increased the survival of a mouse model of amyotrophic lateral sclerosis (431). Furthermore, KDACi have also neuroprotective properties in several other neurodegenerative diseases models: sodium butyrate, a pan-KDAC inhibitor, restored normal locomotion in a *Drosophila* PD model (432); 4b, a HDAC1 and HDAC3 selective inhibitor, improved motor and cognitive parameters and prevented huntingtin aggregation formation in HD mice brain (433); in a mouse model of AD, HDAC6 knockout restored learning and memory, associated with mitochondrial trafficking improvement mediated by α-tubulin acetylation (434).

Zebrafish became a popular biomedical due to several advantageous features, such as embryonic and larval transparency, rapid embryonic development, and high physiological and genetic homology to mammals (280). The neuronal pathways involved in physiology and disease are similar between zebrafish and mammals (300), thus allowing the use of zebrafish to model several human diseases, including neurodegenerative disorders such as HD (304), AD (309), amyotrophic lateral sclerosis (308) and PD. PD may be induced in zebrafish by genetic manipulation or by drug treatment. Gene silencing has been used to study PD-related genes, such as presenilin-associated rhomboid-like (*PARL*) (312) or PTEN induced putative kinase 1 (*PINK1*) (313). Drugs used to induce Parkinsonism in zebrafish include rotenone, paraquat, 6-hydroxydopamine and 1-methyl-4-phenyl-1,2,3,6-tetrahydropyridine (MPTP) (319, 320). MPTP's active metabolite [1-methyl-4-phenylpyridinium (MPP^+)] selectively accumulates in dopaminergic neurons where it inhibits complex I, inducing neuronal cell death (248). Zebrafish is susceptible to MPTP/MPP^+ toxicity through reduction of dopaminergic neurons in the posterior tuberculum and, presumably, serotonergic neurons in the paraventricular organ and hypothalamus (435). However, characterization of zebrafish locomotor changes induced by MPP^+ is currently scarce. MPTP decreased tail reflexes (257, 258), travelled distance, swimming period (259) and speed (319).

Ubiquinone (coenzyme Q_{10}) has been studied as neuroprotective agent in mouse models of MPTP/MPP^+ toxicity, attenuating dopaminergic degeneration (436). Mito-Q_{10}, a positive-charged UQ analogue, inhibited the MPTP- and MPP^+-induced neurotoxicity in mouse and cellular models (437), but as far as we could find, there are no published studies with idebenone and other ubiquinone analogues in MPTP-induced Parkinson models. Regarding KDACi, VPA, sodium butyrate, suberoylanilide hydroxamic acid, phenylbutyrate and TSA decreased MPTP/MPP^+ toxicity in mouse and/or cellular models (438). The main objectives of this work were to: characterize the locomotor profile and mitochondrial function of the zebrafish MPP^+ Parkinson model; validate HDAC1 and HDAC6 as targets by monitoring their expression in zebrafish and by confirming their respective *in vivo* inhibition with MS-275 and tubastatin A. Additionally, we tested the rescuing potential of ubiquinone analogues (idebenone and decylubiquinone) and KDACi (MS-275 and tubastatin A) upon the MPP^+-induced Parkinsonian phenotypes in zebrafish.

Methods

Drugs, solvents and solutions

The 1-methyl-4-phenylpyridinium (MPP^+), UQ analogues (idebenone and decylubiquinone), tricaine methanesulfonate and mitochondrial complex inhibitors (rotenone, sodium malonate and antimycin A) were from Sigma-Aldrich (St. Louis, MO, USA). Tubastatin A and MS-275, which are selective inhibitors of HDAC6 (439) and HDAC1

(440) respectively, were from Selleckchem (Munich, Germany). EX-527 and AGK2, which are selective inhibitors of SIRT1 (441) and SIRT2 (442) respectively, were from Tocris Bioscience (Abingdon, UK). MPP^+ stock solution was prepared in water, idebenone stock solution was prepared in methanol and stock solutions for other drugs were prepared in dimethyl sulfoxide (DMSO). The maximal concentration of solvents used was 0.1% and the solvent effects in all assays were studied (**Figure 3.4.S1**).

Zebrafish maintenance and drug treatments

Adult wild-type zebrafish (*Danio rerio*) were maintained at 28 ± 1ºC, on a 14h:10h light:dark cycle, and handled for egg production as we previously described (443). Briefly, on the day before egg collection adults (7 females and 14 males) were placed in a 30 L breeding tank and the time of egg collection (1.5h after starting the light period) was registered as zero hours post fertilization (hpf).

At 3 days post fertilization (dpf), hatched larvae were randomly distributed into multi-well plates and maintained at the same temperature and light conditions of the adults. According to the number of larvae per condition required for each experiment, two types of plates were used: 12-well plates with 15-30 larvae in 1 mL per well, or 48-well plates with 5 larvae in 0.5 mL per well. Solutions in wells containing larvae (water with or without solvent or drugs) were renewed daily (half volume). Larvae were continuously exposed to drugs from 3 dpf onwards. Exceptions were the survival tests with rotenone pre-exposure, where treatment with 0.3 µM rotenone started at 1 dpf to precede the 500 µM MPP^+ exposure starting at 3 dpf. No food was added to larvae throughout the experiments. Larvae were imaged daily with an inverted microscope (Eclipse TE300, Nikon, Tokyo, Japan) and scored as normomorphic (no apparent abnormality), dysmorphic (one or more abnormalities) or dead, using previously described normal development as reference (292). Dead larvae were removed daily during the readings.

Neuromast labeling

Control larvae and MPP^+-treated larvae at 6 dpf were incubated for 30 min with 100 nM MitoTracker® Green FM. After incubation, larvae were anesthetized with 0.8 mM tricaine methanesulfonate. Fluorescent images were captured at 10x magnification with 488 nm excitation and > 510 nm emission using an inverted epifluorescence microscope (Eclipse TE300, Nikon, Tokyo, Japan), a monochromator (Polychrome II, TILL Photonics, Martinsried, Germany), a CCD camera (C6790, Hammatsu, Photonics, Hamamatsu, Japan) and a computer with the Aquacosmos 2.5 software (Hammatsu Photonics).

Behavioural evaluation

Behavioural evaluation (sensorimotor reflex and locomotion profile) was initially assessed daily in control larvae from 3-7 dpf, identifying 6 dpf as the suitable time period for analysis of maximal responses (**Figure 3.4.3*B*** and **Table 3.4.2**). Subsequently, 10 larvae per condition (in duplicate wells: 5+5) were treated from 3 to 6 dpf and the behavioural profile of normomorphic larvae assessed at 6 dpf.

Sensorimotor reflex (Touch responses). Normomorphic larvae capable of spontaneous swimming were distributed into 12-well plates (1 larvae per well) and allowed to acclimate for at least 1 min. When larvae were spontaneously immobilized, they were gently touched with a micropipette tip (20 µL) in the head or tail for the recording of either positive (immediate swimming) or negative reflexes (no movement upon touch).

Locomotion profile (Spontaneous swimming). Normomorphic larvae were distributed into 12-well plates (1 larvae per well), allowed to acclimate for 5 min, and their locomotor profile recorded for 10 min at 28 ± 1ºC with a HD digital camera (C525, Logitech). Native videos with 15 frames per second (fps) were converted into 5 fps with iWisoft Free Video Converter (www.iwisoft.com/videoconverter) before analysis with the Image J particle tracker plugin ((444); http://mosaic.mpi-cbg.de/ParticleTracker/). We determined the following parameters: total travelled distance, time in movement, movement speed (total travelled distance divided by time in movement), number of initiations and time in movement per initiation. We also determined the movement distribution throughout the well, the number of circles, and the time in centre. For these last three parameters, we divided the well into virtual quadrants (**Figure 3.4.3*A***). A low or high standard deviation (SD) of the time per quadrant reports, respectively, a homogeneous or heterogeneous movement distribution. Larvae complete one circle when they pass sequentially through four sequenced quadrants in either clockwise or in counter-clockwise direction (**Figure 3*A***, Left). The central division out of 9 was used to determine “time in centre” (**Figure 3.4.3*A***, Right). Locomotion profiles were scored as uniform, circular, one-sided, and others (**Figure 3.4.3*Ciii***). All larvae analysed were capable of swimming, although a few did not move during the 10 min recording period (scored together with “others” in

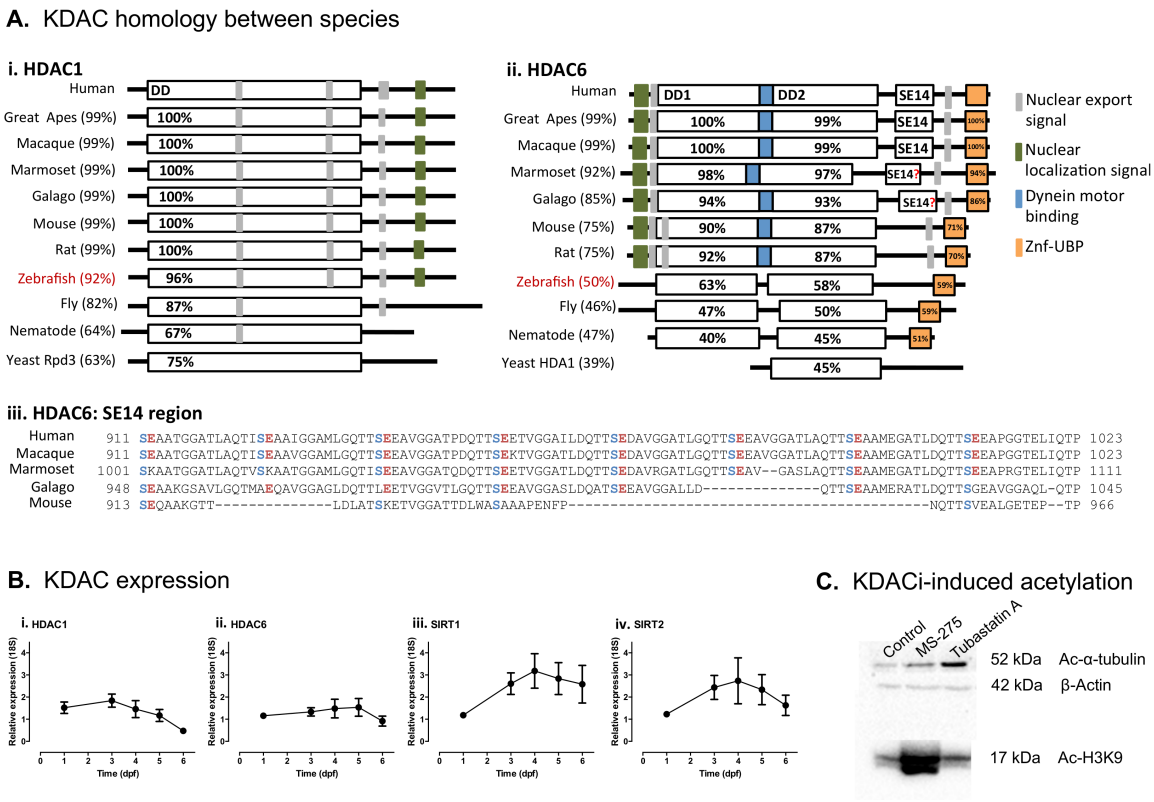

Figure 3.4.1.Structure, expression and activity of zebrafish KDACs (HDAC1 and HDAC6). ***A***, HDAC1 (***i***) and HDAC6 (***ii***) homology comparison: Human, *Homo sapiens*; great apes (bonobo, *Pan paniscus*; chimpanzee, *Pan troglodytes*; gorilla, *Gorilla gorilla*); macaque, *Macaca mullata*; marmoset, *Callithrix jacchus*; galago, *Otolemur garnettii*; mouse, *Mus musculus*; rat, *Rattus norvegicus*; zebrafish, *Danio rerio*; fly, *Drosophila melanogaster*; nematode, *Caenorhabditis elegans*; yeast, *Saccharomyces cerevisiae*. Percentages of identity *vs*. human are shown for the entire protein (% in front of species name), deacetylase domains (DD) and zinc-finger ubiquitin-binding domain (Znf-UBP). (***iii***) Amino acid comparison of the serine-glutamate tetradecapeptide (SE14) region for the indicated mammals. ***B***, Developmental expression of zebrafish KDACs by qPCR. Data are mean ± SEM, relative to 18S expression, of *n* independent experiments: (***i***) HDAC1, *n*=3-8; (***ii***) HDAC6, *n*=3-8; (***iii***) SIRT1, *n*=3-7; (***iv***) SIRT2, *n*= 3-6. ***C***, KDAC inhibitors (KDACi)-induced changes in histone and tubulin acetylation in 6 dpf zebrafish by Western blotting. Larvae treatment (3-6 dpf) with 10 µM MS-275 or 1 µM tubastatin A induced acetylation in histone H3 (H3K9) or α-tubulin, respectively. β-Actin was used as loading control.

locomotion profile).

Activity of mitochondrial respiratory complexes

Sample preparation. At 6 dpf, 30 whole larvae per treatment condition were sonicated (Sonics Vibra-cell) in ice-cold lysis buffer (250 mM sucrose; 20 mM HEPES; 3 mM EDTA, pH 7.5) (403) followed by 3 freeze-thaw cycles. Samples were then centrifuged at 600 g (10 min, 4ºC) and the supernatant re-centrifuged at 20,000 g (25 min, 4ºC) yielding the mitochondrial pellet that was resuspended in ice-cold lysis buffer. For separate head *vs*. body mitochondria assays, 100 larvae per treatment condition were divided with a scalpel blade in ice-cold lysis buffer prior to sonication. Protein concentration in mitochondrial samples was quantified via Bradford method using bovine serum albumin (BSA) standards (445).

Citrate synthase. Citrate synthase activity was determined by measuring 5-thio-2-nitrobenzoate absorvance, spectrophotometrically at 405 nm in a microplate reader (Biotek Synergy HT®). Kinetic-readings were performed at 30ºC in 30s intervals, in 96-well plates containing 25 µL of mitochondrial suspension (approximately 3 µg of protein) and 200 µL of assay buffer [10mM Tris-HCl, 500 µM 5,5'-dithiobis-(2-nitrobenzoic acid), pH=8.1] with 200 µM acetyl coenzyme A. After 5 min of basal readings, 1 mM oxaloacetate was added to the wells and changes in signal recorded for 30 min (446).

Complex I. Complex I activity was quantified by monitoring 2,6-dichlorophenolindophenol (DCPIP) reduction (decreased DCPIP absorbance at 600 nm). Kinetic-readings at 30s intervals were performed at 30ºC with a microplate reader (Biotek Synergy HT®). Mitochondrial suspensions (25 µL with approximately 3 µg of protein) were incubated

in 96-well plates with 150 µL of assay buffer (25 mM KH_2PO_4, 5mM $MgCl_2$, pH=7.2) supplemented with 3.5 mg/mL BSA, 120 µM DCPIP and 50 µM ubiquinone Q_1, during 5 min. 125 µM β-nicotinamide adenine dinucleotide (NADH) was then added and absorbance changes recorded for 15 min, followed by rotenone (7 µM) addition to determine the rotenone-insensitive DCPIP reduction rate (taken as non-complex I mediated) for an additional 15 min (**Figure 3.4.4*B***) (447).

Complex II. Complex II activity was determined similarly to complex I (DCPIP reduction) except that the assay buffer was supplemented with 4 µM antimycin A, 7 µM rotenone, 50 µM DCPIP and 50 µM ubiquinone Q_1. Also, different from complex I determination was the use of 20 mM succinate and 5 mM malonate instead of NADH and rotenone, respectively (403).

KDAC sequence homology

HDAC1 and HDAC6 protein sequences were obtained from NCBI (http://ncbi.nlm.nih.gov/protein). For HDAC1: *Homo sapiens* CAG46518.1; *Pan paniscus* XP_003828201.1; *Pan troglodytes* JAA34765.1; *Gorilla gorilla* XP_004025419.1; *Macaca mulatta* AFJ71458.1; *Callithrix jacchus* JAB49873.1; *Otolemur garnettii* XP_003801297; *Mus musculus* AAI08372.1; *Rattus norvigecus* NP_001020580.1; *Danio rerio* AAI65208.1; *Drosophila melanogaster* AAC61494; *Caenorhabditis elegans* O17695.1; *Saccharomyces cerevisiae* AAB20328.1. For HDAC6: *H. sapiens* NP_006035.2; *P. paniscus* XP_003807271.1; *P. troglodytes* JAA44515.1; *G. gorilla* XP_004064155.1; *M. mulatta* AFI34191.1; *C. jacchus* XP_002762913.2; *O. garnettii* XP_003799739.1; *M. musculus* AAH41105.1; *R. norvigecus* XP_001057931.1; *D. rerio* XP_693858.5; *D. melanogaster* AFI26269.1; *C. elegans* Q20296.2; *S. cerevisiae* CAA95883.1. Percentages of identity were calculated using BLAST (http://ncbi.nlm.nih.gov/Blast.cgi).

KDAC gene transcription (qPCR)

In each experiment, 15 larvae per condition at 3, 4, 5 and 6 dpf were collected and stored in RNA*later*®. RNA was extracted with illustra RNAspin Mini RNA isolation kit (GE Healthcare, Piscataway, NJ, USA), according to manufacturer's instructions, and quantified spectrophotometrically at 260 nm. RNA purity was assessed by 260/280 nm absorbance ratio and by agarose (1.2%) gel electrophoresis. cDNA were synthesized from 0.5 µg RNA using the iScript™ cDNA synthesis kit (Bio-Rad, Hercules, CA, USA), according to manufacturer's instructions. KDAC expression levels were determined using qPCR (Bio-Rad, iQ™5): 4 µL cDNA diluted 1:10 was added to the reaction mixture containing 1x iQ™ SYBR Green supermix (Bio-Rad) and 200 nM of each primer (**Table 3.4.1**), in a final volume of 20 µL. qPCR primers for HDAC1 and HDAC6 were designed with Primer-BLAST (http://www.ncbi.nlm.nih.gov/tools/primer-blast/) using the zebrafish KDAC DNA sequences available in Ensembl (http://www.ensembl.org/index.html). Primers were synthetized by Stab-Vida (Setúbal, Portugal). 18S was used as a reference gene (448). qPCR primers for SIRT1, SIRT2 and 18S were previously described in literature (449-451). qPCR initiated with 3 min denaturation at 95ºC, followed by 40 cycles of denaturation, annealing and extension with conditions summarized in **Table 3.4.1** for each gene. A melting curve and a standard curve with 5-fold serial dilutions of cDNA were generated in each qPCR reaction. PCR products were analysed in an agarose (1.2 %) gel electrophoresis to confirm the presence of single bands and the respective size of the amplified product (**Figure 3.4.S2**). Relative gene expression was calculated using the $2^{-\Delta\Delta Ct}$ procedure (452) and normalized to 18S expression.

Western blot

30 Larvae per condition at 6 dpf were sonicated (Sonics Vibra-cell) in ice-cold lysis buffer (50 mM Tris-HCl, pH 7.4, 1% NP-40, 0.25% Na-deoxycholate and 1 mM EDTA) supplemented with protease and phosphatase inhibitor cocktail (10085973, Fisher Scientific, Loures, Portugal). After sonication, lysates were incubated during 1h, at 4ºC, and then centrifuged at 12,000 g for 10 min. Supernatant protein concentrations were quantified by the Bradford method (445). Lysate samples were heated at 95ºC for 5 min in the presence of 6x sodium dodecyl sulphate (SDS) sample buffer and 5% β-mercaptoethanol, as previously described (453). Equal amounts of protein (50 µg) were loaded into 12% SDS-PAGE (polyacrylamide gel electrophoresis) gel and the electrophoresis run at 125 V, for 70 min, using the Mini-PROTEAN® Tetra Cell (Bio-Rad). Proteins were then transferred into a nitrocellulose membrane, during 1.5 h, at 40 V, using the Mini Trans-Blot® Cell (Bio-Rad) (4ºC). Protein transference was assessed by Ponceau S staining. Membranes were blocked with 5% non-fat dry milk in PBST [phosphate buffered solution (PBS) with 0.05% Tween 20], overnight, at 4ºC. Membranes were incubated with primary antibodies during 1h, at room temperature: rabbit polyclonal anti-histone H3 (acetyl K9) (1:1000) (ab10812; Abcam, Cambridge, UK); mouse monoclonal anti-acetylated-α-tubulin (1:5000) (T6793; Sigma-Aldrich); rabbit polyclonal anti-β-actin (1:5000) (ab8227; Abcam). After washing with

Table 3.4.1. Primer sequences and qPCR conditions during 40 cycles for the indicated genes.

Target	Primer F	Primer R	qPCR conditions
HDAC1	ACATCAAGTTCCTCCGCTCC	TGTAGACCTCCTGCCCA TT	95ºC 15s 58.1ºC 30s 68ºC 20s #
HDAC6	CTGCACAGGCCATA TC CA	TTCCATGGTGAACGTCCCAG	95ºC 15s 60ºC 60s #
SIRT1	ACTGATGAAGGTGTTCATCCCA	GAGATGTTGATGATGATCTGCCA	95ºC 15s 57.2ºC 30s 68ºC 20s #
SIRT2	TCTCTGAAGAAATTCCTAAGTGCGATTCC	TTATCTGAATCAAAATCCATTCCGCCTC	95ºC 15s 59.9ºC 30s 68ºC 20s #
18s	TTGTTGGTGTTGTTGCTGGT	GGATGCTCAACAGGGTTCAT	95ºC 15s 58.9ºC 30s 68ºC 20s #

Data collection

PBST, membranes were incubated with secondary antibodies conjugated with horseradish peroxidase (HRP) for 1 h, at room temperature [donkey polyclonal HRP-conjugated secondary antibody anti-rabbit (1:50000) (ab98503; Abcam) and donkey polyclonal HRP-conjugated secondary antibody anti-mouse (1:10000) (ab98799; Abcam)]. β-actin was used as loading control. Proteins were detected using Immun-Star™ WesternC™ Chemiluminescence kit (Bio-Rad) and ChemiDoc™ MP Imaging System (Bio-Rad).

Statistical analysis

Results are shown as mean ± standard error of mean (SEM) from *n* independent experiments, unless otherwise stated in Figure Legends. In each experiment, individual larvae values were averaged prior to ratio calculations (e.g. time in movement per initiation). Survival tests of larvae treated with MPP^+ or with MPP^+ and rotenone were analysed via Kaplan-Meier. One-way ANOVA with post test for linear trend was used to evaluate concentration- or time-dependent effects. Results were considered statistically different when $P < 0.05$. All statistical analyses and graphical presentations were performed with GraphPad Prism version 6.0 (San Diego, CA, USA).

Results

HDAC1 and HDAC6 expression in zebrafish

KDAC inhibition, mainly as a sytrategy to modulate gene expression, has been investigated as a therapeutic approach for some diseases, including cancer and neurodegenerative disorders (425). The study of the therapeutic potential of KDACi requires animal models with characterised KDAC expression and function. Therefore, in order to validate zebrafish as a model for testing epigenetic modulatory drugs such as KDACi, we performed homology comparisons of zebrafish HDAC1 and HDAC6 with that of other species, and monitored their expression profile during zebrafish embryonic development. Using the NCBI protein database, zebrafish HDAC1 and HDAC6 sequences were compared with respective homologues in primates and in other species that, like zebrafish, are commonly used as experimental models, i.e., mouse, rat, fly, nematode and yeast (**Figure 3.4.1*A***). HDAC1 is highly conserved in the species analysed. Human and zebrafish HDAC1 exhibit 92% global homology (96% at the deacetylase domain; DD) and both contain 4 other key structural elements, namely, one nuclear localization signal (NLS) and three nuclear export signal (NES) sequences. *Drosophila melanogaster* (fly), *Saccharomyces cerevisiae* (yeast), or *Caenorhabditis elegans* (nematode), respectively, lack 2, 3 or 4 of the additional structural elements (**Figure 3.4.1*Ai***).

Regarding HDAC6, there is a higher variability between species. Human HDAC6 is constituted by two DD (DD1 and DD2), two NES sequences, one NLS, one dynein motor binding (DMB) sequence, one zinc-finger ubiquitin-binding protein domain (Znf-UBP) and one serine-glutamate tetradecapeptide repeat domain (SE14). Yeast HDAC6 homologue, HDA1, which presents one DD, has only 39% of percentage of identity in relation to human HDAC6, while zebrafish presents 50% (**Figure 3.4.1*Aii***). The inter DD domain sequence described as dynein motor binding (DMB) in human HDAC6 (454) lacks homology (according to BLAST, NCBI), with the respective inter DD sequence of non-mammalian organisms, rendering uncertain the existence of a functionally equivalent DMB domain in these species. Additionally, known NES and NLS sequences were also absent from the HDAC6 protein of zebrafish, fly, nematode and yeast, meaning that their relative HDAC6 cellular distribution may differ from human HDAC6 (**Figure 3.4.1*Aii***). SE14 is suggested responsible for stable HDAC6 cytoplasmic retention (455) and present in

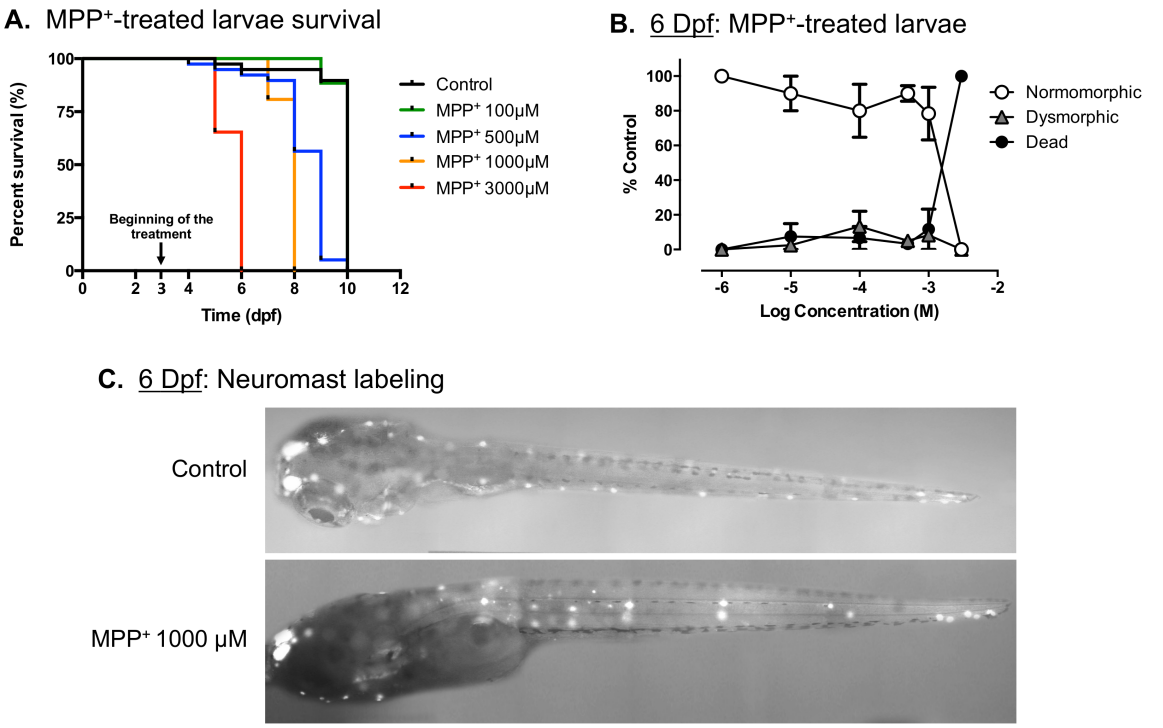

Figure. 3.4.2. Survival and neuromast labelling in MPP$^+$-treated zebrafish larvae. ***A***, Time-dependent survival of control larvae *vs*. MPP$^+$ treatment (0.1 – 3 mM) starting at 3dpf. Each treatment condition was assessed in 26-39 individual larvae, randomly sampled from a synchronized multiparental clutch. ***B***, Normomorphic (white circles), dysmorphic (grey triangles) and dead (black circles) larvae, at 6 dpf, after 3 days of treatment (3-6 dpf) with MPP$^+$ at the indicated concentrations. Data are mean ± SEM of 3-9 independent experiments. ***C***, Representative neuromast labelling in control and MPP$^+$- treated larvae (1 mM from 3 to 6 dpf). Both images were taken at 6 dpf.

higher primates. Marmoset and galago present only 5 and 1 SE14 repetitions, respectively, while higher primates present 8, being uncertain whether this domain is functional in marmoset and galago (**Figure 3.4.1*Aiii***).

Zebrafish expressed HDAC1 and HDAC6 during the studied period: 1-6 dpf (**Figure 3.4.1*B***). HDAC6 expression is almost constant during the embryonic development, whereas HDAC1 expression decreases from 3 to 6 dpf. In order to better characterize the KDAC expression, the SIRT1 and SIRT2 expression were also studied during zebrafish embryonic development: SIRT1 and SIRT2 showed a robust increase in expression until 4 dpf, and subsequently declined. We tested whether KDAC inhibitors (HDAC1, 10 µM MS-275; HDAC6, 1 µM tubastatin A; SIRT1, 10 µM EX-527; SIRT2, 1 µM AGK2) would induce compensatory changes in transcription of their target enzyme, but found no changes in larvae treated from 3 to 6 dpf (**Figure 3.4.S3**). In spite of structural differences between zebrafish and human HDAC6, the selective HDAC6 inhibitor, tubastatin A, increased acetylation of zebrafish α-tubulin K40, a HDAC6 target (439) (**Figure 3.4.1*C***). Similarly, MS-275, a selective inhibitor of human HDAC1 (440), increased acetylation of zebrafish histone H3K9 (**Figure 3.4.1*C***).

MPP$^+$ induced locomotor abnormalities in zebrafish

MPP$^+$ is a known dopaminergic neurotoxin (248), previously tested in zebrafish, but with limited characterization of associated locomotor changes (257-259, 319). For MPP$^+$ concentration selection we tested different concentrations in a larvae survival test without feeding. Control larvae survived until 10 dpf. MPP$^+$ treatment, starting at 3 dpf, accelerated larval death in a concentration-dependent manner, with 100 µM being the highest concentration where survival was no different from control (**Figure 3.4.2*A***). Considering the experimental time period 3-6 dpf, 1 mM (1000 µM) MPP$^+$ was the highest concentration without significant changes in dysmorphic or dead embryos (**Figure 3.4.2*B***), and it also did not affect neuromast labelling at 6 dpf (**Figure 3.4.2*C***).

Neuromasts are sensory structures, rich in mitochondria (456), which help in evaluating the MPP$^+$ selective toxicity to central nervous system (CNS).

Sensorimotor reflexes (tail and head touch responses) and locomotor profiles monitored daily from 3-7 dpf under control conditions highlighted 6 dpf as the best period for these behavioural

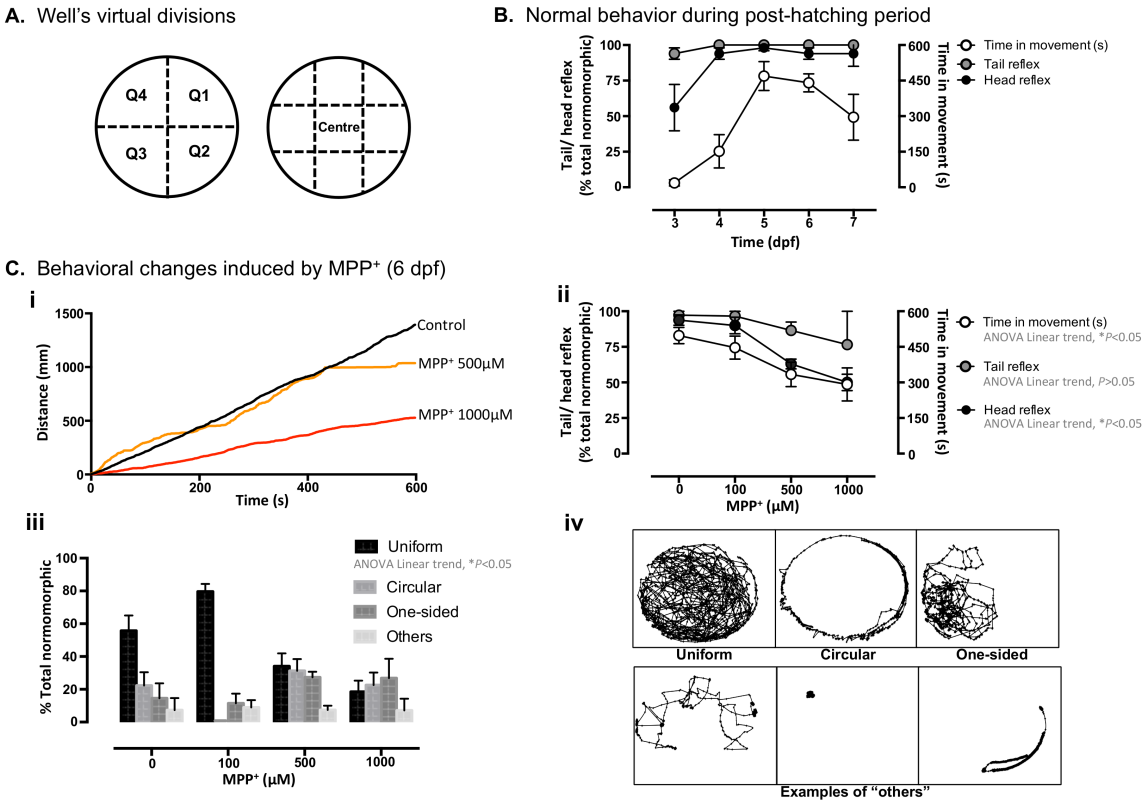

Figure 3.4.3. Behaviour analysis in control and MPP$^+$–treated larvae. ***A***, Virtual quadrant (Q) division for automated locomotion analysis in microplate wells. ***B***, Developmental-dependent (3-7dpf) changes in time in movement (white circles; right Y axis; 0-600 seconds), and sensorimotor reflexes evoked by tail- (grey circles) or head-touch (black circles) in % of control normomorphic larvae (left Y axis). Data are mean ± SEM, of 5 independent experiments, each performed with 10 larvae. ***C***, (***i***) Representative time (s) *vs.* distance (mm) profile of control and MPP$^+$-treated (3-6 dpf) larvae at the indicated concentrations, with readings at 6 dpf; (***ii***) time in movement, tail and head reflexes; (***iii***) locomotion patterns scored as uniform, circular, one-sided and others, according to representative tracings shown in (***iv***). Data are mean ± SEM, of 3-8 independent experiments, each with at least 10 larvae per treatment condition. *P<0.05, One-way ANOVA with post test for linear trend: (***ii***) time in movement, tail and head reflex; (***iii***) uniform profile.

analyses. More than 95% of larvae presented a positive tail reflex at 3 dpf, whereas only about 56% presented head reflex, the latter reaching maximum at 4 dpf (**Figure 3.4.3*B***). Locomotor parameters were maximal at 5–6 dpf (**Table 3.4.2**), as represented by 'time in movement' (**Figure 3.4.3*B***). Higher locomotion corresponded to increased time in movement, travelled distance, number of described circles, time in centre and higher time in movement per initiation (**Table 3.4.2**). We stress that the number of initiations must be analysed together with other parameters (e.g. time in movement), as initiations can be low for larvae with very low motility, as well as for those with high motility that do not stop. Higher locomotion was also associated with lower SD for movement distribution (**Table 3.4.2**), meaning uniform movement (**Figure 3.4.3*Civ***, Top Left) across the well's quadrants (**Figure 3.4.3*A***, Left). We thus chose 6 dpf as the time for behavioural evaluation. We started treatments at 3 dpf, not only because hatched larvae avoid chorion permeability issues, but also because at 3 dpf their CNS is significantly developed and with a spatial distribution of dopaminergic neurons similar to that found in adult zebrafish (316).

MPP$^+$ (100, 500 and 1000 µM; from 3-6 dpf) concentration-dependently induced behavioural abnormalities at 6 dpf (**Figure 3.4.3*C***; **Table 3.4.2**). 100 µM MPP$^+$ changed little or none of the parameters *vs.* control, whereas 500 and 1000 µM MPP$^+$ significantly affected multiple parameters. We thus focused on 500 µM MPP$^+$, as the minimal effective concentration (**Figure 3.4.3*C***, **Table 3.4.2**) and with arguably selective dopaminergic toxicity at 6 dpf (no effect on survival, morphology or neuromasts; **Figure 3.4.2**). 500 µM MPP$^+$ selectively decreased the head touch response, without affecting the tail response (**Figure 3*Cii***, black *vs.* grey circles, as % of total normomorphic larvae – Left Y axis). Interestingly, MPP$^+$ did not change movement speed, but increased the number of initiations (or stops) albeit swimming for shorter periods, thus resulting in decreased total distance, total time in movement, and time in movement per initiation (**Table 3.4.2**). Also, 500 µM

Table 3.4.2. Locomotor parameters of control and drug-treated larvae at the indicated dpf. Drug treatment was from 3 to 6 dpf. Larvae locomotion was analysed during 600s. Data are mean ± SEM of 3-8 independent experiments, each with at least 10 larvae per treatment condition.

		Locomotor parameters (600s)								
Treatment	**Time (dpf)**	Distance (mm)	Time (s) in movement	Initiations / 10 s	Time (s) in movement / initiation	Movement speed (mm/s)	SD (quadrant permanence)	Circles (nr)	Time in centre (% total)	Larvae without movement (% total)
Control	3	83.0 ± 51.1	18.5 ± 13	2.4 ± 0.9	5.4 ± 2.4	7.2 ± 1.5	39 ± 1.7	0.6 ± 0.5	2.0 ± 1.5	61 ± 7.5
	4	429 ± 251	152 ± 70	9.0 ± 2.5	13 ± 4.4	3.2 ± 1.1	31 ± 4.2	2.9 ± 1.9	3.3 ± 1.7	28 ± 10
	5	976 ± 213	469 ± 61	16 ± 3.5	48 ± 23	2.0 ± 0.2	15 ± 4.4	11 ± 3.1	8.6 ± 2.2	2.5 ± 2.5
	6	903 ± 181	441 ± 38	16 ± 2.6	36 ± 14	2.0 ± 0.2	13 ± 2.3	9.6 ± 2.0	7.8 ± 1.8	2.2 ± 2.2
	7	488 ± 108	295 ± 43	23 ± 4.0	14 ± 2.8	1.6 ± 0.3	21 ± 2.8	5.4 ± 1.7	5.5 ± 1.7	0.0 ± 0.9
Control	6	1230 ± 155	497 ± 34	13 ± 1.1	41 ± 5.0	2.4 ± 0.2	11 ± 1.4	14 ± 2.3	3.8 ± 0.5	2.9 ± 2.9
MPP^+ 100 µM	6	1188 ± 155	460 ± 31	12 ± 1.7	41 ± 8.1	2.6 ± 0.3	12 ± 2.8	12 ± 5.3	5.7 ± 0.9	3.3 ± 3.3
MPP^+ 500 µM (M500)	6	↓839 ± 167	↓334 ± 51	↑18 ± 2.0	↓19 ± 2.1	2.4 ± 0.1	↑20 ± 2.2	↓7.0 ± 1.9	3.5 ± 1.1	3.7 ± 2.4
MPP^+ 1000 µM	6	811 ± 253	292 ± 79	14 ± 1.9	21 ± 4.4	2.6 ± 0.3	22 ± 2.5	4.7 ± 1.4	2.3 ± 1.2	12 ± 5.9
MS-275 10 µM	6	522 ± 259	244 ± 109	29 ± 9.6	10 ± 5.7	2.0 ± 0.4	19 ± 1.5	4.3 ± 2.5	3.3 ± 1.0	0.0 ± 0.0
TUB 1 µM	6	1342 ± 15.7	532 ± 4.4	14 ± 4.0	49 ± 18	2.5 ± 0.02	17 ± 6.2	13 ± 0.7	4.1 ± 1.4	0.0 ± 0.0
IDB 3 µM	6	1176 ± 3.65	530 ± 38	12 ± 1.3	45 ± 8.2	2.2 ± 0.2	14 ± 2.3	12 ± 0.2	5.9 ± 1.1	0.0 ± 0.0
DCB 10 µM	6	1178 ± 164	451 ± 29	16 ± 4.3	31 ± 5.8	2.6 ± 0.4	15 ± 0.6	11 ± 3.5	4.1 ± 2.2	0.0 ± 0.0
MS-275 10 µM + M500	6	222 ± 35.0	117 ± 7.8	18 ± 2.8	6.7 ± 0.9	1.9 ± 0.2	26 ± 0.5	1.2 ± 0.4	3.1 ± 1.9	3.7 ± 3.7
TUB 1 µM + M500	6	1045 ± 114	401 ± 64	17 ± 0.4	24 ± 4.5	2.7 ± 0.2	18 ± 2.6	9.4 ± 1.6	1.6 ± 0.2	3.3 ± 3.3
IDB 3 µM + M500	6	558 ± 4.71	248 ± 24	13 ± 5.4	22 ± 7.3	2.3 ± 0.3	23 ± 2.7	2.6 ± 0.9	3.7 ± 3.2	5.5 ± 5.5
DCB 10 µM + M500	6	1084 ± 170	440 ± 37	19 ± 2.0	24 ± 3.8	2.4 ± 0.2	20 ± 1.6	7.8 ± 1.2	2.9 ± 0.7	6.7 ± 3.3

MPP^+ decreased the number of circles and movement uniformity (increased SD for quadrant permanence – **Table 3.4.2**, and decreased % larvae with uniform movement – **Figure 3.4.3*Ciii***, ***iv***).

MPP^+ inhibited zebrafish complex I activity.

MPP^+ toxicity is typically associated with complex I inhibition (248). To verify this assumption in the zebrafish model and test for additional MPP^+ mitochondrial effects, we assessed the activity of mitochondrial complex I, complex II, and citrate synthase, together with the quantification of the total mitochondrial protein per larvae. Larvae treated with MPP^+ (100, 500 or 1000 µM) from 3 to 6 dpf exhibited no change in complex I, complex II and citrate synthase activity nor in total mitochondrial protein per larvae (**Figure 3.4.4*A***). In contrast, low concentrations of the complex I inhibitor rotenone (0.1 µM from 3-6 dpf) sufficed to decrease complex I activity by 49.3 ± 25.4 %, and also decreased mitochondrial protein by 32.2 ± 5.32 % (**Figure 3.4.4*A***). We then tested whether MPP^+ (100, 500 and 1000 µM from 3-6 dpf) differentially affected head (enriched in brain mitochondria) *vs*. body (enriched in muscle) mitochondria (**Figure 3.4.4*C***). When corrected for total mitochondrial protein, complex I, complex II and citrate synthase activity were lower in head *vs*. body mitochondria under control conditions, possibly due to functional differences between brain and muscle mitochondria. The positive control rotenone (0.1 µM) strongly reduced complex I but not complex II or citrate synthase activity, with a modest reduction in both head and body mitochondria protein per larvae (**Figure 3.4.4*Ci-iv***). Interestingly, MPP^+ at 100 and 500 µM exhibited a trend towards increased complex I and II activity in head, but not body mitochondria, that disappeared at 1000 µM together with a trend for decreased citrate synthase activity (**Figure 3.4.4*Ci-iii***).

Given the modest changes observed in mitochondrial extracts from MPP^+ exposed larvae, we tested the effects of directly adding MPP^+ to control mitochondrial extracts. Direct MPP^+ addition to mitochondrial extracts concentration-dependently inhibited complex I but not complex II activity, with 1 mM and 5 mM, respectively, reaching 41.0 ± 5.63 % and 62.3 ± 9.50 % inhibition, One-Way ANOVA with test for linear trend $P < 0.05$ (**Figure 3.4.4*D***). While substantial complex I inhibition in mitochondrial extracts was only achieved with high MPP^+ concentration, lower concentrations added to live larvae are likely to accumulate selectively in dopaminergic neurons via dopamine transporter uptake (258). Moreover, mitochondrial membrane potential ($\Delta\psi_m$)-dependent MPP^+ accumulation should substantially increase the actual concentration in the vicinity of mitochondrial complexes (261). We thus tested whether combined chronic exposure of MPP^+ (500 µM) with rotenone (0.3 µM; aiming to depolarize mitochondria) would modify larvae survival. In co-exposure, the mean survival of rotenone plus MPP^+ (CI 95% = 8.3-8.7 days) overlapped that of MPP^+ alone (CI 95% = 8.0-8.7 days). In pre-exposure experiments, however, rotenone (starting at 1 dpf) combined with MPP^+ (starting at 3 dpf) allowed for a modest increase in mean survival (CI 95% = 8.3-

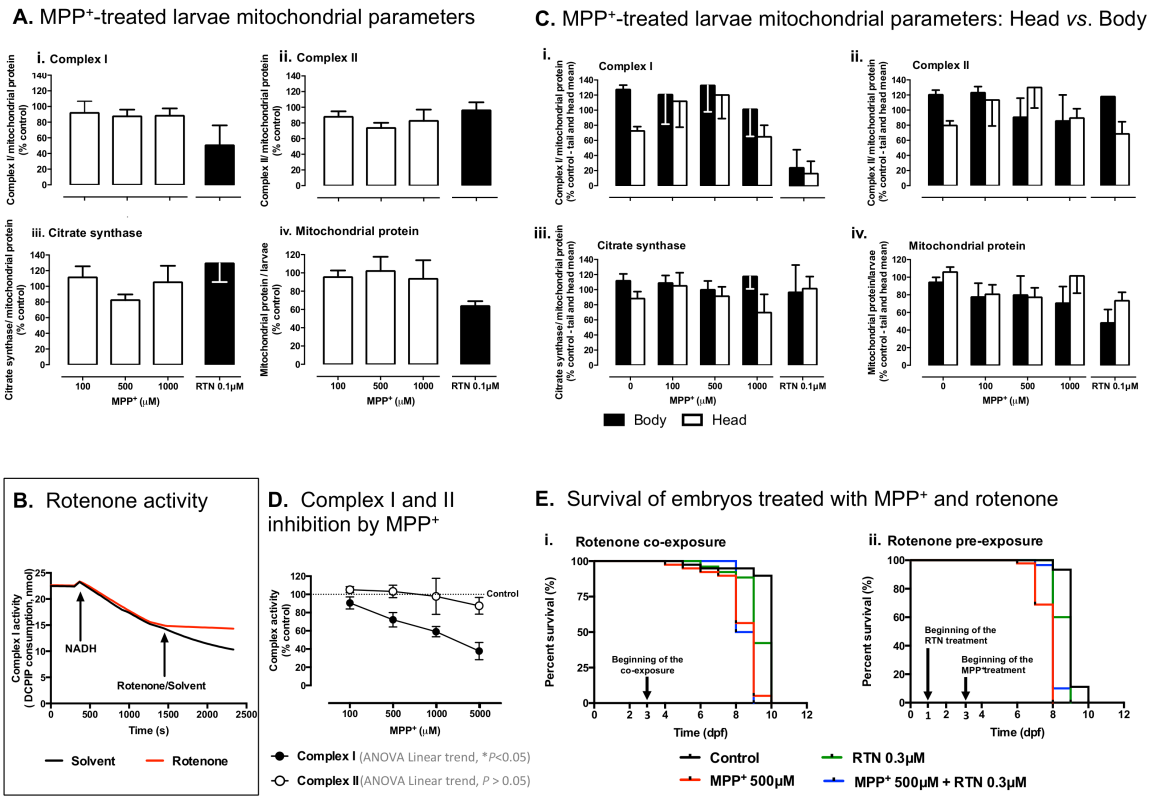

Figure 3.4.4. Mitochondrial parameters in control, MPP$^+$-, and rotenone-treated larvae. ***A***, Complex I (***i***), complex II (***ii***) and citrate synthase (***iii***) activity and mitochondrial protein (***iv***), at 6 dpf, in larvae treated with MPP$^+$ (white bars) or 0.1 µM rotenone (black bars), in % of control. Data are mean ± SEM of 4 independent experiments, each with at least 30 larvae per treatment condition. ***B***, Representative graph of complex I activity assessment, shown as DCPIP consumption (nmol) over time (s). Reaction started with NADH addition at 300s and stopped with rotenone at 1200s. ***C***, Complex I (***i***), complex II (***ii***) and citrate synthase (***iii***) activity and mitochondria protein (***iv***), at 6 dpf, in MPP$^+$ and 0.1 µM rotenone treated-larvae, separated into head (white bars) and body (black bars) prior to measurements. Data are mean ± SEM of 3-5 independent experiments, each with at least 100 larvae per treatment condition, expressed in % control (mean value between control head and tail data = 100%). ***A***, ***C***, Larvae treatment occurred from 3 to 6 dpf. ***D***, Complex I and II activity quantification in control mitochondrial extracts acutely exposed to MPP$^+$ at the indicated concentrations. Data are mean ± SEM in % control (no MPP$^+$) of 4-5 independent experiments, each with at least 30 larvae per treatment condition. *P< 0.05, One-way ANOVA with post test for linear trend. ***E***, Time-dependent survival in larvae treated with MPP$^+$ (500 µM) with or without rotenone (0.3 µM) co-exposure (Left; ***i***) or pre-exposure (Right, ***ii***). Data are from 30-45 larvae per treatment in rotenone pre-exposure assay and 26-39 larvae per treatment in rotenone co-exposure assay, randomly sampled from a synchronized multiparental clutch.

-8.6 days) *vs*. MPP$^+$ alone (CI 95% = 7.9-8.2 days) (**Figure 3.4.4*E***). Thus, these findings are compatible with the hypothesis that MPP$^+$ toxicity for zebrafish larvae is $\Delta\psi_m$-dependent.

Discussion

Zebrafish express HDAC1 and HDAC6 with deacetylase activity

KDAC inhibitors are putative neuroprotective compounds (457), and have the potential to modulate mitochondrial dynamics (425). Here we investigated the impact of HDAC1 or HDAC6 inhibition upon the MPP$^+$-induced Parkinsonian phenotype in zebrafish. HDAC6 partakes in several mechanisms often impaired in neurodegenerative disorders, e.g. microtubule transport, misfolded-protein degradation and autophagy (425, 458). Human HDAC6 has a preferential cytoplasmic localization where it deacetylates targets such as α-tubulin, cortactin or heat shock protein 90 (HSP90). In higher mammals, HDAC6 has a serine-glutamate tetradecapeptide (SE14) domain (459) promoting its stable cytoplasmic retention in a leptomycin B resistant manner (455). Leptomycin B inhibits nuclear export by alkylating the NES receptor, CRM-1 (chromosome region maintenance 1) (460). Mice, and possibly most animals other than higher primates, lack the SE14 domain in their HDAC6 homologue (**Figure 3.4.1*Aii-iii***), with leptomycin B promoting mouse HDAC6 nuclear localization (461). Despite the SE14 absence, mouse HDAC6 is also predominantly cytoplasmic, which is reported to be

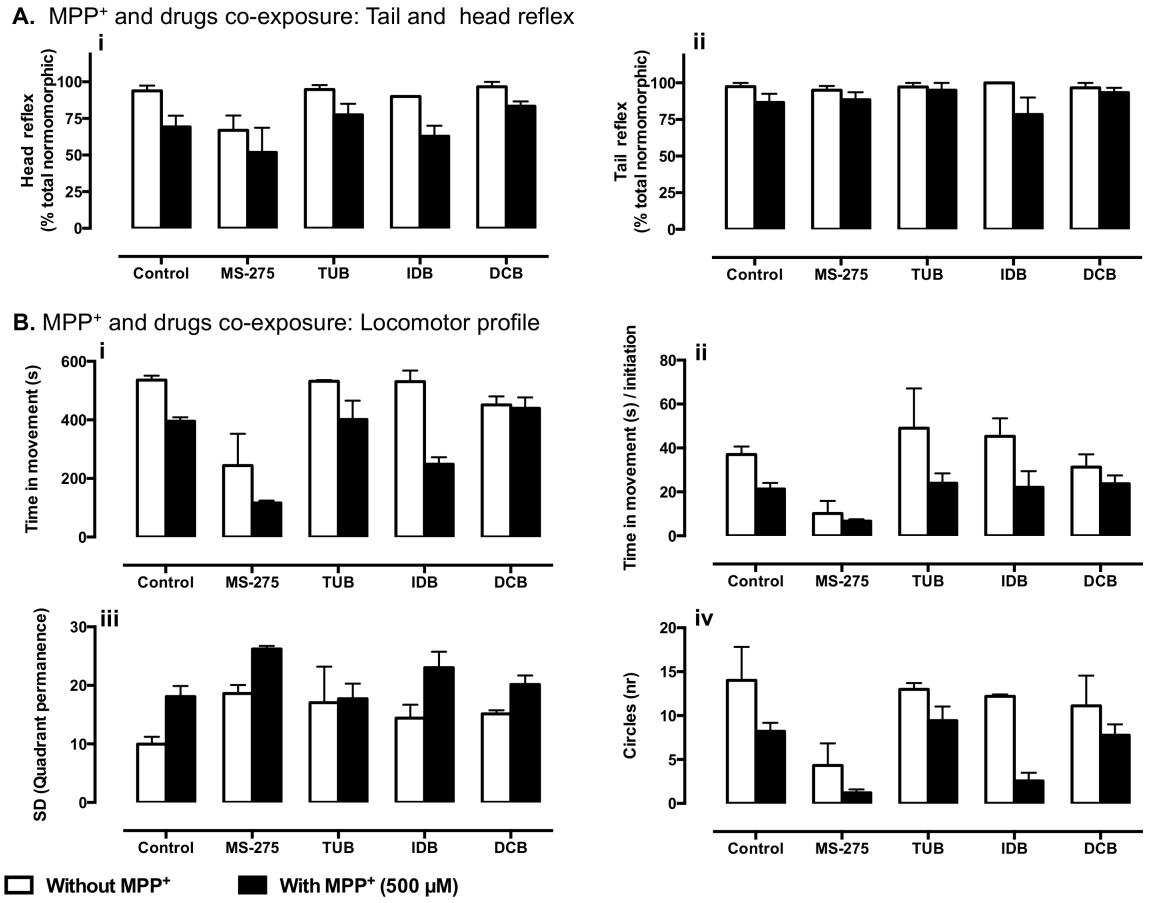

Figure 3.4.5. Sensorimotor reflexes and locomotor profile in 6 dpf zebrafish following drug-treatment. Larvae were treated from 3 to 6 dpf without (white bars) or with (black bars) 500 µM MPP^+, in co-exposure with solvent (control), 10 µM MS-275, 1 µM tubastatin A (TUB), 3 µM idebenone (IDB) or 10 µM decylubiquinone (DCB). ***A***, Head (***i***) and tail (***ii***) reflex expressed in total normomorphic percentage. ***B***, Time in movement (***i***), time in movement per initiation (***ii***), standard deviation of quadrant permanence (***iii***) and number of circles (***iv***). Data are mean ± SEM of 3 independent experiments, each with at least 10 larvae per treatment condition.

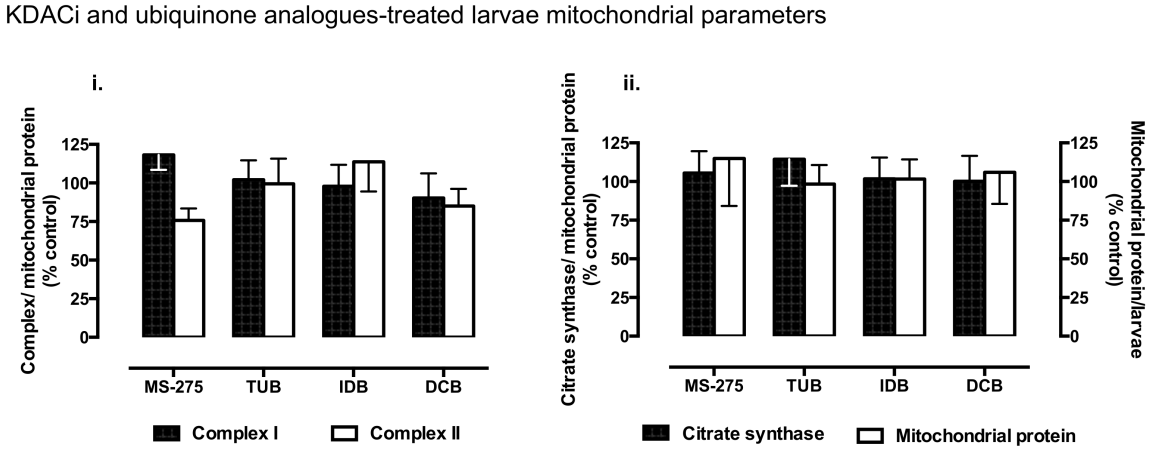

Figure 3.4.6. Effect of KDAC inhibitors and ubiquinone analogues upon zebrafish mitochondrial parameters. Complex I, complex II (***i***) and citrate synthase activity and mitochondrial protein (***ii***) of 6 dpf larvae, treated from 3 to 6 dpf with 10 µM MS-275, 1 µM tubastatin A (TUB), 3 µM idebenone (IDB) or 10 µM decylubiquinone (DCB). Data are mean ± SEM of 3-5 independent experiments, each with at least 30 larvae per treatment condition.

due to the first NES that is also found in other mammals (461).

Zebrafish and *Drosophila* HDAC6 homologues lack a known NES or NLS (**Figure 3.4.1*Aii***), but *Drosophila* HDAC6 is nevertheless preferentially cytoplasmically located (462). Subcellular localization of human HDAC6 is also regulated by acetylation, which favours cytosolic retention by preventing NLS interaction with importin-α (463). HDAC6 dynein motor binding domain (DMB) assists trafficking and clearance of ubiquitinated proteins by agressome formation: HDAC6 DMB binds dynein whereas the Znf-UBP domain binds ubiquitin (464). Zebrafish HDAC6 lacks a known DMB, with uncertain functional consequences. Currently, little is known about HDAC6 in zebrafish. HDAC6 seems necessary for zebrafish angiogenesis, an effect dependent of cortactin deacetylation (465). Thus, by lacking NES, NLS and DMB, the precise nature and mechanisms of zebrafish HDAC6 subcellular distribution and activity remain uncertain. Still, as with *Drosophila* HDAC6, the zebrafish homologue may also be preferentially cytosolic, and its cytosolic deacetylase activity is supported both by domain homology (**Figure 3.4.1*Aii***) as well as by our current data showing enhanced α-tubulin K40 acetylation with tubastatin A treatment (**Figure 3.4.1*C***).

HDAC1 is evolutionarily more conserved, and more extensively studied than HDAC6 in zebrafish. Unlike HDAC6, mammalian HDAC1 is predominantly nuclear (466), regulating the expression of a wide variety of genes. Zebrafish neurogenesis requires HDAC1 that regulates several genes associated with neuronal specification and CNS patterning (467). Additionally, zebrafish heart, exocrine pancreas, liver, retina, craniofacial cartilage and pectoral fin development (468-470), melanocyte differentiation (471) and haematopoiesis (472), all require HDAC1. We show that HDAC6 gene expression is relatively stable throughout zebrafish development, whereas HDAC1 expression decreases after 3 dpf (**Figure 3.4.1*B***), possibly coincident with completion of HDAC1-dependent organogenesis. Zebrafish HDAC1 and HDAC6 are functionally active, with selective pharmacological inhibition increasing physiological substrate acetylation (**Figure 3.4.1*C***). Structurally, zebrafish HDAC1 exhibits all key domains of the human isoform, some of which are absent from fly, nematode and yeast models. All non-primate models fail to fully recapitulate key human HDAC6 features. Even though mice and rats possess the DMB domain absent from zebrafish HDAC6, all these models lack the SE14 domain, as do other key small organism models also lacking DMB (fly and nematode) or even one deacetylase domain (yeast). Nevertheless, our data suggests that cytosolic localization and at least tubulin deacetylase activity are conserved in zebrafish HDAC6.

Mitochondrial and behavioural deficits in the zebrafish MPP^+ Parkinson model

The similarity between zebrafish and mammalian nervous systems, particularly dopaminergic neuronal network organization (292), has supported its use as PD model (259, 403). We used the dopaminergic toxin MPP^+ instead of the pre-toxin MPTP, due to higher handling safety, but also because MPP^+ activity is monoamine oxidase (MAO) independent (**Figure 3.4.7**) (248), thus overcoming the reported potential problem of MPTP being a weak substrate to zebrafish MAO (473). Nevertheless, studies with zebrafish embryos (1-4 dpf) have reported equal susceptibility to MPP^+ or MPTP (259).

Here we report a detailed analysis of the MPP^+-induced behavioural changes (locomotion + sensorimotor reflexes) in zebrafish larvae (**Figure 3.4.3** and **Table 3.4.2**). MPP^+ (500 μM)-treated larvae presented a locomotor profile characterised by short periods of acceleration, pausing more frequently than control larvae (**Figure 3.4.3*Ci***). Thus, MPP^+-treated larvae are in movement during less time and present a higher number of initiations. This profile resembles PD motor symptoms, where patients may present unwanted accelerations, rigidity, postural instability, and freezing of gait (474). Additionally, MPP^+-treated larvae showed an uneven movement distribution (**Figure 3.4.3*Ciii***, ***iv***), possibly due to disorientation. MPP^+ also reduced sensorimotor reflexes, specifically the escape response induced by head touch, without affecting the tail touch response (**Figure 3.4.3*Cii***). Different neuronal circuits are involved in these responses. The head reflex requires trigeminal sensory neurons, whereas the tail reflex requires the spinal Rohon-Bead sensory neurons (475). As far as we could find, there is no evidence that MPP^+ selectively targets trigeminal *vs*. Rohon-Bead sensory neurons. MPP^+ may, however, delay/impair maturation of neuronal pathways involved in the head reflex, since the percentage of MPP^+-treated larvae without head reflex at 6 dpf resembles that of control larvae at 3 dpf (when MPP^+ treatment started) (**Figure 3.4.3*B***, ***Cii***). The delayed maturation hypothesis is supported by previous studies showing rescue of zebrafish larvae motor profile following 48h MPTP washout (259). There are, however, studies suggesting that MPTP induces dopaminergic and some serotoninergic neurodegeneration in transgenic zebrafish with GFP labelled monoaminergic neurons, where decreased *in situ* tyrosine

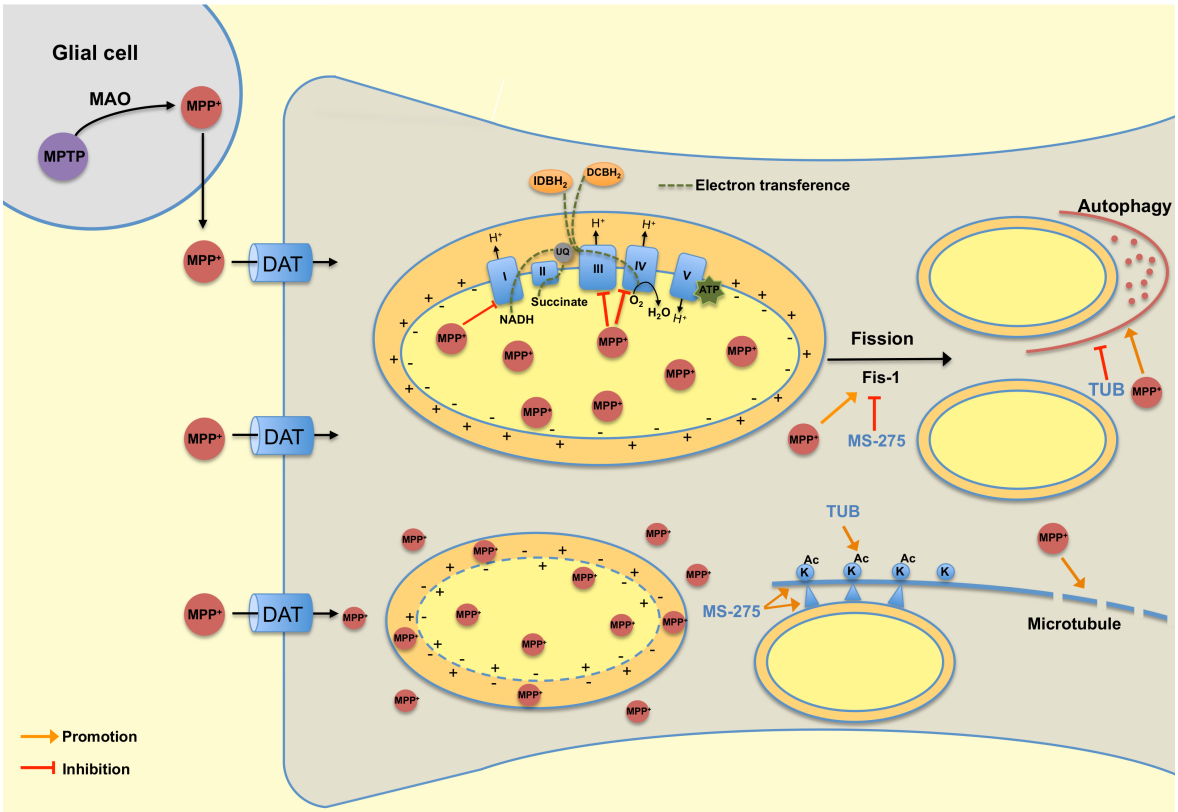

Figure 3.4.7. Mechanisms of drug-induced changes in mitochondrial bioenergetics and dynamics. MPP^+, the active metabolite of MPTP, selectively accumulates in dopaminergic neurons via the dopamine transporter (DAT) (248). MPP^+ is driven to mitochondria in a $\Delta\psi_m$-dependent manner, inhibiting complex I, and possibly complexes III and IV (264). Mitochondrial and cytosolic dehydrogenases reduce ubiquinone analogues (idebenone, $IDBH_2$ and decylubiquinone, $DCBH_2$) that in turn transfer electrons to complex III (9). MPP^+ increases mitochondrial fission (476) and autophagy (477), processes that might be affected by MS-275 (478) and tubastatin A (TUB) (425), respectively. Both tubastatin A and MS-275 promote mitochondrial trafficking (425, 479), while MPP^+ induces microtubule fragmentation, thus impairing mitochondrial transport (480).

hydroxylase hybridization also suggested neurodegeneration (435). Rescued locomotion following MPTP washout may thus involve the high capacity of zebrafish for axonal or even neuronal regeneration after local lesions (300). Significantly, 16 regions capable of neurogenesis are reported in zebrafish, contrasting with two particularly involved in formation of new neurons in mammals (481).

Neuromast labelling was unaffected in MPP^+-treated zebrafish larvae (**Figure 3.4.2*C***). Neuromasts are sensory structures arranged in the lateral line and head, detecting nearby vibrations and thus assisting behaviours such as schooling, prey capture, and predator escape (482). Positive neuromast labelling suggests that MPP^+ impairments in the head reflex are not due to an abnormal lateral line, a condition that could also impair escape behaviour (483). Moreover, the neuromast core of sensory hair cells (482), highly enriched in mitochondria (456), should have displayed decreased MitoTracker labelling if MPP^+ was acting globally via its main mechanism of complex I inhibition (248). Also, mitochondrial complex I activity was unaffected in MPP^+-treated zebrafish, either in whole larvae or even in head *vs*. body mitochondrial extracts (**Figure 3.4.4*A***, ***C***). Nevertheless, MPP^+-treated zebrafish showed locomotor defects, suggesting that MPP^+ (500 µM) is selectively targeting dopaminergic neurons [estimated less than 1% of total human brain neurons (484)], thus explaining lack of complex I inhibition in whole mitochondria extracts. In higher concentrations, however and when directly exposed to mitochondrial extracts, MPP^+ inhibited complex I but not complex II (**Figure 3.4.4*D***).

MPP^+ is a cation that accumulates inside polarized mitochondria, whereby disruption of $\Delta\psi_m$ may avoid the MPP^+ mitochondrial accumulation and consequently its effects (**Figure 3.4.7**) (261), which explains the higher MPP^+ toxicity verified in intact mitochondria *vs*. submitochondrial particles (263). Therefore, rotenone, which causes a complex I inhibition and consequently disruption of $\Delta\psi_m$ (320), could decrease the MPP^+ toxicity. In fact, when larvae were treated with a moderate concentration of rotenone able to inhibit complex I

before of MPP^+ exposure, there was a slight increase of larval mean survival in relation with larvae treated alone with MPP^+ (**Figure 3.4.4*E***). Summing up, MPP^+ induced a locomotor phenotype that may be compared with motor symptoms present in PD without detectable non-selective effects.

Effect of ubiquinone analogues and lysine deacetylase inhibitors upon MPP^+ behavioural deficits

KDACi and UQ analogues were reported neuroprotective in several neurodegenerative diseases models (427, 428, 432-434). In addition to respiratory chain dysfunction via complex I inhibition, MPP^+ has also been associated with disturbed mitochondrial dynamics, namely enhanced fission (476) and decreased microtubule dynamics with specific disruption of mitochondrial axonal transport (480) (**Figure 3.4.7**). Given the KDACi potential for modulating mitochondrial dynamics (425) and the electron carrier properties of UQ analogues capable of enhancing mitochondrial respiratory chain activity (9, 135), we tested whether these compounds could prevent/rescue MPP^+-induced behavioural phenotypes. No protection from MPP^+, however, was detected in larvae co-treated with ubiquinone analogues or KDACi (**Figure 3.4.5** and **Table 3.4.2**).

Tubulin acetylation enhances axonal transport (425) whereby selective tubulin deacetylase (HDAC6) inhibition with tubastatin A (439) might in principle rescue MPP^+-induced impairment in axonal transport (480) (**Figure 3.4.7**). However, HDAC6 presents other key homeostatic roles in neurons, namely regulating autophagy and misfolded protein degradation (454), whose inhibition might explain lack of tubastatin A protection against MPP^+. In fact, autophagy is reportedly increased in the presence of MPP^+ (477), possibly as a protective response since autophagy induction with rapamycin rescued MPP^+-induced toxicity in mice (485).

HDAC1 inhibition with MS-275 has been associated with several biological responses that might afford protection against MPP^+. MS-275 improved axonal transport in neuronal cultures (479); MS-275 induced mitochondrial elongation through fission inhibition (478) (**Figure 3.4.7**), a process reportedly protective against MPP^+ in human neuronal cell lines (486); and MS-275 increased mitochondrial biogenesis in mice skeletal muscle and adipose tissue (487), a process reported protective against MPTP in *in vitro* (SH-SY5Y cells) and *in vivo* (mice) models (488, 489). Nevertheless, our data with 10 μM MS-275 showed no protection and even worsening of MPP^+ effects in zebrafish larvae, with 10 μM MS-275 alone impairing locomotion (**Figure 3.4.5** and **Table 3.4.2**).

In spite of studies showing beneficial effects of KDACi in PD models (490, 491, these are not consensual findings. A higher prevalence of Parkinsonism was reported in patients treated with valproate {Jamora, 2007 #608). Additionally, the pan-KDACi, TSA, decreased rat, mouse and human neuronal cell line survival at nanomolar range, increasing apoptosis and neurotoxicity induced by MPTP and rotenone (492). Paraquat, another dopaminergic toxin, induced histone H3 acetylation in the rat N27 neuronal cell line, decreasing the total KDAC activity. Paraquat toxicity was reduced by inhibition of acetylation by anacardic acid, a histone acetyltransferase inhibitor (493). As far we could find, contradictory information exists about MPTP-induced histone acetylation in mouse models. Despite different doses, treatment period and analysed tissue: no increase of histone H3 acetylation was found on frontal cortex (490), whereas increased histone H3 acetylation was reported for the striatum of MPTP-treated mice (494). Furthermore a slight increase of acetylated tubulin was observed in striatum and substantia nigra of MPTP-treated mice (495).

We previously reported that UQ analogues, idebenone and decylubiquinone, delayed rotenone induced cardiac failure (443). This effect was attributed to the electron carrier properties of UQ analogues, transferring electrons from mitochondrial or cytosolic dehydrogenases to complex III (9). However, MPP^+ may inhibit other mitochondrial complexes beyond complex I, disrupting the electron respiratory chain without an alternative pathway to oxidative phosphorylation energy production. Mitochondrial complex III and IV inhibition by 200 μM MPP^+ was previously shown in isolated mice brain mitochondria (496) (**Figure 3.4.7**). Furthermore, considering that MPP^+ activity depends on $\Delta\psi_m$ (261), drugs that maintain/ increase $\Delta\psi_m$ may boost MPP^+ accumulation and thus its toxicity. Previous studies support the beneficial effect of KDACi on mitochondrial activity. Pan- and class I-specific KDACi preserve mitochondrial function and ATP levels in neurons subjected to hypoxia and glucose deprivation (497). Idebenone protected a rodent retina ganglion cell line against complex I inhibition (120); while decylubiquinone increased mitochondrial complex I and II activities in synaptosomes (135) and restored respiratory chain activity in yeast mitochondria lacking endogenous ubiquinone (117). Thus, it is conceivable that by improving mitochondrial function and holding $\Delta\psi_m$ KDACi or ubiquinone analogues may fail to rescue or even aggravate MPP^+ toxicity.

Concluding remarks

The present work shows that HDAC1 and HDAC6 are expressed and display functional deacetylase activity in zebrafish. While zebrafish HDAC1 is similar to mammalian HDAC1, more studies are needed to clarify some questions about HDAC6, namely whether zebrafish HDAC6 binds to dynein. MPP^+ induced a locomotor phenotype resembling PD motor symptoms. However, $\Delta\psi_m$-dependent MPP^+ toxicity may at least partly explain the lack of protection verified with UQ analogues and HDAC1 or HDAC6 inhibitors. In future studies, it will be valuable to assess UQ analogues and KDACi ability to rescue genetic PD models in zebrafish, namely those displaying Parkin/Pink1 mutations/ deficits.

Acknowledgments. This work was supported by "Fundação para a Ciência e a Tecnologia" (FCT), Strategic Project: PEst-C/EQB/LA006/2013, and by the Research Grants (PI: JMA Oliveira) PTDC/NEU-NMC/0237/2012 (FCT), FCOMP-01-0124-FEDER-029649 (COMPETE), and PPII_ZEBRA (Universidade do Porto and Santander-Totta). BR Pinho acknowledges FCT for her PhD grant (SFRH/BD/63852/2009).

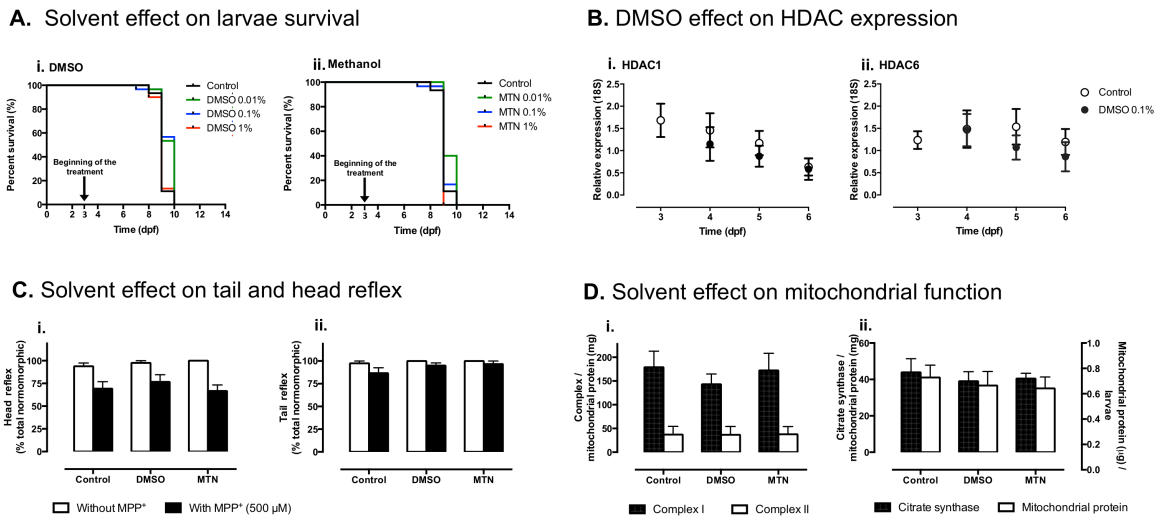

E. Solvent effect on larvae locomotion

Treatment	Time (dpf)	Locomotor parameters (600s)								
		Distance (mm)	Time (s) in movement	Initiations/ 10 s	Time (s) in movement / initiation	Movement speed (mm/s)	SD (quadrant permanence)	Circles (nr)	Time in centre (% total)	Larvae without movement (% total)
Control	6	1242 ± 129	535 ± 16	15 ± 1.2	37 ± 3.7	2.3 ± 0.2	10 ± 1.3	14 ± 3.8	4.1 ± 0.1	0.0 ± 0.0
MPP^+ 500 µM (M500)	6	989 ± 65.8	395 ± 14	19 ± 2.6	21 ± 2.8	2.5 ± 0.08	18 ± 1.8	8.2 ± 1.0	3.0 ± 0.7	3.9 ± 3.9
DMSO 0.1%	6	1097 ± 51.6	513 ± 15	17 ± 1.7	30 ± 2.2	2.1 ± 0.05	15 ± 1.8	7.9 ± 1.4	4.9 ± 2.0	0.0 ± 0.0
MTN 0.1%	6	1176 ± 99.6	527 ± 24	15 ± 3.2	42 ± 13	2.2 ± 0.1	13 ± 2.4	11 ± 2.4	6.3 ± 2.4	0.0 ± 0.0
DMSO 0.1% + M500	6	819 ± 44.8	378 ± 34	17 ± 2.1	23 ± 4.9	2.2 ± 0.2	19 ± 0.5	6.8 ± 1.6	2.9 ± 1.6	0.0 ± 0.0
MTN 0.1% + M500	6	1191 ± 53.4	460 ± 22	16 ± 3.9	33 ± 7.4	2.6 ± 0.005	15 ± 0.9	7.0 ± 0.8	3.0 ± 0.9	3.3 ± 3.3

Figure 3.4.S1. Solvent controls. ***A***, Time-dependent survival *vs*. control (water) in larvae treated with DMSO (***i***) or methanol (***ii***) at the indicated concentrations (% solvent / water volume). Data are from 30-45 larvae per condition, randomly sampled from a synchronized multiparental clutch. ***B***, HDAC1 (***i***) and HDAC6 (***ii***) expression in 0.1% DMSO-treated larvae *vs*. control (water) from 3 to 6 dpf. Data are mean ± SEM, relative to 18S expression, of 3 independent experiments, each with at least 15 larvae per treatment condition. ***C***, Head (***i***) and tail (***ii***) reflex at 6 dpf in 0.1% DMSO and 0.1% methanol-treated larvae from 3-6 dpf *vs*. control (water), without (white bars) or with (black bars) 500 µM MPP^+. Data are mean ± SEM of 4 independent experiments, each with at least 10 larvae per treatment condition. ***D***, Complex I *vs*. complex II activities (***i***); Citrate synthase activity and mitochondrial protein (***ii***) in 0.1% DMSO and 0.1% methanol-treated (3-6 dpf) larvae at 6 dpf. Data are mean ± SEM of 5 independent experiments, each with at least 30 larvae per treatment condition. ***E***, Locomotor parameters at 6 dpf of 0.1% DMSO or 0.1% methanol-treated larvae (3-6 dpf) with or without 500 µM MPP^+. Larvae locomotion was analysed during 600 s. Data are mean ± SEM of 3 independent experiments, each with at least 10 larvae per treatment condition.

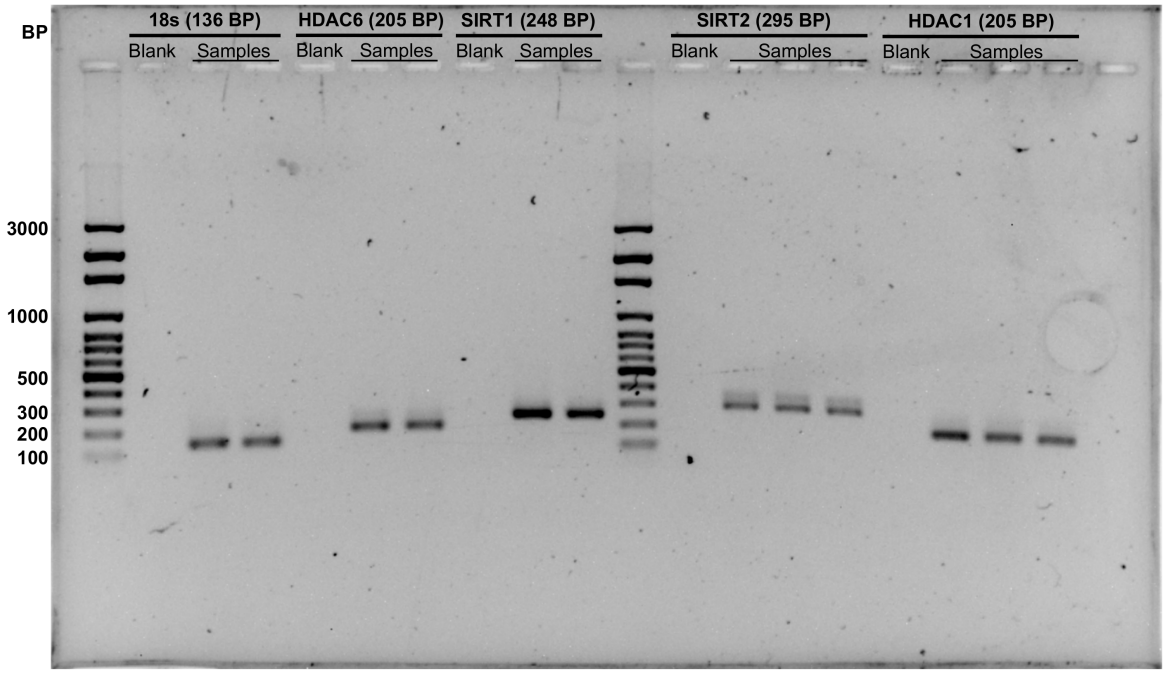

Figure 3.4.S2. qPCR products from KDAC expression study. Representative agarose electrophoresis gel (1.2%) of qPCR products derived from KDAC gene transcription quantification and theoretical size product attending to gene sequence and primers used. BP, base pairs.

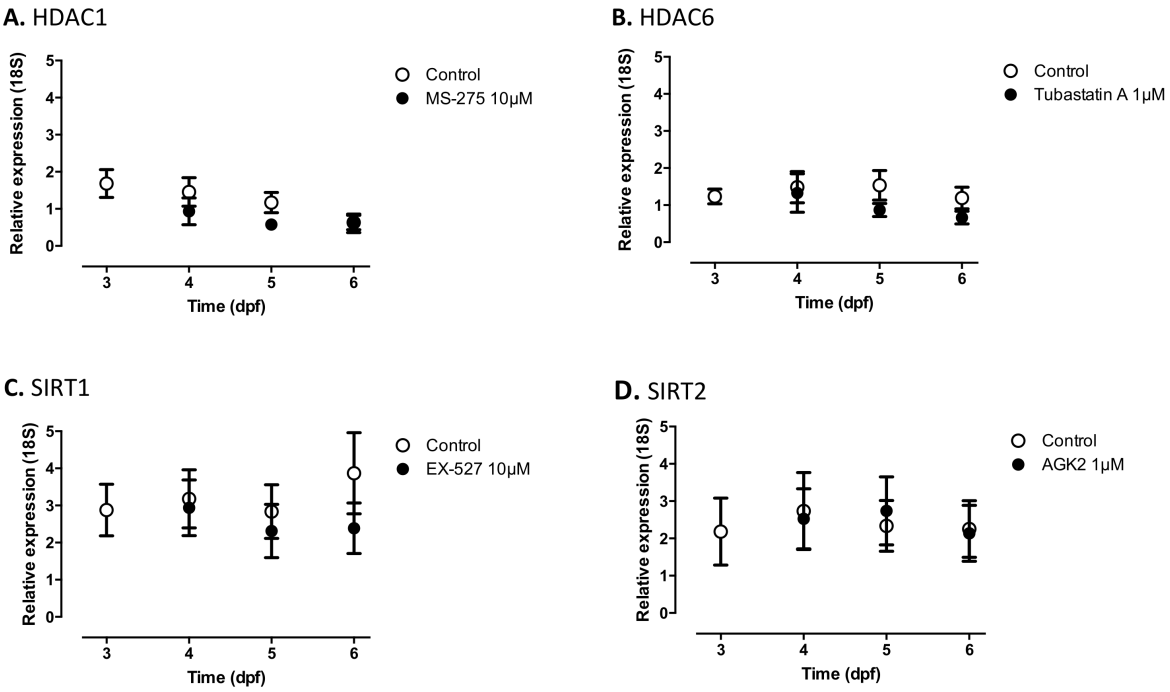

Figure 3.4.S3. KDAC expression in zebrafish treated with the respective enzyme inhibitor over the time. ***A***, HDAC1 expression in 10 µM MS-275-treated larvae. ***B***, HDAC6 expression in 1 µM tubastatin A-treated larvae. ***C***, SIRT1 expression in 10 µM EX-527-treated larvae. ***D***, SIRT2 expression in 1 µM AGK2-treated larvae. Larvae treatment started at 3 dpf. Data are mean ± SEM, relative to 18S expression, of 3-5 independent experiments, each with at least 15 larvae per treatment condition.

Table 3.4.S1. Normomorphic, dysmorphic and dead larvae at 6 dpf under control *vs*. the indicated drug concentrations from 3 to 6 dpf. Data are mean ± SEM of the relative proportions (% total), from *n*=3-8 independent experiments, each with at least 10 larvae per treatment conditions.

		% Total		
		Normomorphic	Dysmorphic	Dead
	Control	92.3 ± 4.0	0.84 ± 0.84	6.9 ± 4.1
	MPP^+ 500 µM	97.0 ± 1.8	0.0 ± 0.0	3.0 ± 1.8
	MPP^+ 1000 µM	78.9 ± 14	8.6 ± 3.0	13 ± 13
	MS-275 10 µM	98.6 ± 1.4	0.0 ± 0.0	1.4 ± 1.4
	TUB 1 µM	95.7 ± 2.0	1.4 ± 1.4	2.9 ± 1.8
	IDB 3 µM	100 ± 0.0	0.0 ± 0.0	0.0 ± 0.0
	DCB 10 µM	96.7 ± 3.3	3.3 ± 3.3	0.0 ± 0.0
Coexposure with MPP^+ 500 µM	MS-275 10 µM	85.0 ± 8.7	5.0 ± 2.9	10 ± 10
	TUB 1 µM	100 ± 0.0	0.0 ± 0.0	0.0 ± 0.0
	IDB 3 µM	96.7 ± 3.3	3.3 ± 3.3	0.0 ± 0.0
	DCB 10 µM	100 ± 0.0	0.0 ± 0.0	0.0 ± 0.0
Coexposure with MPP^+ 1000 µM	MS-275 10 µM	46.7 ± 8.8	6.7 ± 3.3	46.7 ± 12.0
	TUB 1 µM	73.3 ± 15	6.7 ± 6.7	20.0 ± 15.3
	IDB 3 µM	53.3 ± 29	0.0 ± 0.0	46.7 ± 29.1
	DCB 10 µM	56.7 ± 20	0.0 ± 0.0	43.3 ± 20.3

CHAPTER III

GENERAL DISCUSSION
CONCLUSIONS

4. General Discussion

Quinones are compounds with multiple biological activities. In this thesis, naphthoquinones and ubiquinone analogues were the main object of study. Attending to all known biological activities of naphthoquinones, their potential in the modulation of immune system remained underexplored. Ubiquinone analogues are benzoquinones with high biological interest, since they act as electron carriers potentially rescuing mitochondrial ETC dysfunction (9). Ubiquinone analogues in models of mitochondrial dysfunction were thus also studied in this thesis.

4.1. Naphthoquinones

4.1.1. Modulation of the immune system

The immune system is essential for protection against infectious agents (140). However, immune system deregulation is linked to several pathological conditions, including autoimmune diseases, chronic inflammation and allergic disorders. While inflammation may be required against an infectious agent, allergy can be qualified as an undesirable process. Little information exists on naphthoquinones' anti-inflammatory or anti-allergic activity. The majority of the available literature on naphthoquinones' anti-inflamatory activity is focused on shikonin and β-lapachone (see General Introduction). This thesis, therefore, addresses the anti-infllammatory and anti-allergic properties of 1,4-naphthoquinones (diosquinone, juglone, menadione, naphthazarin and plumbagin), and the anti-allergic activity of diospyrin.

Both anti-inflammatory and anti-allergic activities were studied using cell systems: RAW 264.7 macrophages for inflammation and RBL-2H3 basophils for allergy. For both studies, naphthoquinones' non-toxic concentration was determined using the 3-(4,5-dimethylthiazol-2-yl)-2,5-diphenyltetrazolium bromide (MTT) reduction assay. In both RAW 264.7 and RBL-2H3 cells, menadione and juglone were the least toxic compounds, while naphthazarin was the most toxic one, with the maximal non-toxic concentration of 0.1 μM (**Table 4.1**). The same order of toxicity was previously reported in primary rat hepatocytes, which was related with reduced glutathione depletion (498). Öllinger and Brunmark (498) justified the highest naphthazarin toxicity with its highly stabilized semiquinone form (**Figure 4.1**).

Table 4.1. Naphthoquinones' maximal non-toxic concentrations for RAW 264.7 and RBL-2H3 cells and concentrations lethal for 50% of a population (LC_{50}) of zebrafish embryos. LC_{50} values as shown as mean ± standard error of the mean (SEM).

Naphthoquinones	Maximal non-toxic concentration (μM)		LC_{50} (μM)
	RAW 264.7	RBL-2H3	Zebrafish
Diospyrin	N.T.	1	2.00 ± 0.06
Diosquinone	1.5	1	0.54 ± 0.17
Juglone	5	10	0.62 ± 0.03
Menadione	10	5	1.56 ± 0.25
Naphthazarin	0.1	0.1	4.85 ± 0.37
Plumbagin	1	1	0.51 ± 0.08

N.T. Not tested

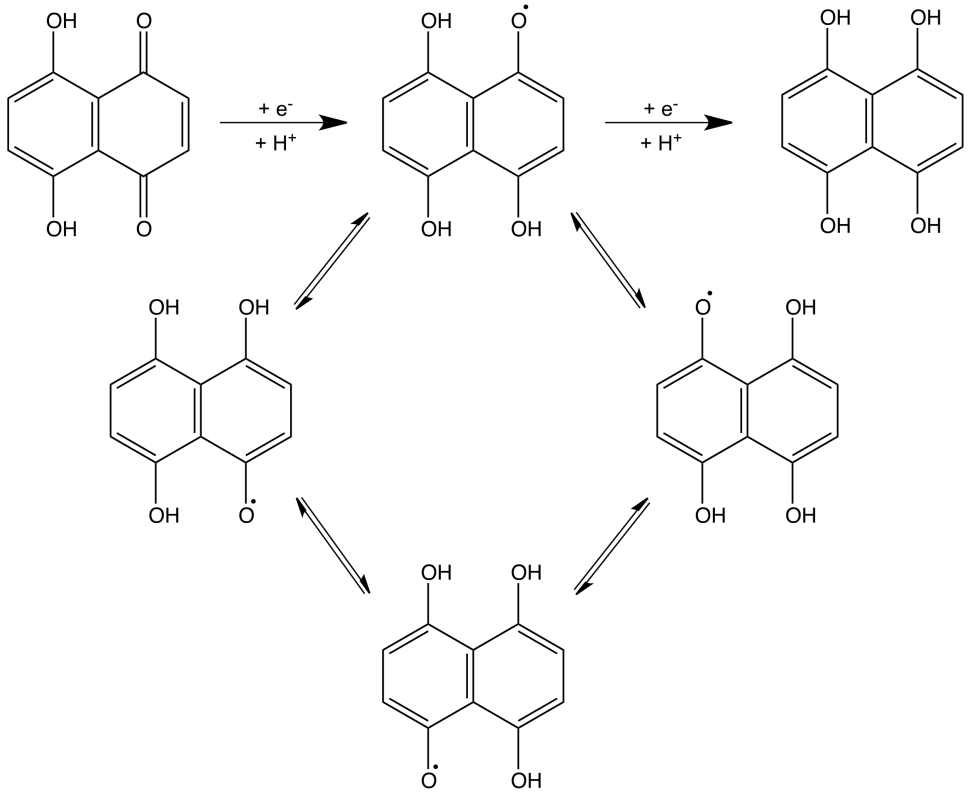

Figure 4.1. Stabilization of naphthazarin's semiquinone radical.

Electron resonance stabilizes naphthazarin's semiquinone radical (**Figure 4.1**), thus increasing the probability of autoxidation with ROS generation (498). Other work confirmed a direct relation in ROS generation and naphthoquinones cytotoxicity, indicating that higher ROS production induces higher toxicity (346). ROS generation has also been reported as a mechanism by which naphthoquinones have antitumoral effects, since cell death is reverted by the presence of antioxidants (499, 500).

The anti-inflammatory screening of naphthoquinones was based in the reduction of NO production by LPS-induced macrophages (**Figure 4.2**).

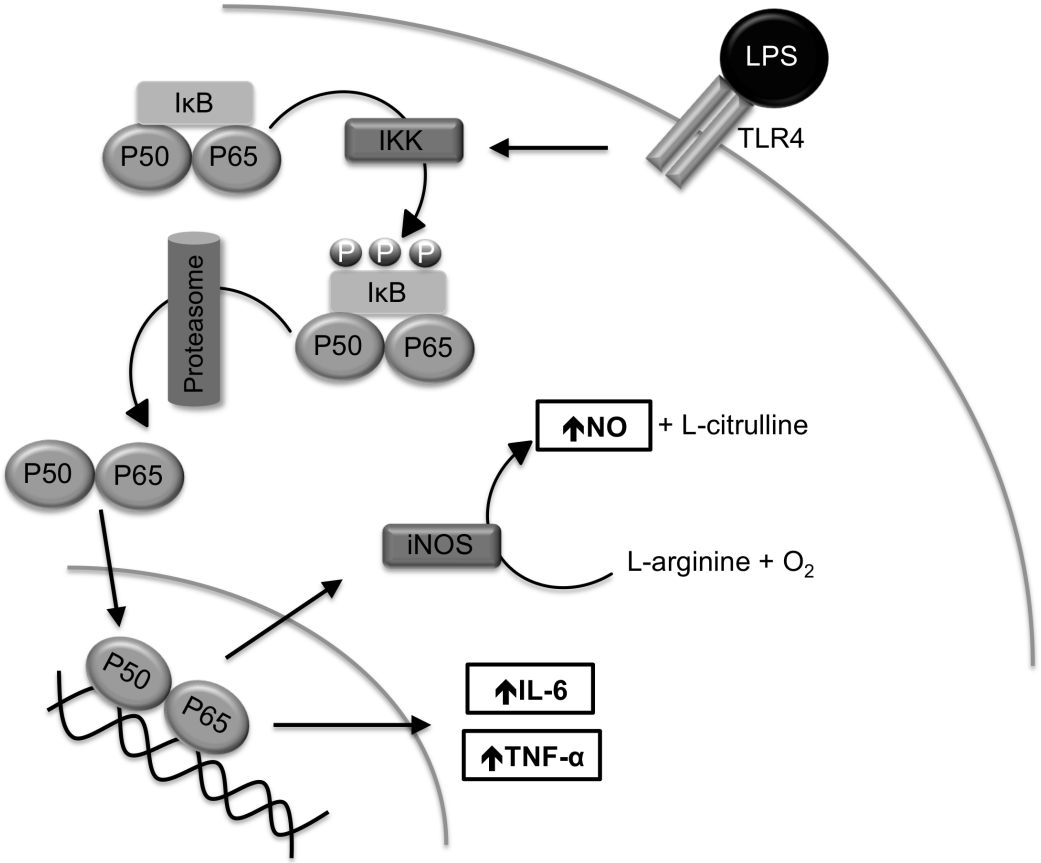

Figure 4.2. **LPS induces an increase of NO, IL-6 and TNF-α levels through NF-κB activation.** LPS promotes phosphorylation of IκB through activation of IKK complex. IκB phosphorylation induces its degradation, allowing the translocation of NF-κB dimer (e.g. P50-P65 dimer) to the nucleus, where the transcription of genes linked to inflammation occurs.

Besides being an ubiquitous intercellular messenger regulating several physiologic processes, NO is also an important non-specific host defence, being highly toxic towards infectious agents (501). In addition, NO has vasodilator properties and regulates the

function of host immune cells (502). NO reduction also contributes to allergy modulation: NO promotes Th2 responses (169) that are associated to allergic disorders and helminthic infections (166). Also, NO may be synthetized by cells involved in allergic responses, such as eosinophils and mast cells (503). Therefore, anti-inflammatory drugs may also have an interesting application in allergic disorders. In fact, allergy and inflammation are not completely separated pathologies, the first being considered a chronic inflammatory disease (504): in an IgE-mediated allergic reaction, the recruitment and activation of inflammatory cells starts an inflammatory process, which is characteristic of the late phase (172).

Diosquinone was the only tested naphthoquinone that reduced NO release without cell toxicity (**Figure 3.1.4** and **3.1.7**). However, NO reduction alone is not a good parameter for anti-inflammatory screening, because superoxide generated during oxidative stress or naphthoquinones' redox cycle may react with NO, reducing its bioavailability (**Figure 4.3**). The reaction of NO with superoxide is irreversible, forming peroxynitrite (a very toxic oxidant), possibly the main responsible for NO attributed toxicity (501). Nitration of tyrosine residues (**Figure 4.3**) is a hallmark of peroxynitrite toxicity (501).

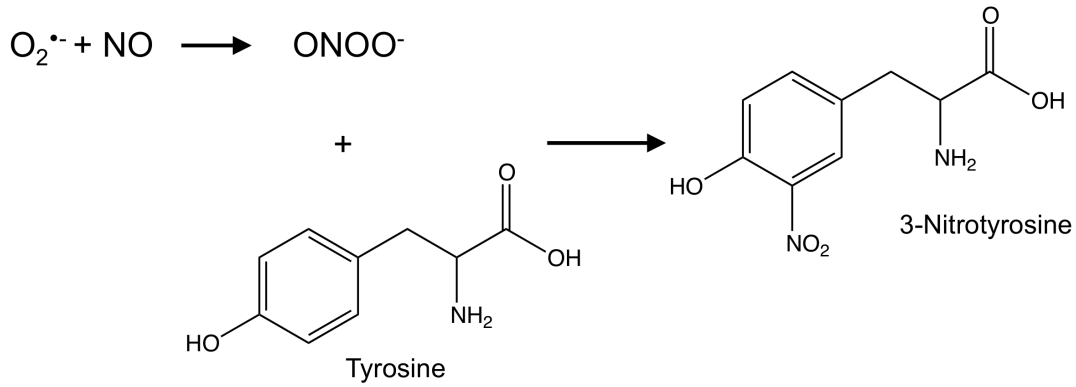

Figure 4.3. **3-Nitrotyrosine formation from superoxide ($O_2^{\bullet-}$) and nitric oxide (NO).**

Quantification of superoxide and 3-nitrotyrosine was made after cell treatment with diosquinone, to evaluate if the observation of reduced NO release was a consequence of oxidative stress. Since neither superoxide (**Figure 3.1.8**) nor 3-nitrotyrosine increased (**Figure 3.1.9**), diosquinone might be interfering with the LPS pathway (**Figure 4.2**) (74). NF-κB is a transcription factor that regulates expression of cell proliferation and inflammatory genes, including iNOS and inducible cytokines (74). Contrarily to the degranulation process that is preceded by a calcium influx, iNOS is not calcium activated, and is continuously active (503). We found no previous studies on the inhibition of NF-κB by diosquinone, but NF-κB might be inhibited by diosquinone, since other naphthoquinones [shikonin (73), β-lapachone (78) and plumbagin (85)] are known NF-κB

inhibitors. NF-κB inhibition is interesting in allergy management because NF-κB activation was found in the airway epithelium of patients with allergic asthma (505), and because allergens may activate NF-κB through IκB degradation (506).

The anti-inflammatory activity of diosquinone was also assessed by reduced TNF-α and IL-6, two pro-inflammatory cytokines enhanced by LPS (**Figure 4.2**) (507). TNF-α plays several inflammatory roles: NF-κB transcriptional regulation, production of IL-6 and other cytokines (508), and expression of COX-2, pro-coagulant proteins and adhesion molecules (509). However, TNF-α is also involved in allergy, promoting Th2 cell response to allergens (510). TNF-α may be produced by mast cells, the first line of response to IgE-mediated allergy (503). Increased TNF-α was observed in human lung samples after IgE-treatment (511). Furthermore, anti-TNF-α antibodies reduced allergic symptoms, eosinophilic infiltration, IgE levels, adhesion molecules expression and Th2 type cytokines transcription in mouse model of allergic rhinitis (512). On the other hand, IL-6 is considered the major stimulus for acute-phase protein synthesis, whose serum levels increase in acute and chronic inflammation. IL-6, in particular, promotes B cell differentiation into antibody-producing cells (513). Similarly to TNF-α, IL-6 promotes Th2 cells differentiation, determining the type of adaptative immune response (514). IL-6 release causes dysfunction of allergic asthmatic airways, through an inflammation-independent process (514). Additionally, IL-6 associates with allergen cutaneous response in atopic individuals (515).

Regarding anti-allergic activity, naphthazarin was the only naphthoquinone reducing IgE-antigen complex mediated degranulation (**Figure 3.2.2**), inhibiting a step upstream to intracellular calcium increase, since naphthazarin was unable to avoid calcium ionophore mediated degranulation. Conceivably, naphthazarin acts mechanistically similarly to shikonin, another naphthoquinone with 5,8-dihydroxy-1,4-naphthoquinone core. Shikonin inhibited spleen tyrosine kinase (Syk), downstream of FcεRI activation by IgE-antigen complex (372). Unlike naphthazarin, diospyrin reduced calcium ionophore-stimulated-basophils' degranulation (**Figure 3.2.3**), suggesting that naphthazarin and diospyrin have different mechanisms of action.

Despite being weak hyaluronidase inhibitors, naphthoquinones inhibited soybean lipoxidase (**Figure 3.2.6*A***), used to model the structurally similar human 5-, 12- and 15-lipoxygenases (377). Naphthoquinones may inhibit lipoxidase through competition with endogenous lipophilic substrates, since higher inhibitory activity correlated with higher lipophilicity (i.e. menadione and the dimeric naphthoquinones diospyrin and diosquinone). Leukotrienes inhibition in cells was only confirmed for menadione. Effective menadione concentrations for reducing LTC_4 in cells (0.005 – 5 μM) (**Figure 3.2.6*C***) were lower than for *in vitro* lipoxidase inhibition (IC_{50}, 128 ± 9.38 μM). Menadione may reduce leukotriene

production in IgE-antigen complex-induced cells by inhibiting 5-lipoxygenase and/or by reducing arachidonic acid availability (**Figure 4.4**). Menadione is a known ROS generator and the associated oxidative stress was reported for similar concentrations to those required for leukotriene reduction (380). Menadione-generated ROS may thus react with arachidonic acid forming oxidized lipids (**Figure 4.4**) (379). Eosinophils, macrophages and monocytes are also important sources of cysteinyl leukotrienes (169). Since leukotrienes are pro-inflammatory (516), menadione-related drugs may help understand the role of leukotriene reduction in non-allergic inflammatory conditions.

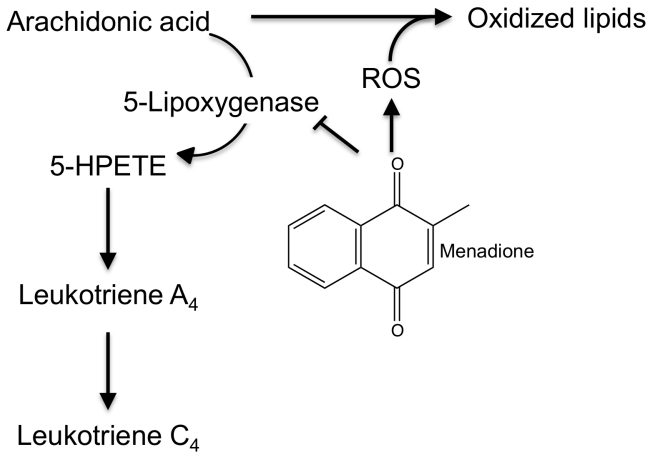

Figure 4.4. **Menadione reduces leukotriene production.** Menadione may directly inhibit 5-lipoxygenase and it may produce ROS, which induces arachidonic acid oxidation, reducing its bioavailability.

4.1.2. Naphthoquinones' toxicity profile in an *in vivo* model

Little information exists concerning the effects of naphthoquinones in zebrafish. In zebrafish embryos: menadione was studied as ROS generator (517) and as anti-cancer drug (518). β-lapachone and plumbagin were also studied as anticancer drugs (518) and dehydro-α-lapachone was identified as anti-vascular drug (519). Additionally, β-lapachone-induced cardiovascular toxicity was previously evaluated in 24 hpf zebrafish (520). Naphthoquinones' toxicity profile in zebrafish (*in vivo* model) was different than that obtained in cell lines (RAW 264.7 and RBL-2H3). Except for naphthazarin and diospyrin, naphthoquinones' LC_{50} values in zebrafish were lower than their toxic concentrations for RAW 264.7 macrophages and RBL-2H3 basophils (**Table 4.1**). This difference of concentrations is probably related with the zebrafish embryonic development: during embryonic development, cells are highly susceptible to oxidative stress or other

mechanisms that may interfere with signalling pathways. In addition, the order of less toxic naphthoquinones to more toxic ones in zebrafish was naphthazarin, diospyrin, menadione, juglone, diosquinone and plumbagin. Curiously, naphthazarin that was the most toxic naphthoquinone in cell culture was the less toxic for zebrafish embryos, at 80 hpf (**Table 4.1**). Naphthazarin induced an all or none effect, allowing directly killing normomorphic embryos, as indicated by the LC_{50}/NC_{50} ratio (naphthazarin LC_{50}/NC_{50} = 1.0 ± 0.04). When LC_{50}/NC_{50} ratio ~1, the concentration required to kill 50% embryos equals that required to halve normomorphic embryos, without dysmorphic embryos. Since naphthazarin was the most hydrophilic naphthoquinone it may lack chorion permeability at low concentrations. In contrast, plumbagin and menadione were the only naphthoquinones inducing abnormalities, which may be related with these naphthoquinones being the most lipophilic of the monomeric ones. Possibly, their lipophilicity allows gradual chorion permeation, allowing the progressive toxicity required for inducing non-lethal abnormalities.

Menadione mainly induced hypochromic anaemia in zebrafish (**Figure 3.3.4*H***), decreasing erythocytes and their red colour, possibly by decreases haemoglobin or even erythrocyte production. A short exposure (24-32 hpf) sufficed to induce hypochromic anaemia. Exposures excluding the 24-32 hpf period allowed normally coloured erythrocytes at 80 hpf. Thus, menadione's effect on haematopoiesis is not acute. Instead, menadione impairs haematopoiesis in the specific period known as transient haematopiesis in zebrafish (400). Menadione may act by complex I inhibition (414), compromising $\Delta\psi_m$ that is required for producing the iron-sulfur cluster in haemoglobin (415). Menadione's toxicity to erythrocytes is consistent with menadione inducing haemolysis in people with glucose-6-phosphate dehydrogenase deficiency (413).

Other naphthoquinones such as atovaquone, β-lapachone and lapachol were also tested in zebrafish in the present thesis. Atovaquone is a synthetic naphthoquinone therapeutically used against *Plasmodium* spp. and *Pneumocystis jiroveci* infections, since its toxicity is selective to parasites *vs*. human cells (521). In fact, atovaquone LC_{50} for *Plasmodium falciparum* (0.001 ± 0.0002 μM) (522) is muchs lower than that for mammalian cells (15-30 μM) (523). Atovaquone induced progressive toxicity in zebrafish embryos, characterized by oedema without significant bradycardia and focal lesions (necrosis and bleedings/clots) (**Figure 3.3.4*A***). Despite lapachol being a β-lapachone isomer (**Figure 1.8**), they presented different toxicity patterns. Lapachol induced a wide range of zebrafish abnormalities, most frequently decreased pigmentation, head defects, gastrula arrest and oedema. β-Lapachone did not induce abnormalities, but had a lower LC_{50} than lapachol for zebrafish (**Figure 3.3.4*F, I*** and **Table 3.3.2**).

4.2. Ubiquinone analogues

4.2.1. UQ analogues in a mitochondrial dysfunction model

Idebenone and decylubiquinone were tested in zebrafish, in order to study the modulation of respiratory chain by UQ analogues. We found no previous information about UQ analogues' effects in zebrafish. Idebenone and decylubiquinone were less toxic than naphthzarin, the naphthoquinone with lower toxicity. Despite differing only in one functional group, idebenone was 4x more lethal than decylubiquinone, at 80 hpf (**Table 3.3.2**). The toxicity of decylubiquinone increased abruptly at 80 hpf, coinciding with peak hatching, suggesting that it may be dependent on increased chorion permeability/dysruption.

4.2.1.1. Mitochondrial dysfunction-induced toxicity in zebrafish

To allow the study of UQ analogues upon the modulation of respiratory chain dysfunction, the effects of mitochondrial complexes inhibitors were characterized in zebrafish. Rotenone (complex I inhibitor) and 3-nitropropionic acid (complex II inhibitor) induced abnormalities, while myxothiazol and antimycin A (complex III inhibitors) directly induced embryonic death without previous abnormalities (**Figure 4.5**). Strong complex III inhibitor toxicity results from lack of alternative pathways for downstream electron flow in the mitochondrial ETC. ATP synthase inhibition (oligomycin) arrested embryonic development at the gastrula stage, revealing the strict dependence of mitochondrial ATP at or past zebrafish gastrulation.

Atovaquone also a complex III inhibitor (521), showed a distinct toxicity profile from myxothiazol and antimycin A, suggesting that atovaquone has additional effects beyond complex III inhibition. In fact, it was previously described that atovaquone inhibits UQ synthesis in *Pneumocystis* spp. by reducing 4-hydroxybenzoate incorporation into UQ (**Figure 4.6**) (62). Consistently, 4-nitrobenzoate, another UQ synthesis inhibitor (411), induced a similar toxicity profile to that described to atovaquone. Therefore, the main mechanism of action of atovaquone in zebrafish may not be the mitochondrial complex III inhibition, but rather the inhibition of UQ biosynthesis. This hypothesis was strenghtened by rescuing atovaquone's decrease in normomorphic embryos with the UQ precursor 4-hydroxybenzoate (**Figure 3.3.6*B***) (62). Significantly, 4-hydroxybenzoate failed to rescue the toxicity of other complex III inhibitors (myxothiazol and antimycin A), and also that of 4-nitrobenzoate. However, lack of protection against 4-nitrobenzoate is probably related to

the use of very different molar concentrations (5 µM 4-hydroxybenzoate - the highest concentration without toxicity *vs.* 10 mM 4-nitrobenzoate - the lowest toxic concentration). It is worth mentioning that 4-hydroxybenzoate toxicity precluded equimolar concentration testing *vs*. 4-nitrobenzoate.

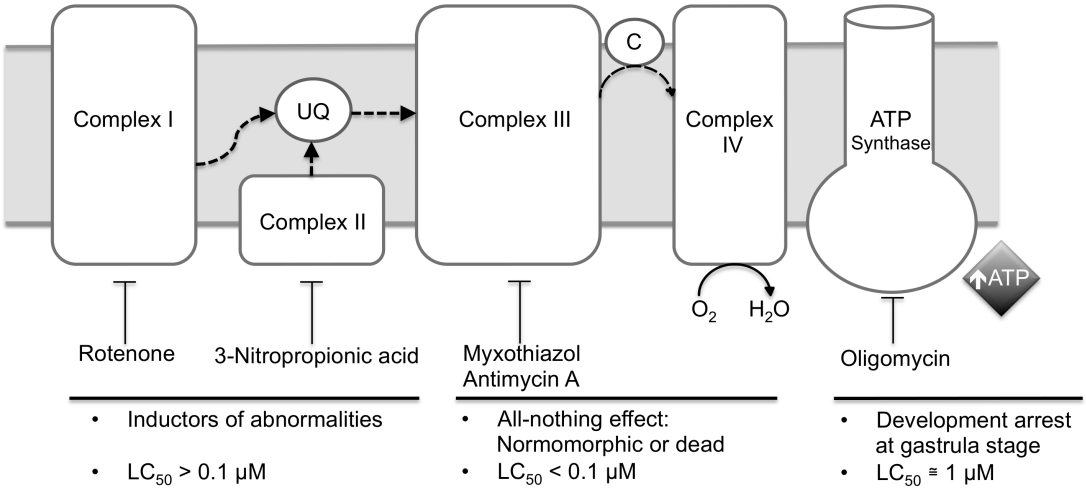

Figure 4.5. **Main effects of mitochondrial complex inhibitors in zebrafish embryonic development.**

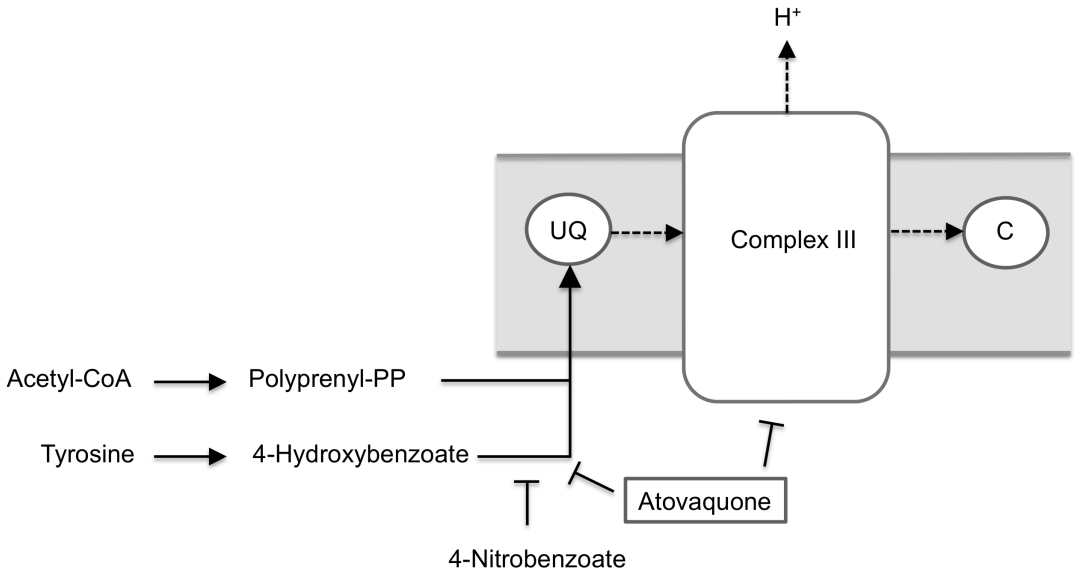

Figure 4.6. **Atovaquone's mechanisms of action.** Atovaquone inhibits mitochondrial complex III and the ubiquinone (UQ) biosynthesis.

4.2.1.2. Mitochondrial dysfunction rescue by UQ analogues

While UQ analogues did not rescue chronic complexes I, II or III inhibitor toxicity, they delayed the circulation and heart beat arrest induced by acute complex I inhibition (**Figure 4.7**). Again, no rescue of acute mitochondrial complex III dysfunction was observed with UQ analogues (**Figure 3.3.7**). As previously stated, no alternative way to complex III exists to energy production, which explains the lack of protection against complex III toxicity inhibition. However, idebenone and decylubiquinone may be reduced by several dehydrogenases, including cytosolic dehydrogenases, directly feeding complex III and, consequently, allowing ATP production even when complex I was inhibited. Idebenone and decylubiquinone-induced protection against acute complex I inhibition was possibly due to increased ATP production, because rotenone asystole was also delayed by oligomycin (prevents ATP consumption upon rotenone induced ATP synthase reversal) (**Figure 3.3.7**). Therefore, lipophilicity of UQ analogues is a likely advantage *vs*. endogenous UQ_{10}, because UQ analogues may be present in cytosol or in mitochondria, crossing biological membranes. Haefeli and collaborators suggested that the same does not occur with UQ_{10}, which failed to restore the ATP levels following complex I inhibition (9).

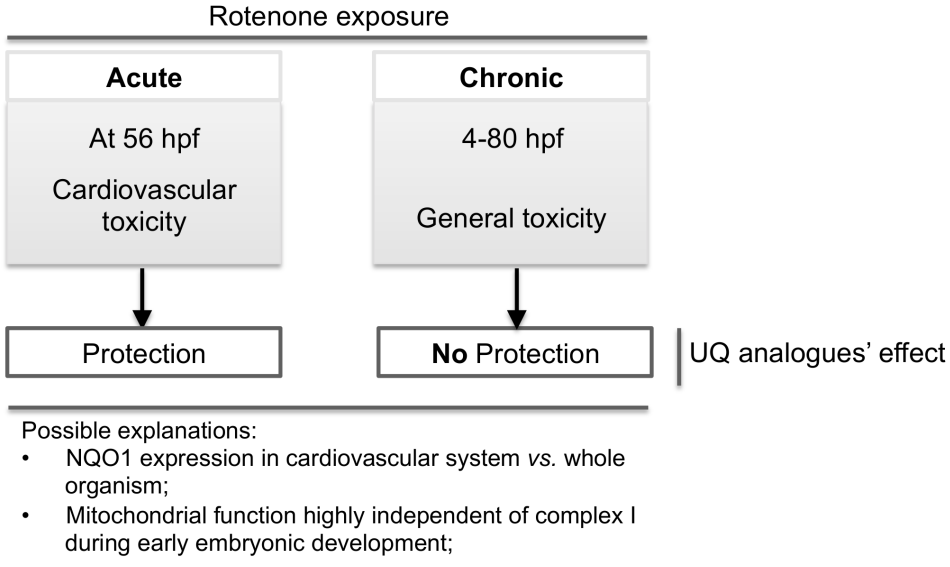

Figure 4.7. **Ubiquinone analogues' effects in zebrafish embryos acutely and chronically treated with rotenone.** UQ analogues induced protection against acute rotenone exposure, but not against chronic exposure.

UQ analogues were also expected to protect against acute complex II inhibition. However, it was not possible to test this hypothesis, because no bradycardia and

circulation/heartbeat arrest were verified in a short period of time using with 3-nitropropionic acid. Additionally, chronic and simultaneous inhibitions of complex I and II did not induced any additive or synergic toxicity (**Figure 3.3.6*C***), as expected if zebrafish had a low dependence of complex I and II to feed complex III. This hypothesis is also supported by other observed evidences: a) LC_{50} of 3-nitropropionic acid in zebrafish was 10 times higher than the LC_{50} described for rat neurons, suggesting that mitochondrial complex II has a lower contribution to energy production (**Table 3.3.2**); b) dysmorphic embryos treated with rotenone or 3-nitropropionic acid survived beyond gástrula (**Figure 3.3.1**), which is not possible without mitochondrial ATP, as it was verified using oligomycin. Thus, in zebrafish early embryonic development, oxidative phosphorylation is perhaps highly dependent on other dehydrogenases beyond complex I and II, such as dihydroorotate dehydrogenase, electron transfer flavoprotein dehydrogenase or glycerol-3-phosphate dehydrogenase. The last two are involved in lipid metabolism, which is expected to be increased during early embryonic development, given the high lipid content of the zebrafish yolk (524). This lack of complex I and II dependence in early embryogenesis may explain why no rescue of chronic complex I and II inhibition was verified with UQ analogues, being also possible that chronic toxicity with rotenone and 3-nitropropionic acid may involve off-target effects.

Another explanation for acute complex I-induced toxicity's rescue verified with UQ analogues and not against chronic toxicity is related with NQO1 expression. NQO1 is reported by Haefeli and collaborators to reduce UQ analogues, allowing them to restore ATP levels in a model of complex I dysfunction (9). NQO1 expression in zebrafish needs clarification; however, it is known that NQO1 is expressed in zebrafish's cardiovascular system and that its inhibition by dicoumarol decreases β-lapachone [predicted to be bioactivated by NQO1 (401)]-induced cardiovascular toxicity in embryos at 24 hpf (520). However, considering whole embryos, dicoumarol-induced NQO1 inhibition did not reduce β-lapachone toxicity, neither increase the menadione toxicity (**Figure 3.3.4*J***), which is detoxified by NQO1 (402). Furthermore, NQO1 is known to have an essential role in zebrafish melanogenesis (406), being expected that NQO1 inhibition induces pigmentation abnormalities. In fact, dicoumarol and lapachol (also known NQO1 inhibitor) induced a pigmentation decrease, having been lapachol the most potent. However, attending to lapachol [IC_{50} = 150 nM (407)] and dicoumarol [IC_{50} = 10 nM (408)] IC_{50} for NQO1, it would be expected that dicoumarol would be more potent than lapachol concerning toxic effects from NQO1 inhibition, whereby lapachol effects may be, perhaps, due to the inhibition of other enzyme, such as dihydroorotate dehydrogenase, for which lapachol is more potent than dicoumarol (409, 410). Together, these findings suggest that NQO1 levels in whole zebrafish embryos may be low. Considering that NQO1 reduces

naphthoquinones into hydroquinones, generally more stable than the oxidized form (8), low NQO1 activity may also explain higher naphthoquinones' toxicity to zebrafish *vs*. RAW 264.7 and RBL-2H3 cells (**Table 4.1**).

4.2.2. Ubiquinone analogues in a Parkinson model

Despite the study of UQ analogues in several neurodegenerative disorders, including Friedrich's ataxia (126) or Leber's hereditary optic neuropathy (130), fewer studies have been done regarding PD. Idebenone increased lifespan and improved motor function of mice with mitochondrial dysfunction induced by knockout of HtrA2, a mitochondrial protease linked to PD (428). In order to test the UQ analogues as possible therapeutic option for PD, a parkinsonian phenotype was created in zebrafish using the neurotoxin MPP^+.

4.2.2.1. MPP^+-induced Parkinsonian phenotype in zebrafish

MPP^+ is a selective dopaminergic toxin, whose main mechanism of action is mitochondrial complex I inhibition (248). MPP^+, at 500 and 1000 µM, induced locomotor abnormalities without apparent morphological changes in zebrafish. MPP^+-induced phenotype in zebrafish was characterized by a modest increase in the number of initiations, a decrease in travelled distance, and in time in movement (**Table 3.4.2**). Therefore, MPP^+-induced a locomotor profile characterized by accelerations intercalated by pauses. Additionally, MPP^+-treated larvae movement lacked uniformity, possibly due to lack of orientation. MPP^+ also compromised sensorimotor reflexes (**Figure 4.8**), namely reducing the number of larvae with head reflex. Since the tail reflex was not affected, MPP^+ may exert toxicity in specific neurons required to head reflex and not to tail reflex, such as trigeminal sensory neurons (475), but this lacks experimental demonstration. On the other hand, MPP^+ may delay zebrafish development, since at 6 dpf the proportion of MPP^+-treated larvae without head reflex resembled the proportion of control larvae wihout head reflex at 3 dpf (when MPP^+ treatment started) (**Figure 3.4.3**).

MPP^+ did not change zebrafish neuromast labelling (**Figure 3.4.2**). Neuromasts are sensory structures in the lateral line that detect surrounding water movements, contributing to fish navigation (482). Thus, some alterations in fish movement, such as an abnormal escape response, may be related with neuromast abnormalities (483). Moreover, neuromasts are constituted by a core of sensory cells, named hair cells that are rich in

mitochondria (456). Therefore, neuromast labelling is a simple technique that helps evaluating a possible non-selective toxicity of MPP^+.

Figure 4.8. **MPP^+-induced effects in zebrafish larvae.** UQ analogues did not induced protection against MPP^+-induced phenotype.

In order to confirm complex I inhibition by MPP^+ in zebrafish, the quantification of complex I activity was made in MPP^+-treated larvae at 6 dpf. Nevertheless, as it is estimated that dopaminergic neurons are less than 1% of the total neurons in human brain (484), the use of whole larvae may dilute the possible complex I inhibition by MPP^+, since no inhibition of complex I was verified in MPP^+-treated embryos (**Figure 3.4.4**). In order to overcome this problem, quantification of complex I was made in head *vs*. body of MPP^+-treated larvae. Again, no inhibition of complex I was verified, but it should be highlighted that mitochondrial data from sectioned larvae typically presented high standard deviations, possibly due to the inherent variability of the sectioning-associated procedure. However, when higher MPP^+ concentrations were added to the control larvae mitochondrial extracts, MPP^+ inhibited complex I but not complex II. Complex I inhibition by MPP^+ may depend on $\Delta\psi_m$, because MPP^+ is a cation that accumulates in polarized mitochondrion (261). This hypothesis is supported by higher MPP^+ toxicity to intact mitochondria than submitocondrial particles (263) and by a modest increase in MPP^+-treated larvae mean survival in the presence of rotenone (reducing $\Delta\psi_m$) (**Figure 3.4.4*E***). Additionally, mitochondrial complexes III and IV inhibition was previously proposed for MPP^+ (264).

4.2.2.2. UQ analogues in MPP^+-induced Parkinsonism

Idebenone (3 μM) and decylubiquinone (10 μM) *per se* did not modify zebrafish locomotion (**Table 3.4.2**). Attending to the protection provided by UQ analogues against

rotenone-induced acute complex I inhibition, it would be expected that idebenone or decylubiquinone could rescue the MPP^+ toxicity, since this compound is also a complex I inhibitor. However, no protection against MPP^+ was verified with UQ analogues (**Table 3.4.2**). In addition, results suggest an increase of MPP^+ toxicity in presence of idebenone, attending to reduced travelled distance, time in movement, and number of circles. The possibility of MPP^+ inhibiting complex III and IV (525) precludes the activity of UQ analogues as electron carriers, transporting electrons directly to complex III. Furthermore, and attending to the fact that MPP^+ may need a polarized mitochondrion to inhibit the respiratory chain, if UQ analogues increase the efficacy of electron transference, enhancing $\Delta\psi_m$ (9, 115, 137), they may contribute to higher MPP^+ mitochondrial accumulation. According to this hypothesis, MPP^+ has further limitations as a PD-modeling drug. However, a recent study reported that lycopene protects cells against MPP^+-induced cytotoxicity and maintains mitochondrial function (526). Therefore, more studies are needed to explore this question and to explain how idebenone increases MPP^+ toxicity. Related with this point, it is known that oxidized idebenone inhibits complex I activity *in vitro* (119) and promotes mPTP opening (134). However, mPTP opening seems to be cell-type dependent, because UQ_0 inhibited mPTP opening in isolated hepatocytes and clone-9 cells (non-cancerous hepatocyte cells), while enhancing mPTP opening in MH1C1 cells (cancerous hepatocyte cells) (527). Nevertheless, oxidized idebenone could avoid MPP^+ accumulation in mitochondrial matrix, by decreasing $\Delta\psi_m$. On the other hand, the oxidized/reduced idebenone equilibrium depends on several factors, including NQO1 activity. If dopaminergic neurons have low NQO1 activity, UQ analogues may not be sufficiently reduced to feed mitochondrial complex III and bypass MPP^+-induced complex I inhibition. In fact, NQO1 expression in human *substantia nigra* from normal individuals was found mainly in astroglial and endothelial cells, being less frequently found in dopaminergic neurons (244).

5. Conclusions

Experimental results from this thesis allowed the following conclusions:

1. Diosquinone was the only tested naphthoquinone that reduced NO from LPS-stimulated cells. The anti-inflammatory activity of diosquinone includes inhibition of inflammatory cytokines release (TNF-α and IL-6).
2. In RAW 264.7 macrophages, diosquinone did not induce oxidative stress, as evaluated by quantifying superoxide and 3-nitrotyrosine levels.
3. Naphthazarin and diospyrin were the only tested naphthoquinones that inhibited basophils' degranulation.
4. Naphthazarin and diospyrin likely have different mechanisms of action: naphthazarin inhibited IgE-antigen complex-induced degranulation, whereas diospyrin inhibited calcium ionophore-induced degranulation.
5. Naphthoquinones are weak hyaluronidase inhibitors.
6. Most tested naphthoquinones inhibit soybean lipoxidase.
7. Menadione, diospyrin and diosquinone, the most lipophilic tested naphthoquinones, presented the highest lipoxidase inhibitory activity, with the proposed mechanism being competition with endogenous lipophilic substrates.
8. Menadione decreased leukotriene C_4 release in IgE-antigen complex-induced basophils, possibly by a mechanims involving 5-lipoxygenase inhibition and decreased arachidonic acid bioavailability.
9. With the exception of naphthazarin and diospyrin, tested naphthoquinones showed higher toxicity to zebrafish embryos than to RAW 264.7 or RBL-2H3 cell lines.
10. Menadione induced hypochromic anaemia in zebrafish embryos, possibly by disrupting haematopoiesis.
11. Rotenone and 3-nitropropionic acid induced abnormalities in zebrafish embryos, while antimycin A and myxothiazol directly killed embryos.
12. Mitochondrial ATP is required for zebrafish embryonic development past the gastrula stage, as verified with oligomycin.
13. Since the atovaquone's toxicity profile differs from other complex III inhibitors, but resembles that of 4-nitrobenzoate, and atovaquone's toxicity is partially rescued by 4-hydroxybenzoate, the main mechanism of atovaquone toxicity in zebrafish might be UQ biosynthesis inhibition.
14. Idebenone and decylubiquinone failed to protection against mitochondrial complex III inhibition in zebrafish.

15. Idebenone and decylubiquinone failed to protect against chronic complex I inhibition during embryonic development.
16. Idebenone and decylubiquinone delayed circulation and heartbeat arrest induced by acute mitochondrial complex I inhibition. Direct feeding of mitochondrial complex III by reduced UQ analogues may underlie the observed protection.
17. Early zebrafish embryonic development appears to lack a strong dependency on mitochondrial complexes I and II. Other dehydrogenases, mainly those involved in lipid metabolism, may thus be responsible for most complex III feeding.
18. NQO1 activity in whole embryo should be low, because its inhibition by dicoumarol neither potentiated menadione toxicity nor decreased β-lapachone toxicity (compounds respectively bioactivated or detoxified by NQO1),
19. MPP^+ induced locomotor abnormalities and abnormal head reflexes in zebrafish larvae.
20. MPP^+ did not induce detectable toxicity in neuromasts.
21. High MPP^+ concentrations were required to inhibited zebrafish complex I in mitochondrial extracts. Results support the hypothesis that MPP^+-induced mitochondrial complex I inhibition depends on mitochondrial membrane potential.
22. Idebenone and decylubiquinone failed to rescue MPP^+-induced locomotor phenotype.

Conclusions concerning naphthoquinones and UQ analogues are summarized in **Table 5.1**.

Table 5.1. Main findings related with each compound.

Quinone	Main findings
Diospyrin	Reduced Calcium mobilization-induced degranulation
Diosquinone	Anti-inflammatory properties: reduced nitric oxide, IL-6 and TNF-α release
Juglone	No significant results obtained
Menadione	Lipoxidase inhibition and reduced leukotrienes synthesis in cells Possible haematopoiesis impairment
Naphthazarin	Inhibited IgE-antigen complex-induced degranulation
Plumbagin	No significant results obtained
Idebenone	Delayed acute rotenone cardiovascular toxicity in zebrafish embryos
Decylubiquinone	Lack of protection against MPP^+-induced locomotor phenotype in zebrafish

CHAPTER IV

BIBLIOGRAPHIC REFERENCES

6. Bibliographic References

1. Bernards MA. Plant natural products: A primer. Can J Zool 2010 Jul; 88 (7): 601-14.
2. Neilson EH, Goodger JQ, Woodrow IE, Moller BL. Plant chemical defense: At what cost? Trends Plant Sci 2013 May; 18 (5): 250-8.
3. Hadacek F, Kraus GF. Plant root carbohydrates affect growth behaviour of endophytic microfungi. FEMS Microbiol Ecol 2002 Aug; 41 (2): 161-70.
4. Hartmann T. From waste products to ecochemicals: Fifty years research of plant secondary metabolism. Phytochemistry 2007 Nov-Dec; 68 (22-24): 2831-46.
5. Zhao N, Wang G, Norris A, Chen X, Chen F. Studying plant secondary metabolism in the age of genomics. Crit Rev Plant Sci 2013 Jul; 32 (6): 369-82.
6. Bruneton J. Pharmacognosy, Phytochemistry Medicinal Plants. 4th ed. Paris: Lavoisier; 2009.
7. Babula P, Adam V, Havel L, Kizek R. Noteworthy secondary metabolites naphthoquinones - their occurrence, pharmacological properties and analysis. Curr Pharm Anal 2009 Feb; 5: 47-68.
8. O'Brien PJ. Molecular mechanisms of quinone cytotoxicity. Chem Biol Interact 1991 May; 80 (1): 1-41.
9. Haefeli RH, Erb M, Gemperli AC, Robay D, Courdier Fruh I, Anklin C, et al. NQO1-dependent redox cycling of idebenone: Effects on cellular redox potential and energy levels. PLoS One 2011 Mar; 6 (3): e17963.
10. Powis G, Hodnett EM, Santone KS, See KL, Melder DC. Role of metabolism and oxidation-reduction cycling in the cytotoxicity of antitumor quinoneimines and quinonediimines. Cancer Res 1987 May; 47 (9): 2363-70.
11. Pinho BR, Sousa C, Oliveira JMA, Valentão P, Andrade PB. Naphthoquinones' biological activities and toxicological effects. In: Bitterlich A, Fischl S, editors. Bioactive compounds: types, biological activities and health effects. New York, USA: Nova Science Publishers; 2012. p. 181-218.
12. Murakami K, Haneda M, Iwata S, Yoshino M. Effect of hydroxy substituent on the prooxidant action of naphthoquinone compounds. Toxicol In Vitro 2010 Apr; 24 (3): 905-9.
13. Joosten V, van Berkel WJ. Flavoenzymes. Curr Opin Chem Biol 2007 Apr; 11 (2): 195-202.
14. Malorni W, Campesi I, Straface E, Vella S, Franconi F. Redox features of the cell: A gender perspective. Antioxid Redox Signal 2007 Nov; 9 (11): 1779-801.

15. Ross D, Kepa JK, Winski SL, Beall HD, Anwar A, Siegel D. NAD(P)H:quinone oxidoreductase 1 (NQO1): Chemoprotection, bioactivation, gene regulation and genetic polymorphisms. Chem Biol Interact 2000 Dec; 129 (1-2): 77-97.
16. Paululat T, Katsifas EA, Karagouni AD, Fiedler H-P. Grecoketides A and B: New naphthoquinones from *Streptomyces* sp. Acta 1362. Eur J Org Chem 2008 Nov; 2008 (31): 5283-8.
17. Bringmann G, Haagen Y, Gulder TA, Gulder T, Heide L. Biosynthesis of the isoprenoid moieties of furanonaphthoquinone I and endophenazine A in *Streptomyces cinnamonensis* DSM 1042. J Org Chem 2007 May; 72 (11): 4198-204.
18. Cao S, Clardy J. New naphthoquinones and a new δ-lactone produced by endophytic fungi from Costa Rica. Tetrahedron Lett 2011 Apr; 52 (17): 2206-8.
19. Kharwar RN, Verma VC, Kumar A, Gond SK, Harper JK, Hess WM, et al. Javanicin, an antibacterial naphthoquinone from an endophytic fungus of neem, *Chloridium* sp. Curr Microbiol 2009 Mar; 58 (3): 233-8.
20. Yamamoto Y, Kinoshita Y, Ran Thor G, Hasumi M, Kinoshita K, Koyama K, et al. Isofuranonaphthoquinone derivatives from cultures of the lichen *Arthonia cinnabarina* (DC.) Wallr. Phytochemistry 2002 Aug; 60 (7): 741-5.
21. Stepanenko LS, Krivoshchekova OE, Dmitrenok PS, Maximov OB. Quinones of *Cetraria islandica*. Phytochemistry 1997 Oct; 46 (3): 565-8.
22. Perry NB, Blunt JW, Munro MH. A cytotoxic and antifungal 1,4-naphthoquinone and related compounds from a New Zealand brown algae, *Landsburgia quercifolia*. J Nat Prod 1991 Jul-Aug; 54 (4): 978-85.
23. Babula P, Adam V, Kizek R, Sladký Z, Havel L. Naphthoquinones as allelochemical triggers of programmed cell death. Environ Exp Bot 2009 Nov; 65: 330-7.
24. Willis RJ. The historical bases of the concept of allelopathy. J Hist Biol 1985 Mar; 18 (1): 71-102.
25. Meazza G, Scheffler BE, Tellez MR, Rimando AM, Romagni JG, Duke SO, et al. The inhibitory activity of natural products on plant *p*-hydroxyphenylpyruvate dioxygenase. Phytochemistry 2002 Jun; 60 (3): 281-8.
26. Hejl AM, Koster KL. Juglone disrupts root plasma membrane H^+-ATPase activity and impairs water uptake, root respiration, and growth in soybean (*Glycine max*) and corn (*Zea mays*). J Chem Ecol 2004 Feb; 30 (2): 453-71.
27. Shearer MJ. Vitamin K. Lancet 1995 Jan; 345 (8944): 229-34.
28. Weber P. Vitamin K and bone health. Nutrition 2001 Oct; 17 (10): 880-7.

29. Ferland G. Vitamin K and the nervous system: An overview of its actions. Adv Nutr 2012 Mar; 3 (2): 204-12.
30. Mallavadhani UV, Panda AK, Rao YR. Pharmacology and chemotaxonomy of *Diospyros*. Phytochemistry 1998 Oct; 49 (4): 901-51.
31. Costa MA, Alves AC, Seabra RM, Andrade PB. Naphthoquinones of *Diospyros chamaethamnus*. Planta Med 1998 May; 64 (4): 391.
32. Lee CH, Lee HS. Acaricidal activity and function of mite indicator using plumbagin and its derivatives isolated from *Diospyros kaki* Thunb. roots (Ebenaceae). J Microbiol Biotechnol 2008 Feb; 18 (2): 314-21.
33. Papageorgiou VP, Assimopoulou AN, Couladouros EA, Hepworth D, Nicolaou KC. The chemistry and biology of alkannin, shikonin, and related naphthazarin natural products. Angew Chem Int Ed 1999 Feb; 38 (3): 270-301.
34. Sandur SK, Ichikawa H, Sethi G, Ahn KS, Aggarwal BB. Plumbagin (5-hydroxy-2-methyl-1,4-naphthoquinone) suppresses NF-κB activation and NF-κB-regulated gene products through modulation of p65 and IκBα kinase activation, leading to potentiation of apoptosis induced by cytokine and chemotherapeutic agents. J Biol Chem 2006 Jun; 281 (25): 17023-33.
35. Gómez Castellanos JR, Prieto JM, Heinrich M. Red Lapacho (*Tabebuia impetiginosa*) - a global ethnopharmacological commodity? J Ethnopharmacol 2009 Jan; 121 (1): 1-13.
36. Powolny AA, Singh SV. Plumbagin-induced apoptosis in human prostate cancer cells is associated with modulation of cellular redox status and generation of reactive oxygen species. Pharm Res 2008 Sep; 25 (9): 2171-80.
37. Lee JH, Yeon JH, Kim H, Roh W, Chae J, Park HO, et al. The natural anticancer agent plumbagin induces potent cytotoxicity in MCF-7 human breast cancer cells by inhibiting a PI-5 kinase for ROS generation. PLoS One 2012 Sep; 7 (9): e45023.
38. Sinha S, Pal K, Elkhanany A, Dutta S, Cao Y, Mondal G, et al. Plumbagin inhibits tumorigenesis and angiogenesis of ovarian cancer cells *in vivo*. Int J Cancer 2013 Mar; 132 (5): 1201-12.
39. Montenegro RC, Araújo AJ, Molina MT, Marinho Filho JD, Rocha DD, López-Montero E, et al. Cytotoxic activity of naphthoquinones with special emphasis on juglone and its 5-*O*-methyl derivative. Chem Biol Interact 2010 Mar; 184 (3): 439-48.
40. Choi EK, Terai K, Ji IM, Kook YH, Park KH, Oh ET, et al. Upregulation of NAD(P)H:quinone oxidoreductase by radiation potentiates the effect of bioreductive β-lapachone on cancer cells. Neoplasia 2007 Aug; 9 (8): 634-42.

41. Ough M, Lewis A, Bey EA, Gao J, Ritchie JM, Bornmann W, et al. Efficacy of β-lapachone in pancreatic cancer treatment: Exploiting the novel, therapeutic target NQO1. Cancer Biol Ther 2005 Jan; 4 (1): 95-102.
42. Ravelo AG, Estévez-Braun A, Chávez-Orellana H, Pérez-Sacau E, Mesa-Siverio D. Recent studies on natural products as anticancer agents. Curr Top Med Chem 2004 Jan; 4 (2): 241-65.
43. Suffnes M, Douros JD. Miscellaneous natural productswith antitumor activity. In: Cassady JM, Douros JD, editors. Anticancer Agents Based on Natural Product Models. NewYork: Academic Press; 1980. p. 474.
44. Huang J, Wang X, Fei D, Ding L. Interactions of vitamin K3 with herring-sperm DNA using spectroscopy and electrochemistry. Appl Spectrosc 2010 Oct; 64 (10): 1126-30.
45. Kawiak A, Piosik J, Stasilojc G, Gwizdek-Wisniewska A, Marczak L, Stobiecki M, et al. Induction of apoptosis by plumbagin through reactive oxygen species-mediated inhibition of topoisomerase II. Toxicol Appl Pharmacol 2007 Sep; 223 (3): 267-76.
46. Paulsen MT, Ljungman M. The natural toxin juglone causes degradation of p53 and induces rapid H2AX phosphorylation and cell death in human fibroblasts. Toxicol Appl Pharmacol 2005 Nov; 209 (1): 1-9.
47. Stout DL, Becker FF. Xenobiotic metabolizing enzymes in genetically and chemically initiated mouse liver tumors. Cancer Res 1986 Jun; 46 (6): 2693-6.
48. Deeley TJ. A clinical trial of synkavit in the treatment of carcinoma of the bronchus. Br J Cancer 1962 Sep; 16 (3): 387-9.
49. Ganasoundari A, Zare SM, Devi PU. Modification of bone marrow radiosensensitivity by medicinal plant extracts. Br J Radiol 1997 Jun; 70 (834): 599-602.
50. Nutter LM, Cheng AL, Hung HL, Hsieh RK, Ngo EO, Liu TW. Menadione: Spectrum of anticancer activity and effects on nucleotide metabolism in human neoplastic cell lines. Biochem Pharmacol 1991 May; 41 (9): 1283-92.
51. Gold J. *In vivo* synergy of vitamin K3 and methotrexate in tumor-bearing animals. Cancer Treat Rep 1986 Dec; 70 (12): 1433-5.
52. Park BS, Kim JR, Lee SE, Kim KS, Takeoka GR, Ahn YJ, et al. Selective growth-inhibiting effects of compounds identified in *Tabebuia impetiginosa* inner bark on human intestinal bacteria. J Agric Food Chem 2005 Feb; 53 (4): 1152-7.
53. Adeniyi BA, Fong HH, Pezzuto JM, Luyengi L, Odelola HA. Antibacterial activity of diospyrin, isodiospyrin and bisisodiospyrin from the root of *Diospyros piscatoria* (Gurke) (Ebenaceae). Phytother Res 2000 Mar; 14 (2): 112-7.

54. Oliveira RA, Azevedo-Ximenes E, Luzzati R, Garcia RC. The hydroxy-naphthoquinone lapachol arrests mycobacterial growth and immunomodulates host macrophages. Int Immunopharmacol 2010 Nov; 10 (11): 1463-73.

55. Kuete V, Tangmouo JG, Meyer JJ, Lall N. Diospyrone, crassiflorone and plumbagin: three antimycobacterial and antigonorrhoeal naphthoquinones from two *Diospyros* spp. Int J Antimicrob Agents 2009 Oct; 34 (4): 322-5.

56. Vegara S, Funes L, Martí N, Saura D, Micol V, Valero M. Bactericidal activities against pathogenic bacteria by selected constituents of plant extracts in carrot broth. Food Chem 2011 Oct; 128 (4): 872-7.

57. Sasaki K, Abe H, Yoshizaki F. *In vitro* antifungal activity of naphthoquinone derivatives. Biol Pharm Bull 2002 May; 25 (5): 669-70.

58. Sritrairat N, Nukul N, Inthasame P, Sansuk A, Prasirt J, Leewatthanakorn T, et al. Antifungal activity of lawsone methyl ether in comparison with chlorhexidine. J Oral Pathol Med 2011 Jan; 40 (1): 90-6.

59. Sakunphueak A, Panichayupakaranant P. Comparison of antimicrobial activities of naphthoquinones from *Impatiens balsamina*. Nat Prod Res 2012 Jun; 26 (12): 1119-24.

60. Medeiros CS, Pontes-Filho NT, Camara CA, Lima-Filho JV, Oliveira PC, Lemos SA, et al. Antifungal activity of the naphthoquinone β-lapachone against disseminated infection with *Cryptococcus neoformans* var. *neoformans* in dexamethasone-immunosuppressed Swiss mice. Braz J Med Biol Res 2010 Apr; 43 (4): 345-9.

61. Errante G, La Motta G, Lagana C, Wittebolle V, Sarciron ME, Barret R. Synthesis and evaluation of antifungal activity of naphthoquinone derivatives. Eur J Med Chem 2006 Jun; 41 (6): 773-8.

62. Kaneshiro ES, Sul D, Hazra B. Effects of atovaquone and diospyrin-based drugs on ubiquinone biosynthesis in *Pneumocystis carinii* organisms. Antimicrob Agents Chemother 2000 Jan; 44 (1): 14-8.

63. Nakato H, Vivancos R, Hunter PR. A systematic review and meta-analysis of the effectiveness and safety of atovaquone proguanil (Malarone) for chemoprophylaxis against malaria. J Antimicrob Chemother 2007 Nov; 60 (5): 929-36.

64. Lorsuwannarat N, Saowakon N, Ramasoota P, Wanichanon C, Sobhon P. The anthelmintic effect of plumbagin on *Schistosoma mansoni*. Exp Parasitol 2013 Jan; 133 (1): 18-27.

65. Garnier T, Mantyla A, Jarvinen T, Lawrence J, Brown M, Croft S. *In vivo* studies on the antileishmanial activity of buparvaquone and its prodrugs. J Antimicrob Chemother 2007 Oct; 60 (4): 802-10.

66. Croft SL, Hogg J, Gutteridge WE, Hudson AT, Randall AW. The activity of hydroxynaphthoquinones against *Leishmania donovani*. J Antimicrob Chemother 1992 Dec; 30 (6): 827-32.
67. Muraguri GR, Kiara HK, McHardy N. Treatment of East Coast fever: A comparison of parvaquone and buparvaquone. Vet Parasitol 1999 Nov; 87 (1): 25-37.
68. Khraiwesh MH, Lee CM, Brandy Y, Akinboye ES, Berhe S, Gittens G, et al. Antitrypanosomal activities and cytotoxicity of some novel imido-substituted 1,4-naphthoquinone derivatives. Arch Pharm Res 2012 Jan; 35 (1): 27-33.
69. Henderson GB, Ulrich P, Fairlamb AH, Rosenberg I, Pereira M, Sela M, et al. "Subversive" substrates for the enzyme trypanothione disulfide reductase: Alternative approach to chemotherapy of Chagas disease. Proc Natl Acad Sci USA 1988 Aug; 85 (15): 5374-8.
70. Sharma N, Shukla AK, Das M, Dubey VK. Evaluation of plumbagin and its derivative as potential modulators of redox thiol metabolism of *Leishmania* parasite. Parasitol Res 2012 Jan; 110 (1): 341-8.
71. Lee JH, Cheong J, Park YM, Choi YH. Down-regulation of cyclooxygenase-2 and telomerase activity by β-lapachone in human prostate carcinoma cells. Pharmacol Res 2005 Jun; 51 (6): 553-60.
72. Liu SH, Tzeng HP, Kuo ML, Lin-Shiau SY. Inhibition of inducible nitric oxide synthase by β-lapachone in rat alveolar macrophages and aorta. Br J Pharmacol 1999 Feb; 126 (3): 746-50.
73. Tzeng HP, Ho FM, Chao KF, Kuo ML, Lin-Shiau SY, Liu SH. β-Lapachone reduces endotoxin-induced macrophage activation and lung edema and mortality. Am J Respir Crit Care Med 2003 Jul; 168 (1): 85-91.
74. Li Q, Verma IM. NF-κB regulation in the immune system. Nat Rev Immunol 2002 Oct; 2 (10): 725-34.
75. Xu J, Wagoner G, Douglas JC, Drew PD. β-Lapachone ameliorization of experimental autoimmune encephalomyelitis. J Neuroimmunol 2013 Jan; 254 (1-2): 46-54.
76. Yoshida LS, Kawada T, Irie K, Yuda Y, Himi T, Ikemoto F, et al. Shikonin directly inhibits nitric oxide synthases: Possible targets that affect thoracic aorta relaxation response and nitric oxide release from RAW 264.7 macrophages. J Pharmacol Sci 2010 Mar; 112 (3): 343-51.
77. Cheng YW, Chang CY, Lin KL, Hu CM, Lin CH, Kang JJ. Shikonin derivatives inhibited LPS-induced NOS in RAW 264.7 cells via downregulation of MAPK/NF-κB signaling. J Ethnopharmacol 2008 Nov; 120 (2): 264-71.

78. Andújar I, Recio MC, Bacelli T, Giner RM, Rios JL. Shikonin reduces oedema induced by phorbol ester by interfering with IκBα degradation thus inhibiting translocation of NF-κB to the nucleus. Br J Pharmacol 2010 May; 160 (2): 376-88.
79. Nam KN, Son MS, Park JH, Lee EH. Shikonins attenuate microglial inflammatory responses by inhibition of ERK, Akt, and NF-κB: neuroprotective implications. Neuropharmacology 2008 Oct; 55 (5): 819-25.
80. Xiong J, Ni J, Hu G, Shen J, Zhao Y, Yang L, et al. Shikonin ameliorates cerulein-induced acute pancreatitis in mice. J Ethnopharmacol 2013 Jan; 145 (2): 573-80.
81. Staniforth V, Wang SY, Shyur LF, Yang NS. Shikonins, phytocompounds from *Lithospermum erythrorhizon*, inhibit the transcriptional activation of human tumor necrosis factor α promoter *in vivo*. J Biol Chem 2004 Feb; 279 (7): 5877-85.
82. Lu L, Qin A, Huang H, Zhou P, Zhang C, Liu N, et al. Shikonin extracted from medicinal Chinese herbs exerts anti-inflammatory effect via proteasome inhibition. Eur J Pharmacol 2011 May; 658 (2-3): 242-7.
83. Dai Q, Fang J, Zhang FS. Dual role of shikonin in early and late stages of collagen type II arthritis. Mol Biol Rep 2009 Jul; 36 (6): 1597-604.
84. Lee CC, Wang CN, Lai YT, Kang JJ, Liao JW, Chiang BL, et al. Shikonin inhibits maturation of bone marrow-derived dendritic cells and suppresses allergic airway inflammation in a murine model of asthma. Br J Pharmacol 2010 Dec; 161 (7): 1496-511.
85. Checker R, Sharma D, Sandur SK, Khanam S, Poduval TB. Anti-inflammatory effects of plumbagin are mediated by inhibition of NF-kappaB activation in lymphocytes. Int Immunopharmacol 2009 Jul; 9 (7-8): 949-58.
86. Luo P, Wong YF, Ge L, Zhang ZF, Liu Y, Liu L, et al. Anti-inflammatory and analgesic effect of plumbagin through inhibition of nuclear factor-κB activation. J Pharmacol Exp Ther 2010 Dec; 335 (3): 735-42.
87. Kohli V, Sharma D, Sandur SK, Suryavanshi S, Sainis KB. Immune responses to novel allergens and modulation of inflammation by vitamin K3 analogue: A ROS dependent mechanism. Int Immunopharmacol 2011 Feb; 11 (2): 233-43.
88. Jia Y, Jing J, Bai Y, Li Z, Liu L, Luo J, et al. Amelioration of experimental autoimmune encephalomyelitis by plumbagin through down-regulation of JAK-STAT and NF-κB signaling pathways. PLoS One 2011 Oct; 6 (10): e27006.
89. Checker R, Sharma D, Sandur SK, Subrahmanyam G, Krishnan S, Poduval TB, et al. Plumbagin inhibits proliferative and inflammatory responses of T cells independent of ROS generation but by modulating intracellular thiols. J Cell Biochem 2010 Aug 110 (5): 1082-93.

90. Maruo S, Kuriyama I, Kuramochi K, Tsubaki K, Yoshida H, Mizushina Y. Inhibitory effect of novel 5-*O*-acyl juglones on mammalian DNA polymerase activity, cancer cell growth and inflammatory response. Bioorg Med Chem 2011 Oct; 19 (19): 5803-12.
91. Kawamura F, Nakanishi M, Hirashima N. Effects of menadione, a reactive oxygen generator, on leukotriene secretion from RBL-2H3 cells. Biol Pharm Bull 2010 May; 33 (5): 881-5.
92. Tewtrakul S, Tansakul P, Panichayupakaranant P. Anti-allergic principles of *Rhinacanthus nasutus* leaves. Phytomedicine 2009 Oct; 16 (10): 929-34.
93. Lien JC, Huang LJ, Wang JP, Teng CM, Lee KH, Kuo SC. Synthesis and antiplatelet, antiinflammatory, and antiallergic activities of 2-substituted 3-chloro-1,4-naphthoquinone derivatives. Bioorg Med Chem 1997 Dec; 5 (12): 2111-20.
94. Hennig L, Christner C, Kipping M, Schelbert B, Rucknagel KP, Grabley S, et al. Selective inactivation of parvulin-like peptidyl-prolyl *cis*/*trans* isomerases by juglone. Biochemistry 1998 Apr; 37 (17): 5953-60.
95. Esnault S, Rosenthal LA, Shen ZJ, Sedgwick JB, Szakaly RJ, Sorkness RL, et al. A critical role for Pin1 in allergic pulmonary eosinophilia in rats. J Allergy Clin Immunol 2007 Nov; 120 (5): 1082-8.
96. Nowicka B, Kruk J. Occurrence, biosynthesis and function of isoprenoid quinones. Biochim Biophys Acta 2010 Sep; 1797 (9): 1587-605.
97. Lenaz G, Fato R, Formiggini G, Genova ML. The role of Coenzyme Q in mitochondrial electron transport. Mitochondrion 2007 Jun; 7 Suppl: S8-33.
98. Bentinger M, Tekle M, Dallner G. Coenzyme Q-biosynthesis and functions. Biochem Biophys Res Commun 2010 May; 396 (1): 74-9.
99. Ernster L, Dallner G. Biochemical, physiological and medical aspects of ubiquinone function. Biochim Biophys Acta 1995 May; 1271 (1): 195-204.
100. Szkopińska A. Ubiquinone. Biosynthesis of quinone ring and its isoprenoid side chain. Intracellular localization. Acta Biochim Pol 2000 May; 47 (2): 469-80.
101. Geromel V, Darin N, Chrétien D, Bénit P, DeLonlay P, Rotig A, et al. Coenzyme Q_{10} and idebenone in the therapy of respiratory chain diseases: rationale and comparative benefits. Mol Genet Metab 2002 Sep-Oct; 77 (1-2): 21-30.
102. Elmberger PG, Kalen A, Brunk UT, Dallner G. Discharge of newly-synthesized dolichol and ubiquinone with lipoproteins to rat liver perfusate and to the bile. Lipids 1989 Nov; 24 (11): 919-30.
103. Kalen A, Norling B, Appelkvist EL, Dallner G. Ubiquinone biosynthesis by the microsomal fraction from rat liver. Biochim Biophys Acta 1987 Oct; 926 (1): 70-8.

104. Turunen M, Olsson J, Dallner G. Metabolism and function of coenzyme Q. Biochim Biophys Acta 2004 Jan; 1660 (1-2): 171-99.

105. Krisans SK, Ericsson J, Edwards PA, Keller GA. Farnesyl-diphosphate synthase is localized in peroxisomes. J Biol Chem 1994 May; 269 (19): 14165-9.

106. Runquist M, Ericsson J, Thelin A, Chojnacki T, Dallner G. Isoprenoid biosynthesis in rat liver mitochondria. Studies on farnesyl pyrophosphate synthase and trans-prenyltransferase. J Biol Chem 1994 Feb; 269 (8): 5804-9.

107. Tekle M, Bentinger M, Nordman T, Appelkvist EL, Chojnacki T, Olsson JM. Ubiquinone biosynthesis in rat liver peroxisomes. Biochem Biophys Res Commun 2002 Mar; 291 (5): 1128-33.

108. Teclebrhan H, Olsson J, Swiezewska E, Dallner G. Biosynthesis of the side chain of ubiquinone:trans-prenyltransferase in rat liver microsomes. J Biol Chem 1993 Nov; 268 (31): 23081-6.

109. Walter L, Nogueira V, Leverve X, Heitz MP, Bernardi P, Fontaine E. Three classes of ubiquinone analogs regulate the mitochondrial permeability transition pore through a common site. J Biol Chem 2000 Sep; 275 (38): 29521-7.

110. Echtay KS, Winkler E, Frischmuth K, Klingenberg M. Uncoupling proteins 2 and 3 are highly active H^+ transporters and highly nucleotide sensitive when activated by coenzyme Q (ubiquinone). Proc Natl Acad Sci USA 2001 Feb; 98 (4): 1416-21.

111. James AM, Smith RA, Murphy MP. Antioxidant and prooxidant properties of mitochondrial Coenzyme Q. Arch Biochem Biophys 2004 Mar; 423 (1): 47-56.

112. Gómez-Díaz C, Rodriguez-Aguilera JC, Barroso MP, Villalba JM, Navarro F, Crane FL, et al. Antioxidant ascorbate is stabilized by NADH-coenzyme Q_{10} reductase in the plasma membrane. J Bioenerg Biomembr 1997 Jun; 29 (3): 251-7.

113. Ebadi M, Sharma SK, Wanpen S, Amornpan A. Coenzyme Q_{10} inhibits mitochondrial complex-I down-regulation and nuclear factor-kappa B activation. J Cell Mol Med 2004 Apr-Jun; 8 (2): 213-22.

114. González-Rubio S, Hidalgo AB, Ferrín G, Bello RI, González R, Gahete MD, et al. Mitochondrial-driven ubiquinone enhances extracellular calcium-dependent nitric oxide production and reduces glycochenodeoxycholic acid-induced cell death in hepatocytes. Chem Res Toxicol 2009 Dec; 22 (12): 1984-91.

115. Fash DM, Khdour OM, Sahdeo SJ, Goldschmidt R, Jaruvangsanti J, Dey S, et al. Effects of alkyl side chain modification of coenzyme Q_{10} on mitochondrial respiratory chain function and cytoprotection. Bioorg Med Chem 2013 Apr; 21 (8): 2346-54.

116. Smith RA, Porteous CM, Gane AM, Murphy MP. Delivery of bioactive molecules to mitochondria *in vivo*. Proc Natl Acad Sci USA 2003 Apr; 100 (9): 5407-12.

117. James AM, Cocheme HM, Smith RA, Murphy MP. Interactions of mitochondria-targeted and untargeted ubiquinones with the mitochondrial respiratory chain and reactive oxygen species. Implications for the use of exogenous ubiquinones as therapies and experimental tools. J Biol Chem 2005 Jun; 280 (22): 21295-312.

118. Rauchová H, Vokurková M, Drahota Z. Idebenone-induced recovery of glycerol-3-phosphate and succinate oxidation inhibited by digitonin. Physiol Res 2012 Jul; 61 (3): 259-65.

119. Esposti MD, Ngo A, Ghelli A, Benelli B, Carelli V, McLennan H, et al. The interaction of Q analogs, particularly hydroxydecyl benzoquinone (idebenone), with the respiratory complexes of heart mitochondria. Arch Biochem Biophys 1996 Jun; 330 (2): 395-400.

120. Heitz FD, Erb M, Anklin C, Robay D, Pernet V, Gueven N. Idebenone protects against retinal damage and loss of vision in a mouse model of Leber's hereditary optic neuropathy. PLoS One 2012 Sep; 7 (9): e45182.

121. Kutz K, Drewe J, Vankan P. Pharmacokinetic properties and metabolism of idebenone. J Neurol 2009 Mar; 256 Suppl 1: 31-5.

122. López LC, Quinzii CM, Area E, Naini A, Rahman S, Schuelke M, et al. Treatment of CoQ_{10} deficient fibroblasts with ubiquinone, CoQ analogs, and vitamin C: Time- and compound-dependent effects. PLoS One 2010 Jul; 5 (7): e11897.

123. Seznec H, Simon D, Monassier L, Criqui-Filipe P, Gansmuller A, Rustin P, et al. Idebenone delays the onset of cardiac functional alteration without correction of Fe-S enzymes deficit in a mouse model for Friedreich ataxia. Hum Mol Genet 2004 May; 13 (10): 1017-24.

124. Soriano S, Llorens JV, Blanco-Sobero L, Gutiérrez L, Calap-Quintana P, Morales MP, et al. Deferiprone and idebenone rescue frataxin depletion phenotypes in a *Drosophila* model of Friedreich's ataxia. Gene 2013 Jun; 521 (2): 274-81.

125. Rustin P, von Kleist-Retzow JC, Chantrel-Groussard K, Sidi D, Munnich A, Rotig A. Effect of idebenone on cardiomyopathy in Friedreich's ataxia: A preliminary study. Lancet 1999 Aug; 354 (9177): 477-9.

126. Di Prospero NA, Baker A, Jeffries N, Fischbeck KH. Neurological effects of high-dose idebenone in patients with Friedreich's ataxia: A randomised, placebo-controlled trial. Lancet Neurol 2007 Oct; 6 (10): 878-86.

127. Velasco-Sánchez D, Aracil A, Montero R, Mas A, Jiménez L, O'Callaghan M, et al. Combined therapy with idebenone and deferiprone in patients with Friedreich's ataxia. Cerebellum 2011 Mar; 10 (1): 1-8.

128. Jauslin ML, Wirth T, Meier T, Schoumacher F. A cellular model for Friedreich Ataxia reveals small-molecule glutathione peroxidase mimetics as novel treatment strategy. Hum Mol Genet 2002 Nov; 11 (24): 3055-63.
129. Napolitano A, Salvetti S, Vista M, Lombardi V, Siciliano G, Giraldi C. Long-term treatment with idebenone and riboflavin in a patient with MELAS. Neurol Sci 2000 Dec; 21 (3): S981-2.
130. Rudolph G, Dimitriadis K, Büchner B, Heck S, Al-Tamami J, Seidensticker F, et al. Effects of idebenone on color vision in patients with Leber Hereditary Optic Neuropathy. J Neuroophthalmol 2013 Mar; 33 (1): 30-6.
131. Barboni P, Valentino ML, La Morgia C, Carbonelli M, Savini G, De Negri A, et al. Idebenone treatment in patients with OPA1-mutant dominant optic atrophy. Brain 2013 Feb; 136 (Pt 2): e231.
132. Buyse GM, Goemans N, van den Hauwe M, Thijs D, de Groot IJ, Schara U, et al. Idebenone as a novel, therapeutic approach for Duchenne muscular dystrophy: results from a 12 month, double-blind, randomized placebo-controlled trial. Neuromuscul Disord 2011 Jun; 21 (6): 396-405.
133. Buyse GM, Goemans N, van den Hauwe M, Meier T. Effects of glucocorticoids and idebenone on respiratory function in patients with Duchenne muscular dystrophy. Pediatr Pulmonol 2013 Sep; 48 (9): 912-20.
134. Giorgio V, Petronilli V, Ghelli A, Carelli V, Rugolo M, Lenaz G, et al. The effects of idebenone on mitochondrial bioenergetics. Biochim Biophys Acta 2012 Feb; 1817 (2): 363-9.
135. Telford JE, Kilbride SM, Davey GP. Decylubiquinone increases mitochondrial function in synaptosomes. J Biol Chem 2010 Mar; 285 (12): 8639-45.
136. Sobreira C, Hirano M, Shanske S, Keller RK, Haller RG, Davidson E, et al. Mitochondrial encephalomyopathy with coenzyme Q_{10} deficiency. Neurology 1997 May; 48 (5): 1238-43.
137. Erb M, Hoffmann-Enger B, Deppe H, Soeberdt M, Haefeli RH, Rummey C, et al. Features of idebenone and related short-chain quinones that rescue ATP levels under conditions of impaired mitochondrial complex I. PLoS One 2012 Apr; 7 (4): e36153.
138. Civenni G, Bezzi P, Trotti D, Volterra A, Racagni G. Inhibitory effect of the neuroprotective agent idebenone on arachidonic acid metabolism in astrocytes. Eur J Pharmacol 1999 Apr; 370 (2): 161-7.
139. Inatsu S, Ohsaki A, Nagata K. Idebenone acts against growth of *Helicobacter pylori* by inhibiting its respiration. Antimicrob Agents Chemother 2006 Jun; 50 (6): 2237-9.

140. Akira S, Uematsu S, Takeuchi O. Pathogen recognition and innate immunity. Cell 2006 Feb; 124 (4): 783-801.
141. Janeway CA, Jr., Medzhitov R. Innate immune recognition. Annu Rev Immunol 2002 Oct; 20: 197-216.
142. West AP, Shadel GS, Ghosh S. Mitochondria in innate immune responses. Nat Rev Immunol 2011 Jun; 11 (6): 389-402.
143. Parkin J, Cohen B. An overview of the immune system. Lancet 2001 Jun; 357 (9270): 1777-89.
144. Kumar H, Kawai T, Akira S. Pathogen recognition by the innate immune system. Int Rev Immunol 2011 Feb; 30 (1): 16-34.
145. Coussens LM, Werb Z. Inflammation and cancer. Nature 2002 Dec; 420 (6917): 860-7.
146. Gabay C. Interleukin-6 and chronic inflammation. Arthritis Res Ther 2006 Jul; 8 (2): S3.
147. Libby P. Inflammation in atherosclerosis. Nature 2002 Dec; 420 (6917): 868-74.
148. Raetz CR. Biochemistry of endotoxins. Annu Rev Biochem 1990 Nov; 59: 129-70.
149. Kaminska B. MAPK signalling pathways as molecular targets for anti-inflammatory therapy - From molecular mechanisms to therapeutic benefits. Biochim Biophys Acta 2005 Dec; 1754 (1-2): 253-62.
150. Ji RR, Gereau RWt, Malcangio M, Strichartz GR. MAP kinase and pain. Brain Res Rev 2009 Apr; 60 (1): 135-48.
151. Saklatvala J. The p38 MAP kinase pathway as a therapeutic target in inflammatory disease. Curr Opin Pharmacol 2004 Aug; 4 (4): 372-7.
152. Brasier AR. The NF-κB regulatory network. Cardiovasc Toxicol 2006; 6 (2): 111-30.
153. Shen HM, Tergaonkar V. NF-κB signaling in carcinogenesis and as a potential molecular target for cancer therapy. Apoptosis 2009 Apr; 14 (4): 348-63.
154. Turini ME, DuBois RN. Cyclooxygenase-2: A therapeutic target. Annu Rev Med 2002 Feb; 53: 35-57.
155. Bos CL, Richel DJ, Ritsema T, Peppelenbosch MP, Versteeg HH. Prostanoids and prostanoid receptors in signal transduction. Int J Biochem Cell Biol 2004 Jul; 36 (7): 1187-205.
156. Warner TD, Mitchell JA. Cyclooxygenases: New forms, new inhibitors, and lessons from the clinic. FASEB J 2004 May; 18 (7): 790-804.
157. Aggarwal BB. Nuclear factor-κB: The enemy within. Cancer Cell 2004 Sep; 6 (3): 203-8.

158. Jeon YJ, Han SH, Lee YW, Lee M, Yang KH, Kim HM. Dexamethasone inhibits IL-1β gene expression in LPS-stimulated RAW 264.7 cells by blocking NF-κB/Rel and AP-1 activation. Immunopharmacology 2000 Jul; 48 (2): 173-83.

159. Tseng CH, Cheng CM, Tzeng CC, Peng SI, Yang CL, Chen YL. Synthesis and anti-inflammatory evaluations of β-lapachone derivatives. Bioorg Med Chem 2013 Jan; 21 (2): 523-31.

160. Osawa Y, Lee HT, Hirshman CA, Xu D, Emala CW. Lipopolysaccharide-induced sensitization of adenylyl cyclase activity in murine macrophages. Am J Physiol Cell Physiol 2006 Jan; 290 (1): C143-51.

161. Phillips TA, Kujubu DA, MacKay RJ, Herschman HR, Russell SW, Pace JL. The mouse macrophage activation-associated marker protein, p71/73, is an inducible prostaglandin endoperoxide synthase (cyclooxygenase). J Leukoc Biol 1993 Apr; 53 (4): 411-9.

162. Mayo JC, Sainz RM, Tan DX, Hardeland R, Leon J, Rodriguez C, et al. Anti-inflammatory actions of melatonin and its metabolites, N1-acetyl-N2-formyl-5-methoxykynuramine (AFMK) and N1-acetyl-5-methoxykynuramine (AMK), in macrophages. J Neuroimmunol 2005 Aug; 165 (1-2): 139-49.

163. Kim E, Kang BY, Kim TS. Inhibition of interleukin-12 production in mouse macrophages by hydroquinone, a reactive metabolite of benzene, via suppression of nuclear factor-κB binding activity. Immunol Lett 2005 Jun; 99 (1): 24-9.

164. Delgado MA, Elmaoued RA, Davis AS, Kyei G, Deretic V. Toll-like receptors control autophagy. EMBO J 2008 Apr; 27 (7): 1110-21.

165. Zhang Y, Hogg N. The mechanism of transmembrane *S*-nitrosothiol transport. Proc Natl Acad Sci USA 2004 May; 101 (21): 7891-6.

166. Galli SJ, Tsai M, Piliponsky AM. The development of allergic inflammation. Nature 2008 Jul; 454 (7203): 445-54.

167. Yazdanbakhsh M, Kremsner PG, van Ree R. Allergy, parasites, and the hygiene hypothesis. Science 2002 Apr; 296 (5567): 490-4.

168. Umetsu DT, DeKruyff RH. The regulation of allergy and asthma. Immunol Rev 2006 Aug; 212: 238-55.

169. Kay AB. Overview of 'allergy and allergic diseases: with a view to the future'. Br Med Bull 2000; 56 (4): 843-64.

170. Johansson SG, Bieber T, Dahl R, Friedmann PS, Lanier BQ, Lockey RF, et al. Revised nomenclature for allergy for global use: Report of the Nomenclature Review Committee of the World Allergy Organization, October 2003. J Allergy Clin Immunol 2004 May; 113 (5): 832-6.

171. Prussin C, Metcalfe DD. 4. IgE, mast cells, basophils, and eosinophils. J Allergy Clin Immunol 2003 Feb; 111 (2): S486-94.
172. Gould HJ, Sutton BJ. IgE in allergy and asthma today. Nat Rev Immunol 2008 Mar; 8 (3): 205-17.
173. Anand P, Singh B, Jaggi AS, Singh N. Mast cells: An expanding pathophysiological role from allergy to other disorders. Naunyn Schmiedebergs Arch Pharmacol 2012 Jul; 385 (7): 657-70.
174. Amin K. The role of mast cells in allergic inflammation. Respir Med 2012 Jan; 106 (1): 9-14.
175. Shea-Donohue T, Stiltz J, Zhao A, Notari L. Mast cells. Curr Gastroenterol Rep 2010 Oct; 12 (5): 349-57.
176. Bhargava KP, Nath R, Palit G. Nature of histamine receptors concerned in capillary permeability. Br J Pharmacol 1977 Feb; 59 (2): 349-51.
177. Rådmark OP. The molecular biology and regulation of 5-lipoxygenase. Am J Respir Crit Care Med 2000 Feb; 161 (2 Pt 2): S11-5.
178. Engels F, Nijkamp FP. Pharmacological inhibition of leukotriene actions. Pharm World Sci 1998 Apr; 20 (2): 60-5.
179. Singh RK, Gupta S, Dastidar S, Ray A. Cysteinyl leukotrienes and their receptors: molecular and functional characteristics. Pharmacology 2010 Jun; 85 (6): 336-49.
180. Holgate ST, Polosa R. Treatment strategies for allergy and asthma. Nat Rev Immunol 2008 Mar; 8 (3): 218-30.
181. Choi Y, Kim MS, Hwang JK. Inhibitory effects of panduratin A on allergy-related mediator production in rat basophilic leukemia mast cells. Inflammation 2012 Dec; 35 (6): 1904-15.
182. Vandecasteele G, Szabadkai G, Rizzuto R. Mitochondrial calcium homeostasis: mechanisms and molecules. IUBMB Life 2001 Sep-Nov; 52 (3-5): 213-9.
183. Miller WL. Steroid hormone synthesis in mitochondria. Mol Cell Endocrinol 2013 Apr; 379 (1-2): 62-73.
184. Schon EA, Przedborski S. Mitochondria: The next (neurode)generation. Neuron 2011 Jun; 70 (6): 1033-53.
185. Modre-Osprian R, Osprian I, Tilg B, Schreier G, Weinberger KM, Graber A. Dynamic simulations on the mitochondrial fatty acid beta-oxidation network. BMC Syst Biol 2009 Jan; 3: 2.
186. Lill R, Hoffmann B, Molik S, Pierik AJ, Rietzschel N, Stehling O, et al. The role of mitochondria in cellular iron-sulfur protein biogenesis and iron metabolism. Biochim Biophys Acta 2012 Sep; 1823 (9): 1491-508.

187. Wang C, Youle RJ. The role of mitochondria in apoptosis*. Annu Rev Genet 2009 Aug; 43: 95-118.

188. Pienaar IS, Chinnery PF. Existing and emerging mitochondrial-targeting therapies for altering Parkinson's disease severity and progression. Pharmacol Ther 2013 Jan; 137 (1): 1-21.

189. Anderson S, Bankier AT, Barrell BG, de Bruijn MH, Coulson AR, Drouin J, et al. Sequence and organization of the human mitochondrial genome. Nature 1981 Apr; 290 (5806): 457-65.

190. Tuppen HA, Blakely EL, Turnbull DM, Taylor RW. Mitochondrial DNA mutations and human disease. Biochim Biophys Acta 2010 Feb; 1797 (2): 113-28.

191. Schapira AH. Complex I: Inhibitors, inhibition and neurodegeneration. Exp Neurol 2010 Aug; 224 (2): 331-5.

192. Sun F, Zhou Q, Pang X, Xu Y, Rao Z. Revealing various coupling of electron transfer and proton pumping in mitochondrial respiratory chain. Curr Opin Struct Biol 2013 Aug; 23 (4): 526-38.

193. Vartak R, Porras CA, Bai Y. Respiratory supercomplexes: Structure, function and assembly. Protein Cell 2013 Aug; 4 (8): 582-90.

194. Bratic I, Trifunovic A. Mitochondrial energy metabolism and ageing. Biochim Biophys Acta 2010 Jun-Jul; 1797 (6-7): 961-7.

195. Wallace DC, Fan W, Procaccio V. Mitochondrial energetics and therapeutics. Annu Rev Pathol 2010 Feb; 5: 297-348.

196. Winklhofer KF, Haass C. Mitochondrial dysfunction in Parkinson's disease. Biochim Biophys Acta 2010 Jan; 1802 (1): 29-44.

197. Lai B, Zhang L, Dong LY, Zhu YH, Sun FY, Zheng P. Impact of inhibition of Q_o site of mitochondrial complex III with myxothiazol on persistent sodium currents via superoxide and protein kinase C in rat hippocampal CA1 cells. Neurobiol Dis 2006 Jan; 21 (1): 206-16.

198. Nicholls DG. Mitochondrial function and dysfunction in the cell: Its relevance to aging and aging-related disease. Int J Biochem Cell Biol 2002 Nov; 34 (11): 1372-81.

199. Bartoschek S, Johansson M, Geierstanger BH, Okun JG, Lancaster CR, Humpfer E, et al. Three molecules of ubiquinone bind specifically to mitochondrial cytochrome bc_1 complex. J Biol Chem 2001 Sep; 276 (38): 35231-4.

200. Devenish RJ, Prescott M, Boyle GM, Nagley P. The oligomycin axis of mitochondrial ATP synthase: OSCP and the proton channel. J Bioenerg Biomembr 2000 Oct; 32 (5): 507-15.

201. Krab K. Kinetic and regulatory aspects of the function of the alternative oxidase in plant respiration. J Bioenerg Biomembr 1995 Aug; 27 (4): 387-96.
202. Dumont M, Beal MF. Neuroprotective strategies involving ROS in Alzheimer disease. Free Radic Biol Med 2011 Sep; 51 (5): 1014-26.
203. Brown GC, Borutaite V. There is no evidence that mitochondria are the main source of reactive oxygen species in mammalian cells. Mitochondrion 2012 Jan; 12 (1): 1-4.
204. Keane PC, Kurzawa M, Blain PG, Morris CM. Mitochondrial dysfunction in Parkinson's disease. Parkinsons Dis 2011 Mar; 2011: 716871.
205. Finsterer J. Treatment of mitochondrial disorders. Eur J Paediatr Neurol 2010 Jan; 14 (1): 29-44.
206. Beal MF. Mitochondria take center stage in aging and neurodegeneration. Ann Neurol 2005 Oct; 58 (4): 495-505.
207. Coleman R, Weiss A, Finkelbrand S, Silbermann M. Age and exercise-related changes in myocardial mitochondria in mice. Acta Histochem 1988; 83 (1): 81-90.
208. Lin MT, Beal MF. Mitochondrial dysfunction and oxidative stress in neurodegenerative diseases. Nature 2006 Oct; 443 (7113): 787-95.
209. Li H, Kumar Sharma L, Li Y, Hu P, Idowu A, Liu D, et al. Comparative bioenergetic study of neuronal and muscle mitochondria during aging. Free Radic Biol Med 2013 Oct; 63: 30-40.
210. Berardo A, Musumeci O, Toscano A. Cardiological manifestations of mitochondrial respiratory chain disorders. Acta Myol 2011 Jun; 30 (1): 9-15.
211. Nunnari J, Suomalainen A. Mitochondria: In sickness and in health. Cell 2012 Mar; 148 (6): 1145-59.
212. Smith RA, Hartley RC, Cocheme HM, Murphy MP. Mitochondrial pharmacology. Trends Pharmacol Sci 2012 Jun; 33 (6): 341-52.
213. Büeler H. Impaired mitochondrial dynamics and function in the pathogenesis of Parkinson's disease. Exp Neurol 2009 Aug; 218 (2): 235-46.
214. Schapira AH, Jenner P. Etiology and pathogenesis of Parkinson's disease. Mov Disord 2011 May; 26 (6): 1049-55.
215. Gasser T. Mendelian forms of Parkinson's disease. Biochim Biophys Acta 2009 Jul; 1792 (7): 587-96.
216. Yong-Kee CJ, Sidorova E, Hanif A, Perera G, Nash JE. Mitochondrial dysfunction precedes other sub-cellular abnormalities in an *in vitro* model linked with cell death in Parkinson's disease. Neurotox Res 2012 Feb; 21 (2): 185-94.

217. Haas RH, Nasirian F, Nakano K, Ward D, Pay M, Hill R, et al. Low platelet mitochondrial complex I and complex II/III activity in early untreated Parkinson's disease. Ann Neurol 1995 Jun; 37 (6): 714-22.

218. Schapira AH, Cooper JM, Dexter D, Clark JB, Jenner P, Marsden CD. Mitochondrial complex I deficiency in Parkinson's disease. J Neurochem 1990 Mar; 54 (3): 823-7.

219. Bindoff LA, Birch-Machin MA, Cartlidge NE, Parker WD, Jr., Turnbull DM. Respiratory chain abnormalities in skeletal muscle from patients with Parkinson's disease. J Neurol Sci 1991 Aug; 104 (2): 203-8.

220. Mann VM, Cooper JM, Krige D, Daniel SE, Schapira AH, Marsden CD. Brain, skeletal muscle and platelet homogenate mitochondrial function in Parkinson's disease. Brain 1992 Apr; 115 (Pt 2): 333-42.

221. Parker WD, Jr., Parks JK, Swerdlow RH. Complex I deficiency in Parkinson's disease frontal cortex. Brain Res 2008 Jan; 1189: 215-8.

222. Shinde S, Pasupathy K. Respiratory-chain enzyme activities in isolated mitochondria of lymphocytes from patients with Parkinson's disease: Preliminary study. Neurol India 2006 Dec; 54 (4): 390-3.

223. Polymeropoulos MH, Lavedan C, Leroy E, Ide SE, Dehejia A, Dutra A, et al. Mutation in the α-synuclein gene identified in families with Parkinson's disease. Science 1997 Jun; 276 (5321): 2045-7.

224. Shimura H, Hattori N, Kubo S, Mizuno Y, Asakawa S, Minoshima S, et al. Familial Parkinson disease gene product, parkin, is a ubiquitin-protein ligase. Nat Genet 2000 Jul; 25 (3): 302-5.

225. Valente EM, Abou-Sleiman PM, Caputo V, Muqit MM, Harvey K, Gispert S, et al. Hereditary early-onset Parkinson's disease caused by mutations in PINK1. Science 2004 May; 304 (5674): 1158-60.

226. Paisán-Ruíz C, Jain S, Evans EW, Gilks WP, Simón J, van der Brug M, et al. Cloning of the gene containing mutations that cause PARK8-linked Parkinson's disease. Neuron 2004 Nov; 44 (4): 595-600.

227. Kuroda Y, Mitsui T, Kunishige M, Shono M, Akaike M, Azuma H, et al. Parkin enhances mitochondrial biogenesis in proliferating cells. Hum Mol Genet 2006 Mar; 15 (6): 883-95.

228. McBride HM. Parkin mitochondria in the autophagosome. J Cell Biol 2008 Dec; 183 (5): 757-9.

229. Deng H, Dodson MW, Huang H, Guo M. The Parkinson's disease genes pink1 and parkin promote mitochondrial fission and/or inhibit fusion in *Drosophila*. Proc Natl Acad Sci USA 2008 Sep; 105 (38): 14503-8.

230. Liu S, Sawada T, Lee S, Yu W, Silverio G, Alapatt P, et al. Parkinson's disease-associated kinase PINK1 regulates Miro protein level and axonal transport of mitochondria. PLoS Genet 2012 Mar; 8 (3): e1002537.

231. Alves-Rodrigues A, Gregori L, Figueiredo-Pereira ME. Ubiquitin, cellular inclusions and their role in neurodegeneration. Trends Neurosci 1998 Dec; 21 (12): 516-20.

232. Kim YM, Jang WH, Quezado MM, Oh Y, Chung KC, Junn E, et al. Proteasome inhibition induces α-synuclein SUMOylation and aggregate formation. J Neurol Sci 2011 Aug; 307 (1-2): 157-61.

233. Snyder H, Mensah K, Theisler C, Lee J, Matouschek A, Wolozin B. Aggregated and monomeric α-synuclein bind to the S6' proteasomal protein and inhibit proteasomal function. J Biol Chem 2003 Apr; 278 (14): 11753-9.

234. McNaught KS, Bjorklund LM, Belizaire R, Isacson O, Jenner P, Olanow CW. Proteasome inhibition causes nigral degeneration with inclusion bodies in rats. Neuroreport 2002 Aug; 13 (11): 1437-41.

235. Martin I, Dawson VL, Dawson TM. Recent advances in the genetics of Parkinson's disease. Annu Rev Genomics Hum Genet 2011 Sep; 12: 301-25.

236. Kamp F, Exner N, Lutz AK, Wender N, Hegermann J, Brunner B, et al. Inhibition of mitochondrial fusion by α-synuclein is rescued by PINK1, Parkin and DJ-1. EMBO J 2010 Oct; 29 (20): 3571-89.

237. Devi L, Raghavendran V, Prabhu BM, Avadhani NG, Anandatheerthavarada HK. Mitochondrial import and accumulation of α-synuclein impair complex I in human dopaminergic neuronal cultures and Parkinson disease brain. J Biol Chem 2008 Apr; 283 (14): 9089-100.

238. Sherer TB, Kim JH, Betarbet R, Greenamyre JT. Subcutaneous rotenone exposure causes highly selective dopaminergic degeneration and α-synuclein aggregation. Exp Neurol 2003 Jan; 179 (1): 9-16.

239. Betarbet R, Sherer TB, MacKenzie G, Garcia-Osuna M, Panov AV, Greenamyre JT. Chronic systemic pesticide exposure reproduces features of Parkinson's disease. Nat Neurosci 2000 Dec; 3 (12): 1301-6.

240. Klivenyi P, Siwek D, Gardian G, Yang L, Starkov A, Cleren C, et al. Mice lacking alpha-synuclein are resistant to mitochondrial toxins. Neurobiol Dis 2006 Mar; 21 (3): 541-8.

241. Olanow CW, Perl DP, DeMartino GN, McNaught KS. Lewy-body formation is an aggresome-related process: A hypothesis. Lancet Neurol 2004 Aug; 3 (8): 496-503.

242. Palin EJ, Paetau A, Suomalainen A. Mesencephalic complex I deficiency does not correlate with parkinsonism in mitochondrial DNA maintenance disorders. Brain 2013 Aug; 136 (Pt 8): 2379-92.

243. Spina MB, Cohen G. Dopamine turnover and glutathione oxidation: Implications for Parkinson disease. Proc Natl Acad Sci USA 1989 Feb; 86 (4): 1398-400.

244. van Muiswinkel FL, de Vos RA, Bol JG, Andringa G, Jansen Steur EN, Ross D, et al. Expression of NAD(P)H:quinone oxidoreductase in the normal and Parkinsonian substantia nigra. Neurobiol Aging 2004 Oct; 25 (9): 1253-62.

245. Dexter DT, Carayon A, Javoy-Agid F, Agid Y, Wells FR, Daniel SE, et al. Alterations in the levels of iron, ferritin and other trace metals in Parkinson's disease and other neurodegenerative diseases affecting the basal ganglia. Brain 1991 Aug; 114 (Pt 4): 1953-75.

246. Sonia Angeline M, Chaterjee P, Anand K, Ambasta RK, Kumar P. Rotenone-induced parkinsonism elicits behavioral impairments and differential expression of parkin, heat shock proteins and caspases in the rat. Neuroscience 2012 Sep; 220: 291-301.

247. Berry C, La Vecchia C, Nicotera P. Paraquat and Parkinson's disease. Cell Death Differ 2010 Jul; 17 (7): 1115-25.

248. Smeyne RJ, Jackson-Lewis V. The MPTP model of Parkinson's disease. Brain Res Mol Brain Res 2005 Mar; 134 (1): 57-66.

249. McCormack AL, Thiruchelvam M, Manning-Bog AB, Thiffault C, Langston JW, Cory-Slechta DA, et al. Environmental risk factors and Parkinson's disease: Selective degeneration of nigral dopaminergic neurons caused by the herbicide paraquat. Neurobiol Dis 2002 Jul; 10 (2): 119-27.

250. Kamel F. Epidemiology. Paths from pesticides to Parkinson's. Science 2013 Aug; 341 (6147): 722-3.

251. Lees AJ, Hardy J, Revesz T. Parkinson's disease. Lancet 2009 Jun; 373 (9680): 2055-66.

252. Kaplan S, Tarsy D. Initial treatment of Parkinson's disease: An update. Curr Treat Options Neurol 2013 Aug; 15 (4): 377-84.

253. Dawson TM, Dawson VL. Molecular pathways of neurodegeneration in Parkinson's disease. Science 2003 Oct; 302 (5646): 819-22.

254. Tetrud JW, Langston JW. Tremor in MPTP-induced parkinsonism. Neurology 1992 Feb; 42 (2): 407-10.

255. Langston JW, Ballard P, Tetrud JW, Irwin I. Chronic Parkinsonism in humans due to a product of meperidine-analog synthesis. Science 1983 Feb; 219 (4587): 979-80.

256. Przedborski S, Jackson-Lewis V, Naini AB, Jakowec M, Petzinger G, Miller R, et al. The parkinsonian toxin 1-methyl-4-phenyl-1,2,3,6-tetrahydropyridine (MPTP): A technical review of its utility and safety. J Neurochem 2001 Mar; 76 (5): 1265-74.

257. Lam CS, Korzh V, Strahle U. Zebrafish embryos are susceptible to the dopaminergic neurotoxin MPTP. Eur J Neurosci 2005 Mar; 21 (6): 1758-62.

258. McKinley ET, Baranowski TC, Blavo DO, Cato C, Doan TN, Rubinstein AL. Neuroprotection of MPTP-induced toxicity in zebrafish dopaminergic neurons. Brain Res Mol Brain Res 2005 Nov; 141 (2): 128-37.

259. Sallinen V, Torkko V, Sundvik M, Reenila I, Khrustalyov D, Kaslin J, et al. MPTP and MPP^+ target specific aminergic cell populations in larval zebrafish. J Neurochem 2009 Feb; 108 (3): 719-31.

260. Ramsay RR, Krueger MJ, Youngster SK, Gluck MR, Casida JE, Singer TP. Interaction of 1-methyl-4-phenylpyridinium ion (MPP^+) and its analogs with the rotenone/piericidin binding site of NADH dehydrogenase. J Neurochem 1991 Apr; 56 (4): 1184-90.

261. Ramsay RR, Singer TP. Energy-dependent uptake of N-methyl-4-phenylpyridinium, the neurotoxic metabolite of 1-methyl-4-phenyl-1,2,3,6-tetrahydropyridine, by mitochondria. J Biol Chem 1986 Jun; 261 (17): 7585-7.

262. Cartelli D, Ronchi C, Maggioni MG, Rodighiero S, Giavini E, Cappelletti G. Microtubule dysfunction precedes transport impairment and mitochondria damage in MPP^+ -induced neurodegeneration. J Neurochem 2010 Oct; 115 (1): 247-58.

263. Sayre LM, Singh MP, Arora PK, Wang F, McPeak RJ, Hoppel CL. Inhibition of mitochondrial respiration by analogues of the dopaminergic neurotoxin 1-methyl-4-phenylpyridinium: Structural requirements for accumulation-dependent enhanced inhibitory potency on intact mitochondria. Arch Biochem Biophys 1990 Aug; 280 (2): 274-83.

264. Desai VG, Feuers RJ, Hart RW, Ali SF. MPP^+-induced neurotoxicity in mouse is age-dependent: Evidenced by the selective inhibition of complexes of electron transport. Brain Res 1996 Apr 715; (1-2): 1-8.

265. Del Zompo M, Piccardi MP, Ruiu S, Quartu M, Gessa GL, Vaccari A. Selective MPP^+ uptake into synaptic dopamine vesicles: Possible involvement in MPTP neurotoxicity. Br J Pharmacol 1993 Jun; 109 (2): 411-4.

266. Dauer W, Przedborski S. Parkinson's disease: Mechanisms and models. Neuron 2003 Sep; 39 (6): 889-909.

267. Kowall NW, Hantraye P, Brouillet E, Beal MF, McKee AC, Ferrante RJ. MPTP induces α-synuclein aggregation in the substantia nigra of baboons. Neuroreport 2000 Jan; 11 (1): 211-3.

268. Chan P, DeLanney LE, Irwin I, Langston JW, Di Monte D. Rapid ATP loss caused by 1-methyl-4-phenyl-1,2,3,6-tetrahydropyridine in mouse brain. J Neurochem 1991 Jul; 57 (1): 348-51.

269. Fabre E, Monserrat J, Herrero A, Barja G, Leret ML. Effect of MPTP on brain mitochondrial H_2O_2 and ATP production and on dopamine and DOPAC in the striatum. J Physiol Biochem 1999 Dec; 55 (4): 325-31.

270. Javitch JA, D'Amato RJ, Strittmatter SM, Snyder SH. Parkinsonism-inducing neurotoxin, *N*-methyl-4-phenyl-1,2,3,6-tetrahydropyridine: uptake of the metabolite *N*-methyl-4-phenylpyridine by dopamine neurons explains selective toxicity. Proc Natl Acad Sci USA 1985 Apr; 82 (7): 2173-7.

271. Smith LA, Jackson MJ, Al-Barghouthy G, Rose S, Kuoppamaki M, Olanow W, et al. Multiple small doses of levodopa plus entacapone produce continuous dopaminergic stimulation and reduce dyskinesia induction in MPTP-treated drug-naïve primates. Mov Disord 2005 Mar; 20 (3): 306-14.

272. Mundinano IC, Hernandez M, Dicaudo C, Ordonez C, Marcilla I, Tunon MT, et al. Reduced cholinergic olfactory centrifugal inputs in patients with neurodegenerative disorders and MPTP-treated monkeys. Acta Neuropathol 2013 Sep; 126 (3): 411-25.

273. Campello L, Esteve-Rudd J, Bru-Martínez R, Herrero MT, Fernández-Villalba E, Cuenca N, et al. Alterations in energy metabolism, neuroprotection and visual signal transduction in the retina of Parkinsonian, MPTP-treated monkeys. PLoS One 2013 Sep; 8 (9): e74439.

274. Ma KL, Gao JH, Huang ZQ, Zhang Y, Kuang DX, Jiang QF, et al. Motor Function in MPTP-Treated Tree Shrews (*Tupaia belangeri chinensis*). Neurochem Res 2013 Sep; 38 (9): 1935-40.

275. Chung YC, Kim SR, Park JY, Chung ES, Park KW, Won SY, et al. Fluoxetine prevents MPTP-induced loss of dopaminergic neurons by inhibiting microglial activation. Neuropharmacology 2011 May; 60 (6): 963-74.

276. Haque MM, Panda K, Tejero J, Aulak KS, Fadlalla MA, Mustovich AT, et al. A connecting hinge represses the activity of endothelial nitric oxide synthase. Proc Natl Acad Sci USA 2007 May; 104 (22): 9254-9.

277. Bové J, Prou D, Perier C, Przedborski S. Toxin-induced models of Parkinson's disease. NeuroRx 2005 Jul; 2 (3): 484-94.

278. Johannessen JN, Chiueh CC, Burns RS, Markey SP. Differences in the metabolism of MPTP in the rodent and primate parallel differences in sensitivity to its neurotoxic effects. Life Sci 1985 Jan; 36 (3): 219-24.

279. Lieschke GJ, Currie PD. Animal models of human disease: Zebrafish swim into view. Nat Rev Genet 2007 May; 8 (5): 353-67.

280. Zon LI, Peterson RT. *In vivo* drug discovery in the zebrafish. Nat Rev Drug Discov 2005 Jan; 4 (1): 35-44.

281. Gonzalez C. *Drosophila melanogaster*: A model and a tool to investigate malignancy and identify new therapeutics. Nat Rev Cancer 2013 Mar; 13 (3): 172-83.

282. Schild LC, Glauser DA. Dynamic switching between escape and avoidance regimes reduces *Caenorhabditis elegans* exposure to noxious heat. Nat Commun 2013 Jul; 4: 2198.

283. Nguyen M, Yang E, Neelkantan N, Mikhaylova A, Arnold R, Poudel MK, et al. Developing 'integrative' zebrafish models of behavioral and metabolic disorders. Behav Brain Res 2013 Aug; 256C: 172-87.

284. Moss JB, Koustubhan P, Greenman M, Parsons MJ, Walter I, Moss LG. Regeneration of the pancreas in adult zebrafish. Diabetes 2009 Aug; 58 (8): 1844-51.

285. Cachat J, Stewart A, Utterback E, Hart P, Gaikwad S, Wong K, et al. Three-dimensional neurophenotyping of adult zebrafish behavior. PLoS One 2011 Mar; 6 (3): e17597.

286. Burket CT, Montgomery JE, Thummel R, Kassen SC, LaFave MC, Langenau DM, et al. Generation and characterization of transgenic zebrafish lines using different ubiquitous promoters. Transgenic Res 2008 Apr; 17 (2): 265-79.

287. Thisse C, Thisse B. High-resolution in situ hybridization to whole-mount zebrafish embryos. Nat Protoc 2008 Dec; 3 (1): 59-69.

288. Yuan S, Sun Z. Microinjection of mRNA and morpholino antisense oligonucleotides in zebrafish embryos. J Vis Exp 2009 May; (27): e1113.

289. Peal DS, Peterson RT, Milan D. Small molecule screening in zebrafish. J Cardiovasc Transl Res 2010 Oct; 3 (5): 454-60.

290. Yeh JR, Munson KM, Elagib KE, Goldfarb AN, Sweetser DA, Peterson RT. Discovering chemical modifiers of oncogene-regulated hematopoietic differentiation. Nat Chem Biol 2009 Apr; 5 (4): 236-43.

291. Pappalardo A, Pitto L, Fiorillo C, Alice Donati M, Bruno C, Santorelli FM. Neuromuscular disorders in zebrafish: State of the art and future perspectives. Neuromolecular Med 2013 Jun; 15 (2): 405-19.

292. Kimmel CB, Ballard WW, Kimmel SR, Ullmann B, Schilling TF. Stages of embryonic development of the zebrafish. Dev Dyn 1995 Jul; 203 (3): 253-310.

293. Stainier DY, Fishman MC. The zebrafish as a model system to study cardiovascular development. Trends Cardiovasc Med 1994 Sep-Oct; 4 (5): 207-12.

294. Cross LM, Cook MA, Lin S, Chen JN, Rubinstein AL. Rapid analysis of angiogenesis drugs in a live fluorescent zebrafish assay. Arterioscler Thromb Vasc Biol 2003 May; 23 (5): 911-2.

295. Vogel B, Meder B, Just S, Laufer C, Berger I, Weber S, et al. *In-vivo* characterization of human dilated cardiomyopathy genes in zebrafish. Biochem Biophys Res Commun 2009 Dec; 390 (3): 516-22.
296. Arnaout R, Ferrer T, Huisken J, Spitzer K, Stainier DY, Tristani-Firouzi M, et al. Zebrafish model for human long QT syndrome. Proc Natl Acad Sci USA 2007 Jul; 104 (27): 11316-21.
297. Peterson RT, Shaw SY, Peterson TA, Milan DJ, Zhong TP, Schreiber SL, et al. Chemical suppression of a genetic mutation in a zebrafish model of aortic coarctation. Nat Biotechnol 2004 May; 22 (5): 595-9.
298. Stoletov K, Fang L, Choi SH, Hartvigsen K, Hansen LF, Hall C, et al. Vascular lipid accumulation, lipoprotein oxidation, and macrophage lipid uptake in hypercholesterolemic zebrafish. Circ Res 2009 Apr; 104 (8): 952-60.
299. Fleming A, Diekmann H, Goldsmith P. Functional characterisation of the maturation of the blood-brain barrier in larval zebrafish. PLoS One 2013 Oct; 8 (10): e77548.
300. Sager JJ, Bai Q, Burton EA. Transgenic zebrafish models of neurodegenerative diseases. Brain Struct Funct 2010 Mar; 214 (2-3): 285-302.
301. Kokel D, Bryan J, Laggner C, White R, Cheung CY, Mateus R, et al. Rapid behavior-based identification of neuroactive small molecules in the zebrafish. Nat Chem Biol 2010 Mar; 6 (3): 231-7.
302. Kimmel CB, Patterson J, Kimmel RO. The development and behavioral characteristics of the startle response in the zebra fish. Dev Psychobiol 1974 Jan; 7 (1): 47-60.
303. Friedrich RW, Jacobson GA, Zhu P. Circuit neuroscience in zebrafish. Curr Biol 2010 Apr; 20 (8): R371-81.
304. Lumsden AL, Henshall TL, Dayan S, Lardelli MT, Richards RI. Huntingtin-deficient zebrafish exhibit defects in iron utilization and development. Hum Mol Genet 2007 Aug; 16 (16): 1905-20.
305. Riera M, Burguera D, Garcia-Fernàndez J, Gonzàlez-Duarte R. CERKL knockdown causes retinal degeneration in zebrafish. PLoS One 2013 May; 8 (5): e64048.
306. Blaser RE, Rosemberg DB. Measures of anxiety in zebrafish (*Danio rerio*): Dissociation of black/white preference and novel tank test. PLoS One 2012 May; 7 (5): e36931.
307. Chapman AL, Bennett EJ, Ramesh TM, De Vos KJ, Grierson AJ. Axonal transport defects in a mitofusin 2 loss of function model of Charcot-Marie-Tooth Disease in zebrafish. PLoS One 2013 Jun; 8 (6): e67276.

308. Ramesh T, Lyon AN, Pineda RH, Wang C, Janssen PM, Canan BD, et al. A genetic model of amyotrophic lateral sclerosis in zebrafish displays phenotypic hallmarks of motoneuron disease. Dis Model Mech 2010 Sep-Oct; 3 (9-10): 652-62.
309. Newman M, Verdile G, Martins RN, Lardelli M. Zebrafish as a tool in Alzheimer's disease research. Biochim Biophys Acta 2011 Mar; 1812 (3): 346-52.
310. Anichtchik O, Diekmann H, Fleming A, Roach A, Goldsmith P, Rubinsztein DC. Loss of PINK1 function affects development and results in neurodegeneration in zebrafish. J Neurosci 2008 Aug; 28 (33): 8199-207.
311. Kim SH, Scott SA, Bennett MJ, Carson RP, Fessel J, Brown HA, et al. Multi-organ abnormalities and mTORC1 activation in zebrafish model of multiple acyl-CoA dehydrogenase deficiency. PLoS Genet 2013 Jun; 9 (6): e1003563.
312. Noble S, Ismail A, Godoy R, Xi Y, Ekker M. Zebrafish Parla- and Parlb-deficiency affects dopaminergic neuron patterning and embryonic survival. J Neurochem 2012 Jul; 122 (1): 196-207.
313. Priyadarshini M, Tuimala J, Chen YC, Panula P. A zebrafish model of PINK1 deficiency reveals key pathway dysfunction including HIF signaling. Neurobiol Dis 2013 Jun; 54: 127-38.
314. Lichtenberg M, Mansilla A, Zecchini VR, Fleming A, Rubinsztein DC. The Parkinson's disease protein LRRK2 impairs proteasome substrate clearance without affecting proteasome catalytic activity. Cell Death Dis 2011 Aug; 2: e196.
315. Moussavi Nik SH, Wilson L, Newman M, Croft K, Mori TA, Musgrave I, et al. The BACE1-PSEN-AβPP regulatory axis has an ancient role in response to low oxygen/oxidative stress. J Alzheimers Dis 2012 Feb; 28 (3): 515-30.
316. Holzschuh J, Ryu S, Aberger F, Driever W. Dopamine transporter expression distinguishes dopaminergic neurons from other catecholaminergic neurons in the developing zebrafish embryo. Mech Dev 2001 Mar; 101 (1-2): 237-43.
317. Tay TL, Ronneberger O, Ryu S, Nitschke R, Driever W. Comprehensive catecholaminergic projectome analysis reveals single-neuron integration of zebrafish ascending and descending dopaminergic systems. Nat Commun 2011 Jan; 2: 171.
318. Souza BR, Romano-Silva MA, Tropepe V. Dopamine D_2 receptor activity modulates Akt signaling and alters GABAergic neuron development and motor behavior in zebrafish larvae. J Neurosci 2011 Apr; 31 (14): 5512-25.
319. Bretaud S, Lee S, Guo S. Sensitivity of zebrafish to environmental toxins implicated in Parkinson's disease. Neurotoxicol Teratol 2004 Nov-Dec; 26 (6): 857-64.

320. Giordano S, Lee J, Darley-Usmar VM, Zhang J. Distinct effects of rotenone, 1-methyl-4-phenylpyridinium and 6-hydroxydopamine on cellular bioenergetics and cell death. PLoS One 2012 Sep; 7 (9): e44610.

321. Schmidt R, Strähle U, Scholpp S. Neurogenesis in zebrafish - from embryo to adult. Neural Dev 2013 Feb; 8: 3.

322. Theerachayanan T, Sirithunyalug B, Piyamongkol S. Antimalarial and antimycobacterial activities of dimeric naphthoquinone from *Diospyros glandulosa* and *Diospyros rhodocalyx*. CMU J Nat Sci 2007 Jul-Dec; 6 (2): 253-9.

323. Hernández-Pérez M, Rabanal RM, de la Torre MC, Rodríguez B. Analgesic, anti-inflammatory, antipyretic and haematological effects of aethiopinone, an *o*-naphthoquinone diterpenoid from *Salvia aethiopis* roots and two hemisynthetic derivatives. Planta Med 1995 Dec; 61 (6): 505-9.

324. Chakrabarty S, Roy M, Hazra B, Bhattacharya RK. Induction of apoptosis in human cancer cell lines by diospyrin, a plant-derived bisnaphthoquinonoid, and its synthetic derivatives. Cancer Lett 2002 Dec; 188 (1-2): 85-93.

325. Kuke C, Williamson EM, Roberts MF, Watt R, Hazra B, Lajubutu BA, et al. Antiinflammatory activity of binaphthoquinones from *Diospyros* species. Phytother Res 1998; 12: 155-8.

326. Subbaramaiah K, Bulic P, Lin Y, Dannenberg AJ, Pasco DS. Development and use of a gene promoter-based screen to identify novel inhibitors of cyclooxygenase-2 transcription. J Biomol Screen 2001 Apr; 6 (2): 101-10.

327. Wang JP, Raung SL, Chang LC, Kuo SC. Inhibition of hind-paw edema and cutaneous vascular plasma extravasation in mice by acetylshikonin. Eur J Pharmacol 1995 Jan; 272 (1): 87-95.

328. Han AR, Min HY, Nam JW, Lee NY, Wiryawan A, Suprapto W, et al. Identification of a new naphthalene and its derivatives from the bulb of *Eleutherine americana* with inhibitory activity on lipopolysaccharide-induced nitric oxide production. Chem Pharm Bull (Tokyo) 2008 Sep; 56 (9): 1314-6.

329. Moncada S, Palmer RM, Higgs EA. Nitric oxide: Physiology, pathophysiology, and pharmacology. Pharmacol Rev 1991 Jun; 43 (2): 109-42.

330. Sweet MJ, Hume DA. Endotoxin signal transduction in macrophages. J Leukoc Biol 1996 Jul; 60 (1): 8-26.

331. Andreakos ET, Foxwell BM, Brennan FM, Maini RN, Feldmann M. Cytokines and anti-cytokine biologicals in autoimmunity: Present and future. Cytokine Growth Factor Rev 2002 Aug-Oct; 13 (4-5): 299-313.

332. El-Omar EM, Carrington M, Chow WH, McColl KE, Bream JH, Young HA, et al. Interleukin-1 polymorphisms associated with increased risk of gastric cancer. Nature 2000 Mar; 404 (6776): 398-402.
333. Stein B, Kung Sutherland MS. IL-6 as a drug discovery target. Drug Discov Today 1998 May; 3 (5): 202-13.
334. Maeda S, Omata M. Inflammation and cancer: Role of nuclear factor-kappaB activation. Cancer Sci 2008 May; 99 (5): 836-42.
335. Laskin DL, Pendino KJ. Macrophages and inflammatory mediators in tissue injury. Annu Rev Pharmacol Toxicol 1995 Apr; 35: 655-77.
336. Alves AC, Costa MA, Paul MI. Naphthaquinones of *Diospyros batocana*. Planta Med 1983 Feb; 47 (2): 121-4.
337. Lobner D. Comparison of the LDH and MTT assays for quantifying cell death: Validity for neuronal apoptosis? J Neurosci Methods 2000 Mar; 96 (2): 147-52.
338. Sousa C, Pontes H, Carmo H, Dinis-Oliveira RJ, Valentão P, Andrade PB, et al. Water extracts of *Brassica oleracea* var. *costata* potentiate paraquat toxicity to rat hepatocytes *in vitro*. Toxicol In Vitro 2009 Sep; 23 (6): 1131-8.
339. Moreira-Gonçalves D, Henriques-Coelho T, Fonseca H, Ferreira RM, Amado F, Leite-Moreira A, et al. Moderate exercise training provides left ventricular tolerance to acute pressure overload. Am J Physiol Heart Circ Physiol 2011 Mar; 300 (3): H1044-52.
340. Adams DO, Hamilton TA. The cell biology of macrophage activation. Annu Rev Immunol 1984 Apr; 2: 283-318.
341. Nathan CF, Hibbs JB, Jr. Role of nitric oxide synthesis in macrophage antimicrobial activity. Curr Opin Immunol 1991 Feb; 3 (1): 65-70.
342. De Vera ME, Taylor BS, Wang Q, Shapiro RA, Billiar TR, Geller DA. Dexamethasone suppresses iNOS gene expression by upregulating I-κBα and inhibiting NF-κB. Am J Physiol 1997 Dec; 273 (6 Pt 1): G1290-6.
343. Sun Z, Andersson R. NF-κB activation and inhibition: A review. Shock 2002 Aug; 18 (2): 99-106.
344. Fotakis G, Timbrell JA. *In vitro* cytotoxicity assays: Comparison of LDH, neutral red, MTT and protein assay in hepatoma cell lines following exposure to cadmium chloride. Toxicol Lett 2006 Jan; 160 (2): 171-7.
345. Chia JK, Pollack M, Guelde G, Koles NL, Miller M, Evans ME. Lipopolysaccharide (LPS)-reactive monoclonal antibodies fail to inhibit LPS-induced tumor necrosis factor secretion by mouse-derived macrophages. J Infect Dis 1989 May; 159 (5): 872-80.

346. Klaus V, Hartmann T, Gambini J, Graf P, Stahl W, Hartwig A, et al. 1,4-Naphthoquinones as inducers of oxidative damage and stress signaling in HaCaT human keratinocytes. Arch Biochem Biophys 2010 Apr; 496 (2): 93-100.

347. Inbaraj JJ, Chignell CF. Cytotoxic action of juglone and plumbagin: A mechanistic study using HaCaT keratinocytes. Chem Res Toxicol 2004 Jan; 17 (1): 55-62.

348. Liu X, Chuman H. Determination of solute lipophilicity by reversed-phase high-performance liquid chromatography (RP-HPLC). J Med Invest 2005 Nov; 52 Suppl: 293-4.

349. Gryglewski RJ, Palmer RM, Moncada S. Superoxide anion is involved in the breakdown of endothelium-derived vascular relaxing factor. Nature 1986 Apr; 320 (6061): 454-6.

350. Mallozzi C, Di Stasi AM, Minetti M. Peroxynitrite modulates tyrosine-dependent signal transduction pathway of human erythrocyte band 3. FASEB J 1997 Dec; 11 (14): 1281-90.

351. Pfeiffer S, Mayer B. Lack of tyrosine nitration by peroxynitrite generated at physiological pH. J Biol Chem 1998 Oct; 273 (42): 27280-5.

352. Pfeiffer S, Schmidt K, Mayer B. Dityrosine formation outcompetes tyrosine nitration at low steady-state concentrations of peroxynitrite. Implications for tyrosine modification by nitric oxide/superoxide *in vivo*. J Biol Chem 2000 Mar; 275 (9): 6346-52.

353. Broide DH. Immunomodulation of allergic disease. Annu Rev Med 2009 Jul; 60: 279-91.

354. Holgate ST. The epidemic of allergy and asthma. Nature 1999 Nov; 402 (6760S): B2-4.

355. Chen BH, Hung MH, Chen JYF, Chang HW, Yu ML, Wan L, et al. Anti-allergic activity of grapeseed extract (GSE) on RBL-2H3 mast cells. Food Chem 2012 May; 132 (2): 968-74.

356. Tewtrakul S, Itharat A. Anti-allergic substances from the rhizomes of *Dioscorea membranacea*. Bioorg Med Chem 2006 Dec; 14 (24): 8707-11.

357. Calogiuri G, Foti C, Bonamonte D, Nettis E, Muratore L, Angelini G. Allergic reactions to henna-based temporary tattoos and their components. Immunopharmacol Immunotoxicol 2010 Dec; 32 (4): 700-4.

358. Jovanovic DL, Slavkovic-Jovanovic MR. Allergic contact dermatitis from temporary henna tattoo. J Dermatol 2009 Jan; 36 (1): 63-5.

359. Pinho BR, Sousa C, Valentao P, Andrade PB. Is nitric oxide decrease observed with naphthoquinones in LPS stimulated RAW 264.7 macrophages a beneficial property? PLoS One 2011 Aug; 6 (8): e24098.

360. Subramaniya BR, Srinivasan G, Sadullah SS, Davis N, Subhadara LB, Halagowder D, et al. Apoptosis inducing effect of plumbagin on colonic cancer cells depends on expression of COX-2. PLoS One 2011 May; 6 (4): e18695.

361. Kimata M, Inagaki N, Nagai H. Effects of luteolin and other flavonoids on IgE-mediated allergic reactions. Planta Med 2000 Feb; 66 (1): 25-9.

362. Passante E, Ehrhardt C, Sheridan H, Frankish N. RBL-2H3 cells are an imprecise model for mast cell mediator release. Inflamm Res 2009 Sep; 58 (9): 611-8.

363. Itoh T, Ohguchi K, Nakajima C, Oyama M, Iinuma M, Nozawa Y, et al. Inhibitory effects of flavonoid glycosides isolated from the peel of Japanese persimmon (*Diospyros kaki* Fuyu) on antigen-stimulated degranulation in rat basophilic leukaemia RBL-2H3 cells. Food Chemistry 2011 May; 126: 289-94.

364. Takahashi T, Ikegami-Kawai M, Okuda R, Suzuki K. A fluorimetric Morgan-Elson assay method for hyaluronidase activity. Anal Biochem 2003 Nov; 322 (2): 257-63.

365. Yingprasertchai S, Bunyasrisawat S, Ratanabanangkoon K. Hyaluronidase inhibitors (sodium cromoglycate and sodium auro-thiomalate) reduce the local tissue damage and prolong the survival time of mice injected with Naja kaouthia and Calloselasma rhodostoma venoms. Toxicon 2003 Nov; 42 (6): 635-46.

366. Akula US, Odhav B. *In vitro* 5-Lipoxygenase inhibition of polyphenolic antioxidants from undomesticated plants of South Africa. J Med Plants Res 2008 Sep; 2 (9): 207-12.

367. Malterud KE, Rydland KM. Inhibitors of 15-lipoxygenase from orange peel. J Agric Food Chem 2000 Nov; 48 (11): 5576-80.

368. Huang FH, Zhang XY, Zhang LY, Li Q, Ni B, Zheng XL, et al. Mast cell degranulation induced by chlorogenic acid. Acta Pharmacol Sin 2010 Jul; 31 (7): 849-54.

369. Hsu MF, Chang LC, Huang LJ, Kuo SC, Lee HY, Lu MC, et al. The influence of acetylshikonin, a natural naphthoquinone, on the production of leukotriene B_4 and thromboxane A_2 in rat neutrophils. Eur J Pharmacol 2009 Apr; 607 (1-3): 234-43.

370. Böttjer J, Amon U, Wolff HH. Functional comparison of different histamine-containing Ige-receptor positive cells. Agents Actions 1994 Jun; 41: C28-C9.

371. Demo SD, Masuda E, Rossi AB, Throndset BT, Gerard AL, Chan EH, et al. Quantitative measurement of mast cell degranulation using a novel flow cytometric annexin-V binding assay. Cytometry 1999 Aug; 36 (4): 340-8.

372. Takano-Ohmuro H, Yoshida LS, Yuda Y, Morioka K, Kitani S. Shikonin inhibits IgE-mediated histamine release by human basophils and Syk kinase activity. Inflamm Res 2008 Oct; 57 (10): 484-8.

373. Sarkhel S, Desiraju GR. N-H...O, O-H...O, and C-H...O hydrogen bonds in protein-ligand complexes: Strong and weak interactions in molecular recognition. Proteins 2004 Feb 54 (2): 247-59.

374. Fujitani N, Sakaki S, Yamaguchi Y, Takenaka H. Inhibitory effects of microalgae on the activation of hyaluronidase. J Appl Phycol 2001 Dec; 13 (6): 489-92.

375. Werz O. 5-lipoxygenase: Cellular biology and molecular pharmacology. Curr Drug Targets Inflamm Allergy 2002 Mar; 1 (1): 23-44.

376. Westcott JY, Wenzel SE, Dreskin SC. Arachidonate-induced eicosanoid synthesis in RBL-2H3 cells: Stimulation with antigen or A23187 induces prolonged activation of 5-lipoxygenase. Biochim Biophys Acta 1996 Sep 1303 (1): 74-81.

377. Prigge ST, Boyington JC, Gaffney BJ, Amzel LM. Structure conservation in lipoxygenases: Structural analysis of soybean lipoxygenase-1 and modeling of human lipoxygenases. Proteins 1996 Mar; 24 (3): 275-91.

378. Criddle DN, Gillies S, Baumgartner-Wilson HK, Jaffar M, Chinje EC, Passmore S, et al. Menadione-induced reactive oxygen species generation via redox cycling promotes apoptosis of murine pancreatic acinar cells. J Biol Chem 2006 Dec; 281 (52): 40485-92.

379. Burnett BP, Bitto A, Altavilla D, Squadrito F, Levy RM, Pillai L. Flavocoxid inhibits phospholipase A2, peroxidase moieties of the cyclooxygenases (COX), and 5-lipoxygenase, modifies COX-2 gene expression, and acts as an antioxidant. Mediators Inflamm 2011 Mar; 2011: 385780.

380. Barchowsky A, Tabrizi K, Kent RS, Whorton AR. Inhibition of prostaglandin synthesis after metabolism of menadione by cultured porcine endothelial cells. J Clin Invest 1989 Apr; 83 (4): 1153-9.

381. Oliveira JM. Nature and cause of mitochondrial dysfunction in Huntington's disease: Focusing on huntingtin and the striatum. J Neurochem 2010 Jul; 114 (1): 1-12.

382. Stewart JB, Freyer C, Elson JL, Wredenberg A, Cansu Z, Trifunovic A, et al. Strong purifying selection in transmission of mammalian mitochondrial DNA. PLoS Biol 2008 Jan; 6 (1): e10.

383. Ingham PW. The power of the zebrafish for disease analysis. Hum Mol Genet 2009 Apr; 18 (R1): R107-12.

384. Broughton RE, Milam JE, Roe BA. The complete sequence of the zebrafish (*Danio rerio*) mitochondrial genome and evolutionary patterns in vertebrate mitochondrial DNA. Genome Res 2001 Nov; 11 (11): 1958-67.

385. Vettori A, Bergamin G, Moro E, Vazza G, Polo G, Tiso N, et al. Developmental defects and neuromuscular alterations due to mitofusin 2 gene (MFN2) silencing in

zebrafish: A new model for Charcot-Marie-Tooth type 2A neuropathy. Neuromuscul Disord 2011 Jan; 21 (1): 58-67.

386. Baden KN, Murray J, Capaldi RA, Guillemin K. Early developmental pathology due to cytochrome *c* oxidase deficiency is revealed by a new zebrafish model. J Biol Chem 2007 Nov; 282 (48): 34839-49.
387. Pei W, Kratz LE, Bernardini I, Sood R, Yokogawa T, Dorward H, et al. A model of Costeff Syndrome reveals metabolic and protective functions of mitochondrial OPA3. Development 2010 Aug; 137 (15): 2587-96.
388. Song Y, Selak MA, Watson CT, Coutts C, Scherer PC, Panzer JA, et al. Mechanisms underlying metabolic and neural defects in zebrafish and human multiple acyl-CoA dehydrogenase deficiency (MADD). PLoS One 2009 Dec; 4 (12): e8329.
389. Flinn L, Bretaud S, Lo C, Ingham PW, Bandmann O. Zebrafish as a new animal model for movement disorders. J Neurochem 2008 Sep; 106 (5): 1991-7.
390. Artuso L, Romano A, Verri T, Domenichini A, Argenton F, Santorelli FM, et al. Mitochondrial DNA metabolism in early development of zebrafish (*Danio rerio*). Biochim Biophys Acta 2012 Jul; 1817 (7): 1002-11.
391. Stackley KD, Beeson CC, Rahn JJ, Chan SS. Bioenergetic profiling of zebrafish embryonic development. PLoS One 2011 Sep; 6 (9): e25652.
392. Azzolin L, Basso E, Argenton F, Bernardi P. Mitochondrial Ca^{2+} transport and permeability transition in zebrafish (*Danio rerio*). Biochim Biophys Acta 2010 Nov; 1797 (11): 1775-9.
393. Mather MW, Henry KW, Vaidya AB. Mitochondrial drug targets in apicomplexan parasites. Curr Drug Targets 2007 Jan; 8 (1): 49-60.
394. Soares J, Coimbra AM, Reis-Henriques MA, Monteiro NM, Vieira MN, Oliveira JM, et al. Disruption of zebrafish (*Danio rerio*) embryonic development after full life-cycle parental exposure to low levels of ethinylestradiol. Aquat Toxicol 2009 Dec; 95 (4): 330-8.
395. Gurvich N, Berman MG, Wittner BS, Gentleman RC, Klein PS, Green JB. Association of valproate-induced teratogenesis with histone deacetylase inhibition *in vivo*. FASEB J 2005 Jul; 19 (9): 1166-8.
396. Earley FG, Patel SD, Ragan I, Attardi G. Photolabelling of a mitochondrially encoded subunit of NADH dehydrogenase with [^{3}H]dihydrorotenone. FEBS Lett 1987 Jul; 219 (1): 108-12.
397. Huang LS, Sun G, Cobessi D, Wang AC, Shen JT, Tung EY, et al. 3-Nitropropionic acid is a suicide inhibitor of mitochondrial respiration that, upon oxidation by

complex II, forms a covalent adduct with a catalytic base arginine in the active site of the enzyme. J Biol Chem 2006 Mar; 281 (9): 5965-72.

398. Hughes WT, Gray VL, Gutteridge WE, Latter VS, Pudney M. Efficacy of a hydroxynaphthoquinone, 566C80, in experimental *Pneumocystis carinii* pneumonitis. Antimicrob Agents Chemother 1990 Feb; 34 (2): 225-8.
399. Fry M, Pudney M. Site of action of the antimalarial hydroxynaphthoquinone, 2-[trans-4-(4'-chlorophenyl) cyclohexyl]-3-hydroxy-1,4-naphthoquinone (566C80). Biochem Pharmacol 1992 Apr; 43 (7): 1545-53.
400. Chen AT, Zon LI. Zebrafish blood stem cells. J Cell Biochem 2009 Sep; 108 (1): 35-42.
401. Kishi T, Takahashi T, Mizobuchi S, Mori K, Okamoto T. Effect of dicumarol, a NAD®H: quinone acceptor oxidoreductase 1 (DT-diaphorase) inhibitor on ubiquinone redox cycling in cultured rat hepatocytes. Free Radic Res 2002 Apr; 36 (4): 413-9.
402. Li LS, Bey EA, Dong Y, Meng J, Patra B, Yan J, et al. Modulating endogenous NQO1 levels identifies key regulatory mechanisms of action of β-lapachone for pancreatic cancer therapy. Clin Cancer Res 2011 Jan; 17 (2): 275-85.
403. Flinn L, Mortiboys H, Volkmann K, Koster RW, Ingham PW, Bandmann O. Complex I deficiency and dopaminergic neuronal cell loss in parkin-deficient zebrafish (*Danio rerio*). Brain 2009 Jun; 132 (Pt 6): 1613-23.
404. Choi WS, Palmiter RD, Xia Z. Loss of mitochondrial complex I activity potentiates dopamine neuron death induced by microtubule dysfunction in a Parkinson's disease model. J Cell Biol 2011 Mar; 192 (5): 873-82.
405. Porter DJ, Bright HJ. 3-Carbanionic substrate analogues bind very tightly to fumarase and aspartase. J Biol Chem 1980 May; 255 (10): 4772-80.
406. Choi TY, Sohn KC, Kim JH, Kim SM, Kim CH, Hwang JS, et al. Impact of NAD(P)H:quinone oxidoreductase-1 on pigmentation. J Invest Dermatol 2010 Mar; 130 (3): 784-92.
407. Preusch PC. Lapachol inhibition of DT-diaphorase (NAD(P)H:quinone dehydrogenase). Biochem Biophys Res Commun 1986 Jun; 137 (2): 781-7.
408. Preusch PC, Siegel D, Gibson NW, Ross D. A note on the inhibition of DT-diaphorase by dicoumarol. Free Radic Biol Med 1991; 11 (1): 77-80.
409. Knecht W, Henseling J, Loffler M. Kinetics of inhibition of human and rat dihydroorotate dehydrogenase by atovaquone, lawsone derivatives, brequinar sodium and polyporic acid. Chem Biol Interact 2000 Jan; 124 (1): 61-76.

410. González-Aragón D, Ariza J, Villalba JM. Dicoumarol impairs mitochondrial electron transport and pyrimidine biosynthesis in human myeloid leukemia HL-60 cells. Biochem Pharmacol 2007 Feb; 73 (3): 427-39.

411. Forsman U, Sjoberg M, Turunen M, Sindelar PJ. 4-Nitrobenzoate inhibits coenzyme Q biosynthesis in mammalian cell cultures. Nat Chem Biol 2010 Jul; 6 (7): 515-7.

412. Johnson-Cadwell LI, Jekabsons MB, Wang A, Polster BM, Nicholls DG. 'Mild Uncoupling' does not decrease mitochondrial superoxide levels in cultured cerebellar granule neurons but decreases spare respiratory capacity and increases toxicity to glutamate and oxidative stress. J Neurochem 2007 Jun; 101 (6): 1619-31.

413. Roberts-Harewood M. Inherited haemolytic anaemias. Medicine 2009 Mar; 37 (3): 143-48.

414. Dong CK, Patel V, Yang JC, Dvorin JD, Duraisingh MT, Clardy J, et al. Type II NADH dehydrogenase of the respiratory chain of *Plasmodium falciparum* and its inhibitors. Bioorg Med Chem Lett 2009 Feb; 19 (3): 972-5.

415. Ye H, Rouault TA. Erythropoiesis and iron sulfur cluster biogenesis. Adv Hematol 2010 Aug; 2010.

416. Kessl JJ, Lange BB, Merbitz-Zahradnik T, Zwicker K, Hill P, Meunier B, et al. Molecular basis for atovaquone binding to the cytochrome bc_1 complex. J Biol Chem 2003 Aug; 278 (33): 31312-8.

417. Krungkrai J. The multiple roles of the mitochondrion of the malarial parasite. Parasitology 2004 Nov; 129 (Pt 5): 511-24.

418. Brière JJ, Schlemmer D, Chretien D, Rustin P. Quinone analogues regulate mitochondrial substrate competitive oxidation. Biochem Biophys Res Commun 2004 Apr; 316 (4): 1138-42.

419. Chandel NS, McClintock DS, Feliciano CE, Wood TM, Melendez JA, Rodriguez AM, et al. Reactive oxygen species generated at mitochondrial complex III stabilize hypoxia-inducible factor-1α during hypoxia: A mechanism of O_2 sensing. J Biol Chem 2000 Aug; 275 (33): 25130-8.

420. Palming J, Sjoholm K, Jernas M, Lystig TC, Gummesson A, Romeo S, et al. The expression of NAD(P)H:quinone oxidoreductase 1 is high in human adipose tissue, reduced by weight loss, and correlates with adiposity, insulin sensitivity, and markers of liver dysfunction. J Clin Endocrinol Metab 2007 Jun; 92 (6): 2346-52.

421. Zhu H, Li Y. NAD(P)H: quinone oxidoreductase 1 and its potential protective role in cardiovascular diseases and related conditions. Cardiovasc Toxicol 2012 Mar; 12 (1): 39-45.

422. Mendelsohn BA, Kassebaum BL, Gitlin JD. The zebrafish embryo as a dynamic model of anoxia tolerance. Dev Dyn 2008 Jul; 237 (7): 1780-8.

423. Niethammer P, Grabher C, Look AT, Mitchison TJ. A tissue-scale gradient of hydrogen peroxide mediates rapid wound detection in zebrafish. Nature 2009 Jun; 459 (7249): 996-9.

424. Moreira PI, Zhu X, Wang X, Lee HG, Nunomura A, Petersen RB, et al. Mitochondria: A therapeutic target in neurodegeneration. Biochim Biophys Acta 2010 Jan; 1802 (1): 212-20.

425. Guedes-Dias P, Oliveira JM. Lysine deacetylases and mitochondrial dynamics in neurodegeneration. Biochim Biophys Acta 2013 Aug; 1832 (8): 1345-59.

426. Wang Y, Hekimi S. Mitochondrial respiration without ubiquinone biosynthesis. Hum Mol Genet 2013 Dec 1; 22 (23): 4768-83.

427. Gutzmann H, Kuhl KP, Hadler D, Rapp MA. Safety and efficacy of idebenone versus tacrine in patients with Alzheimer's disease: Results of a randomized, double-blind, parallel-group multicenter study. Pharmacopsychiatry 2002 Jan; 35 (1): 12-8.

428. Gerhardt E, Gräber S, Szegő EM, Moisoi N, Martins LM, Outeiro TF, et al. Idebenone and resveratrol extend lifespan and improve motor function of HtrA2 knockout mice. PLoS One 2011 Dec; 6 (12): e28855.

429. Hasan MR, Kim JH, Kim YJ, Kwon KJ, Shin CY, Kim HY, et al. Effect of HDAC inhibitors on neuroprotection and neurite outgrowth in primary rat cortical neurons following ischemic insult. Neurochem Res 2013 Sep; 38 (9): 1921-34.

430. Zhang ZZ, Gong YY, Shi YH, Zhang W, Qin XH, Wu XW. Valproate promotes survival of retinal ganglion cells in a rat model of optic nerve crush. Neuroscience 2012 Nov; 224: 282-93.

431. Yoo YE, Ko CP. Treatment with trichostatin A initiated after disease onset delays disease progression and increases survival in a mouse model of amyotrophic lateral sclerosis. Exp Neurol 2011 Sep; 231 (1): 147-59.

432. St Laurent R, O'Brien LM, Ahmad ST. Sodium butyrate improves locomotor impairment and early mortality in a rotenone-induced *Drosophila* model of Parkinson's disease. Neuroscience 2013 Aug; 246: 382-90.

433. Jia H, Kast RJ, Steffan JS, Thomas EA. Selective histone deacetylase (HDAC) inhibition imparts beneficial effects in Huntington's disease mice: Implications for the ubiquitin-proteasomal and autophagy systems. Hum Mol Genet 2012 Dec; 21 (24): 5280-93.

434. Govindarajan N, Rao P, Burkhardt S, Sananbenesi F, Schluter OM, Bradke F, et al. Reducing HDAC6 ameliorates cognitive deficits in a mouse model for Alzheimer's disease. EMBO Mol Med 2013 Jan; 5 (1): 52-63.

435. Wen L, Wei W, Gu W, Huang P, Ren X, Zhang Z, et al. Visualization of monoaminergic neurons and neurotoxicity of MPTP in live transgenic zebrafish. Dev Biol 2008 Feb; 314 (1): 84-92.

436. Cleren C, Yang L, Lorenzo B, Calingasan NY, Schomer A, Sireci A, et al. Therapeutic effects of coenzyme Q10 (CoQ10) and reduced CoQ10 in the MPTP model of Parkinsonism. J Neurochem 2008 Mar; 104 (6): 1613-21.

437. Ghosh A, Chandran K, Kalivendi SV, Joseph J, Antholine WE, Hillard CJ, et al. Neuroprotection by a mitochondria-targeted drug in a Parkinson's disease model. Free Radic Biol Med 2010 Dec; 49 (11): 1674-84.

438. Wu JY, Niu FN, Huang R, Xu Y. Enhancement of glutamate uptake in 1-methyl-4-phenylpyridinium-treated astrocytes by trichostatin A. Neuroreport 2008 Aug; 19 (12): 1209-12.

439. Butler KV, Kalin J, Brochier C, Vistoli G, Langley B, Kozikowski AP. Rational design and simple chemistry yield a superior, neuroprotective HDAC6 inhibitor, tubastatin A. J Am Chem Soc 2010 Aug; 132 (31): 10842-6.

440. Tatamiya T, Saito A, Sugawara T, Nakanishi O. Isozyme-selective activity of the HDAC inhibitor MS-275. Proc Amer Assoc Cancer Res 2004; 45.

441. Napper AD, Hixon J, McDonagh T, Keavey K, Pons JF, Barker J, et al. Discovery of indoles as potent and selective inhibitors of the deacetylase SIRT1. J Med Chem 2005 Dec; 48 (25): 8045-54.

442. Outeiro TF, Kontopoulos E, Altmann SM, Kufareva I, Strathearn KE, Amore AM, et al. Sirtuin 2 inhibitors rescue alpha-synuclein-mediated toxicity in models of Parkinson's disease. Science 2007 Jul; 317 (5837): 516-9.

443. Pinho BR, Santos MM, Fonseca-Silva A, Valentao P, Andrade PB, Oliveira JM. How mitochondrial dysfunction affects zebrafish development and cardiovascular function: an in vivo model for testing mitochondria-targeted drugs. Br J Pharmacol 2013 Jul; 169 (5): 1072-90.

444. Sbalzarini IF, Koumoutsakos P. Feature point tracking and trajectory analysis for video imaging in cell biology. J Struct Biol 2005 Aug; 151 (2): 182-95.

445. Bradford MM. A rapid and sensitive method for the quantitation of microgram quantities of protein utilizing the principle of protein-dye binding. Anal Biochem 1976 May; 72: 248-54.

446. Pereira CV, Oliveira PJ, Will Y, Nadanaciva S. Mitochondrial bioenergetics and drug-induced toxicity in a panel of mouse embryonic fibroblasts with mitochondrial

DNA single nucleotide polymorphisms. Toxicol Appl Pharmacol 2012 Oct; 264 (2): 167-81.

447. Moreira AC, Silva AM, Santos MS, Sardao VA. Resveratrol affects differently rat liver and brain mitochondrial bioenergetics and oxidative stress *in vitro*: investigation of the role of gender. Food Chem Toxicol 2013 Mar; 53: 18-26.
448. McCurley AT, Callard GV. Characterization of housekeeping genes in zebrafish: male-female differences and effects of tissue type, developmental stage and chemical treatment. BMC Mol Biol 2008 Nov; 9: 102.
449. Potente M, Ghaeni L, Baldessari D, Mostoslavsky R, Rossig L, Dequiedt F, et al. SIRT1 controls endothelial angiogenic functions during vascular growth. Genes Dev 2007 Oct 15; 21 (20): 2644-58.
450. Pereira TC, Rico EP, Rosemberg DB, Schirmer H, Dias RD, Souto AA, et al. Zebrafish as a model organism to evaluate drugs potentially able to modulate sirtuin expression. Zebrafish 2011 Mar; 8 (1): 9-16.
451. Liu C, Deng J, Yu L, Ramesh M, Zhou B. Endocrine disruption and reproductive impairment in zebrafish by exposure to 8:2 fluorotelomer alcohol. Aquat Toxicol 2010 Jan; 96 (1): 70-6.
452. Livak KJ, Schmittgen TD. Analysis of relative gene expression data using real-time quantitative PCR and the $2^{-\Delta\Delta CT}$ method. Methods 2001 Dec; 25 (4): 402-8.
453. Quintas C, Fraga S, Gonçalves J, Queiróz G. P2Y receptors on astrocytes and microglia mediate opposite effects in astroglial proliferation. Purinergic Signal 2011 Jun; 7 (2): 251-63.
454. Kawaguchi Y, Kovacs JJ, McLaurin A, Vance JM, Ito A, Yao TP. The deacetylase HDAC6 regulates aggresome formation and cell viability in response to misfolded protein stress. Cell 2003 Dec; 115 (6): 727-38.
455. Bertos NR, Gilquin B, Chan GK, Yen TJ, Khochbin S, Yang XJ. Role of the tetradecapeptide repeat domain of human histone deacetylase 6 in cytoplasmic retention. J Biol Chem 2004 Nov; 279 (46): 48246-54.
456. Owens KN, Cunningham DE, MacDonald G, Rubel EW, Raible DW, Pujol R. Ultrastructural analysis of aminoglycoside-induced hair cell death in the zebrafish lateral line reveals an early mitochondrial response. J Comp Neurol 2007 Jun; 502 (4): 522-43.
457. Kazantsev AG, Thompson LM. Therapeutic application of histone deacetylase inhibitors for central nervous system disorders. Nat Rev Drug Discov 2008 Oct; 7 (10): 854-68.

458. Li G, Jiang H, Chang M, Xie H, Hu L. HDAC6 α-tubulin deacetylase: A potential therapeutic target in neurodegenerative diseases. J Neurol Sci 2011 May; 304 (1-2): 1-8.

459. Yang XJ, Seto E. The Rpd3/Hda1 family of lysine deacetylases: From bacteria and yeast to mice and men. Nat Rev Mol Cell Biol 2008 Mar; 9 (3): 206-18.

460. Fornerod M, Ohno M, Yoshida M, Mattaj IW. CRM1 is an export receptor for leucine-rich nuclear export signals. Cell 1997 Sep; 90 (6): 1051-60.

461. Verdel A, Curtet S, Brocard MP, Rousseaux S, Lemercier C, Yoshida M, et al. Active maintenance of mHDA2/mHDAC6 histone-deacetylase in the cytoplasm. Curr Biol 2000 Jun; 10 (12): 747-9.

462. Barlow AL, van Drunen CM, Johnson CA, Tweedie S, Bird A, Turner BM. dSIR2 and dHDAC6: two novel, inhibitor-resistant deacetylases in *Drosophila melanogaster*. Exp Cell Res 2001 Apr; 265 (1): 90-103.

463. Liu Y, Peng L, Seto E, Huang S, Qiu Y. Modulation of histone deacetylase 6 (HDAC6) nuclear import and tubulin deacetylase activity through acetylation. J Biol Chem 2012 Aug; 287 (34): 29168-74.

464. Jiang Q, Ren Y, Feng J. Direct binding with histone deacetylase 6 mediates the reversible recruitment of parkin to the centrosome. J Neurosci 2008 Nov; 28 (48): 12993-3002.

465. Kaluza D, Kroll J, Gesierich S, Yao TP, Boon RA, Hergenreider E, et al. Class IIb HDAC6 regulates endothelial cell migration and angiogenesis by deacetylation of cortactin. EMBO J 2011 Oct; 30 (20): 4142-56.

466. Taplick J, Kurtev V, Kroboth K, Posch M, Lechner T, Seiser C. Homo-oligomerisation and nuclear localisation of mouse histone deacetylase 1. J Mol Biol 2001 Apr; 308 (1): 27-38.

467. Harrison MR, Georgiou AS, Spaink HP, Cunliffe VT. The epigenetic regulator Histone Deacetylase 1 promotes transcription of a core neurogenic programme in zebrafish embryos. BMC Genomics 2011 Jan; 12: 24.

468. Zhou W, Liang IC, Yee NS. Histone deacetylase 1 is required for exocrine pancreatic epithelial proliferation in development and cancer. Cancer Biol Ther 2011 Apr; 11 (7): 659-70.

469. Pillai R, Coverdale LE, Dubey G, Martin CC. Histone deacetylase 1 (HDAC-1) required for the normal formation of craniofacial cartilage and pectoral fins of the zebrafish. Dev Dyn 2004 Nov; 231 (3): 647-54.

470. Stadler JA, Shkumatava A, Norton WH, Rau MJ, Geisler R, Fischer S, et al. Histone deacetylase 1 is required for cell cycle exit and differentiation in the zebrafish retina. Dev Dyn 2005 Jul; 233 (3): 883-9.

471. Ignatius MS, Moose HE, El-Hodiri HM, Henion PD. colgate/hdac1 Repression of foxd3 expression is required to permit mitfa-dependent melanogenesis. Dev Biol 2008 Jan 15; 313 (2): 568-83.

472. Burns CE, Galloway JL, Smith AC, Keefe MD, Cashman TJ, Paik EJ, et al. A genetic screen in zebrafish defines a hierarchical network of pathways required for hematopoietic stem cell emergence. Blood 2009 Jun; 113 (23): 5776-82.

473. Anichtchik O, Sallinen V, Peitsaro N, Panula P. Distinct structure and activity of monoamine oxidase in the brain of zebrafish (*Danio rerio*). J Comp Neurol 2006 Oct; 498 (5): 593-610.

474. Jankovic J. Parkinson's disease: clinical features and diagnosis. J Neurol Neurosurg Psychiatry 2008 Apr; 79 (4): 368-76.

475. Brustein E, Saint-Amant L, Buss RR, Chong M, McDearmid JR, Drapeau P. Steps during the development of the zebrafish locomotor network. J Physiol Paris 2003 Jan; 97 (1): 77-86.

476. Zhang Q, Wu J, Wu R, Ma J, Du G, Jiao R, et al. DJ-1 promotes the proteasomal degradation of Fis1: Implications of DJ-1 in neuronal protection. Biochem J 2012 Oct; 447 (2): 261-9.

477. Lim L, Jackson-Lewis V, Wong LC, Shui GH, Goh AX, Kesavapany S, et al. Lanosterol induces mitochondrial uncoupling and protects dopaminergic neurons from cell death in a model for Parkinson's disease. Cell Death Differ 2012 Mar; 19 (3): 416-27.

478. Lee JS, Yoon YG, Yoo SH, Jeong NY, Jeong SH, Lee SY, et al. Histone deacetylase inhibitors induce mitochondrial elongation. J Cell Physiol 2012 Jul; 227 (7): 2856-69.

479. Kim JY, Shen S, Dietz K, He Y, Howell O, Reynolds R, et al. HDAC1 nuclear export induced by pathological conditions is essential for the onset of axonal damage. Nat Neurosci 2010 Feb; 13 (2): 180-9.

480. Kim-Han JS, Antenor-Dorsey JA, O'Malley KL. The parkinsonian mimetic, MPP^+, specifically impairs mitochondrial transport in dopamine axons. J Neurosci 2011 May; 31 (19): 7212-21.

481. Gould E. How widespread is adult neurogenesis in mammals? Nat Rev Neurosci 2007 Jun; 8 (6): 481-8.

482. Collazo A, Fraser SE, Mabee PM. A dual embryonic origin for vertebrate mechanoreceptors. Science 1994 Apr; 264 (5157): 426-30.

483. Faucher K, Fichet D, Miramand P, Lagardère JP. Impact of acute cadmium exposure on the trunk lateral line neuromasts and consequences on the "C-start"

response behaviour of the sea bass (*Dicentrarchus labrax* L.; Teleostei, Moronidae). Aquat Toxicol 2006 Mar; 76 (3-4): 278-94.

484. Chinta SJ, Andersen JK. Dopaminergic neurons. Int J Biochem Cell Biol 2005 May; 37 (5): 942-6.
485. Liu K, Shi N, Sun Y, Zhang T, Sun X. Therapeutic effects of rapamycin on MPTP-induced Parkinsonism in mice. Neurochem Res 2013 Jan; 38 (1): 201-7.
486. Poltl D, Schildknecht S, Karreman C, Leist M. Uncoupling of ATP-depletion and cell death in human dopaminergic neurons. Neurotoxicology 2012 Aug; 33 (4): 769-79.
487. Galmozzi A, Mitro N, Ferrari A, Gers E, Gilardi F, Godio C, et al. Inhibition of class I histone deacetylases unveils a mitochondrial signature and enhances oxidative metabolism in skeletal muscle and adipose tissue. Diabetes 2013 Mar; 62 (3): 732-42.
488. Horvath TL, Erion DM, Elsworth JD, Roth RH, Shulman GI, Andrews ZB. GPA protects the nigrostriatal dopamine system by enhancing mitochondrial function. Neurobiol Dis 2011 Jul; 43 (1): 152-62.
489. Thomas RR, Khan SM, Portell FR, Smigrodzki RM, Bennett JP, Jr. Recombinant human mitochondrial transcription factor A stimulates mitochondrial biogenesis and ATP synthesis, improves motor function after MPTP, reduces oxidative stress and increases survival after endotoxin. Mitochondrion 2011 Jan; 11 (1): 108-18.
490. Kidd SK, Schneider JS. Protective effects of valproic acid on the nigrostriatal dopamine system in a 1-methyl-4-phenyl-1,2,3,6-tetrahydropyridine mouse model of Parkinson's disease. Neuroscience 2011 Oct; 194: 189-94.
491. Gardian G, Yang L, Cleren C, Calingasan NY, Klivenyi P, Beal MF. Neuroprotective effects of phenylbutyrate against MPTP neurotoxicity. Neuromolecular Med 2004; 5 (3): 235-41.
492. Wang Y, Wang X, Liu L, Wang X. HDAC inhibitor trichostatin A-inhibited survival of dopaminergic neuronal cells. Neurosci Lett 2009 Dec; 467 (3): 212-6.
493. Song C, Kanthasamy A, Jin H, Anantharam V, Kanthasamy AG. Paraquat induces epigenetic changes by promoting histone acetylation in cell culture models of dopaminergic degeneration. Neurotoxicology 2011 Oct; 32 (5): 586-95.
494. Nicholas AP, Lubin FD, Hallett PJ, Vattem P, Ravenscroft P, Bezard E, et al. Striatal histone modifications in models of levodopa-induced dyskinesia. J Neurochem 2008 Jul; 106 (1): 486-94.
495. Cartelli D, Casagrande F, Busceti CL, Bucci D, Molinaro G, Traficante A, et al. Microtubule alterations occur early in experimental parkinsonism and the microtubule stabilizer epothilone D is neuroprotective. Sci Rep 2013; 3: 1837.

496. Desai VG, Feuers RJ, Hart RW, Ali SF. MPP^+-induced neurotoxicity in mouse is age-dependent: evidenced by the selective inhibition of complexes of electron transport. Brain Res 1996 Apr; 715 (1-2): 1-8.

497. Baltan S, Murphy SP, Danilov CA, Bachleda A, Morrison RS. Histone deacetylase inhibitors preserve white matter structure and function during ischemia by conserving ATP and reducing excitotoxicity. J Neurosci 2011 Mar ; 31 (11): 3990-9.

498. Öllinger K, Brunmark A. Effect of hydroxy substituent position on 1,4-naphthoquinone toxicity to rat hepatocytes. J Biol Chem 1991 Nov; 266 (32): 21496-503.

499. Kumar B, Kumar A, Pandey BN, Mishra KP, Hazra B. Role of mitochondrial oxidative stress in the apoptosis induced by diospyrin diethylether in human breast carcinoma (MCF-7) cells. Mol Cell Biochem 2009 Jan; 320 (1-2): 185-95.

500. Sun J, McKallip RJ. Plumbagin treatment leads to apoptosis in human K562 leukemia cells through increased ROS and elevated TRAIL receptor expression. Leuk Res 2011 Oct; 35 (10): 1402-8.

501. Beckman JS, Koppenol WH. Nitric oxide, superoxide, and peroxynitrite: The good, the bad, and ugly. Am J Physiol 1996 Nov; 271 (5 Pt 1): C1424-37.

502. Coleman JW. Nitric oxide in immunity and inflammation. Int Immunopharmacol 2001 Aug; 1 (8): 1397-406.

503. Coleman JW. Nitric oxide: A regulator of mast cell activation and mast cell-mediated inflammation. Clin Exp Immunol 2002 Jul; 129 (1): 4-10.

504. Sarlus H, Hoglund CO, Karshikoff B, Wang X, Lekander M, Schultzberg M, et al. Allergy influences the inflammatory status of the brain and enhances tau-phosphorylation. J Cell Mol Med 2012 Oct; 16 (10): 2401-12.

505. Ather JL, Hodgkins SR, Janssen-Heininger YM, Poynter ME. Airway epithelial NF-κB activation promotes allergic sensitization to an innocuous inhaled antigen. Am J Respir Cell Mol Biol 2011 May; 44 (5): 631-8.

506. Stacey MA, Sun G, Vassalli G, Marini M, Bellini A, Mattoli S. The allergen Der p1 induces NF-κB activation through interference with IκB α function in asthmatic bronchial epithelial cells. Biochem Biophys Res Commun 1997 Jul; 236 (2): 522-6.

507. Schletter J, Heine H, Ulmer AJ, Rietschel ET. Molecular mechanisms of endotoxin activity. Arch Microbiol 1995 Dec; 164 (6): 383-9.

508. Akira S, Hirano T, Taga T, Kishimoto T. Biology of multifunctional cytokines: IL 6 and related molecules (IL 1 and TNF). FASEB J 1990 Aug; 4 (11): 2860-7.

509. Bradley JR. TNF-mediated inflammatory disease. J Pathol 2008 Jan; 214 (2): 149-60.

510. Choi JP, Kim YS, Kim OY, Kim YM, Jeon SG, Roh TY, et al. TNF-alpha is a key mediator in the development of Th2 cell response to inhaled allergens induced by a viral PAMP double-stranded RNA. Allergy 2012 Sep; 67 (9): 1138-48.

511. Casale TB, Costa JJ, Galli SJ. TNF alpha is important in human lung allergic reactions. Am J Respir Cell Mol Biol 1996 Jul; 15 (1): 35-44.

512. Mo JH, Kang EK, Quan SH, Rhee CS, Lee CH, Kim DY. Anti-tumor necrosis factor-alpha treatment reduces allergic responses in an allergic rhinitis mouse model. Allergy 2011 Feb; 66 (2): 279-86.

513. Ataie-Kachoie P, Pourgholami MH, Morris DL. Inhibition of the IL-6 signaling pathway: A strategy to combat chronic inflammatory diseases and cancer. Cytokine Growth Factor Rev 2013 Apr; 24 (2): 163-73.

514. Neveu WA, Allard JL, Raymond DM, Bourassa LM, Burns SM, Bunn JY, et al. Elevation of IL-6 in the allergic asthmatic airway is independent of inflammation but associates with loss of central airway function. Respir Res 2010 Mar; 11: 28.

515. Lee CE, Neuland ME, Teaford HG, Villacis BF, Dixon PS, Valtier S, et al. Interleukin-6 is released in the cutaneous response to allergen challenge in atopic individuals. J Allergy Clin Immunol 1992 May; 89 (5): 1010-20.

516. Rådmark O, Werz O, Steinhilber D, Samuelsson B. 5-Lipoxygenase: Regulation of expression and enzyme activity. Trends Biochem Sci 2007 Jul; 32 (7): 332-41.

517. Bladen CL, Kozlowski DJ, Dynan WS. Effects of low-dose ionizing radiation and menadione, an inducer of oxidative stress, alone and in combination in a vertebrate embryo model. Radiat Res 2012 Nov; 178 (5): 499-503.

518. Li Y, Huang W, Huang S, Du J, Huang C. Screening of anti-cancer agent using zebrafish: Comparison with the MTT assay. Biochem Biophys Res Commun 2012 May; 422 (1): 85-90.

519. Garkavtsev I, Chauhan VP, Wong HK, Mukhopadhyay A, Glicksman MA, Peterson RT, et al. Dehydro-α-lapachone, a plant product with antivascular activity. Proc Natl Acad Sci USA 2011 Jul; 108 (28): 11596-601.

520. Wu YT, Lin CY, Tsai MY, Chen YH, Lu YF, Huang CJ, et al. β-Lapachone induces heart morphogenetic and functional defects by promoting the death of erythrocytes and the endocardium in zebrafish embryos. J Biomed Sci 2011 Sep; 18: 70.

521. Mather MW, Darrouzet E, Valkova-Valchanova M, Cooley JW, McIntosh MT, Daldal F, et al. Uncovering the molecular mode of action of the antimalarial drug atovaquone using a bacterial system. J Biol Chem 2005 Jul; 280 (29): 27458-65.

522. Biagini GA, Viriyavejakul P, O'Neill P M, Bray PG, Ward SA. Functional characterization and target validation of alternative complex I of *Plasmodium falciparum* mitochondria. Antimicrob Agents Chemother 2006 May; 50 (5): 1841-51.

523. Zhou J, Duan L, Chen H, Ren X, Zhang Z, Zhou F, et al. Atovaquone derivatives as potent cytotoxic and apoptosis inducing agents. Bioorg Med Chem Lett 2009 Sep; 19 (17): 5091-4.

524. Hölttä-Vuori M, Salo VT, Nyberg L, Brackmann C, Enejder A, Panula P, et al. Zebrafish: Gaining popularity in lipid research. Biochem J 2010 Jul; 429 (2): 235-42.

525. Mizuno Y, Sone N, Suzuki K, Saitoh T. Studies on the toxicity of 1-methyl-4-phenylpyridinium ion (MPP^+) against mitochondria of mouse brain. J Neurol Sci 1988 Aug; 86 (1): 97-110.

526. Yi F, He X, Wang D. Lycopene protects against MPP^+-induced cytotoxicity by maintaining mitochondrial function in SH-SY5Y cells. Neurochem Res 2013 Aug; 38 (8): 1747-57.

527. Devun F, Walter L, Belliere J, Cottet-Rousselle C, Leverve X, Fontaine E. Ubiquinone analogs: A mitochondrial permeability transition pore-dependent pathway to selective cell death. PLoS One 2010 Jul; 5 (7): e11792.